

STRUCTURE AND PROPERTIES OF COLLAGEN AND GELATIN
IN THE HYDRATED AND ANHYDROUS SOLID STATE

by

NAK-HO SUNG

S.B., Seoul National University, Korea

(1964)

M.S., University of Chicago

(1967)

Submitted in Partial Fulfillment of the
Requirements for the
Degree of Doctor of Science
at the
Massachusetts Institute of Technology
June, 1972

Signature of Author.

Department of Mechanical Engineering
May 5, 1972

Certified by... ..

Thesis Supervisor

Accepted by.... .

Chairman, Departmental Committee on
Graduate Students



ABSTRACT

On the Structure and Properties of Collagen and Gelatin in the Hydrated and Anhydrous Solid State

by
Nak-Ho Sung

Submitted to the Department of Mechanical Engineering on May 5, 1972 in partial fulfillment of the requirements for the Degree of Doctor of Science in Materials Science and Engineering.

Quantitative characterization of the secondary and tertiary structure of non-fibrous (but native) collagen and its denatured form, gelatin is developed using wide-angle x-ray diffraction, infrared spectroscopy and optical rotatory dispersion (ORD).

Four Debye-Scherrer rings in the x-ray pattern obtained with collagen films are identified as characteristic of the triple helical structure (native collagen) in contrast to the total absence of any Debye-Scherrer rings in amorphous collagen films (hot-cast gelatin). The use of x-ray diffraction in the quantitative analysis of the helical content of semi-native collagen (cold-cast gelatin) is found to be unsatisfactory due to near identity of the patterns of collagen films and cold-cast gelatin films.

The infrared absorption spectra of collagen, cold-cast gelatin and hot-cast gelatin films are studied comparatively. Multiplet bands of the Amide I and Amide II bands are resolved into sub-bands, and sub-bands characteristic of the helical structure of collagen and randomly coiled gelatin are assigned. The infrared spectroscopic basis for the quantitative estimation of helical content of semi-crystalline collagen is developed using the ratio of absorbance of the 1235cm^{-1} band to the 1450cm^{-1} band.

Particular emphasis is placed on the development of solid state methodology for obtaining and interpreting ORD spectra of solid specimens (collagen films and fibers). Following recognition of the tensorial character of the optical activity, three non-zero diagonal components of the second-rank tensor are resolved by independent measurements of the optical activity along the three mutually orthogonal axes of the rod-like collagen molecule. The optical rotation along the direction perpendicular to the axis of collagen helix is found to be negative whereas that along the axis of collagen helix is positive.

Using the component values of optical activity, quantitative comparison is made between the optical activity of

collagen in dilute solution and in the solid state. It is concluded that the triple helical structure of collagen is virtually identical in the two states. It is also suggested that several unexplained cases of difference between the optical rotation of various polypeptides and proteins in dilute solution and in the solid state, which have been reported by several workers can be interpreted quantitatively by use of the solid state methodology for the measurement of optical rotation developed in this work. A sensitive quantitative assay of collagen nativity in the solid state is developed based on the remarkable differences in optical activity among the various specimens (films of native, cold-cast gelatin and hot-cast gelatin). By this method, cold-cast gelatin film is found to possess 49.6% of the tertiary structure of native collagen while the infrared spectroscopic method yields the value 45.16% for the same specimen.

The effect of dehydration on the structure of collagen is studied using x-ray, IR and ORD. Dehydration of native specimens to a water content less than 0.1%-wt. causes minor distortion of the triple helical structure of collagen molecules; such distortion is completely reversible upon rehydration. Contrary to current belief, water is found not to be an integral part of the collagen helix since the helix survives severe dehydration. It is believed that the minor distortion of the helical structure of collagen, caused by dehydration, occurs primarily in the polar regions of the molecule.

It is found that soluble collagen becomes insoluble when dehydrated below 0.3%-wt. moisture level by the formation of interchain cross-links. The mechanism of dehydrative cross-linking is found to proceed neither by a free radical mechanism nor by the aldol-condensation mechanism by which intermolecular cross-links are formed biosynthetically in collagen *in vivo*. It is suggested instead that dehydrative cross-linking in collagen most likely proceeds via a condensation reaction between carboxylic groups and amino groups and/or hydroxyl groups.

Thesis Supervisor: Dr. Ioannis V. Yannas
Title: Associate Professor of Mechanical Engineering

ACKNOWLEDGEMENTS

First, the author wishes to thank his thesis supervisor, Professor Ioannis V. Yannas for his enthusiasm, support and guidance. It was through his suggestions that the seemingly diverse content of this work gradually materialized into a unified whole. The author's association with him has been invaluable adjunct to the author's education.

The author is deeply grateful to Professor Stanley Backer who has been a constant source of encouragement through the financial and morale supports which has been far beyond his call of duty.

Occasional discussions and exchanges of ideas with the author's colleagues and in particular Messrs. Chor Huang and Anthony C. Lunn has been so much profitable and are greatly appreciated.

Thanks are also due to Professor Frederic J. McGarry in Civil Engineering and Professor Edward M. Merrill in Chemical Engineering who have given generously of their valuable time to serve on the author's thesis committee.

The author would like to express his appreciation to Mrs. Yang Ja L. Kim in the Department of Nutrition and Food Science, who continuously provided raw materials for collagen.

The author is grateful to miss Dorothy Eastman for her remarkable efficiency in typing the last Chapter of this document.

This work has been supported by the National Institutes of Health and the National Science Foundation under the Grants No.AM11919 NIH and No.GK 19408 NSF.

The author offers his heartfelt gratitude to his fiancée, Chong Sook, who provided every possible help to the author during the preparation of this thesis.

Finally, the author extends his deep gratitude to his parents for their constant encouragement and love, and to whom this thesis is dedicated.

TABLE OF CONTENTS

	<u>PAGE</u>
LIST OF TABLES	10
LIST OF FIGURE CAPTIONS	11
Chapter I INTRODUCTION	16
Chapter II SAMPLE PREPARATION AND CHARACTERIZATION	23
II-1 QUANTITATIVE STUDY OF THE EXTRACTION PROCESS	
1.1 Introduction	23
1.2 Preparation of Acid Soluble Collagen	25
1.3 Characterization of Collagen Solution	27
A. Concentration	29
B. Intrinsic Viscosity	29
C. Specific Rotation	30
D. Stability of Collagen Solution	34
E. Amino Acid Ananysis	37
II-2 QUANTITAVE STUDY OF CASTING PROCESS FOR COLLAGEN AND GELATIN FILMS	
2.1 Introduction	39
2.2 Solution Casting of Films	40
A. General Considerations	41
B. Casting Procedure	42
2.3 Discussion	50
A. Rate of Evaporation	50
B. Changes in Viscoelastic Behavior During Casting	51
C. Birefringence in Films	54
II-3 MOISTURE ASSAY METHODS FOR COLLAGEN AND GELATIN	
3.1 Introduction	58
3.2 Vacuum Drying Method	58
A. Introduction	60
B. Experimental	61
C. results	67
3.3 Fischer Volumetric Titration Method	67
A. Introduction	67
B. Experimental	69
C. Results and Discussion	72

	<u>PAGE</u>
Reference for Chapter I and II	76
Chapter III X-RAY DIFFRACTION AND INFRARED SPECTROSCOPY STUDIES OF COLLAGEN AND GELATIN	
III-1 X-RAY DIFFRACTION STUDIES	79
1.1 Introduction	79
1.2 Theory of X-ray Diffraction by Helical Molecules	81
1.3 Wide-angle X-ray Diffraction Patterns of Collagen Fiber	91
1.4 Wide-angle X-ray Diffraction patterns of Collagen and Gelatin Films	102
A. Experimental	102
B. Results	104
C. Discussion	106
1.5 Summary	113
III-2 INFRARED SPECTROSCOPY STUDIES	115
2.1 Introduction	115
2.2 Experimental	116
2.3 Results and Discussion	117
2.4 Summary	127
Reference for Chapter III	129
Chapter IV OPTICAL ROTATORY DISPERSION (ORD) AND CIRCULAR DICHROISM (CD) STUDIES OF COLLAGEN AND GELATIN	
IV-1 INTRODUCTION	132
IV-2 GENERAL CONSIDERATION OF ORD AND CD	133
2.1 Phenomenon of Optical Activity ; Terms Definitions	133
2.2 Drude Equations	139
2.3 Moffitt-Yang Equation	141
2.4 Cotton Effect and CD	144
IV-3 ORD AND CD OF COLLAGEN GELATIN	150
3.1 Introduction	150
3.2 Experimental	152
A. Materials	152
B. Instrument Description	152

	<u>PAGE</u>
C. ORD Measurements from the Visible to Near UV Region	153
D. ORD Measurements in the Far UV Region	156
E. CD Measurements	157
F. Other Measurements	157
3.3 Results	160
3.4 Discussion	161
A. Dilute Solution Studies	161
B. Studies of Films	172
C. Comparison of Data Obtained in Solution and Solid State	179
3.5 Tensorial Character of Optical Activity	185
A. Gyration Tensor	185
B. Tensor Components in a Uniaxial Crystal and Collagen Molecule	187
C. Interpretation of ORD of Collagen in Solution and in Film	194
3.6 Optical Rotation of Collagen Fiber- $[\alpha_{33}]_{\text{solid}}$	199
A. Experimental	199
B. Results and Discussion	204
C. Indirect Measurement of $[\alpha_{33}]$	208
3.7 Comparison of the Optical Activity of Collagen in Solution and in Solid Film	210
3.8 Assay of Helical Content	217
3.9 Optical Activity of Collagen at Different Hydration Levels	222
A. Experimental	222
B. Results and Discussion	224
3.10 Summary and Conclusions	226
Reference for Chapter IV	231
Chapter V EFFECT OF DEHYDRATION ON THE STRUCTURE AND PROPERTIES OF COLLAGEN	
V-1 INTRODUCTION	237
V-2 AMINO ACID ANALYSIS OF ANHYDROUS COLLAGEN	239

	<u>PAGE</u>
2.1 Experimental	239
2.2 Results and Discussion	240
V.3 WIDE-ANGLE X-RAY DIFFRACTION STUDIES OF ANHYDROUS COLLAGEN	243
3.1 Experimental	243
3.2 Results and Discussion	246
V.4 ORD STUDIES OF ANHYDROUS COLLAGEN FILM	260
4.1 Experimental	261
4.2 Results and Discussion	262
V.5 IR SPECTRA OF ANHYDROUS COLLAGEN FILM	264
5.1 Experimental	265
5.2 Results and Discussion	265
V.6 CONCLUSION ON THE EFFECT OF DEHYDRATION ON THE STRUCTURE OF COLLAGEN	267
V.7 DEHYDRATIVE CROSS-LINKING IN COLLAGEN AND GELATIN	269
7.1 Solubility of the Dehydrated Collagen Film	269
A. Experimental	270
B. Results and Discussion	271
7.2 Study on the Mechanism of Dehydrative Cross-Linking	275
A. Experimental	275
B. Results and Discussion	276
7.3 Solubility of Dehydrated Lathyrctic Collagen	278
A. Experimental	278
B. Results and Discussion	280
7.4 Summary and Conclusions on the Dehydrative Cross-linking in Collagen and Gelatin	283
Reference for Chapter V	287
Recommendations for Future Work	290
Biographical Note	291

LIST OF TABLES

	<u>PAGE</u>
Table II-1 Intrinsic Viscosity and Optical Rotatory Dispersion properties of Collagens of Different Species	33
Table II-2 Amino Acid Compositions of Rat Tail Collagen	38
Table II-3 Change of the Activity of Fischer Reagent during Storage	70
Table II-4 Comparisons of the Moisture Content of collagen and Gelatin Determined by Vacuum Drying Method and by the Fischer Titration Method	73
Table III-1 Wide-Angle X-ray Diffraction Data of Collagen Fiber (unstretched)	95
Table III-2 Orientation of Collagen Molecules in the Wet Rat Tail Tendon and the Film	101
Table III-3 Wide-Angle X-ray Diffraction Data of Collagen, Cold-cast Gelatin and Hot-cast Gelatin Films	107
Table III-4 Major Bands in the Infrared Absorption Spectra of Collagen	119
Table III-5 Changes in IR Spectrum of Collagen Due to Denaturation (Comparison between Collagen and Hot-cast Gelatin Spectra on Five Major Intensive Bands)	123
Table III-6 IR Sub-bands of Amide I and II Absorption Bands in the Infrared Spectra of Collagen and Hot-cast Gelatin	124
Table IV-1 ORD Data of Collagen and Gelatin in Various States	177
Table IV-2 Comparison of the ORD and IR Methods in Evaluating the Helical Content	221
Table V-1 Amino Acid Composition of Native and Dehydrated Rat Tendon Collagen	242
Table V-2 Dehydration History of the Tendon Fiber	245
Table V-3 Dehydration History of the Collagen Films For X-ray Diffraction Studies	261
Table V-4 Solubility of the Dehydrated Collagen Film	272
Table V-5 Solubility of the Dehydrated Gelatin Films	274
Table V-6 Effect of Free Radical Scavengers on the Solubility of Dehydrated Gelatin	277
Table V-7 Solubility of Normal and Lathyrctic Collagen with Various Treatments	281

LIST OF FIGURE CAPTIONS

	<u>PAGE</u>
Figure I-1 Schematic presentation of the structure of collagen at different levels of order	18
Figure II-1 Material balance for the extraction process of rat tail tendon collagen	28
Figure II-2 Intrinsic viscosity of rat tail collagen in 0.05M acetic acid solution	31
Figure II-3 Change in the relative viscosity of collagen solution (0.08%-wt. collagen in 0.05M acetic acid) with time at room temperature	35
Figure II-4 Change in the specific rotation of collagen solution (in 0.05M acetic acid) with time at room temperature	36
Figure II-5 Schematic diagram of the film casting box	45
Figure II-6 Rate of dehydration of the collagen solution under forced convection	48
Figure II-7 Rate of dehydration of the collagen solution under natural convection	49
Figure II-8 Change of the concentration of collagen during casting process	52
Figure II-9 Rate of evaporation vs. concentration of collagen during casting process under forced convection	53
Figure II-10 Birefringence of the collagen films cast under the conditions of natural and forced convection	56
Figure II-11 Variation of the apparent specific rotation of the collagen films cast under different conditions (optical rotation was measured with a film rotating around by 45°)	57
Figure II-12 Rate of dehydration of collagen film (5.6 μ thick) under vacuum (3x10 ⁻⁴ mmHg) at 23°C	63
Figure II-13 Rate of dehydration of gelatin granules (0.4-0.65 mm in diameters) under vacuum (3x10 ⁻⁴ mmHg) at 105°C	64
Figure II-14 Rate of dehydration of collagen film (3.8 μ thick) under vacuum (3x10 ⁻⁴ mmHg) at 105°C	65

	<u>PAC</u>	
Figure II-15	Moisture regain of anhydrous collagen and gelatin at ambient condition	66
Figure II-16	Comparisons between the moisture contents of collagen and gelatin determined by vacuum drying method and by Fischer titration method	74
Figure III-1	Cylindrical coordinates for simple helix; Helical parameters in real and reciprocal space	83
Figure III-2	The Bessel function $J_n(x)$ as functions of n and x	87
Figure III-3	Geometry of coiled-coil	87
Figure III-4	Wide-angle x-ray fiber pattern of wet rat tail tendon collagen	92
Figure III-5	Distribution of the layer line intensities in the diffraction pattern of collagen fiber	97
Figure III-6	(a) Disorientation angle ϕ of the meridional reflection in the wide-angle collagen fiber pattern (b) Wide-angle x-ray diffraction pattern heat shrunken (65°C, 1 hour in water) collagen fiber	99
Figure III-7	Schematic presentation of the specimen preparation for wide angle x-ray diffraction pattern of collagen film obtained with x-ray beam parallel to the plane of the film	102
Figure III-8	Debye-Scherrer Rings in the wide-angle x-ray pattern of collagen film	105
Figure III-9	Wide-angle x-ray diffraction pattern of collagen film (Beam perpendicular to the plane of the film - (a), Beam parallel to the plane of the film - (b))	111
Figure III-10	Wide-angle x-ray diffraction patterns of cold-cast and hot-cast gelatin films	112
Figure III-11	Infrared absorption spectra of collagen and hot-cast gelatin film	118
Figure III-12	Ratio of absorbance of the 1235 cm^{-1} band to 1450 cm^{-1} band in collagen, cold-cast gelatin and hot-cast gelatin	126

	<u>PAGE</u>
Figure IV-1 Schematic presentation of plane polarized and circularly polarized light	136
Figure IV-2 Cotton effect for isolated absorption band at λ_i ((a)Absorption, (b)ORD, (c)CD)	137
Figure IV-3 Cotton effect and absorption spectra	147
Figure IV-4 Schematic diagram for CD spectra in Gaussian form	147
Figure IV-5 Typical CD spectra of polypeptides of α -helical, β and randomly coiled conformations	149
Figure IV-6 Schematic diagram of Cary 60 spectropolarimeter	154
Figure IV-7 Apparent density of collagen and gelatin films as a function of thickness	159
Figure IV-8 ORD of collagen and gelatin in dilute solution(0.05M HAC) in the Visible to near-UV region	164
Figure IV-9 ORD of collagen and gelatin in dilute solution(0.05M HAC) in far UV region	165
Figure IV-10 ORD of collagen, cold-cast gelatin and hot-cast gelatin films in the visible to near UV region	166
Figure IV-11 ORD of collagen film in far UV region	167
Figure IV-12 CD spectra of collagen and gelatin in dilute solution (0.05M HAC)	168
Figure IV-13 CD spectra of collagen and cold-cast gelatin films	169
Figure IV-14 Drude plot of the ORD of gelatin in dilute solution (600m μ -300m μ)	170
Figure IV-15 Drude plot of the ORD of collagen in dilute solution (600m μ -300m μ)	171
Figure IV-16 Drude plot of the ORD of collagen film (600m μ -300m μ)	173
Figure IV-17 Drude plot of the ORD of cold-cast gelatin film (600m μ -300m μ)	174
Figure IV-18 Drude plot of the ORD of hot-cast gelatin film (600m μ -300m μ)	175
Figure IV-19 Comparison of ORD of collagen solution (in 0.05M HAC) and collagen film (Visible to near UV region)	180

	<u>PAGE</u>
Figure IV-20 Comparison of the ORD of collagen solution (in 0.05M HAc) and collagen film (far UV region)	181
Figure IV-21 Comparison of CD spectra of collagen solution(in 0.05M HAc) and collagen film	182
Figure IV-22 Transition of the coordinates of the molecular axes of collagen	190
Figure IV-23 Geometry of the tilted collagen film	197
Figure IV-24 Optical micrograph of the cross-sectional view of the tendon specimen used for the optical rotation measurements	201
Figure IV-25 Specimen holder for the tendon fibers in the measurements of the optical rotation	202
Figure IV-26 ORD of dry collagen fiber (ca.15%-wt. water) measured along the fiber axis $[\alpha_{33}]$	205
Figure IV-27 Comparison of the ORD of collagen measured along the helical axis of molecule($[\alpha_{33}]$)and in perpendicular to the helical axis($[\alpha_{11}]$)	206
Figure IV-28 Specific Rotation of the Collagen Films at Various tilted Positions (Tilt Angle β)	211
Figure IV-29 Specific Rotation of Collagen at Various Hydration Levels from in Dilute Solution to Anhydrous States	225
Figure V-1 Wide-Angle x-ray diffraction pattern of Native Wet (65%-wt. water) Tendon (A) and Dry (~15%-wt.) (B)	247
Figure V-2 Wide-Angle X-ray Diffraction Pattern of Native Tendon: Partially Dehydrated(3.9 %-wt. water)(A) and Anhydrous(<0.1%-wt. water)(B)	248
Figure V-3 Comparison of the Wide-Angle X-ray Pattern of Wet (A) and Rehydrated (B) Tendon	249
Figure V-4 Changes in 10th, 7th, 3rd Layer Line Spacings of the Fiber Pattern with Water Content	250

	<u>PAGE</u>	
Figure V-5	Changes in d_{100} and d_{200} of the Fiber Pattern with Water Content	251
Figure V-6	(A) Unit Twist "t" of the Collagen Helix at Different Levels of Hydration (B) Changes in 10 th Layer Line Breadth with water Content	252
Figure V-7	Specific Rotation of the Collagen Films at Various Dehydration Levels (from 15%-wt. water to 0%-wt.)	263
Figure V-8	Solubility of the Dehydrated Collagen (Solubility vs. Dehydration Levels)	273

CHAPTER I INTRODUCTION

Structure of Collagen; Collagen is one of the most abundant structural proteins found in living systems as a constituent of connective tissue. The basic molecular unit of collagen is a triple helix (51) composed of three similar, but not identical polypeptide unit, termed tropocollagen(TC), is a rigid rod-like macromolecule about 3000\AA long with a diameter of about 15\AA , and has a molecular weight of about 300,000(25,53,54). A schematic diagram for different levels of structure of collagen is shown in Figure I-1.

Several levels of structural complexity can be considered in collagen;

Firstly, primary structure (the complete sequence of amino acids in the polypeptide chain) of collagen is made up of 18 amino acids of varying amounts. The amino acid composition for many different species of collagen is well known, but the amino acid sequences are still largely undetermined. The composition of rat tail collagen is shown in Table II-1.

Some of the characteristic features in primary structure of collagen are as follows (figure I-1.A); (i) the content of glycyl residues is about one-third of total and almost every third residue of the polypeptide chain is glycyl; this provides for relatively free rotation around the chain, thereby rendering flexibility to it, (ii) the imino acids, proline and hydroxyproline constitute about one-fourth of

the residues, which provide the rigidity of the chain due to the hindered rotation of the chain around the pyrrolidine ring of the prolyl residue, (iii) individual chains appears to be made up of block sequences of "polar" regions (mostly α -amino acids) alternating with "apolar" regions (prolyl- and hydroxyprolyl-rich region)

Secondly, conformation of individual chain (secondary structure) of collagen molecule is a left-handed helix, similar to poly-L-proline II type which has a pitch of about 9\AA (Figure I-1,B).

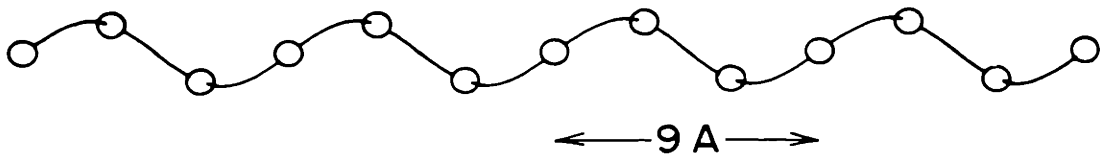
Thirdly, the tertiary structure (large scale folding of the polypeptide chains of collagen) is a right-handed super-helix, made up of a three individual chains of left-handed helix, with a repeat distance of about 90\AA (Figure I-1,C).

Finally, the quaternary structure (structure originating from the aggregation of TC molecules) of collagen shows a variety of different forms of aggregation. Depending on the conditions of aggregation process, different crystallites are formed including the quarter-staggered native type, the segment long spacing (SLS) type, the fibrous long spacing (FLS) type and others. A pattern of fine cross striations with an axial period of about 690\AA (spacing D in Figure I-1,E) for native and about 2800\AA for the FLS forms are the characteristic features of the transmission electron micrographs of stained specimens of these crystallites.

A. TYPICAL SEQUENCE

GLY-X-Y-GLY-PRO-Y-GLY-X-HYP-GLY-PRO-HYP

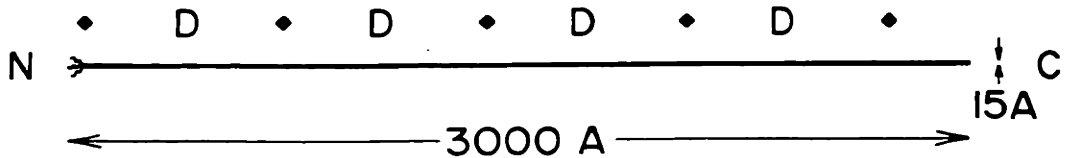
B. MINOR HELIX



C. MAJOR (TRIPLE) HELIX



D. MOLECULE



E. FIBRIL

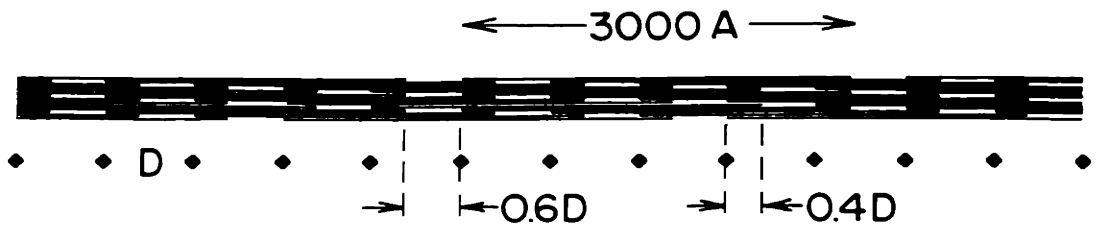


Figure I-1

Higher order structures as well as further details on structure of collagen discussed above have been recently reviewed by Yannas(54) and by others(55).

Scope of this investigation

The secondary and tertiary structure of biological polymers including collagen is commonly studied in the dilute solution state using classical physicochemical methods such as viscometry, light-scattering, osmometry, optical rotation, ultracentrifugation, flow birefringence and several others. By contrast, biopolymers in the solid state can be studied fruitfully only in the form of single crystal or highly ordered states(i.e., fibers) using the x-ray diffraction technique or electron microscopy.

Due to the fact that collagen can not be crystallized, the gross features of the tertiary structure of this biopolymer have been obtained largely from the x-ray diffraction pattern of collagen fibers, a pattern which can provide only limited information compared to the pattern of crystallizable proteins. Higher orders of structural order in collagen fibers have been partly deduced by transmission and scanning electron microscopy.

The lack of methodology for the structural characterization of non-fibrous collagen in the solid state (eg. in the form of films) is even more acute. Virtually no characterization of collagen films, cast from collagen solution has been reported. Such characterization tools must be

developed before an effort is undertaken to use collagen as a material.

This thesis attempts to develop and standardize the methods for quantitative characterization of the secondary and tertiary structure of collagen in the solid state, specifically, of two-component solid films and fibers based on collagen and water. Systematic and comparative use is made of wide-angle x-ray diffraction, infrared spectroscopy and optical rotatory dispersion(ORD) in the quantitative characterization of the native, helical conformation of collagen chains which is contrasted with the denatured, randomly-coiled structure of gelatin.

This study has focused its attention on two regions of concentration range of the collagen-water system, namely, dry(ca.15%-wt. water) and anhydrous (water less than 0.1%-wt.) state. Anhydrous collagen poses an unsolved problem in collagen science. When dehydrated below 0.3%-wt. water level, soluble collagen becomes insoluble(11), by a formation of inter-chain cross-links. Water has been suggested to be an integral part of the collagen structure, i.e., essential in its formation and maintenance(12).

Attempts were, therefore, made in this thesis to assess the effect of severe dehydration on the structure of collagen helix, using the techniques developed in this study, and also to elucidate the mechanism of dehydrative cross-linking by use of a variety of techniques.

Chapter II contains the quantitative characterization

of the sample preparation techniques including the extraction process of collagen from rat tail tendon, the solution casting process for the collagen and gelatin films and their characterization. Also included is a comparative study of moisture assay in collagen by the vacuum drying method on one hand and the Fischer volumetric method on the other.

Chapter III contains the methodology and results of wide-angle diffraction and infrared spectroscopic studies. A brief review is made of diffraction theory by a helical molecule followed by the discussion of the characteristic fiber pattern of native collagen fibers. Debye-Scherrer patterns of collagen, cold-cast gelatin and hot-cast gelatin films are compared.

The infrared absorption spectra of collagen and hot-cast gelatin are discussed. The five most intensive absorption bands are studied in an attempt to establish the IR spectroscopic basis for differentiating the native helical conformation of collagen structure from the randomly-coiled structure of hot-cast gelatin. Quantitative assay of a nativity of solid specimens is developed based on the absorbance of the conformation sensitive bands.

Chapter IV presents the development of the systematic application of ORD and CD to the secondary and tertiary structure of collagen and gelatin in the solid state. Comparative studies are made of the ORD and CD behavior of collagen between dilute solution and the solid states.

Analysis of the tensorial components of the optical activity tensor of tropocollagen molecule is presented followed by the measurements of each component using different specimens of collagen films and fibers. Based on the component values of the optical activity of collagen molecule, quantitative comparison is made of the nativity of the collagen between in dilute solution and in the solid state. A method for assay of relative helicity of the solid specimen of collagen, cold-cast gelatin and hot-cast gelatin films is developed in this section.

Chapter V is devoted to the studies of the effect of dehydration on the structure and properties of collagen. The effect of dehydration on the wide-angle x-ray diffraction patterns, infrared spectra and ORD of collagen is investigated and interpreted in relation to the structural changes. Finally the mechanism of dehydrative cross-linking in collagen is investigated using a variety of techniques including the use of free radical scavenger, EPR measurements, chemical modifications as well as lathyritic collagen.

CHAPTER II

SAMPLE PREPARATION AND CHARACTERIZATION

II-1 Quantitative Study of the Extraction Process

1.1 Introduction

The physicochemical studies to determine the structure, size and shape of the collagen molecule as well as the chemistry of the protein, including amino acid sequence, requires the isolation of collagen from its natural sources in the form of either solid phase or solution.

Although most collagen in natural connective tissues is insoluble, some of the collagen in certain tissues can be extracted in native form. The amount of soluble collagen depends on many variables such as the kind of tissue and the age of animal. (1) In general, the extraction procedure involves grinding of tissues, pre-extraction of the non-collageneous materials, extraction of the soluble fraction of collagen and purification. Depending on the solubilizing medium used, three different methods are known as follows:

- (1) neutral salt extraction
- (2) acid extraction
- (3) chemical or enzymatic solubilization

Detailed discussion of these methods can be found elsewhere; (2) however, some aspects of each methods are dis-

cussed here briefly.

When neutral or alkaline salt solutions are used as an extracting medium, the yield is relatively low (around 15% or less of total collagen in the tissue) and the collagen thus extracted has been known as the fraction which has been recently bio-synthesized; the latter is loosely aggregated (3,4) and is suggested as the precursor of insoluble collagen. (5) Phosphates, citrate and sodium chloride are the commonly used salts. (3-8)

Acid extraction is also widely used; acidic solutions of low ionic strength such as citrate buffer and acetic acid are used as an extracting medium. (9,10) The yield is, in general, higher than that from salt extraction. In either method, the yield depends on various factors such as the amount of extraction solution, duration of extraction, state of subdivision of ground tissue and stirring efficiency as well as the pH of the solution.

The collagens from salt and acid extractions do not differ in their chemical (amino acid composition) and physicochemical properties; (10,11) however, they do differ in their aggregation properties. (12) Acid soluble collagens can be reconstituted to native type fibers by warming (heat gelling) (50) much more readily than salt extracted collagen. Some fractions of salt extractable collagen are reported to be unable to be reconstituted by warming. (12)

Since most collagens in native tissues are insoluble

in the usual extracting solvents, methods have been sought for altering the collagen to be solubilized. The attempt has been made to increase the solubility of the collagen by digesting polysaccharide components of the tissue with enzymes which may be combined with collagen, thereby preventing its solubilization. α -Amylase (13) and hyaluronidase (14) were reported to be successful in this respect. Another approach in applying enzymes to solubilize the collagen is to use proteolytic enzymes such as pepsin and trypsin (15) which cleave a limited number of peptide bonds near the covalent cross-links. The application of other enzymes which are responsible for the insolubility of collagen and the action of these enzymes on native collagen in solution is thoroughly discussed by Piez in his recent summary. (2)

There are, therefore, many ways to prepare soluble collagen from tissue. Selection of any particular method may be determined by criteria, such as accessibility of tissue, simplicity of extracting procedure, yield. On the basis of these considerations, the method reported by Dumitru and Garrett (16) was employed as a standard procedure in preparing soluble collagen from rat tail tendon in this study.

1.2 Preparation of Acid Soluble Collagen from Rat Tail Tendon

Rat tails from Albino rats of varying ages were the

source of collagen in this work, except as otherwise indicated. Tails, collected and stored in a refrigerator at -10° C. were the stock supply for the extraction process.

Frozen tails, stored for about a month, were washed with cold tap water until they became flexible. With a pair of wire-stripping pliers, the tail was cut from the narrow tip in such a way that skin and bone was cut but not through the tendon. Tendon threads were then pulled out together with tail tip from the remaining tail. Exposed tendon was cut from the tail tip using a pair of scissors and immersed immediately in $0.5 \text{ M NaH}_2\text{PO}_4$ solution. This was repeated at 1/2-inch intervals up to the base of the tail. The weight of tendon in a tail varied from 130 mg to 400 mg (wet weight) depending on the size of the tail. The solution of $0.5 \text{ M NaH}_2\text{PO}_4$ was used as a pre-extraction medium. (16) The reticular membrane surrounding the fibrils of the tendon was separated off by $0.5 \text{ M NaH}_2\text{PO}_4$, (24) thereby increasing the speed of dissolution in acetic acid solution in the next step. Approximately 100 ml of the solution was used per gram of wet tendon and the pre-extraction step was carried out at room temperature over four hours. After pre-extraction, tendons were taken out from the solution and washed with distilled water several times to remove any residual NaH_2PO_4 from the solution. Since the tendon became swollen very quickly in distilled water, each rinse did not last more than ten seconds. Tendons

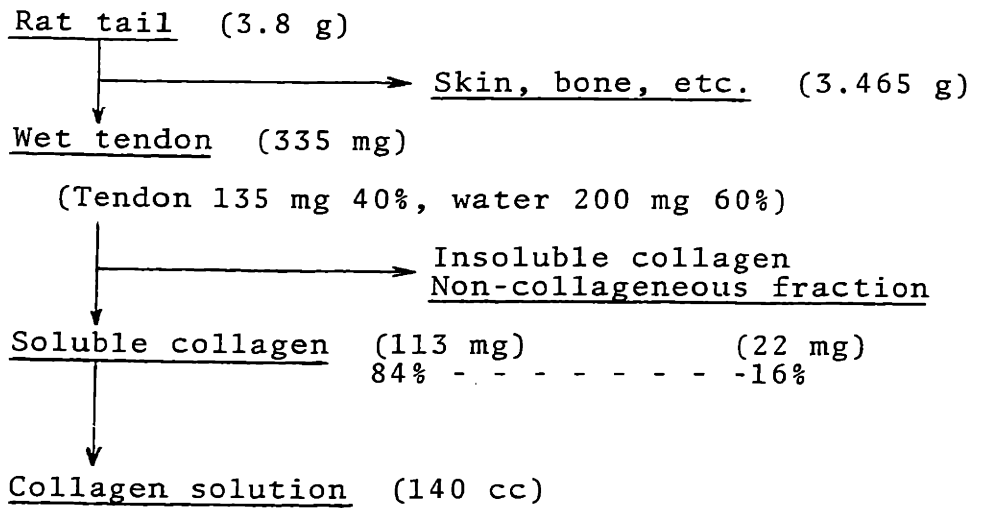
were then put into 0.05 M acetic acid to dissolve. Solubilization was carried out for overnight at room temperature with occasional mild agitation. Tendon fibers dissolved slowly yielding a very viscous solution. Approximately 450 cc of 0.05 M acetic acid solution was used for one gram of wet tendon to yield a solution containing approximately 0.08% collagen by weight after 24 hours of dissolution. Because of foreign materials and insoluble fraction of tendon, collagen solution after dissolution is normally very turbid. Clear solution was obtained by filtering the solution through medium and coarse glass frits. The final solution, thus obtained, contained approximately 0.08% wt. of acid soluble collagen and material balance for the overall extraction procedure is shown in Figure II-1 for the tendon from a medium-size rat tail.

Depending on the use intended for the collagen, further purification was done by precipitating out the collagen with a 2 M KCl solution, dialysing against distilled water over 24 hours at 23^o C. and redissolving in 0.05 M acetic acid solution. The acid soluble rat tail tendon collagen (0.08% wt. in 0.05 M acetic acid) was the standard collagen solution used in later work in this study.

1.3 Characterization of Collagen Solution

Before using the collagen prepared as described above, certain critical physical quantities such as the collagen

MATERIAL BALANCE OF EXTRACTION PROCESS
OF COLLAGEN FROM RAT TAIL (MEDIUM SIZE)



Final conc. = 0.08%-wt.

FIGURE II-1

concentration of the solution. The intrinsic viscosity $[\eta]$, the specific rotation $[\alpha]$ and certain other characteristics of the dissolved collagen were determined routinely following each preparation.

A. Concentration of Collagen Solution

The final concentration of the collagen solution was determined by the gravimetric method. A known amount of solution was first air-dried at room temperature and subsequently dehydrated at 105° C. under vacuum for three days. The weight of dehydrated collagen was determined with an analytical balance and the percentage of the dry weight to the original total weight of the solution was computed. Typical final concentrations of the collagen solution centered around 0.08%-wt. ranging from 0.057%-wt. to 0.098%-wt.

B. Intrinsic Viscosity $[\eta]$

Intrinsic viscosity was estimated by a low shear rate technique. Using an Ubbelohde viscometer (Model 13-614, Fisher Scientific) the relative viscosity of the collagen solution was obtained by measuring the flow times of the solution at different concentrations in 0.05 M acetic acid at 25° C. \pm 0.1° C. The flow time for the 0.05 M acetic acid solution in the Ubbelohde viscometer used was 123 seconds at 25° C. Relative viscosity, η_{rel} and specific

viscosity η_{sp} were calculated from the flow times of the collagen solution (t), of the solvent (t_0) and the concentration (c) using the following equations:

$$\eta_{rel} = \eta_{solution}/\eta_{solvent} = t/t_0$$

$$\eta_{sp} = \eta_{rel} - 1 = (t - t_0)/t_0$$

From the plot of η_{sp}/c vs. c , the intrinsic viscosity $[\eta]$ was estimated by extrapolation to zero concentration.

$$[\eta] = \lim_{c \rightarrow 0} (\eta_{sp}/c)$$

The intrinsic viscosity of acid soluble collagen from rat tail tendon, obtained by the above method was 12.7 ± 0.5 dl/g. The plot of η_{sp}/c versus concentration at 25° C. is shown in Fig. II-2. The intrinsic viscosity of vertebrate collagens varies, in general, from 11.5 to 17.0 dl/g depending on the collagen species, solvent, temperature and the experimental techniques. Data for different collagen species are summarized in Table II-1. The result obtained is somewhat different from that of Nada (27) who reported 15 dl/g for rat tail collagen. Direct comparison is, however, of no significance due to the different extraction procedure and also to the lack of information on the experimental conditions used by Nada. Nevertheless, the results are in fair agreement considering the large variability observed in the data of other collagens.

C. Specific Rotation, $[\alpha]$

The specific optical rotation of the dilute collagen

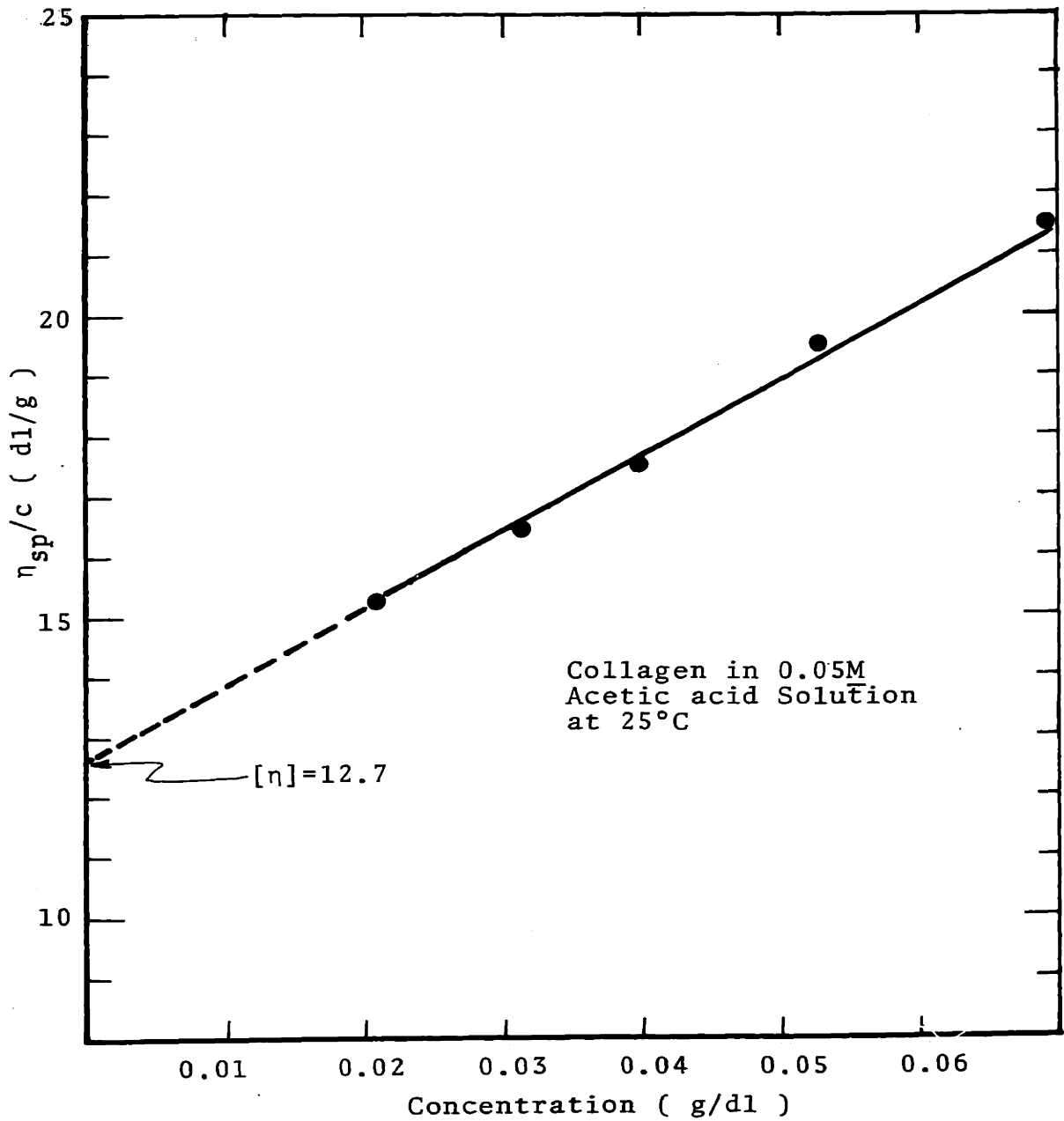


Figure II-2 Intrinsic viscosity of collagen solution

solution was determined with a Cary 60 spectropolarimeter. It is possible to obtain the full spectrum of specific rotation (ORD) of the collagen solution from a wave-length of 190 m μ to 600 m μ with this instrument. However, for the purpose of characterization, the optical rotation was measured only at 365 m μ and 589.5 m μ (sodium D line); at these wavelengths many independently reported values are available for the comparison. Measurements were carried out with a 1 cm quartz solution cell at room temperature for different concentrations of the solution and the blank solvent. (Details of the measurement procedure are to be discussed in Chapter IV.) From the measured angle of optical rotation, the specific rotation, $[\alpha]$ was calculated as follows: $[\alpha] = \alpha/l \cdot c$ (degrees cm³/decimeter g) where α is the rotation angle measured, c is the concentration of the solution in g/cm³, and l is the optical path length of the solution in decimeters. The specific rotation of the rat tail tendon collagen in 0.05 M acetic acid solution, measured at room temperature, was found to be:

$$[\alpha]_{365 \text{ m}}^{\text{R.T.}} = -1300 \pm 50$$

$$[\alpha]_{\text{D}}^{\text{R.T.}} = -380 \pm 10$$

These values agree well with other reported values (table II-1) for many different species of collagen indicating that the extraction method employed in this study yielded a native collagen solution. (Harrington (33) reported a

TABLE II-1 INTRINSIC VISCOSITY AND SPECIFIC ROTATION OF
COLLAGEN

<u>Collagen</u>	<u>Intrinsic Viscosity</u> [η] (dl/g)	<u>Specific Rotation</u> degree/g-cm ²
Ichthyocol	13.2 (citrate, pH 3.7) ⁹	- 350 ³²
	11.5 (citrate, pH 3.7) ²⁵	- 330 ³³
	12-16 (neutral salts) ²⁶	
	15-17 (neutral CaCl ₂) ²¹	
Rat tail tendon	15 (acid) ²⁷	- 289 ³³
	12.7 (0.05 M HA _c) [*]	- 380 [*]
Ratskin	16.5 (citrate, pH 3.7) ²⁸	
	13.7 (citrate, pH 3.7) ²⁹	- 409 ²²
Calfskin	13.5 (citrate, pH 3.7) ³⁰	- 415 ³⁰
	15 (acetic acid) ³¹	
	12	
Perch swim bladder	13.2 (citrate, pH 3.7) ²⁹	- 400 ²²
Cod swim bladder	13.2 (citrate, pH 3.7) ²⁹	- 397 ²²
Codskin	12.8 (citrate, pH 3.7) ¹⁴	-----
Dogfish sharkskin	-----	- 345 ³⁵

*This work

value of -289 for rat tail collagen which is unusually lower than other values.)

D. Stability of the Collagen in Solution

Collagen is well known for its characteristic helix-coil transition in dilute solution where molecules are well isolated from each other. This transition is often called "denaturation", a term referring to the disorganization of the secondary and tertiary structures without affecting the primary structure. (23) The denaturation of collagen in dilute solution occurs at temperatures from 16° to 37°

C. depending on the collagen species. (21) Rat tail tendon collagen is known to have a relatively high denaturation temperature, T_D of 37° C. (21) The helix-coil transition of collagen has been discussed thoroughly by von Hippel. (19)

For the practical purpose of handling collagen in the laboratory, it is necessary to know the extent to which collagen denatures at room temperature during process such as the casting of collagen film from dilute solution. The optical rotation and the relative viscosity of the freshly prepared collagen solution kept at room temperature (23° C.), were determined at various intervals of time over a two-week period. The change of η_{rel} with time is shown in Figure II-3. The ratio of initial specific rotation

$[\alpha]_{365}^{t=0}$ to that at time t , $[\alpha]_{365}^t$ is also plotted ag-

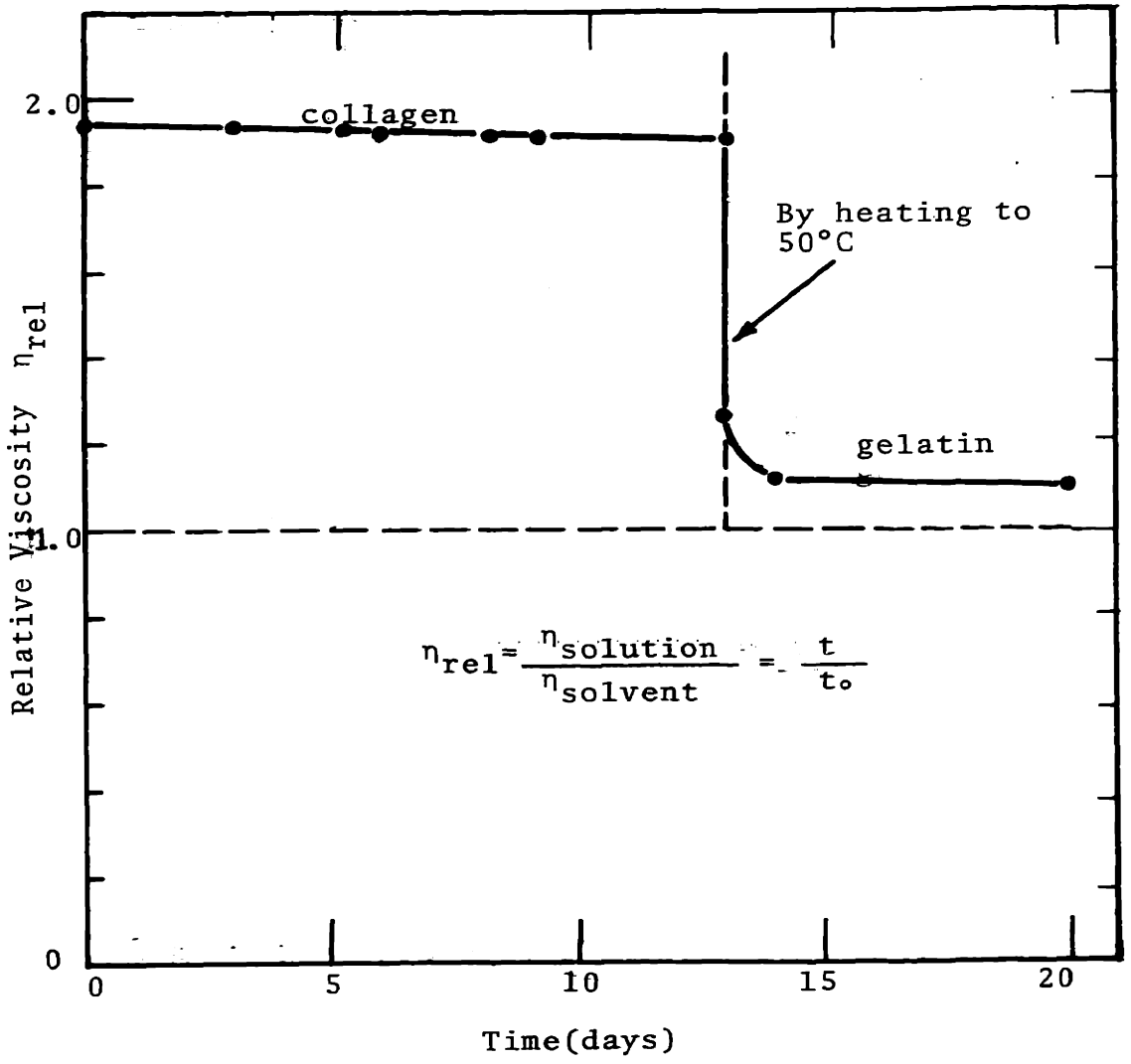


Figure II-3 Change in the relative viscosity of collagen solution(0.08%-wt. collagen in 0.05M acetic acid) with time at room temperature

$$\frac{[\alpha]_{365}^t}{[\alpha]_{365}^0}$$

-36-

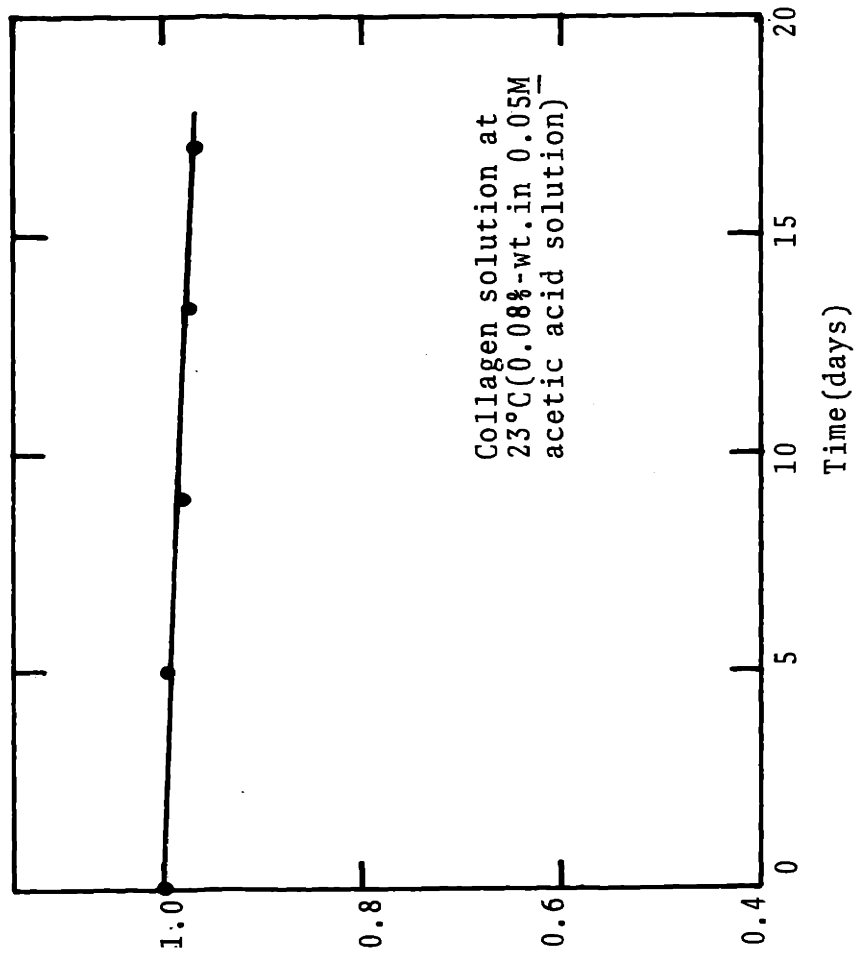


Figure II-4 Change in the specific rotation of collagen solution at room temperature

against time in Figure II-4. For the initial five days, during which most experiments in this work were conducted (including solution casting of films), the relative viscosity changed from its original value of 1.94 to 1.92 while the ratio of specific rotation decreased from 1.0 to 0.99. The small changes in the relative viscosity and the specific rotation indicates that the denaturation of collagen at 23° C. during the two-week period can well be taken as negligible (approximately 4.5% of the total collagen was estimated to be denatured in the two-week period based on the specific rotation values). It is worthwhile to mention that the optical rotation did not change when the collagen solution was stored at 0° C. for more than two months.

E. Amino Acid Analysis of RTT Collagen

The tail tendon was removed from the freshly killed rat tail, and pre-extracted with 0.5 M NaH₂PO₄ solution for four hours at room temperature. The tendon collagen was hydrolysed with 6 M HCl (1 mg collagen/5 ml 6 M HCl) at 120° C. for 22 hours under vacuum. At the end of the hydrolysis, hydrochloric acid was removed by evaporation and the residual amino acids were washed three times with distilled water. Dried amino acids were removed by dissolving in "Trisol" buffer solution and were analyzed with Beckman Automatic Amino Acid Analyzer. (Model 121, Beckman, Fullerton, Calif.) The results are tabulated in Table II-2

TABLE II-2 AMINO ACID COMPOSITION OF RAT TAIL COLLAGEN

<u>Amino Acid</u>	<u>Neuman</u> ^(a)	<u>Piez et al</u> ^(b)	<u>This work</u> ^(c)
Alanine	99.3	107.0	102.0
Glycine	351.0	331.0	336.0
Valine	22.5	22.9	22.7
Leucine	22.5	23.6	27.4
Iso-Leucine	13.2	9.6	11.5
Proline	123.0	122.0	121.0
Phenylalanine	14.3	11.9	13.5
Tyrosine	5.4	3.9	4.7
Serine	27.8	43.0	33.9
Threonine	19.1	19.9	18.0
Methionine	5.8	8.4	5.3
Arginine	46.5	50.0	(50) ^α
Histidine	3.3	4.1	3.9
Lysine	35.6	26.9	31.2
Aspartic Acid	47.1	45.0	46.3
Glutamic Acid	73.7	71.0	71.3
Hydroxy Proline	90.4	94.2	95.2
Hydroxy Lysine	-----	6.6	((6.6) ^α

Note: Data represent the number of amino acid residue/1000 amino acids.

- a) Recalculated (Eastoe and Leach, 1958) from Neuman's data
- b) Soluble rat tail collagen
- c) Native rat tail collagen containing 10% insoluble collagen
- d) Experiment was incomplete. Data are taken from Piez et al

together with other reported values for comparison. Our data show very good agreement with those of others (19) within the experimental error range.

II-2 Solution Casting Process for Collagen and Gelatin Films

2.1 Introduction

In a two-component system of a solvent and a solute, the dilute solution and the solid bulk state might be considered as the two extremes of the concentration range. In the dilute solution state, the solute molecules are sufficiently apart from each other so that the interaction between them is negligible. The structure of macromolecules in dilute solution can be deduced from their hydrodynamic properties (i.e. viscosity, sedimentation) or from their interaction with electromagnetic radiation (i.e. light scattering, IR and UV spectroscopy). In the bulk state, on the other hand, the molecules are closely packed together in aggregates varying in degree of order and ranging from completely amorphous solids to perfectly crystalline solids. The methods applied to study the molecular structure in the solid state differ, in general, from those applicable to dilute solution. X-ray diffraction, electron microscopy and IR spectroscopy are well known techniques for the study of macromolecules in the bulk state.

There is no guarantee that a macromolecule, which can assume different structures, will have the same molecular structure both in dilute solution and in the solid state. Any projection of the structural information obtained from dilute solution studies to the solid state should be made with caution. The properties, such as mechanical or thermodynamic, of polymers in bulk depend not only on the characteristics of isolated molecules but also on the interactions between them (i.e. hydrogen bonding, cohesive energy, etc.). It should be realized that some properties of crucial importance to the behavior of polymers in bulk have little or no relation to their behavior in solution. (39) This requires us to study macromolecules both in dilute solution and in the bulk state in order to understand the relation between molecular structure and physical properties.

In the solution casting process, where the solute molecules are transferred from their original solution environment to the bulk state, it is of interest to study the behavior of individual molecules and their interaction, as well as to monitor the process as a whole in a quantitative manner. In this section, therefore, the solution casting process for collagen and gelatin films is discussed in detail.

2.2 Solution Casting of Collagen and Gelatin Films

A. General Considerations

Collagen film can be prepared by two different methods which yield different types of film morphology. A transparent and optically isotropic film can be cast from a dilute collagen solution containing dispersed tropocollagen molecules. Another type of collagen film, which is opaque, can be cast from a suspension of collagen precipitates. These two types of films differ from each other in that the latter is composed of randomly oriented collagen fibrils (200-2000 Å in diameter) whereas the former is made up of tropocollagen molecules (15 Å in diameter).

It has been well known that tropocollagen can form different types of fibrils. Under different conditions of aggregation fibrils of native type (quarter staggered), segment long spacing type (SLS), fibrous long spacing type (FLS), and fibrils with no evident periodicity can be precipitated. (36) It is, therefore, possible to prepare a variety of different collagen films by evaporating water from a suspension of collagen fibrils of different types. Films of this kind are opaque and have a rough surface and the electron micrographs of the surface of such films have shown clearly that the film is a sort of "felt", made up of fibrils. (37) Because of the opacity and the rough surface, this "felt"-like film is not suitable for spectroscopic work (IR, ORD, etc.).

A transparent and optically isotropic collagen film can be cast from a clear solution of tropocollagen molecules. Such films have proved to be suitable for infrared and optical rotation studies; and so, unless stated otherwise, the collagen films referred to in this study are of this kind.

B. Solution Casting Procedure

(i) Operational Parameters

Before describing the detailed steps of the casting procedure, it is necessary to consider some general requirements for a casting surface, uniformity of the film and other operational ~~variables~~ such as temperature and rate of evaporation of the solvent.

A suitable casting surface must meet certain criteria. The surface must not react chemically with the solution, it must adhere only weakly to the dry film after casting and it must be non-toxic, non-flammable and easily available. The final product, the collagen film, must be optically transparent, optically isotropic and it must have uniform thickness in order to be suitable for spectroscopic measurements. Preliminary experiments were carried out to select an adequate substrate from several different surfaces including glass, mercury, aluminum, polystyrene and polymethyl methacrylate. Glass surfaces were not useful due to the strong adhesion between glass and the dry col-

lagen film; it was almost impossible to remove the film without fracturing it. Mercury, even though providing the perfect levelled surface without a problem of adhesion, was unacceptable because, on prolonged contact with the collagen solution (in 0.05 M acetic acid), a greyish white precipitate was produced at the interface and adhered thereafter to the collagen film. This precipitate is believed to have been the product of a reaction possibly occurring between acetic acid and mercury. An aluminum surface also turned out to be a poor substrate since it did not withstand the acidity of collagen solution but showed, instead, evidence of corrosion during the casting operation. As recommended by Dumitru, (38) both polystyrene (PST) and polymethylmethacrylate (PMMA) provided satisfactory surfaces for the casting of collagen solution into film. Dry collagen film was easily removed from these hydrophobic polymeric surfaces. PST was used in most of the times in this work.

Two operational parameters, namely, the casting temperature and the dehydration rate were controlled in order to prepare different types of films. Three different films were prepared and studied in this work. These are collagen film, cold-cast gelatin film and hot-cast gelatin film. Procedures for each case are as follows.

(ii) Collagen Film

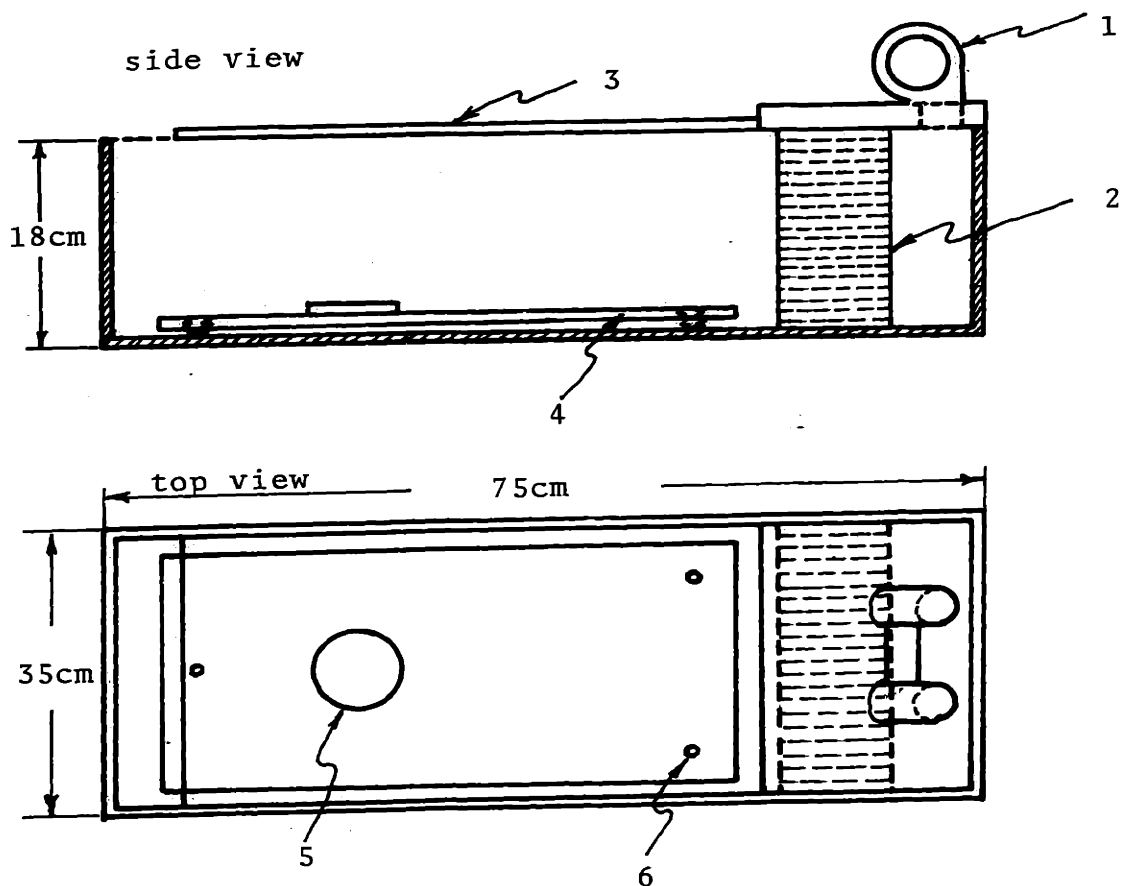
Step 1; A dilute collagen solution (ca. 0.08%-wt.) prepared and stored as described earlier, was first concentrated in a large beaker to approximately 0.5%-wt. by blowing air over the solution at room temperature (23^o C.).

Step 2; The concentrated solution was then poured into a shallow PST dish (about 10 cm in diameter) to the desired amount of depth and the dish was placed on the levelling table which had been carefully adjusted with a levelling device (Figure II-5).

Step 3; Two different conditions were employed for the subsequent evaporation of the solvent to minimize the casting time. When the uniformity of the film is not important, step 3-a was used and for the uniform film suitable for the spectroscopic studies step 3-b was used.

Step 3-a; For rapid casting, air was blown over the casting dish with an air blower installed on the casting box (see Figure II-5) at room temperature (forced convection casting).

Step 3-b; For slow casting, the solution was allowed to evaporate at 23^o C. without any special provision for forced convective flow over the surface (normal convection casting).



1. Air Blower
2. Honey Comb Structured Aluminum Air Distributor
3. Plexiglass Cover
4. Levelling Table
5. Casting Dish
6. Adjustable Screw for Levelling

Figure II-5 Schematic diagram of the film casting box

Step 4; The resulting dry, transparent film was removed by peeling off from the surface of the casting dish and stored in a PMMA container at ambient conditions for future use.

(iii) Cold-Cast Gelatin Film

The steps involved in the casting of cold gelatin film were the same as those in collagen film except for the one additional step necessary to denature collagen.

Step 1; Same as step 1 in the preparation of collagen film.

Step 2; A concentrated collagen solution was denatured to gelatin by warming the solution at 50° C. for one hour in a constant temperature water bath. The denatured solution was allowed to cool down to room temperature.

Steps 3-5; These are the same as steps 2-4 in the preparation of collagen film.

Disposable PST Petri dishes (10 cm in diameter, manufactured by Falcon Plastics Co.) were used as casting dishes. Dishes fabricated by another manufacturer (Fischer Scientific Company) were not suitable because the surface was not adequately flat. The estimated amount of solution adequate for the desired film thickness was based on the concentration of collagen solution and the density of the

dry film which was taken to be 1.32 g/cm^3 (see Chapter IV); i.e. for 5μ thick film, 0.5%-wt. collagen solution was needed to a depth of 1.32 mm.

Casting parameters both for fast (step 3-a) and slow (step 3-b) casting were monitored at room temperature. Figures II-6 and II-7 show a plot of the weight of solution against casting time for step 3-a and step 3-b respectively. The concentration of collagen in solution was also plotted against time (Figure II-8) and against the rate of dehydration (Figure II-9) for fast casting. The merits and drawbacks of the above two different evaporation conditions as well as a discussion of the data obtained will be presented in the later section.

(iv) Hot-Cast Gelatin Film

Step 1; Same as step 1 in the preparation of cold-cast gelatin.

Step 2; Same as step 2 in the preparation of cold-cast gelatin.

Step 3; The denatured gelatin solution was poured into a casting dish and the dish was placed on the leveling table which had been properly levelled in a temperature-controlled environment ("Stabil-Therm" Constant Temperature Cabinet, by Blue M Electric Co., Blue Island, Illinois).

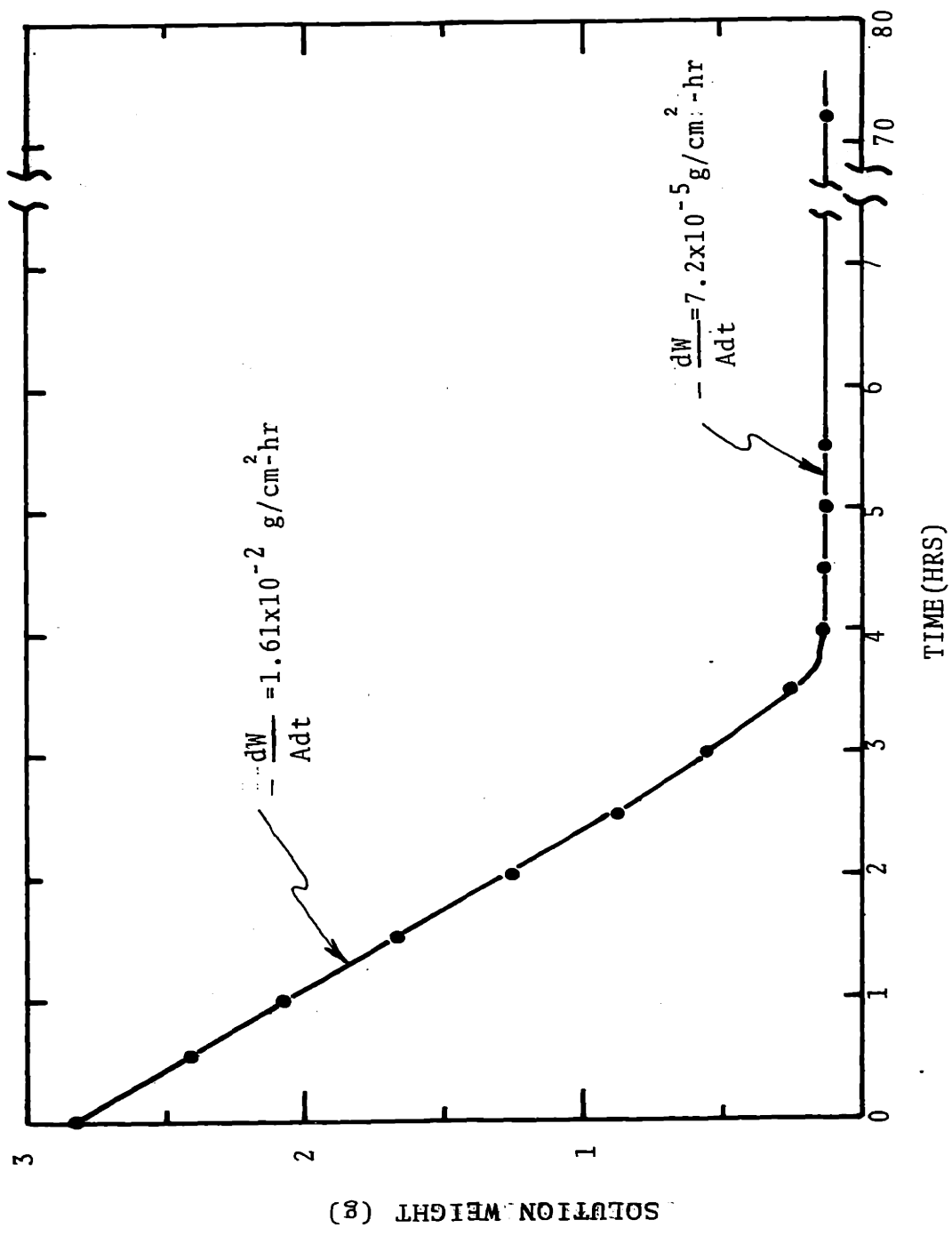


Figure II-6 Rate of dehydration of the collagen solution under forced convection

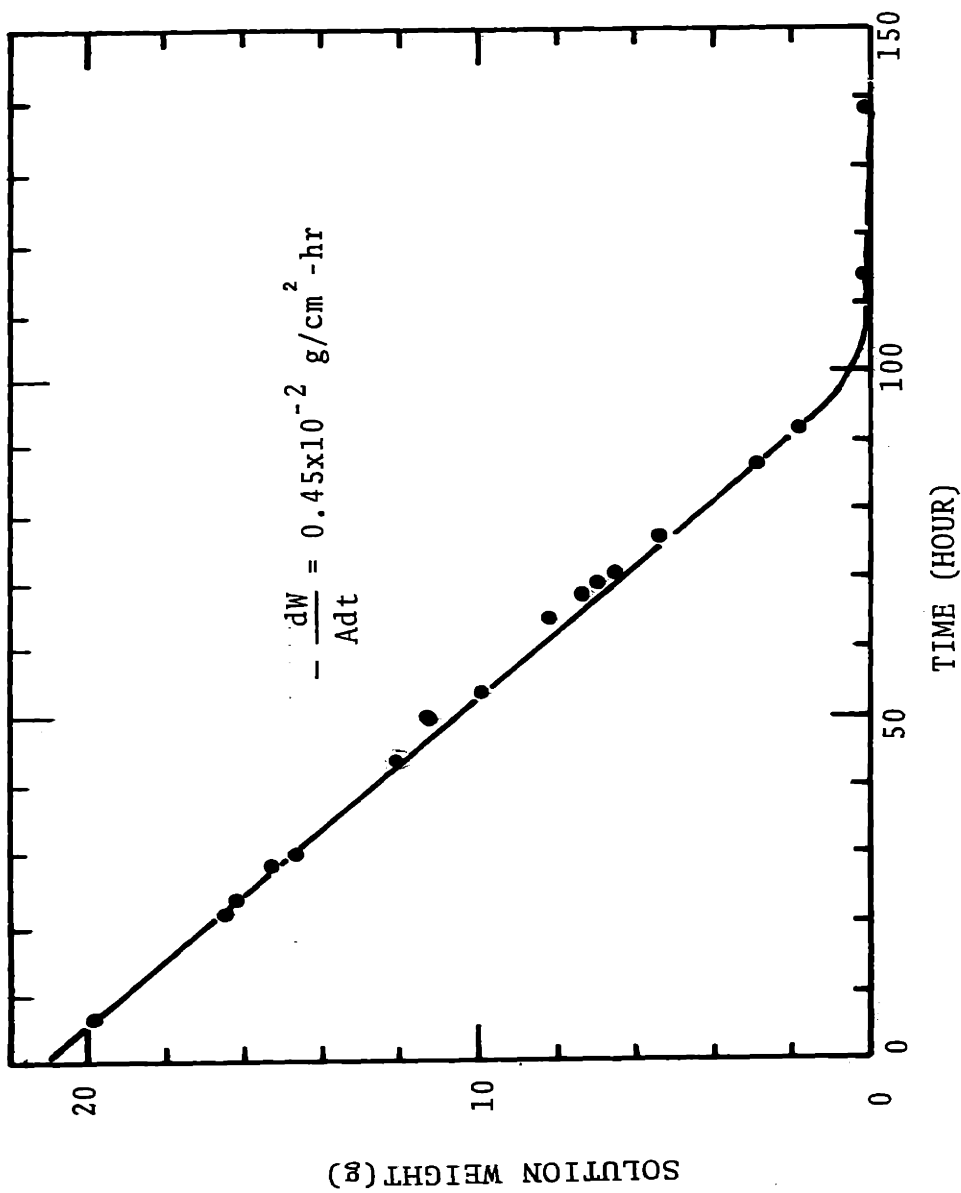


Figure II-7 Rate of dehydration of the collagen solution under natural convection

Step 4; The temperature of the incubator was maintained at $65^{\circ} \pm 1^{\circ}$ C. and air circulation was provided inside the incubator by a fan in order to eliminate temperature gradients. The casting dish was covered with perforated aluminum foil to reduce the higher temperature and air blowing.

Step 5; Same as the step 5 in the preparation of the cold-cast gelatin film.

2.3 Discussion

A. Rate of Evaporation

Collagen and cold-cast gelatin films were cast under two different conditions as mentioned earlier in the procedure. When forced convection was used (step 3-a), the initial rate of evaporation $-dw/A \cdot dt$ (w is the weight of the solution, A is the area of the casting surface, and t is the time) was constant at a value of 1.61×10^{-2} g/cm²-hr as shown in Figure II-6. When casting was done by use of natural convection (step 3-b), the evaporation rate was 0.45×10^{-2} g/cm²-hr, which is about one-fourth of the rate observed when forced convection was used (Figure II-7). The initial rate of evaporation remained unchanged until the concentration increased to about 20%-wt. (Figure II-9); thereafter, the rate decreased rapidly from 1.61×10^{-2} to 7.2×10^{-5} g/cm²-hr as the collagen concentration

increased approximately from 20% to 75%-wt. This transition occurred in relatively short time (less than one hour) compared with the entire casting period of about three days (Figure II-8). It appears to be, therefore, at approximately 20%-wt. collagen, the surface skin forms, which has a much slower diffusivity. At 80%-wt., the rate is almost zero because the film is in equilibrium with ambient moisture. In most of this work, 5-10 μ thick films were cast from approximately 0.5%-wt. collagen solution within three to four days.

B. Changes in Viscoelastic Behavior of Collagen During the Casting

By incorporating increasing amount of diluent to a glassy polymer, it has been shown that one can shift a plasticized polymer to any of the well known five regions of viscoelastic behavior at constant temperature. (49) If we consider the solution casting operation as a reverse process to the addition of diluent to polymer, it is apparent that collagen should exhibit variable viscoelastic behavior during the casting.

The original viscous solution subjected to the casting operation contained about 0.5%-wt. collagen. As the evaporation went on, the concentration of collagen increased and so did the viscosity. Approximately at 7-10%-wt.,

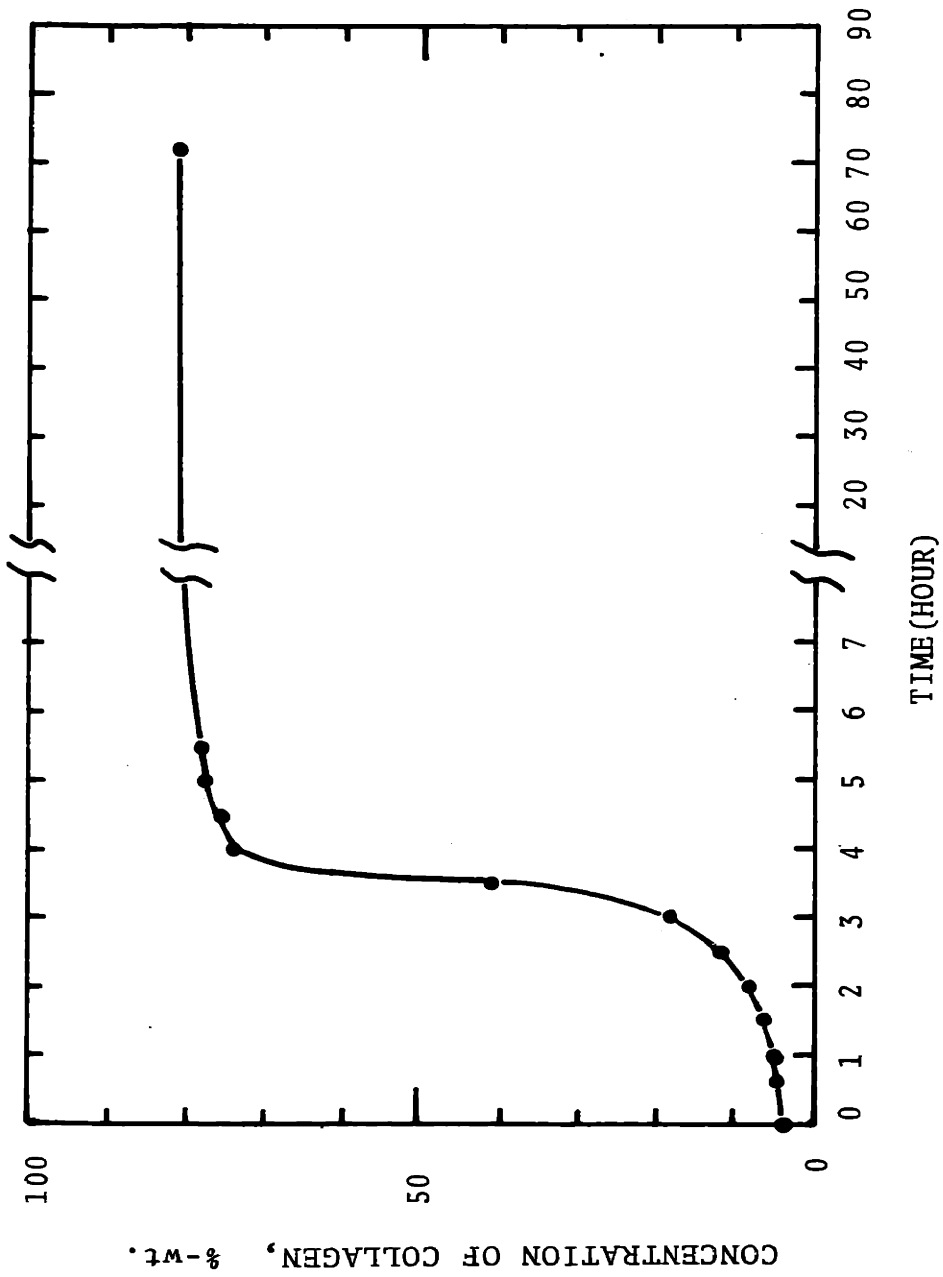
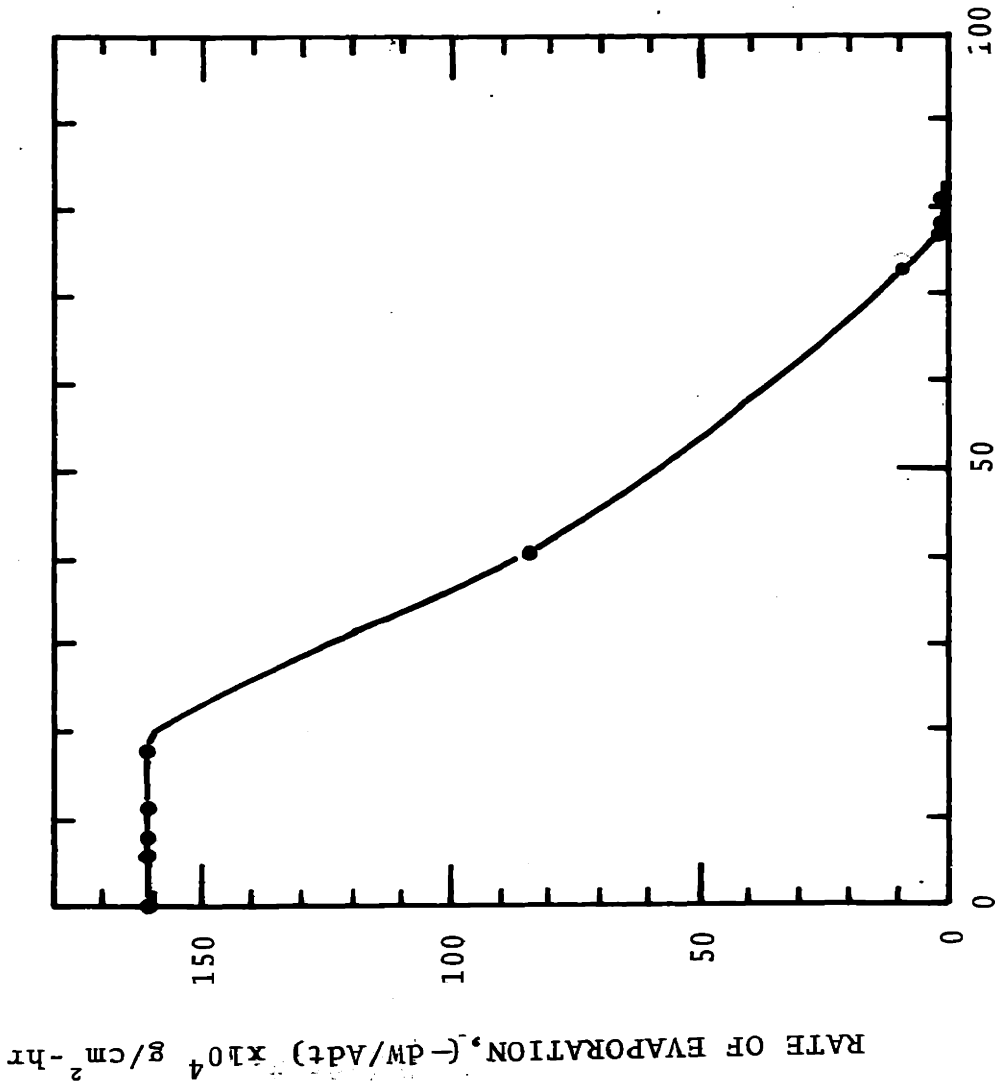


Figure II-8 Change of the concentration of collagen during casting process



CONCENTRATION OF COLLAGEN, %-wt.

Figure II-9 Rate of evaporation vs. concentration of collagen during casting process under forced convection

the solution became very viscous and at 15%-wt. became too viscous to flow, gradually setting into a gel-like state near 20%-wt. As shown in Figure II-8, the highly hydrated gel-like state transformed rapidly to a solid, tenacious film (ca. 75%-wt. collagen) and slowly underwent further dehydration to yield a dry film, which contained approximately 15%-wt. water, a moisture content which was in equilibrium with ambient conditions. Due to the small thickness ($\sim 10\mu$) of the film, the transition from rubbery to glassy state occurred much faster than could be observed conveniently in greater detail. Although the information is more qualitative than quantitative, it indicates the main features of the viscoelastic behavior of collagen film at different levels of hydration.

C. Birefringence in Collagen and Gelatin Films

As mentioned in section A. above, use of forced convection provided much higher rate of evaporation compared to the rate observed under conditions of normal convection and thereby shortened the time of casting considerably. However, films cast by forced convection often exhibited significant optical anisotropy when studied with a Cary 60 Spectropolarimeter. The absolute magnitude of birefringence was much smaller than 0.5 degree, the sensitivity limit of a polariscope which had been used to study the strain birefringence of synthetic polymers. (The highest magnit-

ude of the birefringence, in terms of angle of rotation of the plane of polarization was less than 0.2 degrees in the most anisotropic specimen which is shown in Figure II-10.) For the study of optical activity, however, even a small amount of birefringence became a serious problem because the actual rotation angle due to optical activity alone was about the same order of magnitude (0.2° - 0.3° as shown in Figure II-11 where actual rotation angle is converted to the specific rotation values. Notice that the average rotation angle is in same order as birefringence) which has been shown in Figure II-10. Considering the small magnitude of the birefringence present in collagen films cast by the forced convection method, this anisotropy is believed to be due to partial orientation of the collagen molecules attained during casting as a result of unidirectional mechanical force exerted constantly by blowing air on the surface of the solution. In fact, the effect of forced convection on the optical anisotropy of collagen films is clearly shown in Figure II-10, where two films prepared under different conditions are compared. The film which was cast by forced convection (open circles) showed highly variable optical rotation when it was rotated around the axis of light propagation. The film cast under conditions of normal convection (solid circles) showed fairly uniform values of the optical rotation indicative of the absence of any orientation in the film. Films suitable for

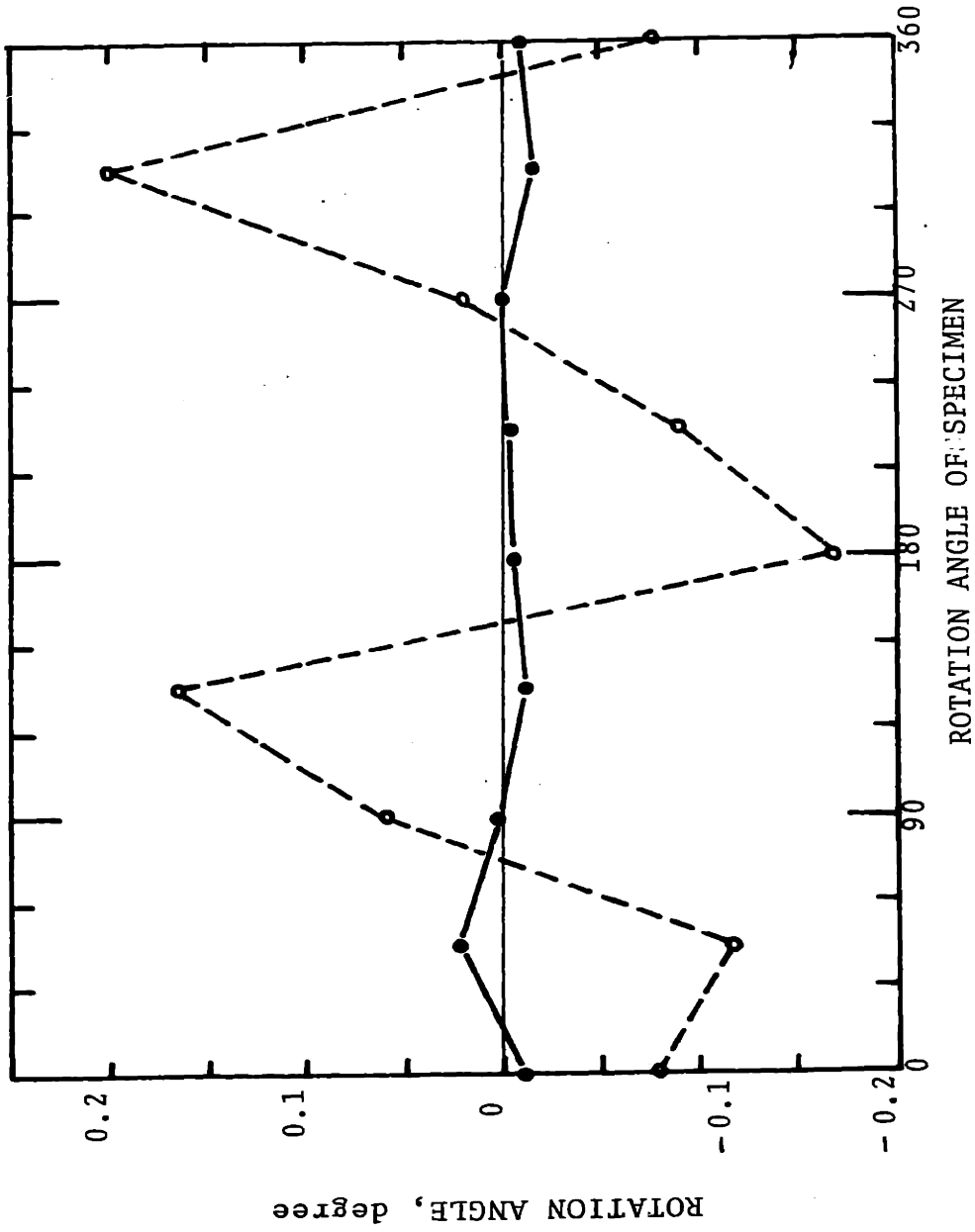


Figure II-10 Birefringence of the collagen films cast under the conditions of natural and forced convection (○ ; cast under forced convection, ● ; cast under natural convection)

APPARENT SPECIFIC ROTATION, $[\alpha]_{365}$, degree/g-cm²

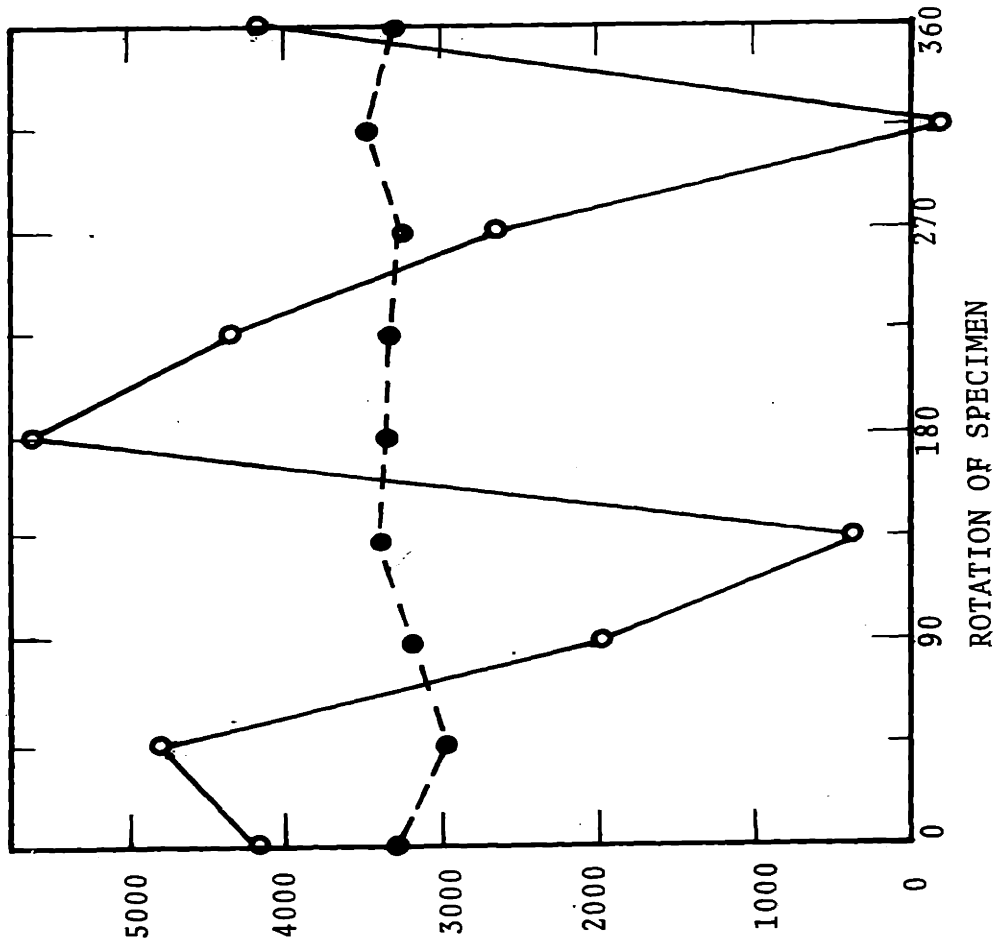


Figure II-11 Variation of the apparent specific rotation of the collagen films cast under different conditions (optical rotation was measured with a film rotating around by 45°)

the study of optical activity were, therefore, cast under conditions of natural convection, whereas those for other studies were prepared by forced air convection (step 3-a). (Optical activity and features of tropocollagen during the casting are presented in Chapter IV.)

II-3 Moisture Assay Methods for Collagen and Gelatin

3.1 Introduction

Due to the importance of moisture content as a parameter in characterizing and monitoring the collagen and the gelatin in the solid state, an attempt was made to establish a standard technique of moisture determination. Considering the complicated nature of interactions between water and non-aqueous constituents, even a clear definition of moisture content is difficult to state. Conceptually, water content could be defined as the relative number of all H₂O molecular units present in which the two hydrogen nuclei and the oxygen nucleus have the same internuclear distances and bond angles as in the water molecule. Practically, however, water content must be defined operationally in terms of the experimental technique; and the results obtained by any one technique may not necessarily coincide with water content according to definition.

Several physical and chemical procedures (40-42) are available for the quantitative assay of water; however, at

present no satisfactory absolute method exists for moisture assay in biopolymers. In general, the choice of techniques best suited to a particular problem depends on several factors, including sensitivity, precision, accuracy required, facilities available, the nature of materials to be analyzed and the level of moisture content. Absolute methods now available are based on the principle of complete removal of water from the sample by vaporization, by extraction, by chemical reaction or by any combination of these processes. NMR (40, 41) and IR (42) techniques are also available which do not require the removal of water and the dichromate oxidation method (43) is also available for organic samples. NMR method, however, can not provide a sensitive assay below 5%-wt. moisture level (40,41). IR method (42) is also not sensitive compared to other methods because the water band at 3450 cm^{-1} arising from free water is too close to the strong NH-band at 3300 cm^{-1} and appears as a small shoulder band, the resolution of which is very difficult. The bound water gives the same absorption band as NH-stretching, 3300 cm^{-1} and quantitative resolution is also very difficult.

In this work, the vacuum drying method and the Fischer volumetric titration method were extensively tested and results from them were cross-compared. The first of these is a physical method while the second involves the water in the specimen in a chemical reaction. Details in procedure

as well as a comparison of these two methods are discussed in the following sections.

3.2 Vacuum Drying Method

A. Introduction

The principle of this method is removal of water from the sample by vaporization. In applying the vacuum drying method, it is assumed that removal of water is complete and effects of any chemical side reactions occurring during the process are negligible. Complete removal of water is not attainable because there always exists an equilibrium moisture content of the system which depends on temperature and pressure. The equilibrium moisture in most cases, however, is very small under conditions of high vacuum at an elevated temperature. For practical purposes, it therefore is quite acceptable to assume that the constancy of weight of sample undergoing dehydration is an indication of a state of complete dehydration.

The rate of approach to equilibrium moisture content is, in general, very slow due to the characteristic slow diffusion coefficient of water in most dehydrated substances. (44, 45, 46) To accelerate the rate of removal of water, methods are used to either decrease the diffusion path length (44, 45) by reducing the particle size of the powdered sample or increase the diffusion coefficient by

raising the temperature. (46)

B. Experimental

Standard conditions for vacuum-drying were set at $105 \pm 1^{\circ}$ C. and a vacuum of 3×10^{-4} mmHg, using a vacuum oven (National Appliance Co., Portland, Oregon, Model 5830-4). The procedures involved the following steps.

(i) Samples of collagen or gelatin of various levels of hydration were taken in a weighing bottle and weighed using an analytical balance. The original sample weight (W) was obtained from the difference between the weight of the bottle with and without sample.

(ii) Depending on the hydration level, different dehydration steps were used to dry the specimen before subjecting it to final vacuum-drying.

(a) Specimen, containing more than 65%-wt. water (swollen gel) was dried first by forced convection at 23° C. The dried specimen normally contained about 15-20% moisture, which is in equilibrium with ambient condition. This step is exactly the same as the casting procedure described in a previous section.

(b) A dry sample or the sample treated as above (a) was transferred into a weighing bottle and dehydrated further to about 4-5%-wt. moisture under vacuum at

23° C. for about five hours (see Figure II-12).

(iii) The final step of vacuum-drying was carried out in a vacuum oven until the weight of the specimen reached a consistent value.

(iv) The completely dehydrated sample was taken out from the oven together with the weighing bottle and was weighed immediately to obtain the anhydrous sample weight (W_0).

(v) The moisture content of the sample was computed from the ration $(W-W_0)/W \times 100 = \% \text{-wt. moisture}$.

When the dehydration was completed the vacuum was broken by introducing air that had been dessicated through a series of drying tubes containing NaOH, CaCl_2 , Silica gel and P_2O_5 . The time required for complete dehydration was found to depend on the size of the samples. For example, the moisture in dry gelatin granules (diameters ranging from 0.40-0.65 mm) was reduced from about 0.5%-wt. to 0.3%-wt. in one hour and down to 0.1%-wt. in two days and the constant weight was attained in five days (Figure II-13). Gelatin and collagen films having thickness less than 15μ reached constant weight in three days (Figure II-14).

When exposed to the atmosphere, an anhydrous specimen quickly regained moisture and a correction for moisture regain during weighing was necessary. Each weighing was

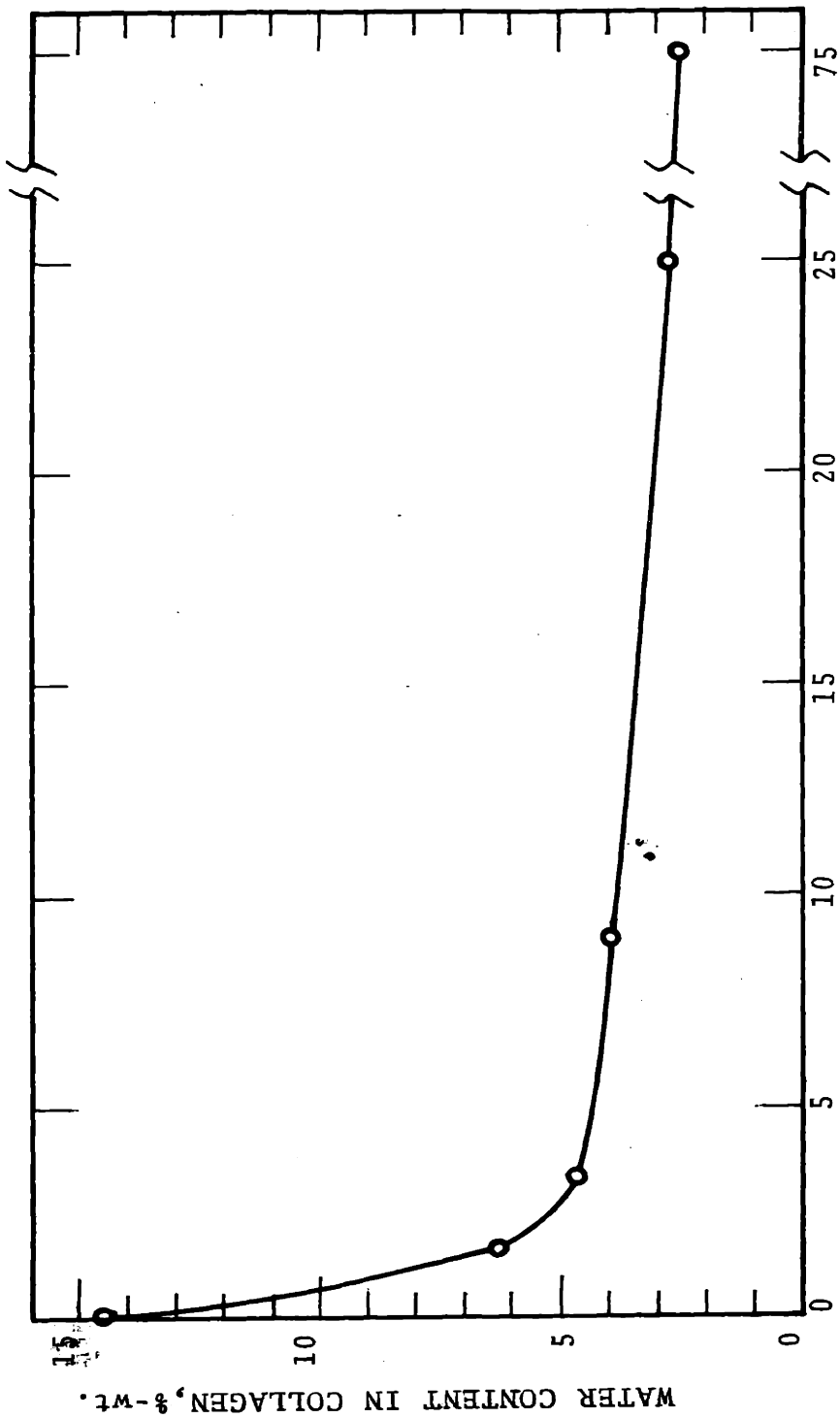


Figure II-12 Rate of dehydration of collagen film (5.6 μ thick) under vacuum
 (3×10^{-4} mmHg) at 23°C

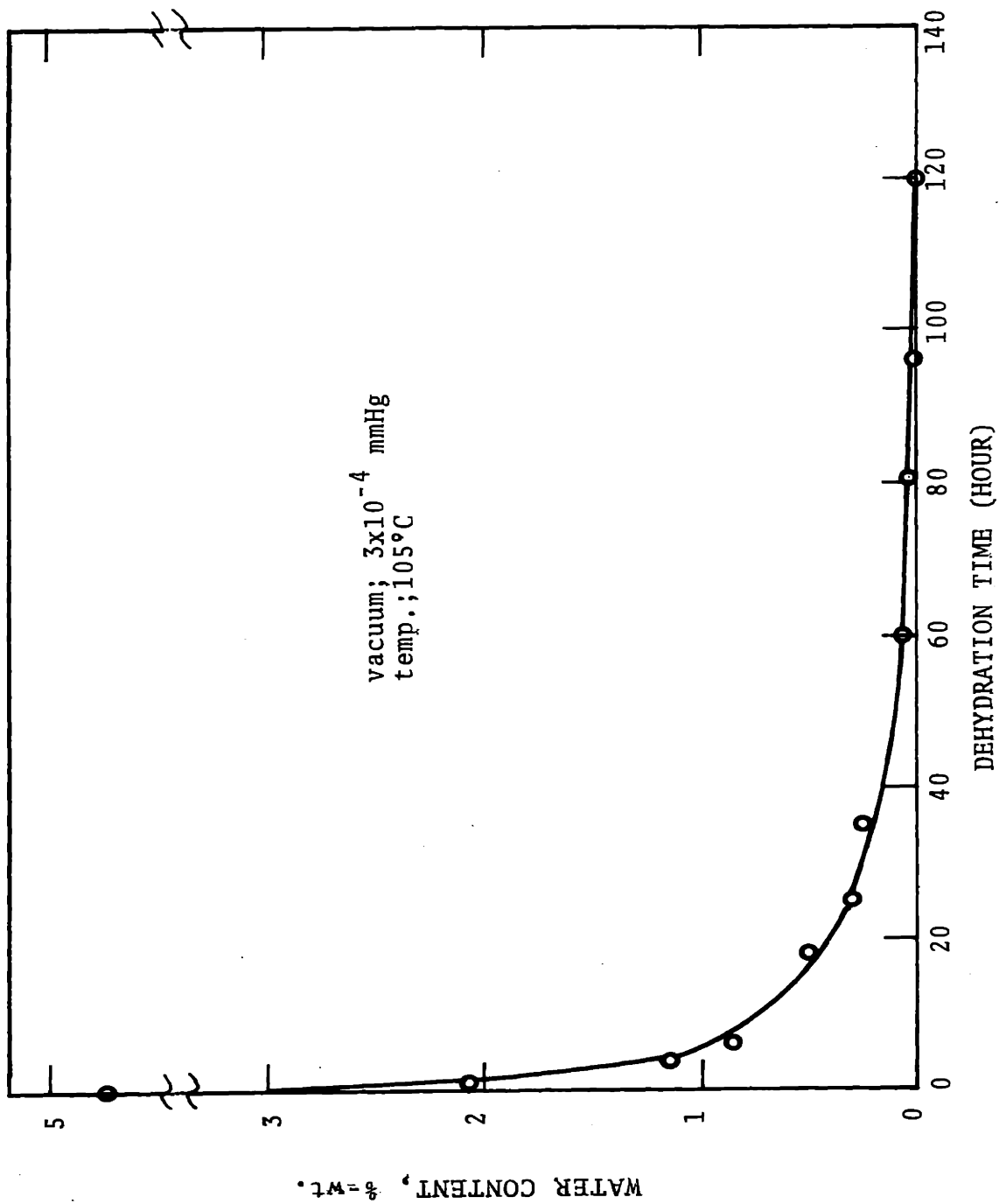


Figure II-13 Rate of dehydration of gelatin granules (0.4-0.65 mm in diameter)

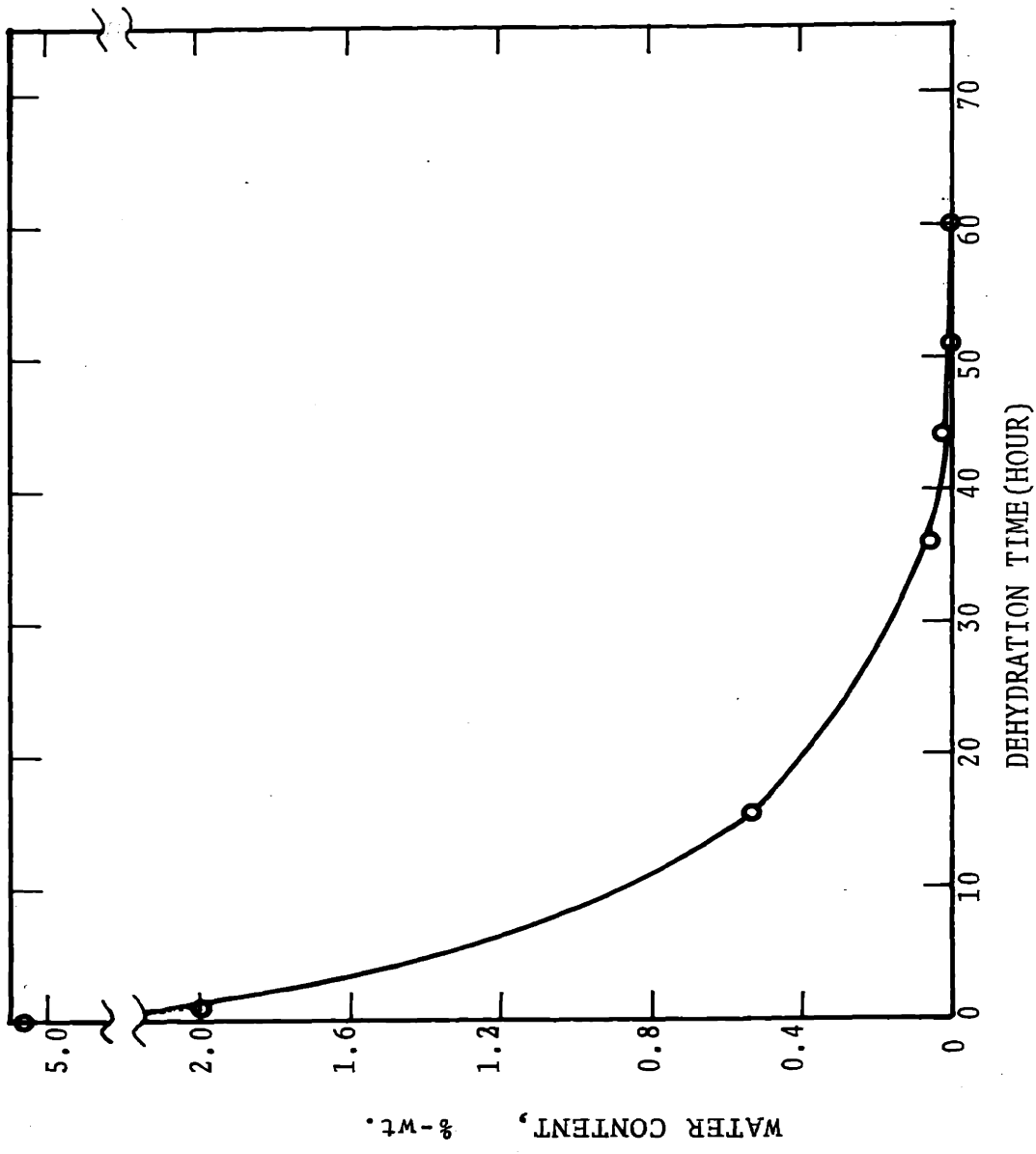


Figure II-14 Rate of dehydration of collagen film (3.8 μ thick) under vacuum (3×10^{-4} mmHg) at 105°C

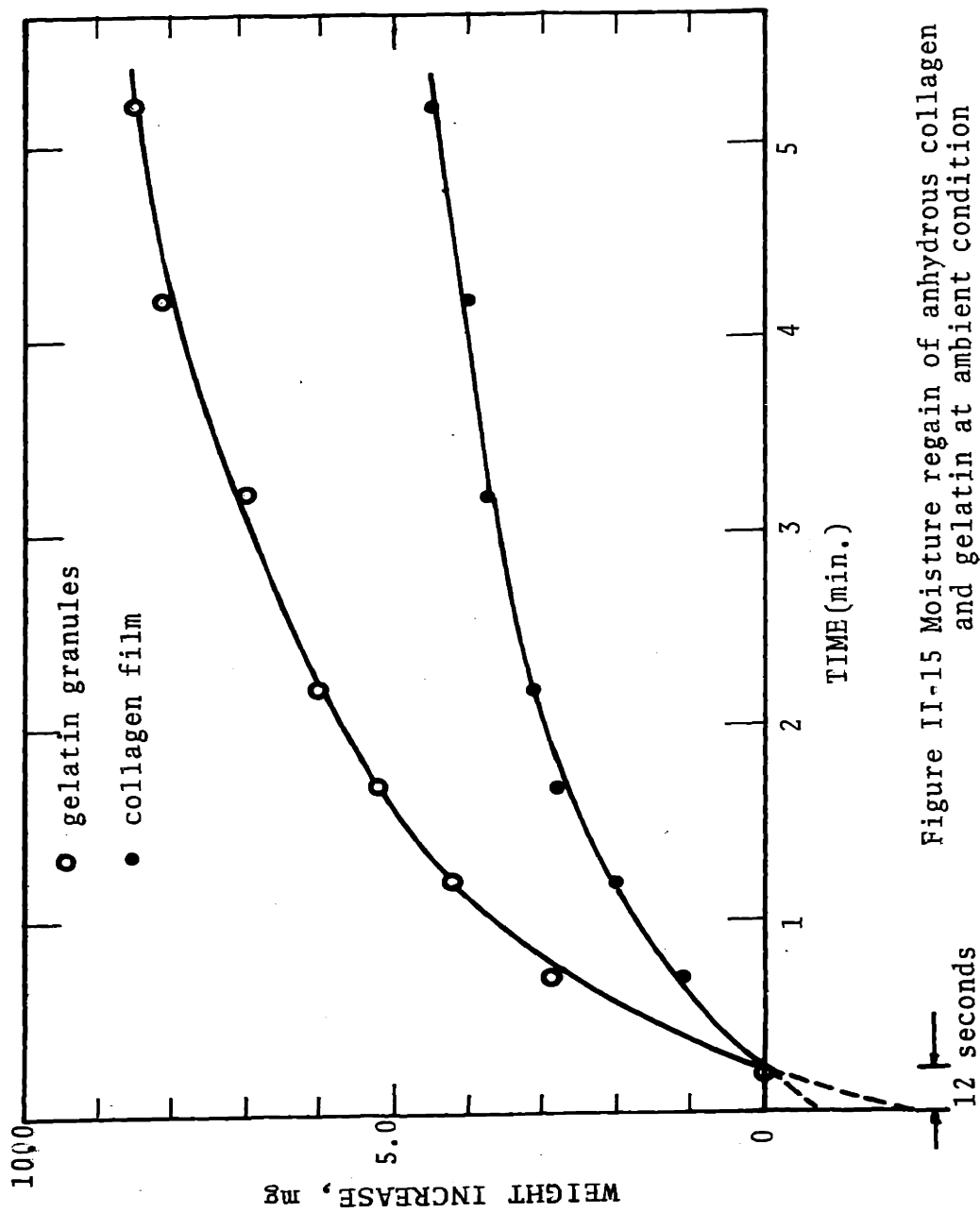


Figure II-15 Moisture regain of anhydrous collagen and gelatin at ambient condition

lasted approximately 12 seconds counted from the time that the specimen was taken out of the oven to the time the weight was read on the balance and corrections were made by extrapolating the weight to zero time (the time when the sample was taken out of the oven) using the moisture regain curves (Figure II-15).

As expected, it was found that the level of moisture regain during weighing depends on the surface area of the specimen exposed directly to the atmosphere rather than on the weight of the specimen. Corrections were, therefore, individually applied to each sample.

C. Results

Collagen and gelatin of different degrees of hydration were tested for their moisture content using the vacuum-drying method. The results of such determinations are shown in Figure II-16 and compared with results obtained by the Fischer volumetric method on samples with identical water content.

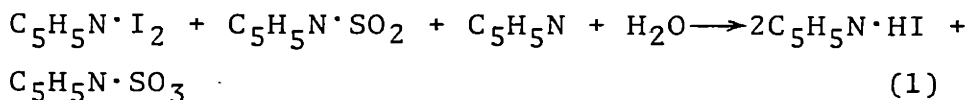
3.3 Fischer Volumetric Titration Method

A. Introduction

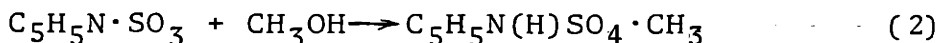
Among the several physical and chemical procedures available for determining water, the most widely applicable chemical method is that based on the Karl Fischer reagent

(KFR). The high sensitivity of the KFR and the rapidity with which analysis can be performed are the main advantages of this method. The basic principle, the method of titration and the applicability have been the subject of numerous publications including those by Mitchell (47) and Smith (48). It is, therefore, considered unnecessary to discuss these topics here in anything but a brief introductory manner.

In this method, the moisture in the samples is made available for volumetric measurement by extraction with a suitable anhydrous solvent. The solvent together with the extracted moisture is, then, titrated with Fischer reagent which reacts exclusively with moisture stoichiometrically. The Fischer reagent is composed of iodine, sulfur dioxide, pyridine and methanol and titration involves the two-step reactions:



and



The reaction (1) is accompanied by color change from canary yellow to chromate yellow to the brown of unused iodine. The titration end-point can be detected either visually or electrometrically. The electrometric method is known to be more sensitive but also more time-consuming and therefore subject to greater error due to contamination of the spec-

imen by environmental moisture. The visual method requires simple apparatus and was found to yield good results.

B. Experimental

In this work, the visual method for end-point detection was employed in the titration. The apparatus consisted of a Machlett automatic buret (2 liter), magnetic stirrer, drying tubes and Erlenmeyer flasks (125 ml). The entire apparatus was efficiently air-tightened against the atmosphere by use of drying tubes containing silica gel.

(i) Standardization of Fischer Reagent

The exactly known amount (ca. 30 ml) of anhydrous methanol (Merck Co.) was transferred into a well dried, 125 ml Erlenmeyer Flask. About 0.2 mg of Sodium Tartrate Dihydrate (Fischer Sci.) was weighed accurately and transferred into the flask containing the methanol. The flask was then placed on the magnetic stirring apparatus and fitted with a rubber stopper at the tip of an automatic buret containing the Fischer reagent. After about 10 minutes stirring, the sodium tartrate was completely dissolved and titration was commenced by adding the Fischer reagent slowly. During the entire titration period, the sample flask was kept airtight. The end point was determined by the color change from yellow to brown which persisted for more

than 30 seconds. In exactly the same manner, a blank test was made for anhydrous methanol. The titer "F" of Fischer reagent was calculated as follows:

$$F = \frac{0.1566 \times W}{A - B} \times 1000 \text{ mg water/ml reagent}$$

where 0.1566 is weight fraction of water in sodium tartrate dihydrate and W is weight of sodium tartrate. A and B are the amount (ml) of Fischer reagent consumed in titrating methanol-sodium tartrate and methanol alone, respectively.

The average value for the titer "F" of the Fischer reagent used in this work was about 5.3 - 5.0 mg H₂O/ml FR. Because of the inherent instability of the Fischer reagent, the titer "F" was measured on each day whenever the test was made. Table II-3 shows the change of titer values during storage; this represents the typical decay in activity of Fischer reagent used in this study. Conditions for storage of the Fischer reagent included protection from direct light and the moisture.

TABLE II-3

Change of the Activity of Fischer Reagent During Storage

<u>Storage Time (Days)</u>	<u>Titer "F" mgH₂O/ml reagent</u>
0	5.39
8	5.30
28	5.16
75	5.00

(ii) Determination of Moisture in Sample

The overall procedure of determining moisture in gelatin and collagen is the same as the procedure used in standardization of Fischer reagent except for the moisture extraction step. The rate of extraction of moisture from the solid samples depends primarily on the type of solvent used, the size of sample (particle size or thickness of films, etc.), and the temperature. All the extraction procedures in this work were done at room temperature (23° C.) with occasional stirring. Five different solvents were tested for their efficiency in extraction. Extraction was faster with methanol and pyridine (one day), moderately fast with dimethyl formamide (three days) and much slower with acetone and acetic acid (never reached the end point in five days). No appreciable differences were found in extraction rate between methanol and pyridine. Methanol, however, was chosen over pyridine as the standard extraction medium for gelatin and collagen based on its lower toxicity and cost. Complete extraction of moisture from films of thickness less than 25 required less than one day whereas two days were needed for the gelatin granules of sizes 0.4-0.65 mm at room temperature. The degree of completeness of the extraction process was tested by determining the moisture content of identical specimens which had been extracted in the solvent for different periods of time up to five days. In general, throughout the entire

experiment, extreme care was taken in dealing with samples so that moisture absorption from the atmosphere was avoided as much as possible and all the glassware and titration apparatus was dried completely and kept free of moisture.

C. Result and Discussion

Specimens with identical moisture content were used to compare results obtained by the two methods. The comparative results are shown in Table II-4 and illustrated in Figure II-16, obtained with gelatin and collagen. In Figure II-16, the solid line represents the relation expected on the assumption of complete agreement. There is no tendency for systematic deviation from the line of complete agreement in the range of 0.3%-wt. to 10%-wt. moisture. This leads to the conclusion that the vacuum drying method and the Fischer volumetric method give results which closely agree with either collagen or gelatin specimens.

With the vacuum drying method, five days were required to obtain a result compared to only two days using the Fischer volumetric method. However, the labor necessary to obtain a result by the Fischer Volumetric method was about three times more than the time required in vacuum drying method which was a much simpler procedure.

Systematic errors are estimated at $\pm 6\%$ for the vacuum drying method and $\pm 5\%$ for the Fischer titration method. These errors are at a level of 1%-wt. moisture

TABLE II-4 MOISTURE CONTENT OF GELATIN AND COLLAGEN BY
DIFFERENT METHODS

<u>Sample No.</u>	<u>Vacuum-Drying</u>	<u>Fischer volumetric</u>
1	1.80	2.08
2	0.76	0.56
3	0.81	0.74
4	0.92	0.90
5	1.09	1.01
6	0.81	0.81
7	0.61	0.58
8	0.89	0.93
9	0.60	0.40
10	0.64	0.71
11	0.73	0.67
12	0.75	0.79
13	0.28	0.31
14	0.38	0.27
15	0.31	0.32
16	0.93	0.71
17	0.80	0.71
18	2.86	2.79
19	10.85	10.68
20	0.53	0.56
21	10.20	9.80

(Samples No. 1-19: gelatin granules

20,21: collagen films

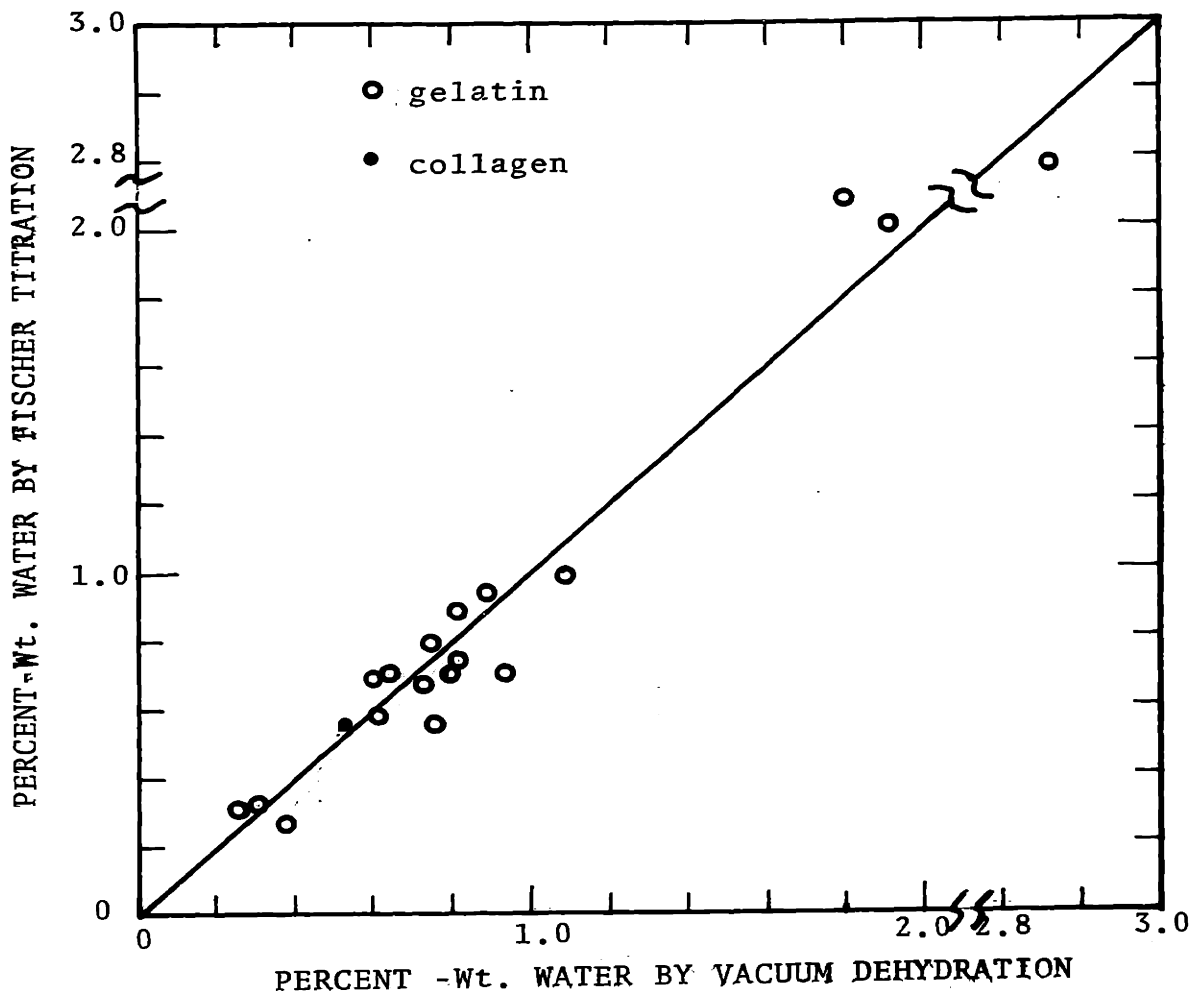


Figure II-16 Comparisons between the moisture contents of collagen and gelatin determined by vacuum drying method and Fischer titration method

with a one-gram sample, based on the uncertainties in balance sensitivity, corrections for moisture regain and in detecting the end point of Fischer titration. Variability in moisture content among samples of supposedly identical moisture content was as much as 10% at a level of 1%-wt. moisture higher than the estimated errors. Such variability accounts for the observed deviation of points in Figure II-16 from the line which indicates complete agreement between the two methods. When the sample has non-aqueous volatile components, vacuum drying method is not acceptable and Fischer volumetric titration has an advantage. In gelatin and collagen, however, no problem with non-aqueous volatile components was encountered. The Fischer volumetric titration provides, therefore, no particular advantage compared to the vacuum drying method which is considerably simpler in operation and, therefore, vacuum drying method was the moisture determination method most often used in this work.

REFERENCES FOR CHAPTER I and II

1. Gross, J. (1958) *J. Exp. Med.*, 107, 265
2. Piez, K.A. (1967) Treatise on Collagen Vol. 1. Ed. by Ramachandran, G.N., p 208
3. Gross, J., Highberger, J.H., and Schmitt, F.O. (1955) *Proc. Natl. Acad. Sci., U.S.A.*, 41, 1
4. Jackson, D.S., and Fessler, J.H. (1955) *Nature, London* 176, 69
5. Harkness, R.D., Mark, A.M., Muir, H.H., and Neuberger, A. (1954) *Biochem. J.* 56, 558
6. Highberger, J.H., Gross, J. and Schmitt, F.O. (1951) *Proc. Natl. Acad. Sci. U.S.A.*, 39, 286
7. Gross, J. (1958) *J. Exp. Med.* 107, 247
8. Jackson, D.S. and Bentley, J.P. (1960) *J. Biophys. Biochem. Cytol.* 7, 37
9. Gallop, P.M. (1944) *Archs. Biochem. Biophys.* 54, 486
10. Piez, K.A., Lewis, M.S., Martin, G.R. and Gross, J. (1961) *Biochem. Biophys. Acta* 53, 596
11. Piez, K.A., Eigner, E.A. and Lewis, M.S. (1963) *Biochemistry*, 2, 58
12. Fessler, J.H. (1960) *Biochem. J.* 76, 452
13. Steven, F.S. (1964) *Ann. Rheum. Dis.* 23, 300
14. Jackson, D.S. (1953) *Biochem. J.* 54, 638
15. Drake, M.P., Davison, P.F., Bump, S. and Schmitt, F.O. (1966) *Biochemistry*, 5, 301
16. Dumitru, E.T. and Garrett, R.R. (1957) *Arch. Biochem. Biophys.* 66, 245
17. Grant, R.A. (1964) *J. Clinic. Pathol.*, 17, 685
18. Nimni, M.E. (1968) *J. Biol. Chem.*, 243, 1457
19. Treatise on Collagen Vol. 1, Ed. by Ramachandran, G.N. Academic Press (1967)
20. Davison, P.F. and Drake, M.P. (1966) *Biochem.* 5, 313

21. Harrington, W.R. and von Hippel, P.H. (1961) Adv. Protein Chem. 16, 1
22. Burge, R.E. and Hynes, R.D. (1959) Nature, 184, 1562
23. Kauzmann, W. (1959) Adv. Protein Chem. 14, 1
24. Huang, Chor (1971) M.S. Thesis M.I.T
25. Boedtke, H. and Doty, P. (1956) J. Am. Chem. Soc. 78, 4267
26. Gallop, P.M., Seifter, S. and Meilman, E. (1957) J. Biophys. Biochem. Cytol. 3, 545
27. Noda, H. (1955) Biochim. et Biophys. Acta 17, 92
28. Orekhovich, V.N. and Shpikiter, V.O. (1955) Biokhimiya 20, 438
29. Burge, R.E. and Hynes, R.D. (1959) J. Mol. Biol. 1, 155
30. Doty, P. and Nishihara, T. (1958) In Recent Advances in Gelatin and Glue Research Ed. by Stainsby, G. Pergammon Press, London
31. Rice, R.V. (1960) Proc. Natl. Acad. Sci. U.S. 46, 1187
32. Cohen, C. (1955) J. Biophys. Biochem. Cytol. 1, 203
33. Harrington, W.F. (1958) Nature, 181, 997
34. Young, E.G. and Lorimer, J.W. (1960) Arch. Biochem. Biophys. 88, 373
35. Lewis, M.S. and Piez, K. (1961) Federation Proc. 20, 308
36. Schmitt, F.O., Gross, J. and Highberger, J. (1955) Symp. Soc. Exptl. Biol., 9, 148
37. Gliozzi, A., Marchio, R. and Ciferri, A. (19) In Chemistry and Molecular Biology of the Intercellular Matrix Ed. by Balazs, E.A. Vol. 1. 313
38. Dumitru, E.T. (1961) U.S. Patent 3, 152, 203
39. Morawetz, H. (1965) Macromolecules in Solution Interscience

40. Shaw, T.M. and Elsken, R.H. (1950) J. Chem. Phys., 18, 1113
41. Elsken, R.H. and Shaw, T.M. (1955) Anal. Chem. 27, 290
42. Bradbury, E.M., Burge, R.E., Randall, J.T. and Wilkinson, G.R. (1958) Disc. Faraday Soc. 21, 173
43. Launer, H.F. and Tomimatsu, T. (1952) Food Tech. 6, 59 and 281
44. Makower, B. and Myers, S. (1943) Proc. Inst. Food Tech. pp 156
45. Makower, B., Chastain, S.M. and Nielson, E. (1946) Ind. Eng. Chem. 38, 721
46. Fish, B. (1957) Food Invest. Tech. Paper No. 5. London
47. Mitchell, J. Jr. (1951) Anal. Chem. 23, 1069
48. Mitchell, J. Jr. and Smith, D.M. (1948) "Aquametry" Interscience
49. Yannas, I.V. (1968) J. Poly. Sci. Part A-2, 6, 687
50. Gross, J. (1963) Biochim. Biophys. Acta 71, 250
51. Ramachandran, G.N. (1967) In Treatise on Collagen, Vol. 1, Chap. 3, Acad. Press
52. Schmitt, F.O., Gross, J. and Highberger, J.H. (1955) J. Exp. Cell Res., Supplement 3, 326
53. Gross, J., Highberger, J.H. and Schmitt, F.O. (1954) Proc. Natl. Acad. Sci. U.S., 40, 679
54. Yannas, I.V. (1972) J. Macromol. Sci.-Rev. C7, 49
55. Hodge, A.J. (1967) In Treatise on Collagen, Vol. 1, Ed. by Ramachandran, G.N., Chap. 4, Acad. Press

CHAPTER III
X-RAY DIFFRACTION AND INFRARED SPECTROSCOPY STUDIES OF
COLLAGEN AND GELATIN

III-1 X-ray diffraction Study of Collagen and Gelatin in
Solid State

1.1 Introduction

In 1951, Pauling and Corey (1) proposed α -helix as the basic structure of a group of fibrous proteins, partly basing themselves on the results of X-ray diffraction studies of single crystals of amino acids. Perutz (2), in 1953, discovered the method of isomorphous attachment of a heavy atom to the hemoglobin molecules in single crystal which produced changes in the diffracted X-ray intensities thereby enabling him to identify the peaks. Using this technique, Kendrew and his coworkers (3) first determined the three dimensional structure of the protein, myoglobin. In 1953, Watson and Crick (4, 5) proposed the double helix structure for DNA, led by the X-ray diffraction studies of it by Wilkison and his coworkers (6). The structure of viruses, such as tobacco mosaic virus, were also studied by X-ray method first by Bernal and Fankuchen (7) and later by Watson. (8) The events mentioned above are some of the numerous X-ray studies in the field of molecular biology which show how X-ray diffraction study played a key role in

obtaining current knowledge of protein structures.

The understanding of the molecular architecture of collagen triple helix was also primarily based on the study of X-ray diffraction on collagen fiber. The characteristics of collagen fiber pattern were recognized as early as the 1920's (15) and since then, based on this pattern, many attempts were made to work out a structure which would fit the X-ray pattern. However, this was not successful until the early 1950's when the Fourier transform theory of the X-ray diffraction by helix was worked out by Cochran et al. (16) and a greatly improved fiber pattern of collagen was made available by Cowan et al. (23)

In 1954, Ramachandran and Kartha (9) proposed three parallel stranded, left-handed helical chains for a structure of collagen. The same authors (1955) (10) proposed a modified structure of a three-stranded non-integral coiled-coil. The same basic three-stranded coiled-coil model for collagen was derived by Rich and Crick (11) following their study on a polyglycine II model. They proposed two possible models which they called collagen I and collagen II. The difference between them is in the sequence of hydrogen bonds between the three helices forming the coiled-coil. Cowan, McGavin and North (12) also arrived at the same two forms of three-stranded coiled-coils as for the structure of collagen based on their study on poly-L-proline. Bear (13) also proposed the same two models.

Therefore, four different groups of workers essentially have come to similar conclusions but differ only in the details of the conformation of peptide chains and their interchain hydrogen bonding. A recent review by Ramachandran (14) provides an excellent discussion of the details of collagen structure as well as of the historical development.

In the following sections, brief review of the diffraction theory by helix and the interpretation of the fiber diffraction pattern of collagen are presented followed by a discussion of the Debye-Scherrer patterns of collagen and gelatin films.

1.2 Theory of X-Ray Diffraction by Helical Array of Atoms

It is well known that the characteristic feature of the X-ray diffraction pattern of a fiber, composed of long chain molecules of helical structure, is not as simple as those patterns found in a single crystal diagram. An interpretation of this effect was not available until the Fourier transform of X-ray diffraction by a helix was worked out by Cochran et al. (16) The treatment was further extended by the analyses of Crick (17), Lang (18) and Ramachandran. (19)

Details in analysis can be found in those original papers and therefore, it is intended to give here only those important consequences of the theory. A concise and

brief review on the theory has been given by Wilson (20) and mathematical aspects of the theory are also made available in the review of Alexander (21) while Ramachandran (14) has also discussed the theory specifically in relation to collagen.

As a first step in developing the theory, Cochran et al. (16) calculated a Fourier transform of a continuous helix of negligible thickness (The helical parameters are shown in Figure III-1.) Using the cylindrical coordinates for both real (r, ϕ, z) and reciprocal (R, Ψ, Z) spaces, they obtained the following equation. The Fourier transform T at (R, Ψ, Z) in reciprocal space is

$$T(R, \Psi, Z) = T(R, \Psi, n/P) = J_n(2\pi Rr) \exp[in(\Psi + \pi/2)] \quad (1)$$

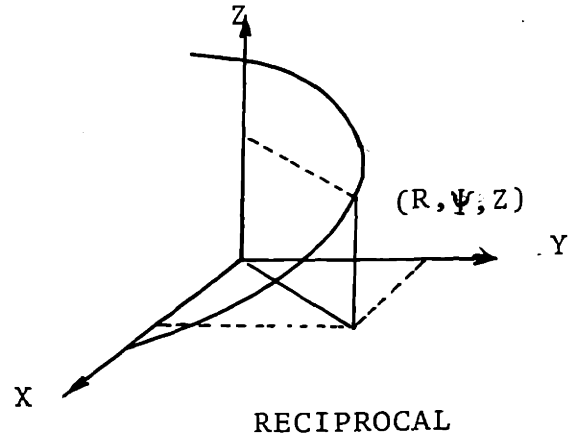
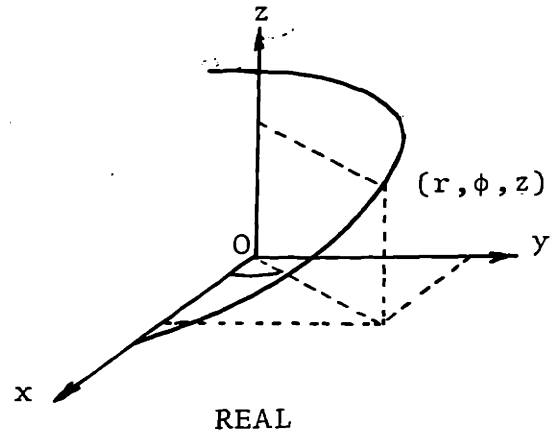
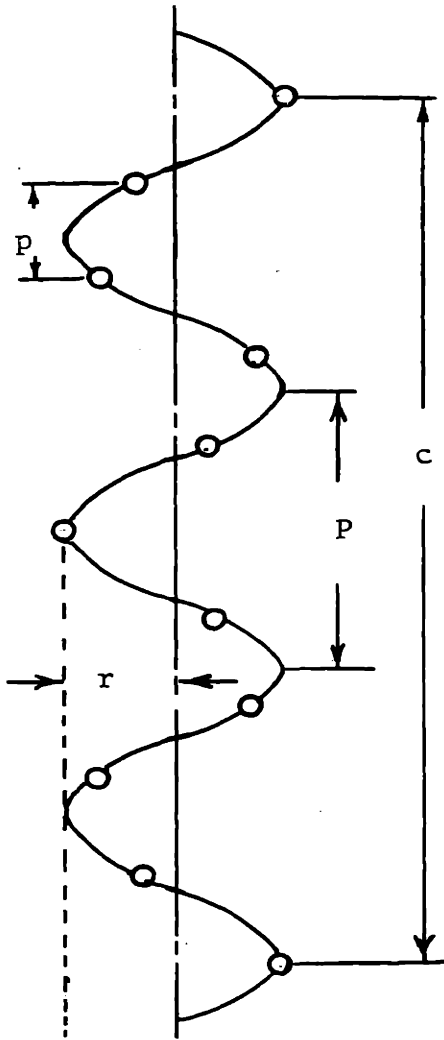
where $J_n(2\pi Rr)$ is a Bessel function of n th order. The transform was non-vanishing only at

$$Z = n/P \quad (2)$$

where n is integer and P is the pitch height of the helix. From this analysis, the following were concluded.

(i) Since P is the repeat distance along the helix, the transform is confined to layer lines at $Z = n \cdot (1/P)$ in reciprocal space.

(ii) The intensity distribution of the n th layer line or at $Z = n/P$ is proportional to $|T(R, \Psi, n/P)|^2$ and hence $|J_n(2\pi Rr)|^2$, which is independent of Ψ .



P ; PITCH OF THE HELIX
 c ; CRYSTALLOGRAPHIC IDENTITY PERIOD PARALLEL TO Z-AXIS
 P ; VERTICAL DISTANCE BETWEEN CONSECUTIVE EQUIVALENT POINTS ON THE HELIX
 r ; RADIUS OF HELIX

a) HELICAL PARAMETERS

b) CYLINDRICAL COORDINATES IN REAL AND RECIPROCAL SPACE

Figure III-1

(iii) Because of the properties of the Bessel function $J_n(x)$ (see Figure III-2), only the zero order Bessel function, $J_0(x)$ has non-zero intensity at $x = 0$. Therefore, the only meridional peak will be at the center of the diffraction pattern and no other meridional intensities will be present.

(iv) As order n increases in $J_n(x)$, the first maximum moves further away from the center (see Figure III-2) and therefore, the center of the diffraction pattern would have a cross-like appearance.

Cochran et al. (16) also advanced one step further to a real molecular model by calculating a transform of a discontinuous helix, i.e.; a set of scattering points equally spaced by a distance p along a helix (see Figure III-1). At this point, it should be mentioned that the number of points per turn, P/p may or may not be an integer and a crystallographically identical period c must be introduced as shown in Figure III-1. The number of turns of the helix per crystallographic period c would be $N = c/P$ and the number of scattering centers per period c would be $M = c/p$. Since the helix repeats itself at a distance c , the layer line spacing becomes $1/c$ in the reciprocal space and the transform is finite only at

$$Z = \ell(1/c) \tag{3}$$

where ℓ is an integer.

Mathematically, a discontinuous helix was defined by a product $K \cdot L$ where the function K is non-zero only on a continuous helix and the function L is non-zero on a set of planes spaced by a distance p along the z -axis. The Fourier transform of a discontinuous helix is, therefore, the transform of the product $K \cdot L$, which is the transform of K convoluted with the transform of L . Cochran et al. (16) showed that the result of this transform is finite only in the planes at

$$Z = n/P + m/p \quad (4)$$

where m, n are integers. From (3) and (4), the transform is non-zero only at

$$Z = \ell/c = n/P + m/p \quad (5)$$

and

$$\ell = c/P \cdot n + c/p \cdot m = N \cdot n + M \cdot m \quad (5')$$

and the transform at $Z = (\ell/c)$ (called ℓ th layer line) is:

$$T(R, \psi, \ell/c) = \sum_n T(R, \psi, n/P) = \sum_n J_n(2\pi R \cdot r) \exp[in(\psi + \pi/2)] \quad (6)$$

The summations are over all values of n which satisfy the condition (5) for all the possible values of $m = 0, \pm 1, \pm 2, \dots$

Two major differences are to be noted here between a continuous and a discontinuous helix.

(i) The fundamental layer line spacing is $1/c$ in a discontinuous helix, compared to $1/P$ in a continuous helix.

Since c is greater, in general, than P ,

$1/c < 1/P$ and so the layer line spacing is much narrower in reciprocal space.

(iii) Since only the zero order Bessel function $J_0(x)$ is finite at $x = 0$, the transform is finite at $R = 0$ only when $n = 0$. From equation (5), therefore,

$$Z = \ell/c = m/p = \pm 1/p, \pm 2/p, \dots \quad (7)$$

and there should be diffracted intensities along the meridian of the diffraction pattern ($R = 0$) at positions $Z = \pm 1/p, \pm 2/p$, etc. (Notice that in a continuous helix no meridional peak would appear as discussed previously.)

The theory of diffraction by a coiled-coil was first developed by Crick (17) and was further studied by Lang (18) and by Ramachandran (19).

Before presenting the results of the theory, it is necessary to introduce the parameters used in describing the major and the minor helices (see Figure III-3). Let c be the repeat distance of coiled-coil in the z -direction (crystallographically identical period) in which a total M units of scattering centers exist. If N_0, N_1 are the number of turns of the major and the minor helix within a repeat distance c in their own frame of reference, the number of turns of the minor helix with respect to the external frame of reference (major helix coordinate) N , is $N_1 \pm N_0$ with positive sign, if the handedness of the major and the minor helices are the same and negative, if opposite. If h, P_0 and P are the vertical heights of the distance between the scattering centers, the pitch of the maj-

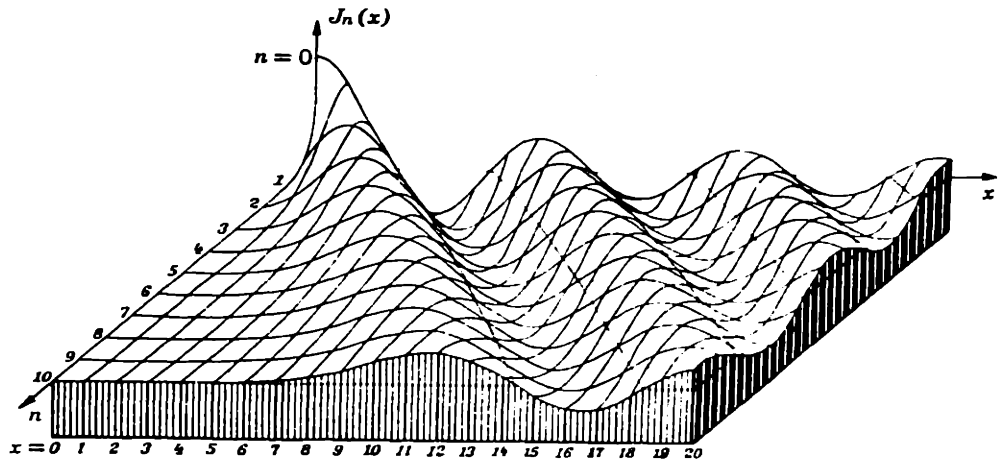


Figure III-2 The Bessel function $J_n(x)$ as functions of n and x

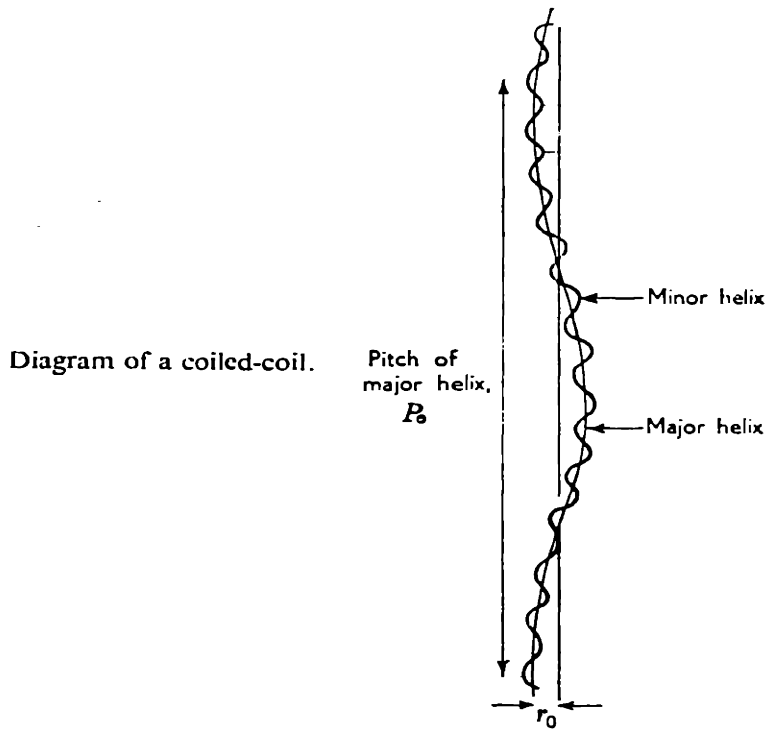


Figure III-3 Geometry of coiled-coil

or and the minor helices, respectively, than

$$c = M \cdot h = N_0 P_0 = NP \quad (8)$$

Now, the transform of the discontinuous coiled-coil, containing M units in a repeat distance c, has the following form according to Crick (17).

$$T(R, \Psi, \ell/c) = \sum_{pqsd} \sum_p J_p(2\pi R \cdot r_0) J_q(2\pi R \cdot \bar{r}_1) J_s(2\pi(\ell/c)r \cdot \sin\alpha) \\ J_d(2\pi R \Delta) \exp[i\{p(\pi/2 + \Psi - \Psi_0) + q(\pi/2 + \psi_1 - \Psi) \\ + s(\psi_1 + \pi) + d(\Psi + \psi_1 - \psi_0 + \pi/2) - m\psi_M + 2\pi Z_0 \ell/c \}] \quad (9)$$

with the condition

$$N_0 p + (N_1 - N_0)q + N_1 s + (N_1 + N_0)d - Mm = \ell \quad (10)$$

where

$$\bar{r}_1 = r_1(1 + \cos\alpha)/2$$

$$\Delta = r_1(1 - \cos\alpha)/2$$

p, q, s, d, m and ℓ are all integers

r_0 , r_1 are radii of the major and the minor helices

α is major helix angle

ψ_0 , ψ_1 are the cylindrical coordinate angles of the scattering center at $z = 0$ in the major and the minor helix coordinates respectively

ψ_M is the difference in coordinate angles between the adjacent scattering centers

Interpretation of this result seems to be much more complicated than for the single helix. However, due to the properties of the Bessel function and the magnitudes of some

parameters, the problem of interpretation becomes simplified. First, the helix angle α of the major helix is considered to be small ($< 10^\circ$) and therefore, $\cos \alpha \approx 1$ so that $\bar{r}_1 \approx r$ and $\Delta \approx 0$. In order to have a non-zero value for $J_d(2\pi R\Delta)$ in equation (9), since $\Delta \approx 0$, d must be zero. This gives a new condition (11) for equation (10).

$$N_0p + (N_1 - N_0)q + N_1s + Mm = \ell \quad (11)$$

$$\text{or } N_0p + Nq + N_1s + Mm = \ell \quad (11)'$$

Now, the meridional intensity (at $R = 0$) could be observed when $p=q=s=0$ but it could be also observed with $s \neq 0$

($J_p(2\pi \cdot \ell / c \cdot r \cdot \sin \alpha)$ does not contain R). A detailed discussion of the cases where $s=0$ and $s \neq 0$ has been given by Ramachandran (19) and Crick (22) and the major conclusions can be summarized as follows:

(i) When $s = 0$ equation (1) becomes

$$N_0p + Nq + Mm = \ell \quad (12)$$

Comparing with the corresponding equation for the simple discontinuous helix, i.e. the equation (5)' ($\ell = N_n + M_m$), equation (12) has an extra term N_0p due to the coiled-coil helix. Since N_q in equation (12) is equivalent to N_n in equation (5)' and $N_0p < N_q$, there will be more layers splitted and closely spaced between the layers given by the simple helix.

(ii) When $s \neq 0$, we have

$$N_0p + Nq + N_1s + N_m = \ell \quad (11)'$$

The function $J_s(2\pi \cdot \ell / c \cdot r \cdot \sin \alpha)$, however, does not take

appreciable values for small λ/c except when $s = 0$, and no layer line will occur at positions other than those given by equation (12) (The contribution of J_s for large value of λ/c is not important because Bessel function $J_n(x)$ has a much smaller amplitude at larger value of x , which also corresponds to the reflection far from the meridian).

In summary, the layer lines have only two types of periodicities, namely, that due to the major helix pitch ($1/P_0$) and that due to the minor helix pitch ($1/P$). The actual layer line spacings are given by equation (12) and the corresponding values for z in reciprocal space are

$$\begin{aligned} Z &= \lambda/c = N_0/c \cdot p + N/c \cdot q + M/c \cdot m \\ &= (1/P_0)p + (1/P)q + (1/h)m \end{aligned} \quad (13)$$

of these, $p=q=0$ gives the intensity on the meridian with $Z = \pm 1/h, \pm 2/h \dots$ and others are non-meridional. Those with $q = 0$ ($p, m \neq 0$) have intensities near the meridional with layer lines

$$Z = (1/P_0)p + (1/h)m \quad (14)$$

Therefore, the positions of layer lines depend only on the reciprocals of the unit heights $1/h, 1/P_0$ and $1/P$. The strongest intensity will be that of the meridional peak with $p=q=0$ and $m = \pm 1$, so that $Z = \pm 1/h$ (negative sign of Z represents the lower half of the diffraction pattern). Next prominent intensity will occur from those with $p = 0$ and $q = \pm 1$ so that $Z = \pm 1/p$ ($m = 0$) and $Z = \pm 1/p \pm 1/h$ ($m = \pm 1$).

If we consider the positive values of Z only (corres-

ponding to those intensities above the equator in diffraction pattern) three prominent layer lines will be $Z_1 = 1/h$, $Z_2 = 1/p$ and $Z_3 = 1/h - 1/p$ and $Z_1 = Z_2 + Z_3$. This gives a useful rule of thumb such that if the molecule has a helical structure, the layer line spacings for three prominent intensities d_1 , d_2 and d_3 should have a relationship $1/d_1 = 1/d_2 + 1/d_3$ among them where d_1 is the layer line spacing on the meridian and d_2 , d_3 are those of non-meridional.

1.3 The Wide Angle X-ray Diffraction Pattern of Collagen Fiber

When a fiber pattern is obtained from native tendon fibers using a flat camera, the following main features are observed as shown in Figure III-4.

- (i) A strong meridional reflection around a spacing of $3\overset{\circ}{\text{Å}}$
- (ii) Strong non-meridional reflections with spacings around $10\overset{\circ}{\text{Å}}$ and $4\overset{\circ}{\text{Å}}$
- (iii) A strong equatorial reflection which changes with moisture from about $10.4\overset{\circ}{\text{Å}}$ for dry to about $14\overset{\circ}{\text{Å}}$ for wet tendon
- (iv) A strong diffuse peak centered around a spacing of about $4.5\overset{\circ}{\text{Å}}$ on the equator

As described in the previous section, the absence of a meridional reflection between the equator and the $3\overset{\circ}{\text{Å}}$ reflection together with the relationship among the layer line

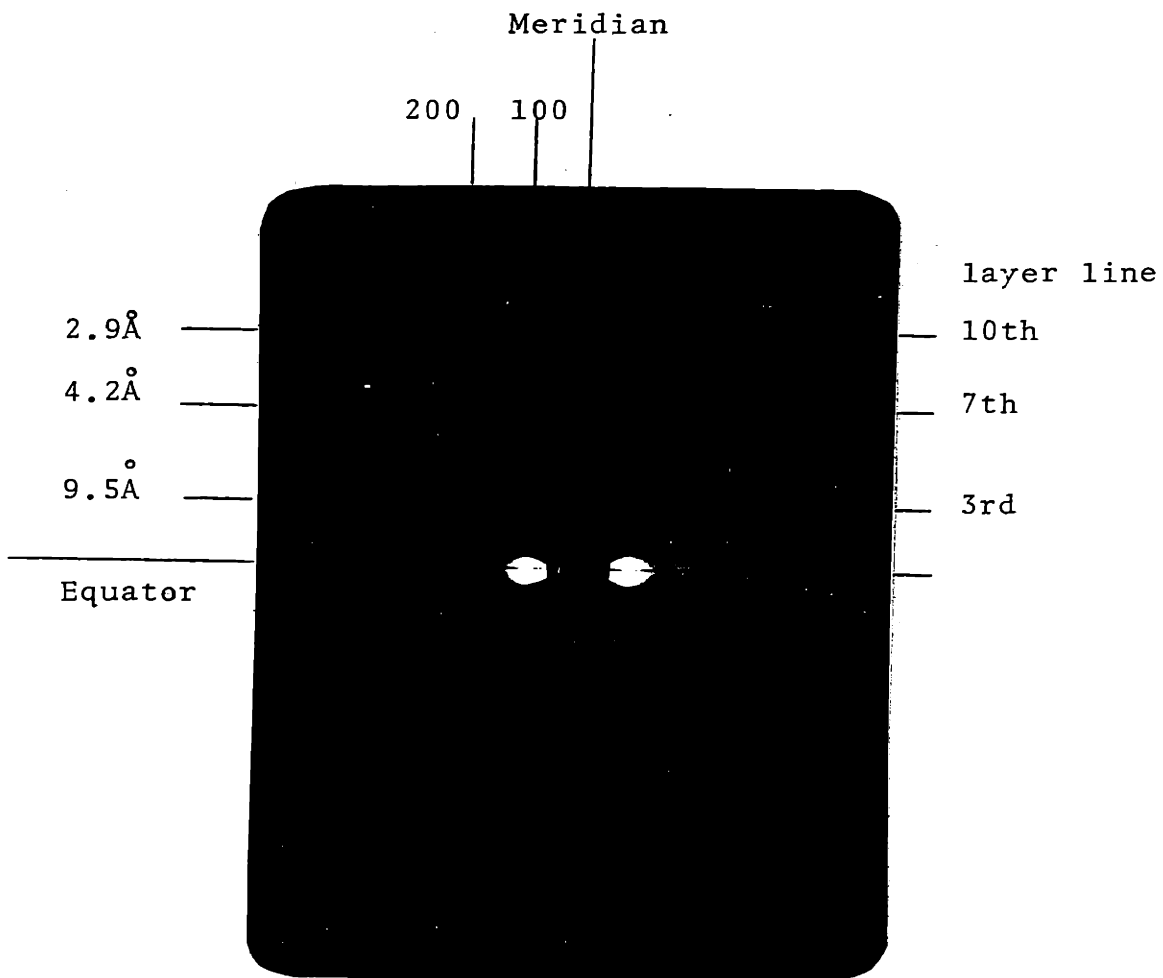


Figure III-4 Wide-angle x-ray fiber pattern of wet rat tail tendon collagen

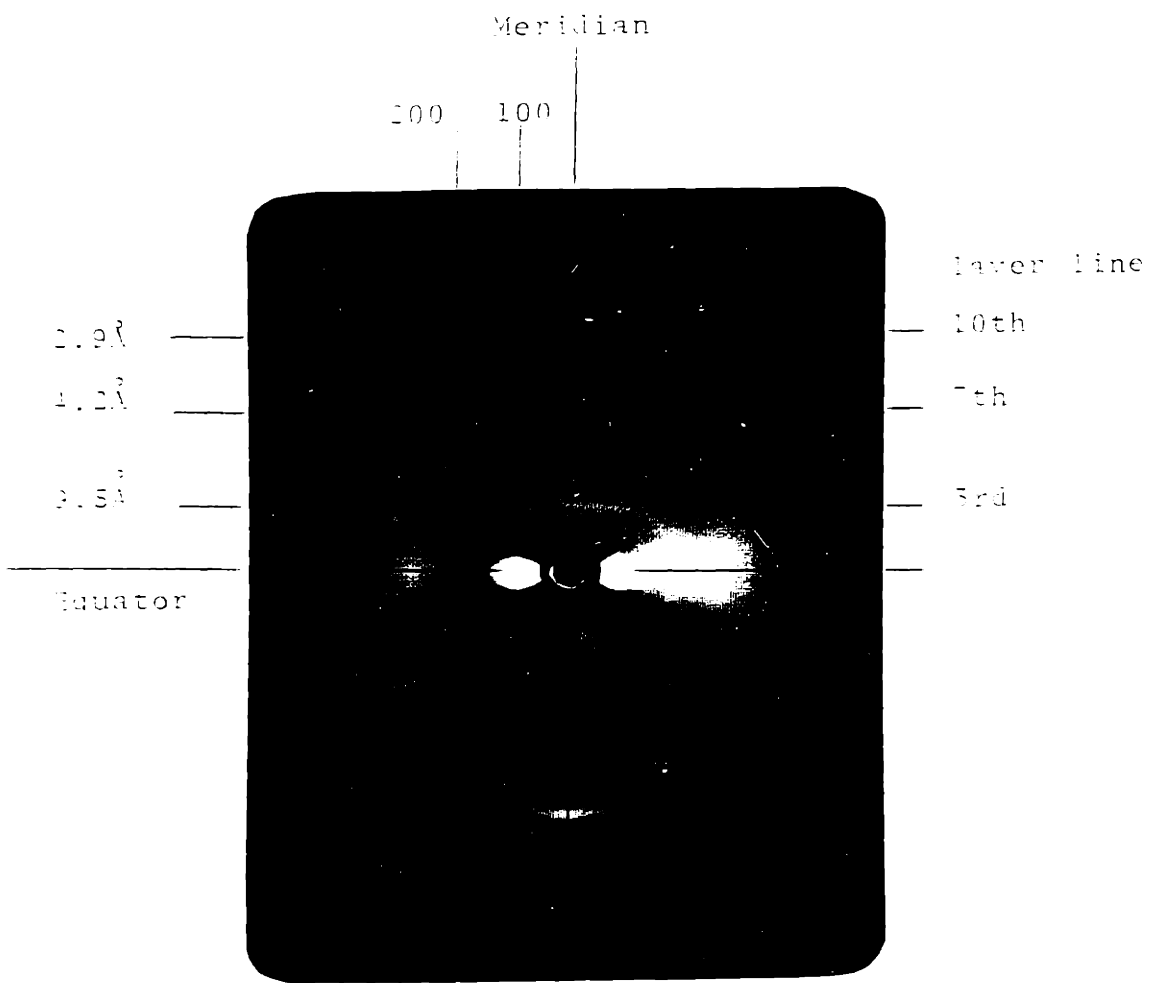


Figure III-1 Wide-angle x-ray fiber pattern of wet rat tail tendon collagen

spacings, $1/3 \cong 1/4 + 1/10$ is characteristic of the X-ray pattern of helical molecules. This led many workers to believe that the structure of collagen must be helical in nature. The theory itself, however, cannot differentiate between a single, double or triple stranded helix. Therefore, as Cowan et al. (24) described, there are three possible cases where the above reflections could be produced. (Rich and Crick (25) showed similar alternatives). They are: (i) a single chain having a pitch of $10 \overset{\circ}{\text{Å}}$ and about $3 \frac{1}{3}$ units per turn, (ii) two intertwined helices each having a pitch of $20 \overset{\circ}{\text{Å}}$ and about $6 \frac{2}{3}$ units per turn, (iii) three intertwined chains, each with a pitch of $30 \overset{\circ}{\text{Å}}$ and 10 units per turn. The idea of a three-stranded helix emerged from the considerations of diffracted intensities and the density of collagen which requires three amino acid residues per $3 \overset{\circ}{\text{Å}}$ in the fiber direction (25). Consequently, all the reflections in the diffraction pattern were indexed based on case (iii) above, where c is taken as $30 \overset{\circ}{\text{Å}}$, and so the $3 \overset{\circ}{\text{Å}}$ reflection is called 10th layer line ($\ell/30 \cong 1/3 \therefore \ell \cong 10$) and the $4 \overset{\circ}{\text{Å}}$ and $10 \overset{\circ}{\text{Å}}$ reflections are indexed as the 7th and the 3rd layer lines respectively ($\ell/30 \cong 1/4 \therefore \ell \cong 7$, $\ell/30 \cong 1/10 \therefore \ell \cong 3$). In what follows, the $3 \overset{\circ}{\text{Å}}$, $4 \overset{\circ}{\text{Å}}$ and $10 \overset{\circ}{\text{Å}}$ reflections are called the 10th, the 7th and the 3rd layer line and their layer line spacings are designated as d_{10} , d_7 and d_3 respectively.

In describing the collagen helix, Ramachandran (19) introduced two parameters, the unit height, h and the unit

twist, t . The unit height is the vertical height of the repeat unit (one amino acid residue in collagen) and the unit twist is defined as the fraction of a full rotation (360°) corresponding to one repeat unit and therefore equal to the reciprocal of the number of units per turn. Using the two parameters, the helix can be generated by the operation of rotating a unit by t turns about a helical axis and translating it along the axis of helix by a distance h . These two parameters are, therefore, the basic parameters in characterizing helix and it is of great importance to obtain their values from the diffraction pattern.

As described in the last part of the previous section, the three prominent layer lines (d_{10} , d_7 and d_3) must correspond to $Z = 1/h$, $1/P$ and $1/h - 1/P$ in reciprocal space. Therefore,

$$d_{10} = h$$

$$d_3 = P$$

$$\text{and } 1/d_{10} = 1/d_3 + 1/d_7 \quad (15)$$

Meridional reflection (d_{10}) gives immediately the value for h and the unit twist t is obtained from the ratio of d_{10}/d_3 ($= h/P$), because P is the height of one complete turn of the helix and P/h is the number of units per turn.

Table III-1 shows the layer line spacings and the helical parameters for an unstretched collagen fiber, obtained in our laboratory and those of the most recently refined values by Ramachandran and Sasisekharan (14,26). (The experimental part of the fiber pattern is presented in the

TABLE III-1 WIDE ANGLE X-RAY DIFFRACTION PATTERN OF
COLLAGEN FIBER (UNSTRETCHED)

Layer Line	Spacing (Å)		Remarks
	(a)	(b)	
10	2.91	2.90±0.02	True meridional reflection, spacing corresponds to the vertical height of one residue
7	4.2	4.05±0.05	Non-meridional reflection
3	9.5	9.35	Non-meridional reflection
d ₁₀₀	10.4-14.6		Equatorial reflection, hydration sensitive, spacing corresponds to the lateral packing distance of tropo-collagen molecule
d ₂₀₀	ca. 1/2(d ₁₀₀)		
----	centered around at 4.5		Strong, diffuse reflections on and near the equator
t=d ₁₀ /d ₃	0.308	0.310	Unit twist

(a) From Ramachandran and Sasisekharan (26)

(b) This work

next section in which collagen and gelatin films are discussed.) The reported layer line spacings are different from group to group (10-13), for example, d_{10} varies from 2.86 Å to 2.95 Å. The best account for this has been given by Ramachandran in his review (14) and so will not be discussed here.

The equatorial spacing (d_{100} in Figure III-4) represents the mean distance between tropocollagen helices packed in collagen fibrils. The spacing d_{100} has been well known for its hydration sensitive nature and varies from 10.4 Å for dry collagen to 14.6 Å wet collagen (27). The other equatorial reflection (d_{200} in Figure III-4) which is not as distinctly clear as d_{100} also varies with hydration level. The d_{200} spacing is found to have a value close to one-half of d_{100} at all the hydration levels. The effect of water molecules on the diffraction pattern of the collagen fiber will be discussed later in Chapter V.

The diffuse "blob" of strong intensity which appears on the equator is considered (14) to be the cluster of intensities of the layer lines of mostly 0th, 1st and 2nd. This is clear when we compare the diffraction pattern with the intensity distribution of the different layer lines observed as shown in Figure III-5. Ramachandran (14) suggested that the spacing of this blob, 4.5 Å, might represent the average distance between the planar peptide units at the same height in the three chains. An accurate analysis of this blob is, however, impossible due to the diffuseness of the reflection.

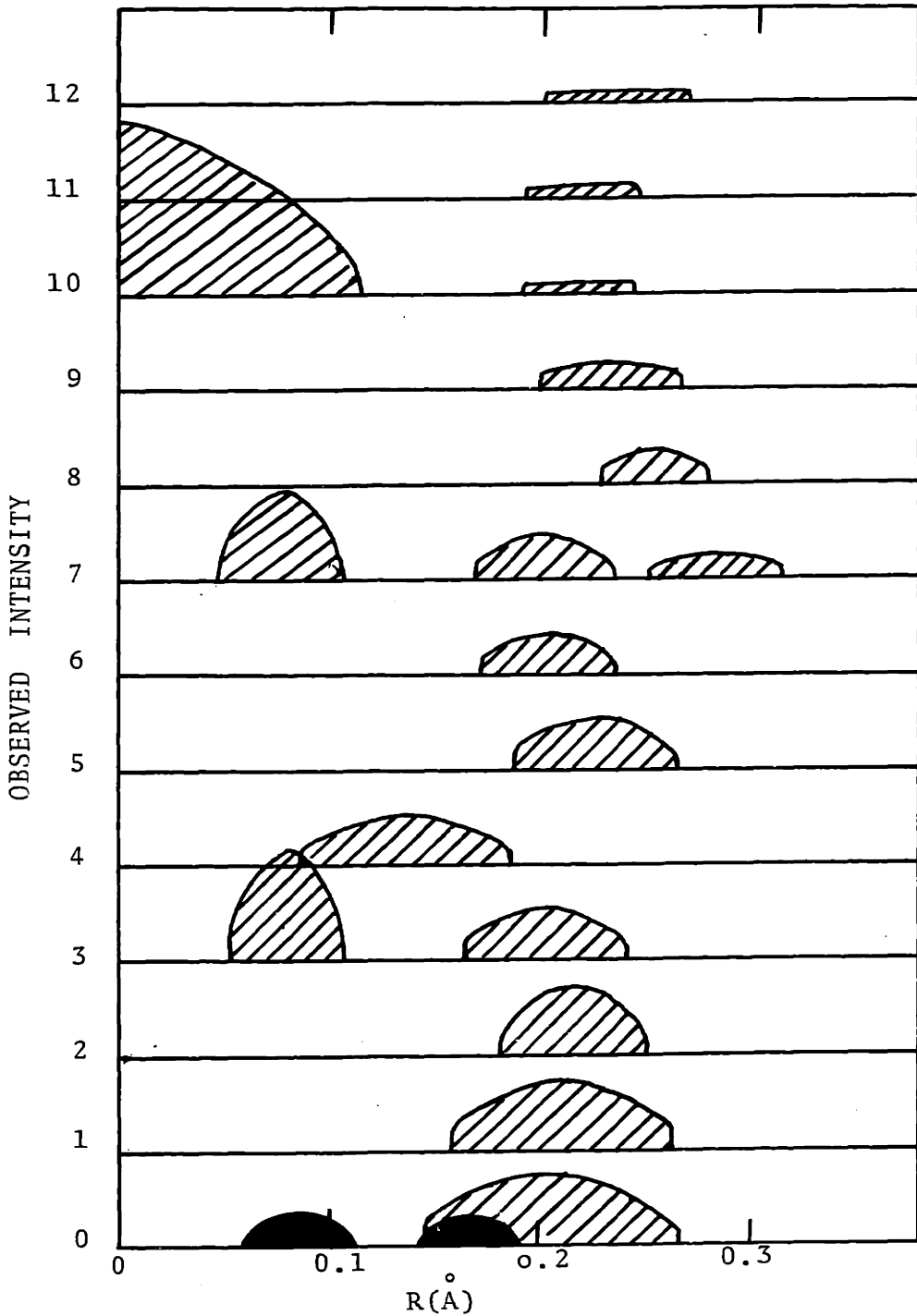


Figure III-5 Intensity distribution of the layer lines in x-ray pattern of collagen fiber

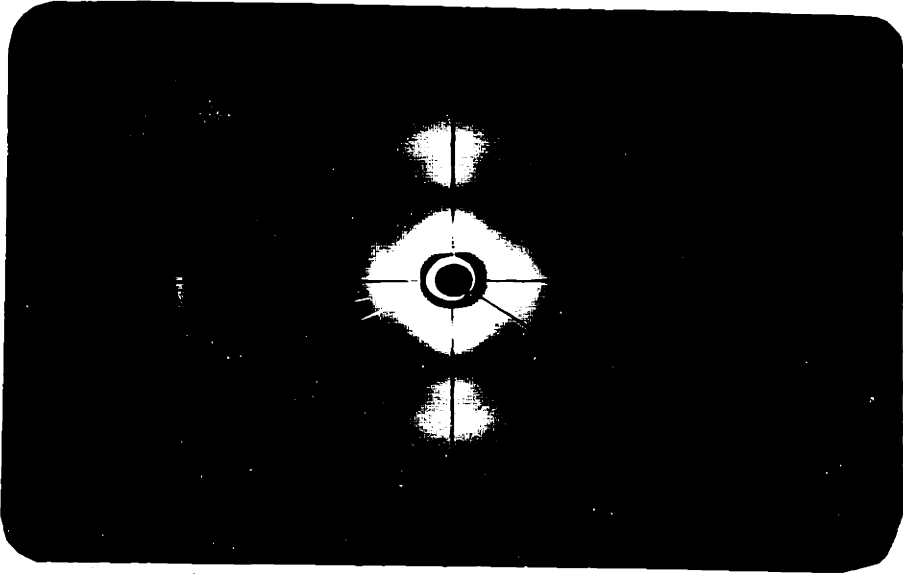
So far discussion has been made of the characteristics of the fibrous pattern of collagen, the identification of each reflection and their relations to the helical structure. Other information, such as, the average orientation of collagen molecules in the native tendon and the average crystallite size can also be obtained from the diffraction pattern.

If the collagen molecules are perfectly oriented along the fiber direction, the meridional peak would appear as a well defined dot right on the meridian. The effect of disorientation on the diffraction pattern is such that as the disorientation increases, the spot will be spread out into streaks to give a reflection arc. Therefore, from the measurement of the angle of the arc (see Figure III-6 (a)) one can estimate the degree of disorientation. For the quantitative expression of the average of the orientation distribution, it has been the general practice to use the "orientation function f" defined as (32)

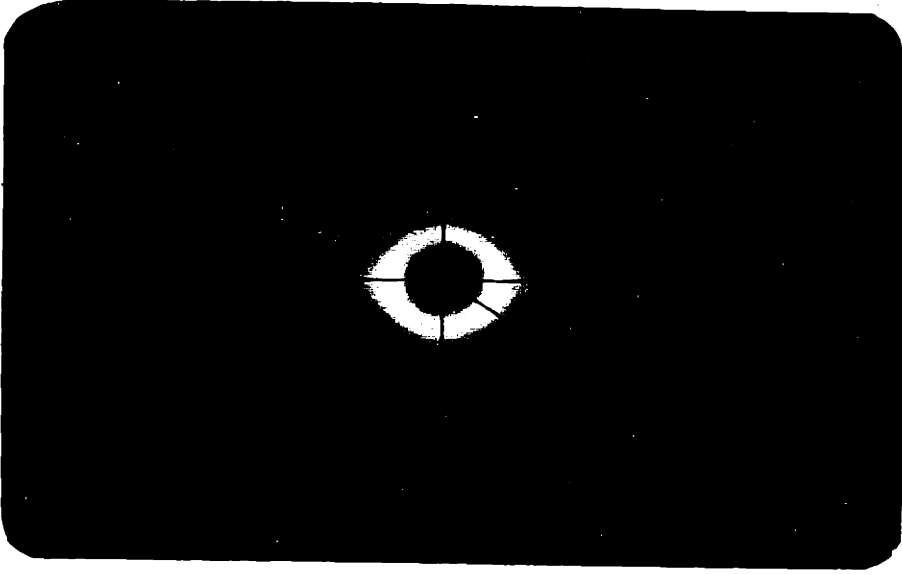
$$f = \frac{3 \overline{\cos^2 \alpha} - 1}{2} \quad (16)$$

where α is the orientation angle and $\overline{\cos^2 \alpha}$ is the average value of the $\cos^2 \alpha$. In general, three different orientation functions are used to describe the orientation of crystallites in space. However, for the case of uniaxial orientation, as is the case with the collagen fiber, only one orientation function is needed.

As is well known, (29,30) the angles of the reflection arcs of either meridional or equatorial peaks repre-

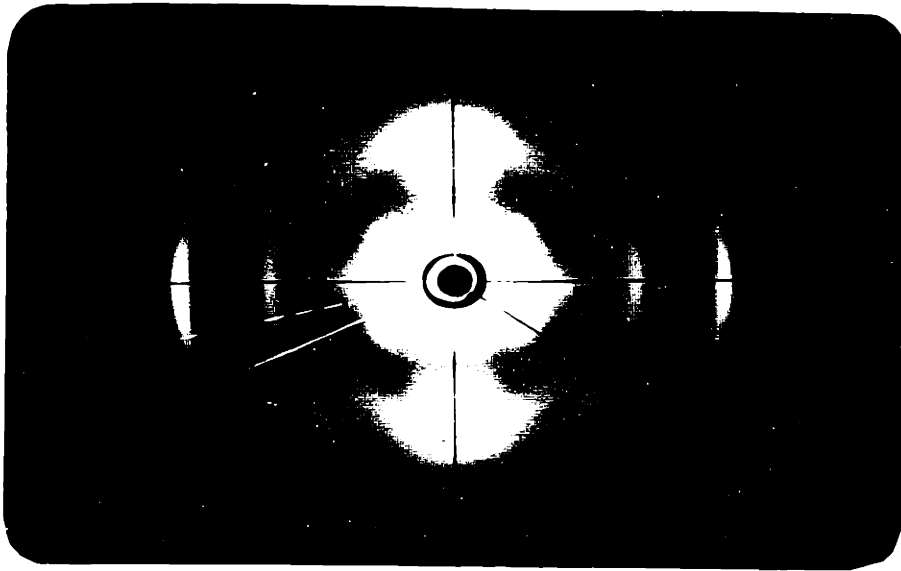


a) DISORIENTATION ANGLE ϕ OF THE
MERIDIONAL REFLECTION OF
COLLAGEN FIBER PATTERN

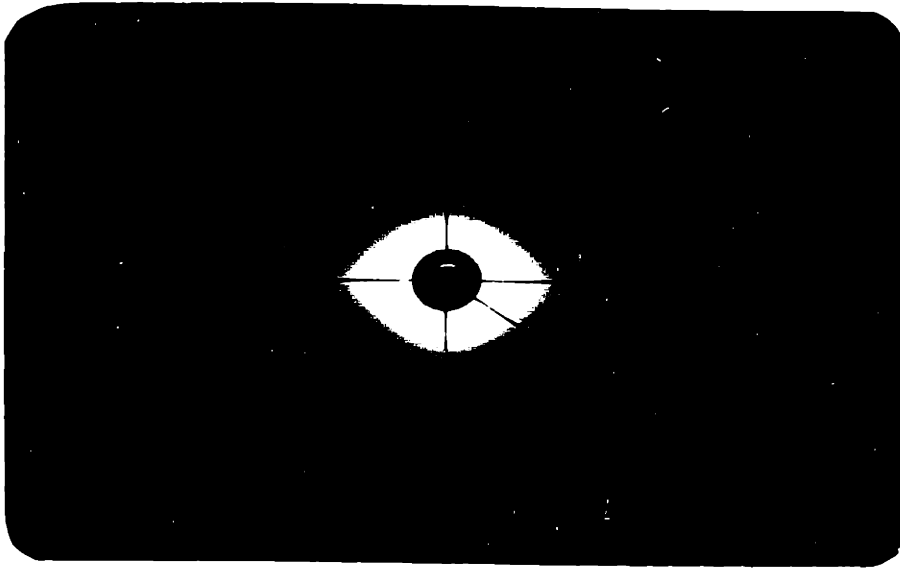


b) X-RAY PATTERN OF SHRUNKEN
COLLAGEN FIBER (IN WATER
AT 65°C, 1 HOUR)

Figure III-6



a) BISO-ORIENTATION ANGLE ϕ OF THE
MERIDIONAL REFLECTION OF
COLLAGEN FIBER PATTERN



b) X-RAY PATTERN OF SHRUNKEN
COLLAGEN FIBER (IN WATER
AT 65°C, 1 HOUR)

Figure 111-6

sent approximately the range of the angles of disorientation of the fibrils. In order to obtain $\overline{\cos^2\alpha}$ however, one has to know the intensity distribution within the reflection arc, which can be obtained with a densitometer. According to Stein (30,31), a good approximation of $\overline{\cos^2\alpha}$ can be obtained from the estimated half-width angle of the arc (Figure III-6 (a)). Using this approximation method, the average orientation of the collagen fibrils in unstretched and stretched (strain $\approx 6\%$) native wet tendon was estimated and is shown in Table III-2, where the estimated half-width angles of the meridional peak, $\overline{\cos^2\alpha}$ values and the values for orientation function f are listed. The half-width angle varied from 13° for unstretched to 9° for stretched (strain $\approx 6\%$) and the value of $\overline{\cos^2\alpha}$ varied accordingly from 0.949 to 0.976. Corresponding values of f varied from 0.923 to 0.964. Using the Scherrer equation (33), the mean crystallite size of the crystalline powders can be estimated from the breadth of the reflections. This requires, however, the crystallites to be of relatively perfect crystalline order so that no other source of line broadening of the reflection exist. In the collagen fiber diagram, it is not considered to be appropriate to apply the Scherrer equation to estimate the crystallite size because the breadth of the meridional reflection can possibly result not only from the size effect but also from the non-uniformity in the vertical height of peptide units along the helical axis. Nevertheless, the line breadth can

TABLE III-2 ORIENTATION OF COLLAGEN MOLECULES IN THE WET RAT TAIL TENDON AND THE FILM

	<u>Tendon Fiber</u>		<u>Film</u>
	<u>un-</u> stretched	stretched	
Angle ϕ of the meridional arc	26°	18°	24°
Half-width angle	13°	9°	12°
$\overline{\cos^2\alpha}$	0.949	0.976	0.957
$f = (3\overline{\cos^2\alpha} - 1) / 2$	0.923	0.964	0.936

Note: For tendon fiber, f is for the uniaxial orientation along the fiber axis. For film, f is for the planar orientation in the plane of the film.

be taken as a good indicator of the lattice imperfection in general, and it will be seen in a later chapter how the breadth of meridional reflection changes with water content. The line breadth of the meridional reflection of the wet collagen fiber diagram was estimated to be 1.25° (or 0.0218 radians). (This is the angle β_0 in Scherrer equation, $L = K\lambda/\beta_0 \cdot \cos \theta$ (17) and is obtained from the difference in Bragg angles of the meridional peak based on the outer and the inner edge of the reflection arc.)

When the collagen fibers were shrunken in water by heating at 65° C. for one hour, the structural order in the fiber became completely destroyed and the diffraction pattern changed dramatically to the pattern shown in Figure III-6 (b).

1.4 Wide Angle X-Ray diffraction Patterns of Collagen and Gelatin Films

A. Experimental

Materials: Three different types of films, collagen, cold-cast and hot-cast gelatin films, were prepared by solution casting from native and denatured collagen solutions as described in the previous chapter on solution casting. The films prepared varied in thickness from 0.25 to 0.5 mm and contained about 10 - 15%-wt. moisture, the equilibrium moisture content under ambient conditions.

Apparatus: A combination of a Norelco X-Ray Analytical

Instrument (manufactured by Phillips Electronics Instruments, N.Y.) and a flat-film camera (or Laue camera) was used to obtain the transmission X-ray diffraction pattern. The X-ray radiation used was $\text{Cu K}_{\alpha}^{\circ}$ ($\lambda = 1.5405 \text{ \AA}$), filtered through nickel and generated at 35 Kilovolts with a current of 15 miliamperes. The beam collimator used was 6 cm in length and the beam cross-section was 1 mm in diameter. The photographic films used were of the high-speed type, Kodak No-Screen (NS-54T), supplied by General Electric, Medical Department, Wellesley, Mass.

Procedure: A rectangular specimen, (1 cm x 2 cm) was cut out from the film, placed in a sample holder and held in front of the collimator such that the X-ray beam was perpendicular to the film surface. The flat film camera, loaded with the Kodak No-Screen film, was placed at a distance of about 6 cm from the specimen. Alignment of X-ray beam was checked with a fluorescence screen and the X-ray beam was exposed by opening the beam cap of the X-ray tube. The exposure time was set by automatic timer at 50 min. to 75 min., depending on the specimen thickness (eg., 1 hour for 0.3 mm thick specimen with 35 Kvolts, 15 mA). At the end of the exposure, the camera was taken into the dark room where the negative photographic films were developed. (A collagen fiber diagram (presented in Figure III-4) was obtained in the same manner as above except for sample preparation. Rat tail tendon fibers were removed from the

tail, washed with 0.5 M NaH_2PO_4 for two hours at room temperature and then mounted on the sample holder. Tendon fibers aligned in parallel of approximately 1.5 mm in diameter, were held vertically, with the fiber axis perpendicular to the X-ray beam in front of the collimator. During the exposure, tendon fibers were kept wet by a few drops of distilled water supplied at a constant interval of about 10 minutes.)

A specimen of collagen film used for the diffraction pattern with the X-ray beam parallel to the plane of the film was prepared as follows: strips of collagen film, about 1 mm x 15 mm in size, were cut out from the large film and placed together by laying one strip on top of others in a specially made sample holder. The detailed steps are illustrated in Figure III-7.

B. Results

The wide angle X-ray diffraction patterns of the collagen film, obtained with the beam perpendicular and parallel to the plane of films are shown in Figure III-9. The patterns of cold- and hot-cast gelatin films are presented in Figure III-10.

In the collagen pattern, four Debye-Scherrer rings were present with different intensities and sharpness. The spacings for each ring (labelled as R_1 , R_2 , R_3 and R_4 in Figure III-8) are 2.90 Å, 4.0-4.3 Å, 7.1-7.8 Å and 11-13 Å. The R_1 ($d = 2.9$ Å) and R_4 ($d = 13$ Å) reflections

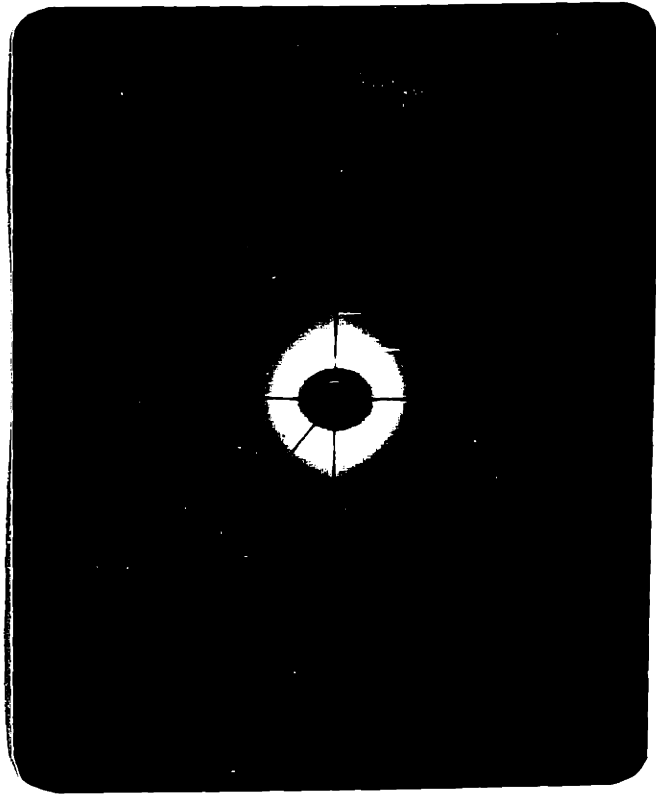


Figure III-8 Debye-Scherrer rings (R_1, R_2, R_3, R_4)
in the wide-angle x-ray pattern
of collagen film

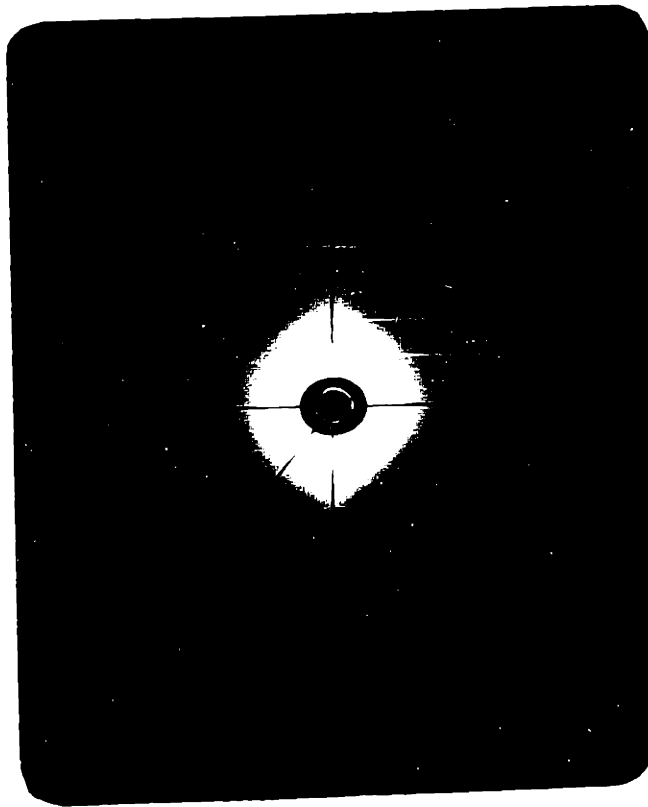


Figure III-3 Debye-Scherrer rings (R_1, D_1, R_2, D_2) in the wide-angle x-ray pattern of collagen film.

are relatively sharp with strong intensities, whereas R_3 ($d = 7.1 - 7.8 \text{ \AA}$) reflection is very weak. The R_2 reflection ring ($d = 4.0-4.3 \text{ \AA}$), often referred to as the amorphous halo, is very diffuse even though the intensity is strong.

Exactly the same feature as above was found in the diffraction pattern of the cold-cast gelatin film. The diffraction of the hot-cast gelatin, however, exhibits no crystalline Debye-Scherrer rings and only very diffuse amorphous halo was present at $4.3-4.5 \text{ \AA}$. The results are summarized in Table III-3.

C. Discussion

By comparison of the film pattern with the fiber pattern, it can readily be recognized that reflections R_1 ($d = 2.9 \text{ \AA}$) and R_4 ($d = 11-13 \text{ \AA}$) in the film pattern correspond to the meridional (10th layer line) and the equatorial reflections in the fiber pattern respectively. The diffuse R_2 reflection ($d = 4.0 \sim 4.5 \text{ \AA}$) would result from both the 7th layer line ($d = 4.0-4.2 \text{ \AA}$) and the large diffuse blob on and near the equator ($d \approx 4.5 \text{ \AA}$) in the fiber pattern. The R_3 reflection ($d = 7.1-7.8 \text{ \AA}$), which is relatively weak, is expected to occur from the 3rd layer line ($d_3 = 9.3-9.5 \text{ \AA}$) in the fiber pattern. It must be noted here that the $d_3 = 9.3-9.5 \text{ \AA}$ is the layer line spacing, obtained from the Bragg angle corresponding to the vertical distance of 3rd layer line reflection from the equator in

TABLE III-3 WIDE ANGLE X-RAY DIFFRACTION DATA OF COLLAGEN
COLD-CAST AND HOT-CAST GELATIN FILMS

Reflections	Spacing (Å)		
	<u>Collagen</u>	<u>Cold-cast gelatin</u>	<u>Hot-cast gelatin</u>
R ₁	2.90	2.90	-----
R ₂	4.0-4.5	4.3	4.3-4.5
R ₃	7.1-7.8	7.3	-----
R ₄	11.0-13.5	11.0-12.0	-----

Note: R₂ reflection is very diffuse
R₃ reflection is very weak
R₄, R₁ reflections are relatively sharper and
stronger in intensities

the fiber pattern. When the spacing is calculated based on the Bragg angle from the distance between the center of the pattern to the 3rd layer line reflection, the value of 7.5 \AA is obtained and this is what is observed in the Debye-Scherrer pattern.

The Debye-Scherrer pattern can be obtained from the results of the fiber pattern by the spherical transforms of each layer line intensity. This involves the summation of all the intensity points on the different layer lines corresponding to the same d-value. Such calculations (35,36) showed that the intensity peaks are expected at $d \approx 3.0 \text{ \AA}$, $d \approx 4.5 \text{ \AA}$ and at $d \approx 12 \text{ \AA}$ in the film pattern which is in good agreement with the experimental observations. The presence of the above four reflection rings, therefore, can be used to identify the structure of collagen.

As shown in Figure III-9 (a), the intensity of the reflection of each Debye-Scherrer ring is uniform all around, indicating that the tropocollagen molecules are uniformly distributed in the two dimensional space of the film plane. The diffraction pattern obtained with the X-ray beam parallel to the plane of the film (Figure III-9 (b)) shows a planar orientation of the molecules in the film plane. The degree of orientation with respect to the plane of the film is comparable to that of unstretched tendon fiber in the fiber direction. The estimated half-width angle of the 10th layer line ($d = 2.9 \text{ \AA}$) reflection arc in the film pattern is ca. 12° which yields the value of 0.045

for the square of the directional cosine ($\overline{\cos^2 \alpha}$) between the normal of the film plane and the axis of the tropocollagen helix.

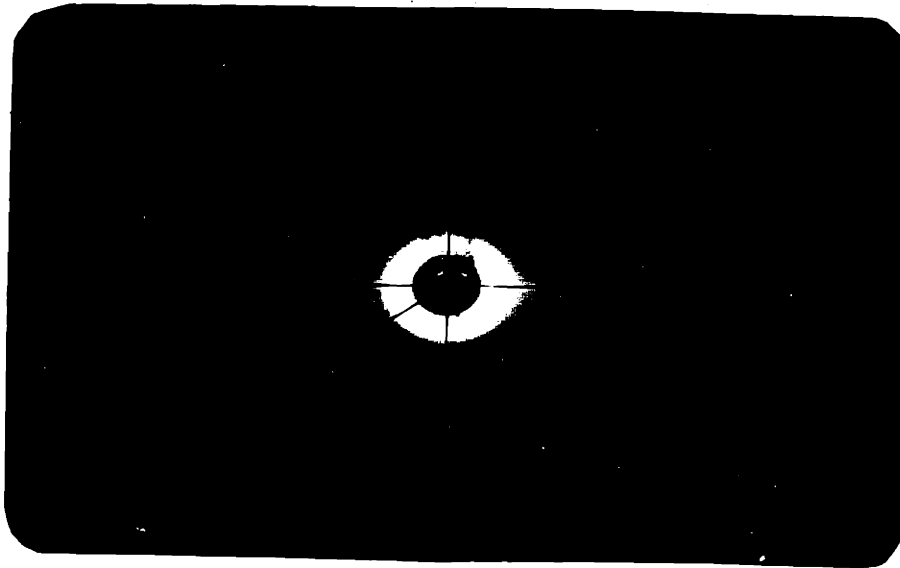
From the above two patterns (III-9 (a) and (b)), it is clear that the tropocollagen molecules are lying in the plane of the film, but are randomly oriented otherwise. It is not clear, however, whether the tropocollagen molecules are packed together as undeformed rigid rod-like macromolecules or relatively flexible, therefore, locally deformed macromolecules. Considering the high ratio (200 to 1) of the length to the diameter of the molecule (aspect ratio) and the difference in the structural order of the polar and apolar regions of tropocollagen (37), these molecules are likely to be deformed, probably at the polar regions (or the regions where prolyl and hydroxyl prolyl residues are largely absent) as Yannas has suggested in his review paper (37).

The diffraction pattern of cold-cast gelatin (Figure III-10 (a)) showed exactly the same crystalline Debye-Scherrer rings as that of collagen film. The hot-cast gelatin pattern, on the other hand, shows total absence of any Debye-Scherrer ring and only an amorphous halo is shown at $d \cong 4.5 \overset{\circ}{\text{A}}$. This agrees well with the patterns published by Bradbury and Martin (38) and Katz et al. (39). The presence of the same Debye-Scherrer rings in cold-cast gelatin (cast at room temperature) pattern as in the collagen film pattern is direct evidence of the partly crystal-

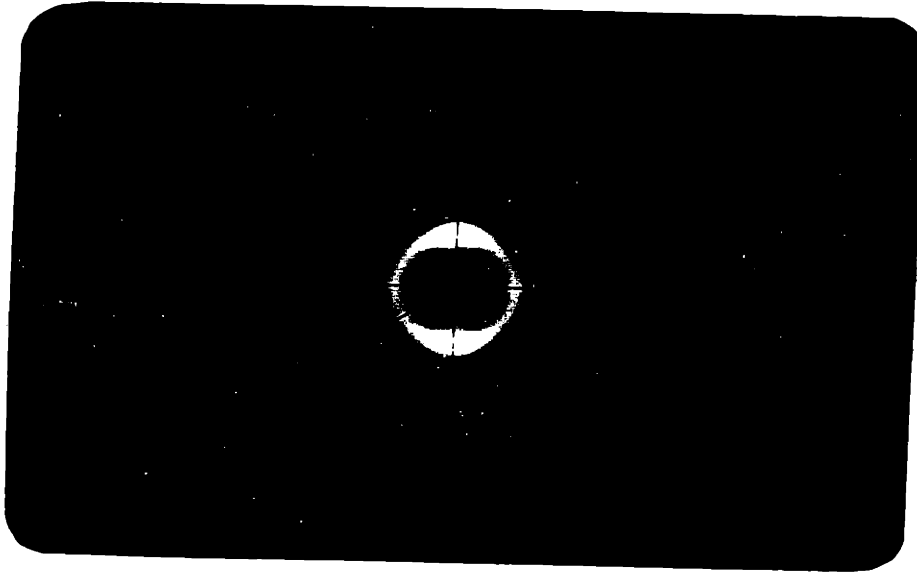
line nature of cold-cast gelatin.

As is well known, the randomly-oriented gelatin molecules can undergo the transition to the helical conformation in solution at temperatures below that of helix-coil transition. Relatively clear understanding of the renaturation process (coil \rightarrow helix) of the gelatin in solution has been obtained in the investigation of Harrington and his coworkers (40,41) through the study of the associated mutarotation phenomenon. The extent to which gelatin regains the collagen structure varies depending on the temperature, and approaches an equilibrium with time (40). Cold-cast gelatin is, therefore, a partially crystalline form of collagen and depending on the casting conditions, the degree of crystallinity can be varied. Hot-cast gelatin (cast at 65^o C.) is totally amorphous indicating that, during the casting process, coil \rightarrow helix transition of the molecules did not occur as the casting temperature (65^o C.) was higher than the helix-coil transition temperature of 37^o C.

As seen in Figure III-9 and III-10, the amorphous and crystalline nature of hot-cast and cold-cast gelatin can be clearly demonstrated by X-ray diffraction pattern. Unfortunately, however, the X-ray diffraction technique is not as sensitive as other experimental techniques (i.e. optical rotation, to be discussed in later chapter) in differentiating cold-cast gelatin from collagen. While the X-ray patterns of collagen and cold-cast gelatin are nearly

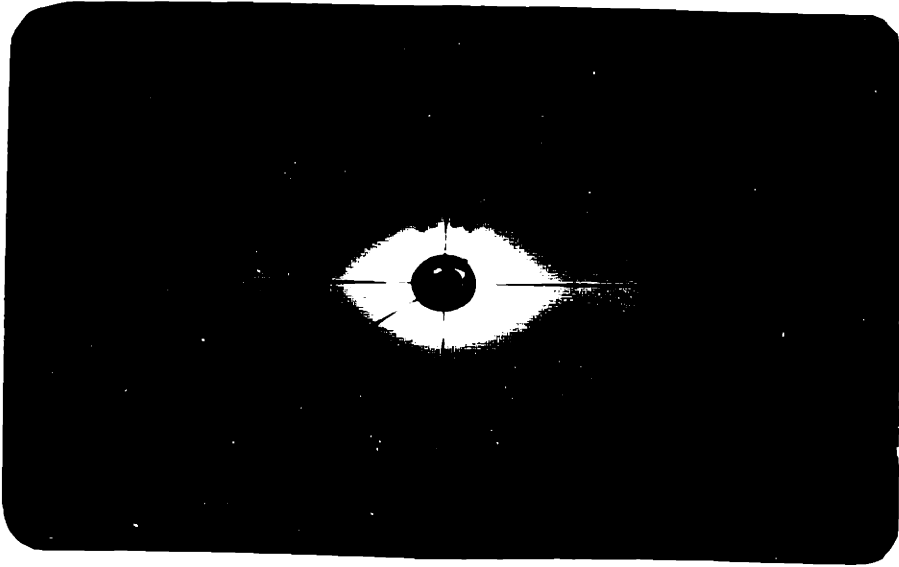


a) X-RAY BEAM PERPENDICULAR
TO THE PLANE OF THE FILM

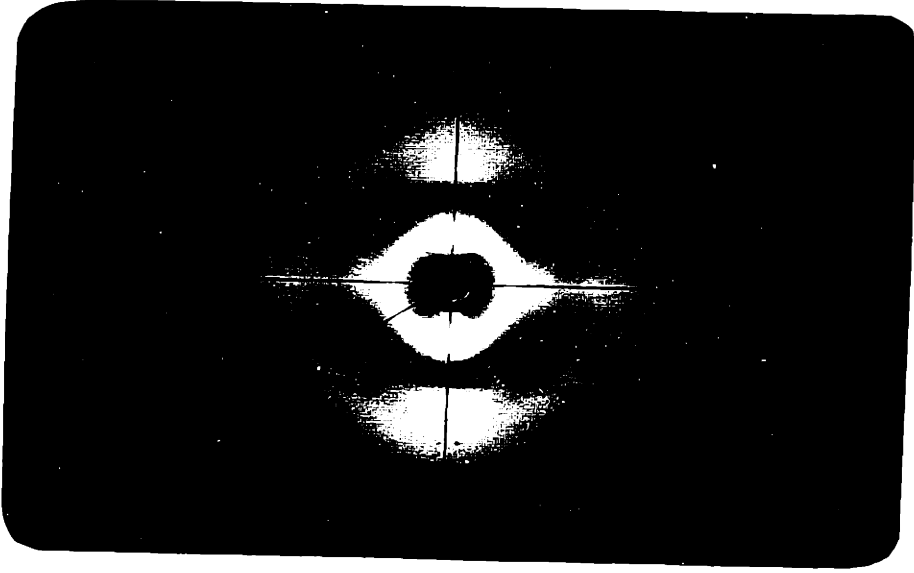


b) X-RAY BEAM PARALLEL
TO THE PLANE OF THE FILM

Figure III-9 Wide-angle x-ray diffraction pattern of collagen film

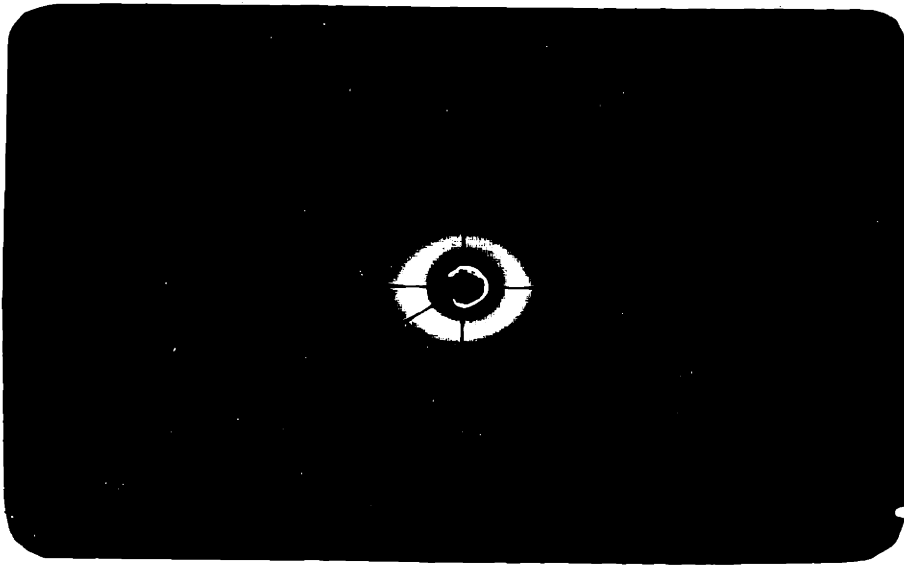


a) X-RAY BEAM PERPENDICULAR
TO THE PLANE OF THE FILM



b) X-RAY BEAM PARALLEL
TO THE PLANE OF THE FILM

Figure 111 9 wide angle x ray diffraction pattern of collagen film

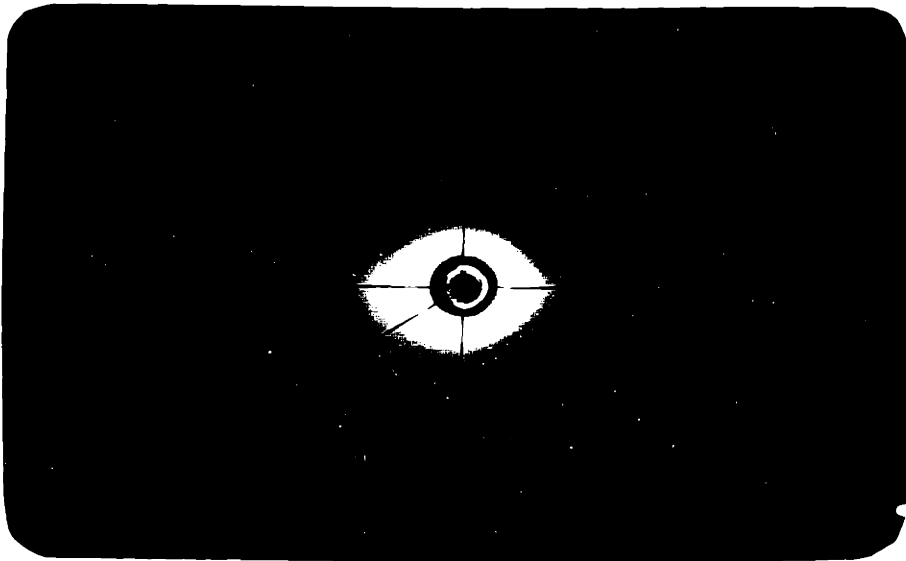


a) COLD-CAST GELATIN

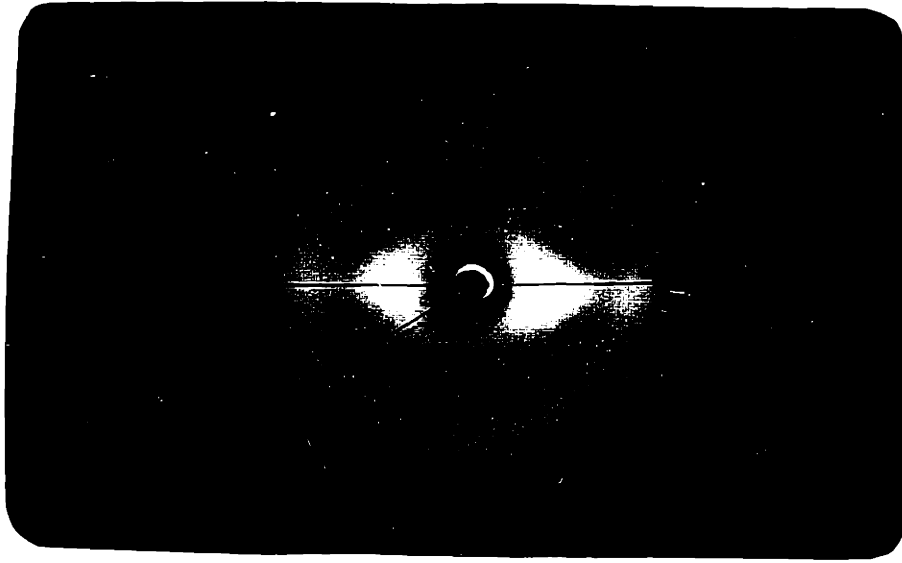


b) HOT-CAST GELATIN

Figure III-10 Wide-angle x-ray diffraction patterns of cold-cast and hot-cast gelatin films



a) COLD-CAST GELATIN



b) HOT-CAST GELATIN

Figure III-10 Wide-angle X-ray diffraction patterns of cold-cast and hot-cast gelatin films

the same, the specific re
other enormously. (i.e.
-1700 for cold-cast gelat

1.5 Summary

The theory of X-ray
was briefly reviewed. Ba
interpretations were made
tern of collagen fibers.

(i) A true meridion

$2.9 \overset{\circ}{\text{Å}}$ corresponds to

(ii) Two non-meridi

$4.2 \overset{\circ}{\text{Å}}$ and $9.35 \overset{\circ}{\text{Å}}$ cor

er lines.

(iii) A relationshi

ings such that $1/d_{10}$

and two helical para

twist (t) are relate

$$h = d_{10} = 2.9 \overset{\circ}{\text{Å}}$$

$$t = d_{10}/d_3 = 2.$$

The average orientat
along the fiber axis in n
half-width angle of the 1
were 9° for wet stretched
stretched fiber.

The wide-angle X-ray
gen, cold-cast and hot-ca

Both collagen and cold-cast gelatin films (cast at 23° C.) showed identical diffraction pattern with four Debye-Scherrer rings, when obtained with the X-ray beam parallel to the normal of the film plane. Four reflection rings are at spacings of 2.9 Å (R₁), 4.0-4.3 Å (R₂), 7.1-7.8 Å (R₃) and 11-13 Å (R₄), which are in good agreement with the expected spacings based on the spherical transform of the layer line intensities of fiber pattern. The presence of these four Debye-Scherrer rings are, therefore, the indication of the presence of the structure of collagen helix. But it is not sufficient to show the nativity of the molecule as seen by the identical pattern of collagen and cold-cast gelatin. Hot-cast gelatin film showed no crystalline Debye-Scherrer rings and only an amorphous halo was present at a spacing of ca. 4.5 Å.

The pattern of a collagen film obtained with X-ray beam parallel to the plane of the film showed a high degree of orientation of collagen molecules in the plane of the film. The average out of plane orientation of the molecules estimated by the half-width angle of the 10th layer line reflections is about 12°, yielding the average value of the square of direction cosine, $\overline{\cos^2\alpha}$ to be 0.045.

Even though X-ray diffraction technique showed a clear distinction between amorphous and crystalline state of collagen (hot-cast gelatin vs. collagen), it did not provide a sensitive basis for the differentiation between collagen and cold-cast gelatin (partially crystalline collagen).

III-2. Infrared Spectroscopic Studies of Collagen and Gelatin

2.1 Introduction

The major features of the infra-red absorption spectrum of collagen have been known since 1950 (42,43). As is the case with many other proteins, the interpretation of the spectra of collagen was the major difficulty in the early application of infrared to the study of collagen structure. Even though a complete analysis of vibrational modes of complex macromolecule is impossible, many of the characteristic absorption bands common to a variety of proteins have been assigned based on the vibrational analysis of simple molecules (45-48, 54). The strongest absorption bands in collagen spectrum are those of the amide peptide group, a repeat unit of the polypeptide chain backbone, and, for this reason, intensive studies have been centered on these bands.

Advancement has been made thereafter in improving the resolution and more accurate assignments of the spectral bands have been made possible by the application of different sample preparation techniques (55), by use of polarized radiation (49,50,51,54) and deuteration studies (50,52,53,54). The infra-red dichromic study of the major amide absorption bands using polarized radiation has successfully led to the screening of various molecular models proposed for collagen (51,54). Deuteration studies com-

bined with infrared spectroscopic analysis have provided additional information on the identification of the vibrations involving the movement of labile hydrogen, as well as in the differentiation of the location of specific group in amorphous and crystalline regions (50,52,53,54). The current state of infrared spectroscopic studies of collagen and gelatin has been reviewed by Yannas (37).

The main purpose of the study described in this section was to provide the infrared spectroscopic basis for the characterization of crystalline (native) and amorphous collagen (gelatin) in the solid state. Since the same principal vibrations are found in both collagen and gelatin, the small differences in frequencies, band contours and intensities of the major peptide bands are of importance and will be discussed this section.

2.2 Experimental

Materials: Films of collagen, cold-cast and hot-cast gelatin were prepared from the aqueous solutions of native and denatured collagen as described in the previous section on solution casting (Chapter II). The differences in crystallinity between collagen and hot-cast gelatin have been discussed in the preceding chapter on X-ray diffraction studies.

The thickness of the films suitable for IR spectroscopy was found to be in the range of 1 - 3 microns. Films were stored and subjected to the spectroscopic meas-

urements in ambient conditions. The equilibrium moisture content of the films was in the range of 10 - 15%-wt.

Measurements: A double-beam grating infrared spectrophotometer (Perkin-Elmer Model 621) was used to obtain the spectra in the frequency range of 200 cm^{-1} to 4000 cm^{-1} . The scan speed was fixed at 16 minutes for the full spectrum. The spectra was recorded both in the transmission and absorption mode. The resolution of the relatively strong bands (i.e. those of amide I,II) was found to be better in the absorption mode, whereas relatively weak absorption bands were resolved better in transmission mode. Operational data on the instrument are as follows: slit program: 1000, gain: 4.5, attenuator speed: 1100, scan time: 16, suppression: 6, scale expansion: 1 and source current: 0.8.

2.3 Results and Discussion

The infrared spectra of collagen and hot-cast gelatin are shown in Figure II-11 recorded in the absorption mode. The interpretation of some of the bands are summarized in Table III-4. The changes in spectra brought about by denaturation of collagen into hot-cast gelatin, shown in Figure III-11, are summarized in Table III-5. Following is the discussion on the five strongest bands (Amide I,II,III, 3330 cm^{-1} and 1450 cm^{-1} band) in the collagen spectrum and their changes in hot-cast gelatin spectrum.

First, the 3330 cm^{-1} NH stretching vibrational fre-

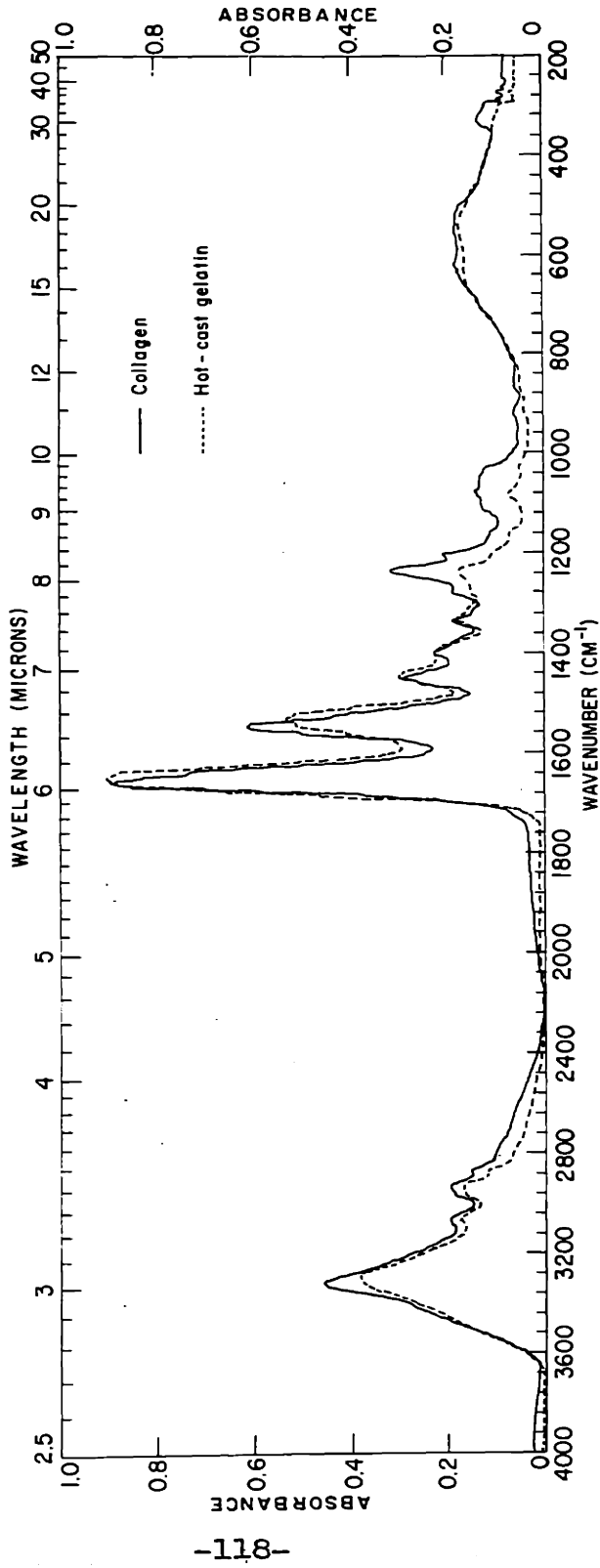


Figure III-11 Infrared absorption spectra of collagen and hot-cast gelatin film

TABLE III-4 MAJOR BANDS IN THE IR SPECTRUM OF COLLAGEN (37)

Frequencies, cm^{-1}	Interpretation	Reference
4850-4890	Overtone of 3300 cm^{-1} and 1550 cm^{-1}	42,51,52
4580-4600	Combination of $c = 0$	42,43,52
3400-3450	Free water	50,55
3290-3335	NH stretch	42,43,49,50,51,54,55
3100	Overtone of amide II	48,50
3060	NH tension	54,55
2930-2950	CH stretch	47,54,55
2870-2885	CH stretch	47,55
2850	CH stretch	55
1710	Non-ionized COOH	55
1640-1660	$c = 0$ stretch (amide I)	42,44,46,47, 48,51,54,55
1560	COO^-	55
1535-1550	NH in-plane deformation and CN stretch (amide II)	42,44,45,48, 51,54,55
1445-1455	CH_2 deformation and CH_3 asymmetric deformation	47,54,55
1407	COO^-	55
1375-1390	CH_3 symmetric deformation	54,55
1310-1340	CH_2 wagging	54
1230-1270	CN stretch and NH in-plane deformation (amide III)	44,45,54,55
1075-1082	CO vibrations of hydroxyl groups	50
920-940	OH deformation of COOH (?)	55
650-700	NH out of plane deformation	51,54

quency of collagen is shifted to 3300 cm^{-1} in the hot-cast gelatin spectrum. The value of 3330 cm^{-1} of collagen has been known to be significantly larger than the value of 3300 cm^{-1} found in most other proteins, indicating the NH---O hydrogen bonds in collagen is longer than those occurring in other protein structures (14,56). Quantitative correlation by Nakamoto et al. (56) of the hydrogen bond length with the NH stretching vibrational frequency showed good agreement with the structural model proposed for collagen (17). Because of the characteristic nature of this frequency in the structure of collagen, the 3330 cm^{-1} absorption peak provides a simple test for the identification of the collagen type structure.

Secondly, the amide I band, corresponding to the $\text{C}=\text{O}$ stretching vibration, consists of several component sub-bands, the strongest having a frequency of 1665 cm^{-1} . The nature of this multiplet peak is not clearly understood; it indicates, however, the existence of non-equivalent $\text{C}=\text{O}$ bonds, with stretching vibration indicative of different vibrational energy levels, the difference due to the environment such as side-chains, polypeptide chain conformation and inter- and intra-molecular hydrogen bonding (50). Careful examination of the relatively well resolved amide I band shows about 9 -10 sub-bands of different intensities which are listed in Table III-6. In the collagen spectrum the strongest sub-band occurs at frequency of 1655 cm^{-1} , whereas, that of 1635 cm^{-1} is the strongest one in the hot-cast gelatin spectrum. The reported shift of this

band (50) from 1660 cm^{-1} for collagen to 1640 cm^{-1} for gelatin is, in fact, an apparent shift resulting from the change in band contour due to the change in the relative intensities of sub-bands (37), particularly, of 1655 cm^{-1} and 1635 cm^{-1} . From the observed increase in relative intensity of the 1635 cm^{-1} sub-band against the 1655 cm^{-1} sub-band upon denaturation, the 1635 cm^{-1} sub-band can be assigned as the $c = 0$ stretching vibrational frequency of the amorphous, random coil peptide (hot-cast gelatin) and the 1655 cm^{-1} peak as that of crystalline helical peptide of collagen. This does not exclude the relative importance of other sub-bands, whose apparent changes are not as clear as for the above two sub-bands.

Similar observations can be made with the amide II absorption band. This band can be assigned to the NH in-plane deformation and CN stretch of the amide groups. This band is composed of many sub-bands (see Table III-6) with the strongest peak at 1550 cm^{-1} in collagen and at 1535 cm^{-1} in hot-cast gelatin. The apparent shift of frequency (50) from 1550 cm^{-1} to 1535 cm^{-1} is again due to the change in relative intensity of sub-bands. The intensity of the 1535 cm^{-1} sub-band is much weaker than the 1550 cm^{-1} sub-band in collagen and increases significantly by denaturation.

The sub-band at a frequency 1550 cm^{-1} of the amide II band can, therefore, be assigned as the characteristic band of the structure of collagen, while the sub-band at

1535 cm^{-1} can be assigned to the randomly coiled form of collagen (hot-cast gelatin). The above assignment of the sub-bands is in good agreement with the similar work by Huc and Sanejouand (55) who assigned the bands of frequencies 1650 cm^{-1} and 1530 cm^{-1} as those of the randomly coiled structure of collagen.

The two absorption bands at frequency of 1450 cm^{-1} and 1235 cm^{-1} (amide III) are the remainder two of the five most intensive peaks in the spectrum. The band at 1450 cm^{-1} which corresponds to the CH_2 deformation and CH_3 asymmetric deformation has changed neither in its frequency nor in intensity upon denaturation. The amide III band at frequency 1235 cm^{-1} , however, shows a markedly reduced intensity in the hot-cast gelatin spectrum compared to the intensity in the collagen spectrum.

The spectrum of cold-cast gelatin is intermediate in character between native collagen and hot-cast gelatin. The NH stretch band frequency is 3320 cm^{-1} , which is in between the frequencies 3330 cm^{-1} of collagen and 3300 cm^{-1} of hot-cast gelatin. The apparent frequencies of amide I and II bands are 1650 cm^{-1} and 1540 cm^{-1} respectively. The intensity of the amide III band at 1235 cm^{-1} is much stronger than in hot-cast gelatin spectrum but is significantly smaller than in collagen.

An attempt was made to use the intensity of the amide III band as an index of helical content. For this, the absorbance of amide III band, A_{1235} was normalized by the

TABLE III-5 CHANGES IN IR SPECTRUM OF COLLAGEN DUE TO DENATURATION (Comparison between collagen and hot-cast gelatin spectra on five most intensive bands)

<u>Absorption Band</u>	<u>Collagen</u>	<u>Hot-cast gelatin</u>
NH stretch	3330 cm^{-1}	3300 cm^{-1}
Amide I(a)	1655	1636
Amide II(b)	1550	1535
1445-1455 cm^{-1} (c)	1450	1450
Amide III(d)	1235	1235

(a) and (b): Frequency shifts are apparent shifts due to the changes in relative intensity of sub-bands, 1655 cm^{-1} , 1635 cm^{-1} and 1550 cm^{-1} , 1535 cm^{-1} .

(c): No change was observed in intensity.

(d): Intensity is much lower in hot-cast gelatin than in collagen spectrum.

TABLE III-6 SUB-BANDS OF AMIDE I AND II ABSORPTION
BANDS IN COLLAGEN AND HOT-CAST GELATIN
SPECTRA

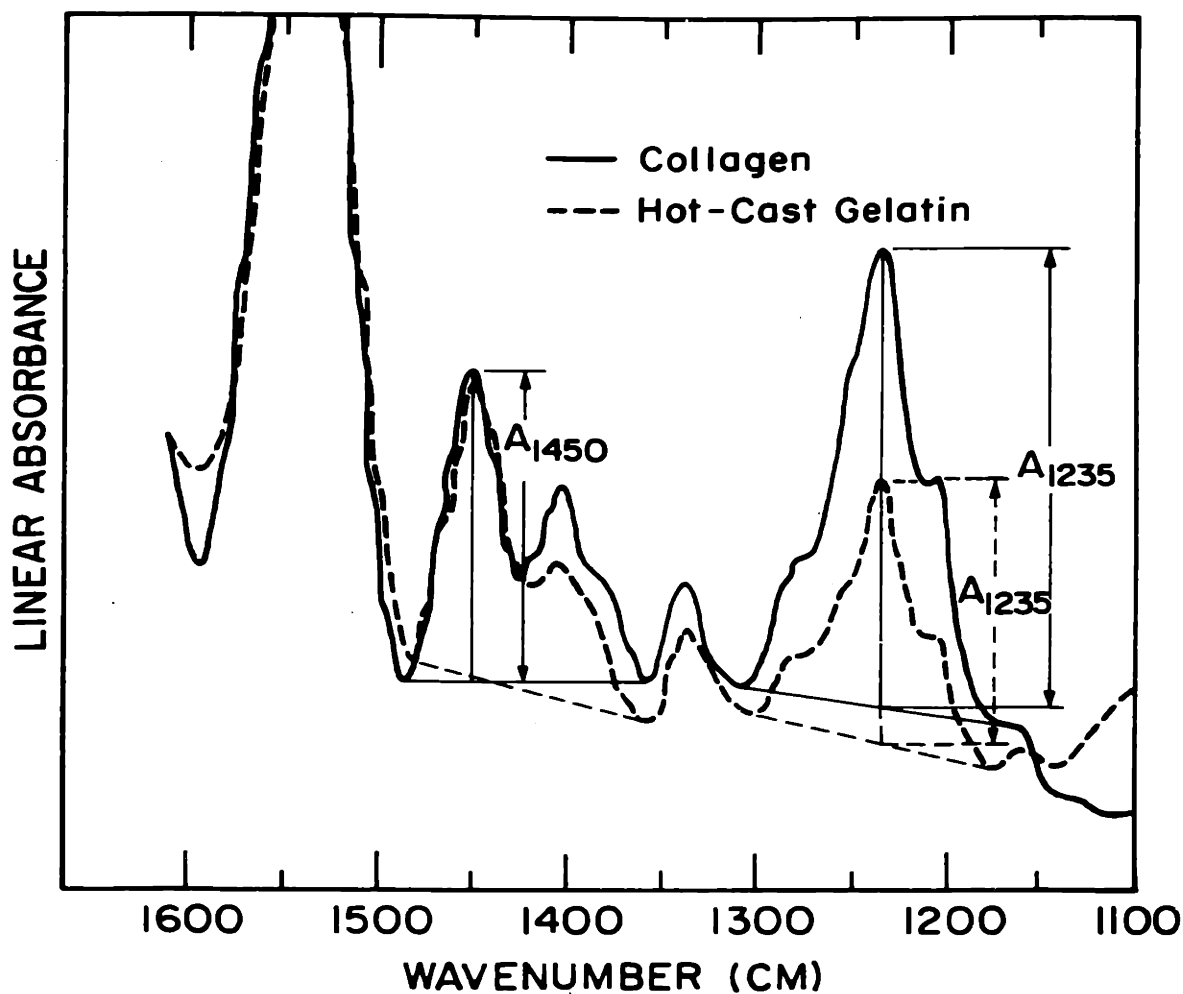
Band	Frequencies, cm^{-1}	Remarks
Amide I-----	1685	
	1675	
	1670	
	1665	
	1655-----	strongest in collagen
	1645	
	1635-----	strongest in hot-cast gelatin
	1625	
	1620	
	Amide II-----	1580
1570		
1560		
1555		
1550-----		strongest in collagen
1545		
1535-----		strongest in hot-cast gelatin
1525		
1520		
1505		

absorbance of the 1450 cm^{-1} band, A_{1450} , because neither the intensity nor the frequency of this band is changed upon denaturation. Figure III-12 shows the absorbance of these two bands for collagen and hot-cast gelatin. The ratio, A_{1235}/A_{1450} , thus obtained was varied from 1.35 ± 0.10 for collagen to 0.89 ± 0.03 for hot-cast gelatin and cold-cast gelatin showed a value of 1.10 ± 0.05 . By assigning the values 1.35 and 0.89 as the characteristic ratio of A_{1235}/A_{1450} for 100% helix and 100% random coil respectively, the helical content of the cold-cast gelatin film was estimated as follows:

$$\% \text{-Helix} = \frac{(1.10 \pm 0.05) - (0.89 \pm 0.03)}{(1.35 \pm 0.10) - (0.89 \pm 0.03)} \times 100 = 45 \pm 16\%$$

(The "%-Helix" obtained is the relative helicity with respect to the helicity of native collagen and is not necessarily the absolute helicity of the polypeptide chains in cold-cast gelatin.)

The interpretation of the IR spectra of complex macromolecules, such as collagen, is far from being clear. Nevertheless, it can be clearly shown that the qualitative identification of collagen in different molecular conformational states, namely, crystalline native and amorphous denatured collagen, can be clearly shown by the infrared spectrum. A quantitative characterization of the molecular conformation of semi-crystalline collagen (cold-cast gelatin) using the ratio of the absorbance of the 1235 cm^{-1} band and the 1450 cm^{-1} band can provide reasonably good



$$R = A_{1235} / A_{1450}$$

Collagen : 1.35 ± 0.10
 Hot-Cast Gelatin : 0.89 ± 0.03
 Cold-Cast Gelatin : 1.10 ± 0.05

Figure III-12 Ratio of absorbance of the 1235cm⁻¹ band to 1450cm⁻¹ band in collagen, cold-cast gelatin and hot-cast gelatin

quantitative data. However, this method seems to be of small practical importance considering the other sensitive method, such as optical rotation measurements, demonstrated in the next chapter.

2.4 Summary

The infra-red spectroscopic basis for the characterization of crystalline (native) collagen and amorphous collagen (gelatin) was established. From the IR spectra of collagen and hot-cast gelatin films, the following major changes were observed which lead to the assignment of certain characteristic absorption bands to different state of collagen.

(i) NH stretch vibrational frequency of native collagen is 3330 cm^{-1} . It shifts to 3300 cm^{-1} in hot-cast gelatin.

(ii) The amide I absorption band is a multiplet, consisting of many sub-bands. Of these, the sub-bands of frequency 1655 cm^{-1} and 1635 cm^{-1} are the characteristic amide I bands for collagen and hot-cast gelatin respectively.

(iii) Similarly, the amide II absorption band is multiplet, and the 1550 cm^{-1} sub-band is the characteristic amide II band of collagen whereas the 1535 cm^{-1} sub-band is characteristic of hot-cast gelatin.

(iv) The frequency of the amide III band, 1235 cm^{-1} , remains unchanged; however, the intensity of the band

reduces significantly upon denaturation of collagen to gelatin.

(v) The IR spectra of cold-cast gelatin (semi-crystalline collagen) is intermediate in character between those of collagen and hot-cast gelatin.

(vi) The helical content of cold-cast gelatin is estimated to be $45\% \pm 16\%$, using the ratio of the absorbance of the 1235 cm^{-1} band to the 1450 cm^{-1} band.

REFERENCES FOR CHAPTER III

1. Pauling, L. and Corey, R.B. (1951) Proc. Nat. Acad. Sci. U.S.A., 37, 235-282
2. Perutz, M.E., Bolton, W., Diamond, R., Muirhead, H., Will, G. and North, A.C.T. (1960) Nature, 185, 416
3. Kendrew, J.C., Bodo, G., Dintzis, H.M., Parrish, R.G. Wyckoff, H. and Phillips, D.C. (1958) Nature, 181, 662
4. Watson, J.D. and Crick, F.H.C. (1953) Nature, 171, 737
5. Ibid., Nature, 171, 964
6. Wilkins, M.H.F., Stokes, A.R. and Wilson, H.R. (1953) Nature, 171, 737
7. Bernal, J.D. and Fankuchen, J. (1941) J. Gen Physiol. 25, 111
8. Watson, J.D. (1954) Biochim. Biophys. Acta 13, 10
9. Ramachandran, G.N. and Kartha, G. (1954) Nature, 174, 269
10. Ramachandran, G.N. and Kartha, G. (1955) Nature, 176, 593
11. Rich, A. and Crick F.H.C. (1955) Nature, 176, 915
12. Cowan, P.M., McGavin, S. and North, A.C.T. (1955) Nature, 176, 1062
13. Bear, R.S. (1956) J. Biophys. Biochem. Cytol. 2, 363
14. Ramachandran, G.N. (1967) in Treatise on Collagen, Vol. 1. Chap. 3, Ed. by Ramachandran, G.N., Academic Press, N.Y. and London
15. Rich, A. and Crick, F.H.C. (1961) J. Mol. Biol., 3, 483
16. Cochran, W., Crick, F.H.C. and Vand, V. (1952) Acta Cryst., 5, 581
17. Crick, F.H.C. (1953) Acta Cryst., 6, 685
18. Lang, A.R. (1956) Acta. Cryst., 9, 436
19. Ramachandran, G.N. (1960) Proc. Indian Acad. Sci., 52, 240

20. Wilson, H.R. (1966) Diffraction of X-rays by Proteins, Nucleic Acids and Viruses, Edward Arnold Ltd, London
21. Alexander, L.E. (1969) X-ray Diffraction Methods in Polymer Science, John Wiley and Sons Inc.
22. Crick, F.H.C. (1953) Acta Cryst., 6, 689
23. Cowan, P.M., North, A.C.T. and Randall, J.T. (1953) in Nature and Structure of Collagen ed. by J.T. Randall p.241 Buttenworth, London
24. Cowan, P.M., North, A.C.T. and Randall, J.T. (1955) Symp. Soc. Exp. Biol. 9, 115
25. Rich, A. and Crick, F.H.C. (1961) J. Mol. Biol. 3, 483
26. Ramachandran, G.N. and Sasisekharan, V. (1965) Biochim. Biophys. Acta., 109, 314
27. Rouguie, M.A. and Bear, R.S. (1953) J. Am. Leather Chem. Assoc. 48, 735
28. Sasisekharan, V. and Ramachandran, G.N. (1957) Proc. Indian Acad. Sci. A45, 363
29. Stokes, A.R. (1955) Progress in Biophys. 5, 140
30. Stein, R.S. (1958) J. Poly. Sci. 31, 327
31. Stein, R.S. and Norris, F.H. (1956) J. Poly. Sci. 21, 381
32. Müller, F.H. (1941) Kolloid-Z. 95, 172 and 307
33. Alexander, L.E. (1969) X-ray Diffraction Method in Science, Wiley-Interscience p 423
34. Flory, P.J. and Garrett, R.R. (1958) J. Am. Chem. Soc. 80, 4836
35. Lakshmanan, B.R., Ramachrishnan, C., Sasisekharan, V. and Thathachari, Y.T. (1962) in Collagen Ed. by Ramanathan, N. p 135. Wiley, N.Y.
36. Arndt, U.W., and Riley, D.P. (1954) Phil. Trans. Roy. Soc., London, A247, 409
37. Yannas, I.V. (1972) J. Macromol. Sci.--Revs., c7, 49
38. Bradbury, E.M. and Martin, C. (1952) Proc. Roy. Soc., A214, 183

39. Katz, J.R., Derksen, J.C. and Bon, W.F. (1931) Rec. Trav. Chim. Pays-Bas, 50, 725
40. von Hippel, P.H. and Harrington, W.F. (1960) Brookhaven Symp. Quant. Biol., 13, 213
41. Harrington, W.F. et al. (1970) Biochem. 9, No. 9 September
42. Ambrose, E.J. and Elliott, A. (1951) Proc. Roy. Soc. A206, 206
43. Fraser, R.D.B. (1950) Disc. Faraday Soc. 9, 378
44. Fraser, R.D.B and Price, W.C. (1952) Nature 170, 490
45. Fraser, R.D.B. and Price, W.C. (1953) Proc. Roy. Soc. B141, 66 (1953)
46. Sutherland, G.B.B.M. (1952) Adv. Protein Chem. 7, 291
47. Berger, A., Kurtz, J. and Katchalski, E. (1954) J. Am. Chem. Soc. 76, 5552
48. Badger, R.M. and Pullin, A.D.E. (1954) J. Chem. Phys. 22, 1142
49. Miyazawa, T. and Blout, E.R. (1961) J. Am. Chem. Soc. 83, 712
50. Bradbury, E.M., Burge, R.E., Randall, J.T. and Wilkinson, G.R. (1958) Disc. Faraday Soc. 25, 173
51. Sutherland, G.B.B.M., Tanner, K.N., and Wood, D.L. (1954) J. Chem. Phys. 22, 1621
52. Fraser, R.D.B. and MacRae, T.P. (1958) J. Chem. Phys. 29, 1024
53. Fraser, R.D.B. and MacRae, T.P. (1959) J. Chem. Phys. 31, 122
54. Beer, M., Sutherland, G.B.B.M., Tanner, K.N. and Wood, D.L. (1959) Proc. Roy. Soc. A249, 147
55. Huc, A. and Sanejouand, J. (1968) Biochim. Biophys. Acta, 154, 408
56. Nakamoto, K., Margoshes, M. and Rundle, R.E. (1955) J. Am. Chem. Soc., 77, 6480

CHAPTER IV

OPTICAL ROTATORY DISPERSION (ORD) AND CIRCULAR DICHROISM (CD) STUDIES OF COLLAGEN AND GELATIN

IV-1 Introduction

In the last decade, since the rebirth of interest in optical activity (1), the study of optical activity has progressed very rapidly both in theories and instrumentation and has become one of the most powerful tools for the conformational study of polypeptides and proteins. Initial application of the optical activity method in the early 1950's was primarily on the structural, stereochemical and conformational problems in rather simple organic molecules (1). The revival of the optical rotatory dispersion method in the study of proteins and peptides structures occurred between 1955 and 1960, when new experimental and theoretical tools became available. This was greatly encouraged by the fact that the helical structures, proposed for polypeptides (2) and polynucleotides (3) in the last decade, have asymmetry, which gives rise to the optical activity and that model substances of the polyamino acids were synthesized (4) which helped the protein chemist considerably in the interpretation of the data obtained with proteins.

Major attempts were made in this period to classify the proteins according to their conformations (5,6,7). The semi-empirical equations of Drude (8) and Moffit-Yang

(9) have been the major analytical tools in describing the optical rotatory dispersion (ORD) data, particularly that of helical macromolecules. However, neither of the two equations was satisfactory for the studies of non-helical proteins (10). Recent discoveries of Cotton effect of poly-amino acids and proteins (11-13) in the far ultraviolet region provided more sensitive data than was the case with the ORD data in the UV-visible region; this allowed more insight into the conformation of non-helical proteins (10, 14).

In this chapter, we propose to outline the fundamental principles of the optical rotatory properties of the collagen molecule and to apply them to the study of collagen structure in various conformational states (native and denatured) both in dilute solution and in the solid state.

IV-2 General Considerations of ORD and CD

2.1 Phenomenon of Optical Activity, Terms and Definitions

The phenomenon of optical activity was first discovered by the French scientist, Biot, more than 150 years ago. Since then, the theoretical aspect of the phenomenon and its wavelength dependence (ORD) had been studied by many scientists including Lowry (15), Drude (8), Kuhn (16), Rosenfeld (17), Kirkwood (18), Eyring and his coworkers (19), Moffitt (20) and Moscovitz (21). Many reviews have also appeared both on theoretical and experimental aspects of optical activity (6,22,24,50). It is, therefore, not

intended here to discuss the details of the theory, but to provide only a brief description of the phenomenon of optical activity.

When plane polarized light enters an optically active medium, it splits up into two circularly polarized waves, known as a left- and a right-handed component. (See Figure IV-1 (a)). Due to the right- or left-handed character of the medium (or asymmetry in structure), these two circularly polarized light waves travel through it with slightly different velocities, corresponding to the different refractive indices n_l and n_r for left- and right-handed light (Figure IV-1 (b)). After passing through the medium, there will be a phase difference between these two waves and upon their recombination, the plane of polarization of the emergent light will have been rotated (Figure IV-1 (b)).

In classical electromagnetic theory, the condition for optical activity is given as follows (33):

$$m = -(\beta/c) \partial \tilde{H} / \partial t \quad (1)$$

$$u = (\gamma/c) \partial \tilde{E} / \partial t \quad (2)$$

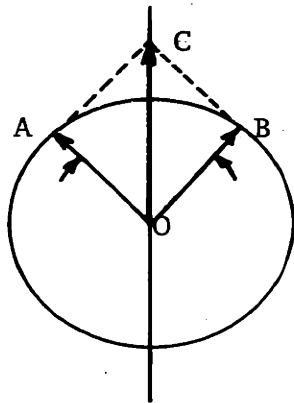
where m , u are the induced electric and magnetic moments, H , E are the magnetic and the electric field of the incident light, c is the velocity of light and β , γ are constants determined by the structure. (β and γ can be shown to be equal in magnitude and the contribution of electric and magnetic fields to the optical activity is therefore the same (33)). The condition above indicates that the optically active material must have a property of inducing electric and magnetic moments when light, an electromag-

netic wave, enters the medium. It has been demonstrated (25) that the induced magnetic and electric moments do not vanish only when the molecule does not have symmetry. This is why the asymmetric molecules are known to be optically active.

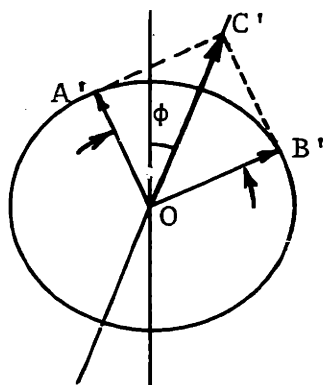
If the events occur at a wavelength far from the absorption bands, the difference in velocities of left- and right-handed circularly polarized light can be expressed in terms of the difference in refractive indices n_l and n_r and the degree of rotation therefore depends on the magnitude of the $\Delta n = n_l - n_r$. If the events occur near and at the absorption bands, however, unequal absorption of the left and the right circularly polarized light occurs in addition to the unequal velocity, which results in elliptically polarized light (Figure IV-1 (c)). This phenomenon is known as circular dichroism and the combined phenomenon of unequal velocity and unequal absorption of the left and the right circularly polarized light is known as "Cotton effect" (26).

For the isolated single absorption band, general spectra for the cases of absorption, optical rotatory dispersion (ORD) and circular dichroism (CD) are shown schematically in Figure IV-2.

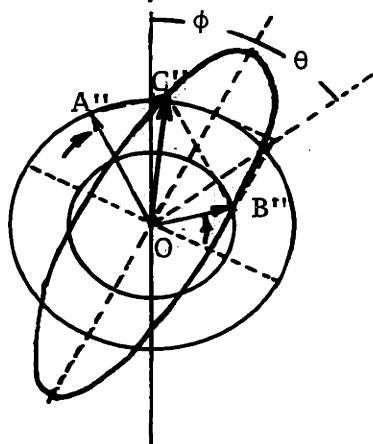
For the quantitative expression for ORD and CD, several different terms have been defined. Biot introduced the term "specific rotation $[\alpha]_\lambda$ ".



- a) OC---linearly polarized light
 OA,OB---left- and right-handed circularly polarized light



- b) linearly polarized light (OC') rotated through an angle ϕ due to the phase difference of 2ϕ between OA' and OB'



- c) elliptically polarized light (OC''). rotation angle is due to the phase difference between OA'' and OB''. ellipticity angle θ is due to the difference in absorption of OA'' and OB''

Figure IV-1 Schematic presentation of plane polarized and circularly polarized light

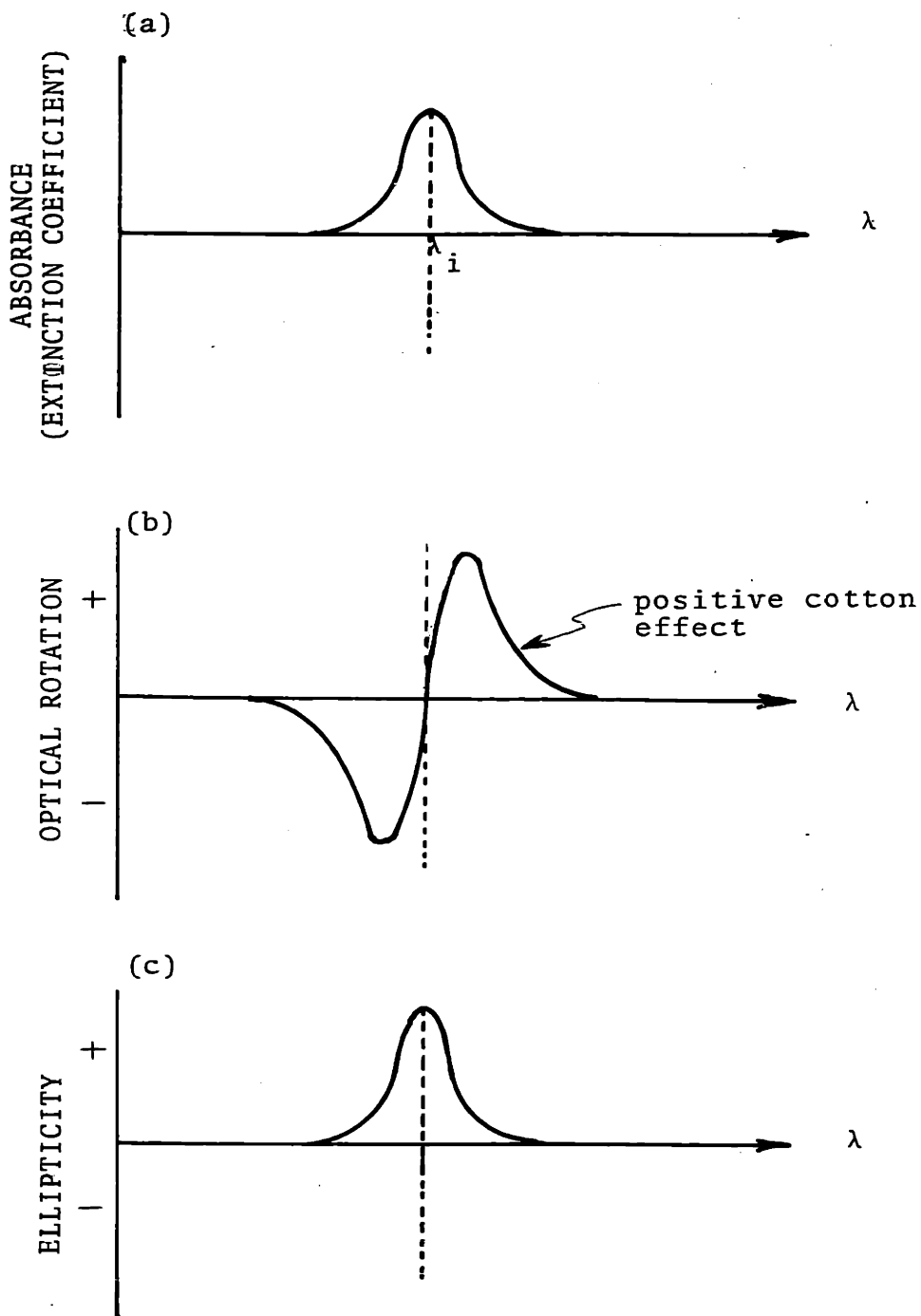


Figure IV-2 Cotton effect for isolated absorption band at λ_i ((a)Absorption, (b)ORD,(c)CD)

$$[\alpha]_{\lambda} = \frac{100 \cdot \alpha_{\lambda}}{\ell \cdot c} \quad (3)$$

where α_{λ} is a rotation angle of the plane of the polarization in degrees at a wavelength λ , ℓ is the pathlength of the sample in decimeters, c is the concentration of the optically active medium in grams/100 ml. For ℓ' in cm and c' in g/cm³,

$$[\alpha]_{\lambda} = \frac{10 \cdot \alpha_{\lambda}}{\ell' \cdot c'} \frac{\text{degrees-cm}}{\text{gram}} \quad (3')$$

The "molar rotation, $[M]$ " is related to the specific rotation by

$$[M]_{\lambda} = \frac{M}{100} [\alpha]_{\lambda} \quad (4)$$

where M is the molecular weight of the sample. For the optical rotation of polymeric substances, the "mean residue rotation, $[m]$ " is defined as below

$$[m]_{\lambda} = \frac{MRW}{100} [\alpha]_{\lambda} \frac{\text{degrees-cm}}{\text{decimole}} \quad (4)$$

in which MRW is the mean residue weight. The ORD depends significantly on the refractive index of the solvent and a correction factor has been introduced (6) to eliminate the variations in rotation due to the solvents (Lorenz correction factor). The corrected rotation is then known as "Reduced mean residue rotation, $[m']_{\lambda}$ ";

$$[m']_{\lambda} = \frac{3}{n^2 + 2} [m]_{\lambda} = \frac{3}{n^2 + 2} \frac{MRW}{100} [\alpha] \quad (6)$$

where n is the refractive index of the solvent. The MRW/100 values vary between 1.0 and 1.2 for most proteins (for collagen, 0.92) and the whole correction factor $MRW/100 \cdot 3/(n^2 + 2)$ is approximately 0.79; (for collagen, 0.74) at the longer wavelengths (10). CD is also expressed in a variety of different forms and the following quantities are among those most frequently appearing in the lit-

erature.

The "Ellipticity, θ " is defined as the arc tangent of the ratio of minor to major axes of the elliptically polarized light (Figure IV-1) so that

$$\theta = \tan^{-1} (b/a) \text{ (degrees)} \quad (7)$$

CK data are often reported in terms of the difference in the extinction coefficient of the sample for left and right circularly polarized light. This is known as "Molar circular dichroism, $\Delta\epsilon$ " and $\Delta\epsilon = \epsilon_L - \epsilon_R$ (liters/mole-cm) (8)

For the purpose of comparing the CK of different samples, a quantity called "Molecular ellipticity, $[\theta]$ " is commonly used which is defined as

$$[\theta] = \frac{180}{\pi} \frac{\theta}{l'c'} \frac{M}{10} = \frac{\theta^\circ}{10} \frac{M}{l'c'} \frac{\text{degrees-cm}^2}{\text{decimole}} \quad (9)$$

where θ is the measured ellipticity (in equ. (7)) in radians (θ° is in degrees)

l' is the path length of the sample in cm

M is the molecular weight of the sample in daltons

c' is the concentration in grams per cm^3 .

θ in equation (9) is related to $\Delta\epsilon$ in equation (8) in the following manner.

$$\theta = 3300 \cdot \Delta\epsilon \quad (10)$$

(For the derivation of this relationship, see reference 54, page 154)

2.2 Drude Equation

As is true of many other optical properties, the op-

tical rotation also depends on the wavelength of light, a phenomenon known as optical rotatory dispersion (ORD). A quantitative of ORD in spectral regions far from the absorption bands was first proposed by Drude (18). Using the theory of classical electromagnetic interaction with electrons, Drude derived the following equation (known as the Drude Equation) based on a model of electrons moving along a helical path.

$$[\alpha]_{\lambda} = \sum_i \frac{K_i}{\lambda^2 - \lambda_i^2} \quad (11)$$

where λ_i is the wavelength of the optically active absorption band and K_i is a constant proportional to the rotational strength of the i th electronic transition. Each term (called partial rotation) represents the contribution of a single transition (i th) and the overall rotation is the sum of all the partial rotations.

Experimental studies with many substances were shown to obey the "simple Drude equation" which is a simplified form of equation (11):

$$[\alpha]_{\lambda} = \frac{A}{\lambda^2 - \lambda_c^2} \quad (12)$$

in which λ_c , called the dispersion constant, is the wavelength corresponding to a dominant electronic transition and A , named the rotatory constant, is a constant characteristic of the given system.

The applicability of the simple Drude equation to a given set of data as well as the determination of constants A and λ_c are essentially based on a graphical procedure.

If any of the plots of $1/[\alpha]_{\lambda}$ vs λ^2 (15), $1/[\alpha]_{\lambda} \cdot \lambda^2$ vs $1/\lambda^2$ (29), or $[\alpha]_{\lambda} \cdot \lambda^2$ vs $[\alpha]_{\lambda}$ (30), is a straight line, the ORD is classified as "simple dispersion" while data which deviate from a straight line are classified as "complex dispersion". In general, globular proteins (both native and denatured) and polypeptides with a random coil conformation show simple dispersion whereas the helical polypeptides (α -helix) exhibit the complex dispersion (6). The values for λ_c of many proteins were obtained in the past and tabulated in the review paper by Urnes and Doty (6). For most proteins, λ_c varies from 180 $m\mu$ to 290 $m\mu$. The significance of this value in relation with the structural characteristics of proteins is not clearly understood (10).

2.3 Moffitt-Yang Equation

As mentioned above, the ORD data of many proteins and particularly those possessing a helical conformation show complex dispersion. This can be treated adequately in linear form by adding a second term to the simple Drude equation as suggested by Lowry (15) and Heller (29).

This is known as the "two term Drude equation".

$$[\alpha]_{\lambda} = \frac{A_1}{\lambda^2 - \lambda_1^2} + \frac{A_2}{\lambda^2 - \lambda_2^2} \quad (13)$$

This treatment is good for empirical comparisons, but a more theoretical approach was attempted by Moffitt (20) in correlating ORD of proteins to the helical secondary structure of the α -helix of Pauling and Corey. He deduced the

phenomenological equation for ORD in wavelengths far from the absorption bands in the following form:

$$[m']_{\lambda} = \sum_i \frac{a_i \lambda_i^2}{\lambda^2 - \lambda_i^2} + \sum_i \frac{b_i \lambda_i^4}{(\lambda^2 - \lambda_i^2)^2} \quad (14)$$

The equation shows that the optical rotation per monomer unit (or amino acid residue) is the sum of the partial rotations from each i -th optically active electronic transition. The second term in the equation gives rise to the curvature in ORD spectra. For the practical application of the theory to experimental data, Moffitt and Yang (9) modified the original equation to the simplified form

$$[m']_{\lambda} = \frac{a_0 \lambda_0^2}{(\lambda^2 - \lambda_0^2)} + \frac{b_0 \lambda_0^4}{(\lambda^2 - \lambda_0^2)^2} \quad (15)$$

This equation has three adjustable parameters, namely, a_0 , b_0 and λ_0 . As with the Drude equation, the test of the applicability and the determination of parameters a_0 , b_0 are normally done graphically by plotting $[m']_{\lambda}(\lambda^2 - \lambda_0^2)$ against $1/(\lambda^2 - \lambda_0^2)$ using arbitrary values of λ_0 and finding out the λ_0 which would yield the best straight line.

A significant volume of ORD study has been done with synthetic polypeptides of α -helical form, of which the structural information has been well established from other studies such as X-ray diffraction, IR spectroscopy, light scattering, hydrodynamic studies. Among many synthetic polypeptides, poly- α -benzyl-L-glutamate (PBLG) and poly-L-glutamic acid (PGA) are representative (9,30,32).

Extensive ORD data for many synthetic polypeptides have been well tabulated by Urnes and Doty (6).

In the light of theory, and on the basis of experimental findings obtained from synthetic polypeptides of known structure, the following generalization was made on the characteristics of the Moffitt parameters, a_0 , b_0 and λ_0 (6). The constant a_0 represents the intrinsic rotation of the constituent residues and their interactions within the structure. This is equivalent to the rotatory constant A in simple Drude equation (12) and varies with solvent and side chain composition. The constants b_0 and λ_0 are primarily a function of secondary structure and are relatively insensitive to the environment. The b_0 values of many known α -helical polymers centered around -630, whereas those of random coil polymers were near zero. The λ_0 of most of the polypeptides which give the best straight line in the Moffitt plot of ORD was $212 \pm 5 \text{ m}\mu$. By the use of characteristic b_0 values of -630 for complete helix and 0 for random coil, helical content of the partially helical polypeptides has been estimated from the ratio of measured b_0 value to the value, 630 of the 100% helix (90,91) (i.e. % Helix = $(b_0/630) \times 100$). This requires the fixed value of λ_0 ($212 \text{ m}\mu$) in the estimation of b_0 values. Many exceptions have been found, of course, for the above general statement and, in particular, non-zero values of b_0 were found in many random coil polymers (32, 34,35). Despite some exceptions on the b_0 values of random coil and

the question on the universally fixed value of $\lambda_0 = 212 \text{ m}$ for both helix and random coil, the estimation of helix content by the " b_0 method" is still being considered as the best method (36). In summary, the Moffitt-Yang equation is an explicitly phenomenological equation which can describe the ORD of many helical polypeptides at visible and near UV regions with constants a_0 , b_0 , and λ_0 . The form of the equation has theoretical origin but is known to be not unique to helix (37). However, in general, λ_0 , b_0 and a_0 can complete the characterization of any single set of data by use of the Moffitt-Yang equation.

2.4 Cotton Effect and CD

So far, we have discussed the ORD in the visible and near UV regions where the Drude and Moffitt equations are valid. In the far UV region (180-240 μ), most proteins have strong absorption bands and because of the fact that the same electronic transitions are responsible also for the optical activity, ORD appears with much more complex dispersion than in the visible region.

Typically, as the wavelength approaches to the absorption band, the OR exhibits maximum (minimum), zero, minimum (maximum) around the absorption band. (Figure IV-2 (b)), which is very different from the ORD in visible region where the OR decreases monotonically with increasing wavelength. This was first discovered by Cotton in 1895, who also found that plane polarized light became ellipti-

cally polarized due to the unequal absorption of left- and right-handed circularly polarized components of the plane polarized light. This latter phenomenon (known as circular dichroism) as well as the observation of anomalous ORD in the far UV region are both called "Cotton Effect".

The relationship between absorption, ORD and CD for isolated optically active absorption band is shown schematically in Figure IV-2.

The Cotton Effect is called "negative" when the negative extremum occurs at the long wavelength side and is "positive" when the positive extremum is at the long wave side. The theoretical treatment of OR in regions of absorption was carried out by Kuhn and Freudenberg (38) based on a classical coupled oscillator model and also by Moffitt and Moscowitz (39) by quantum mechanical approaches. Details of these treatments can be found in many reviews (24,41).

In brief, the following relations were derived between the absorption, OR and CD parameters. Rosenfeld (19) expressed OR as a sum of partial rotations as follows:

$$[m']_{\lambda} = \frac{96\pi N}{hc} \sum_i R_i \frac{\lambda_i^2}{(\lambda^2 - \lambda_i^2)} \quad (16)$$

where $[m']_{\lambda}$ is the OR at λ , N is Avogadro's number, h is Planck's constant, c is the velocity of light, λ_i is the wavelength of the absorption maximum of the i_{th} electronic transition and R_i is the so-called "partial rotation-

al strength". The rotational strength, R_i is related to Cotton effect parameters in the following manner.

$$R_i = \frac{hc}{96\pi N} \frac{A_i G_i}{\lambda_i} \quad (17)$$

in which G_i is called "damping factor" and A_i is magnitude of Cotton effect which can be obtained from experimental data as shown in Figure IV-3. The rotational strength R_i can also be related to the CD data according to Moscowitz (21,27) who derived the following relationship using the Kronig-Kramer's reciprocal relations.

$$R_i \cong 0.696 \times 10^{-42} \pi [\theta]_i^{\circ} \frac{\Delta_i^{\circ}}{\lambda_i^{\circ}} \quad (18)$$

where $[\theta]_i^{\circ}$, Δ_i° and λ_i° are the diagnostic parameters of partial dichroism curves associated with the i -th transition which is assumed as Gaussian inform for isolated transition (See Figure IV-4).

$$[\theta]_i = [\theta]_i^{\circ} \exp\{-(\lambda - \lambda_i^{\circ})^2 / (\Delta_i^{\circ})^2\} \quad (19)$$

Δ_i° is the half width and λ_i° is the wavelength at which $[\theta]_i$ is maximum. (Δ_i° is equivalent to half width of the absorption band or the damping factor G_i in equation (17), and also in Figure IV-3). In principle, one can, therefore, analyze the Cotton effect and correlate OR with CD as long as the absorption bands are isolated from each other so that an assessment of R_i is possible: in practise, however, the ideal shape of the Cotton effect occurs very rarely (1),

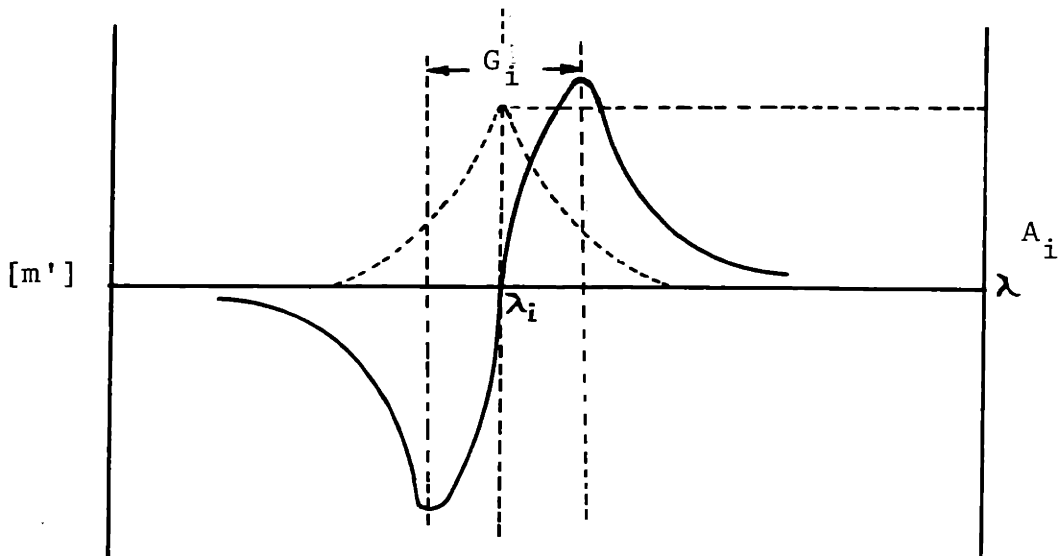


Figure IV-3 Positive cotton effect and absorption
 solid curve--OR, dotted curve---Absorption
 A_i ; amplitude of cotton effect
 G_i ; damping factor or half band width

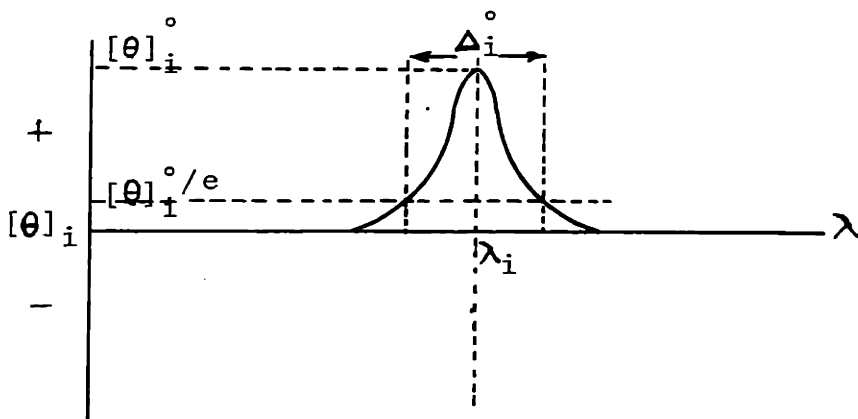


Figure IV-4 CD spectra in Gaussian form

and mostly the curves are more complex due to the superposition of many partial rotations, each with its own Cotton effect. The assessment of R_i 's, accordingly, is very difficult.

Identification of absorption bands and their relation to the Cotton effect is further complicated by the fact that not all the absorption bands are optically active; some weak absorption may have strong rotation and vice versa (28). (This is because absorption is related only to the electric moments of the transition whereas optical activity results from a product of electric and magnetic moments (33)).

In spite of the difficulties in interpreting the actual experimental data, advances have been made in the application of the Cotton effect to the conformational features of many synthetic polypeptides. In particular, CD has been actively used in the study of α -helical, random coiled and β -structure polypeptides (36,14,40). Recently, CD has more popularity than the ORD due to the fact that CD gives more discrete spectral bands than ORD, which normally gives strong overlap, and, therefore, CD provides better resolution for absorption bands. Typical CD spectra for three conformations (α -helical, β and random coil), are shown in Figure IV-5.

These spectra are considered to be unique to each conformation. Based on this, Greenfield and Fasman (40) have developed a method for the estimation of α -helical

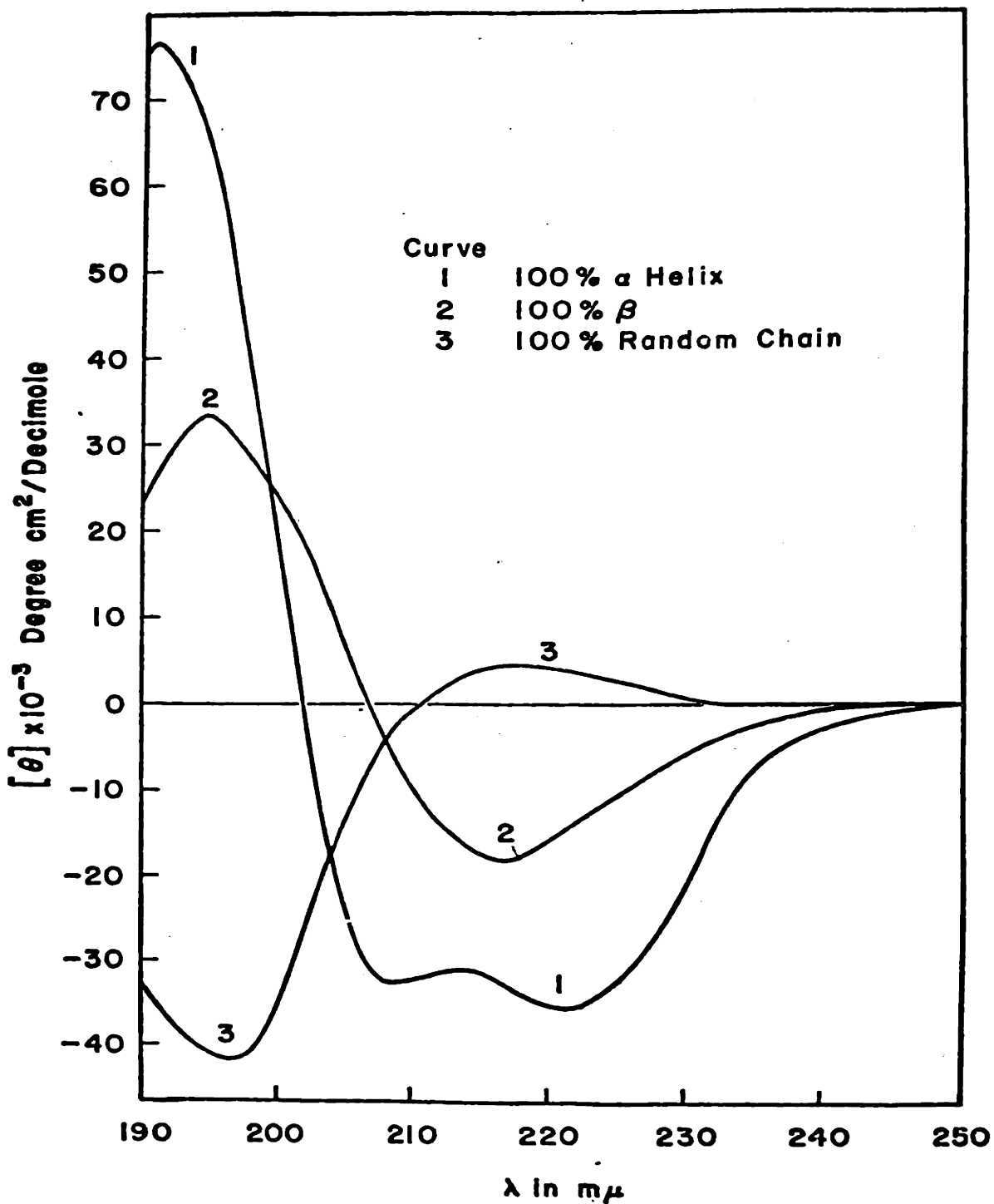


Figure IV-5 Typical CD spectra of polypeptides of α -helical, β , and randomly coiled conformations

content in many proteins and peptides.

IV-3. ORD and CD of Collagen and Gelatin

3.1 Introduction

Despite the fact that the optical rotatory dispersion (ORD) technique has been actively used in the study of conformations of the α -helix, of β -structure and of random coil proteins (6), ORD of collagen has received much less attention and has been considered as an exception to the generalization established empirically in other proteins (6,42). Major characteristics in ORD of collagen in dilute solution which differ from other proteins are:

(i) ORD of collagen exhibits simple dispersion (fit to a one term Drude equation) similar to that of random coil proteins, whereas most other synthetic helical polypeptides show complex dispersion (fit to the Moffitt-Yang equation) (42).

(ii) Upon denaturation, the optical rotation of collagen becomes less levorotatory ($[\alpha]_D^{\text{Collagen}} \cong -400$ and $[\alpha]_D^{\text{Gelatin}} \cong -90$ to -120) while the α -helical polypeptides show increased levorotation ($[\alpha]_D^{\text{helix}} \cong -20$ to -40 and $[\alpha]_D^{\text{denatured}} \cong -90$ to -120).

Because of the sensitive changes in OR values during denaturation, OR studies of collagen have played an important role in helix \leftrightarrow coil transformation studies in dilute solution (52).

Most of the early studies (43-47) on OR properties of collagen and gelatin were limited to the dilute solution state at a few wavelengths of light in the visible region. This work has been reviewed by Harrington and von Hippel (42). Little effort was, however, made on ORD and CD of collagen in the far UV region (250 m μ to 190 m μ). Recent progress in ORD studies of collagen and gelatin has been reviewed by von Hippel (54) and by Carver and Blout (53). Application of this technique has, however, not been made to the studies of collagen in solid state.

In this thesis, therefore, attempts are made to establish a basis for the systematic application of ORD to the study of collagen and gelatin in the solid state. Classical physicochemical methods such as viscometry, light scattering, ultracentrifuge, flow birefringence, osmometry etc., which have been used for the study of macromolecules in the dilute solution state, are not applicable to the solid state X-rays, infrared spectroscopy and electron microscopy which are commonly used for the study of macromolecules in the solid state and are, in general, inappropriate for the study of the dilute solutions. The ORD technique can, however, be applicable to studies in both states and establishment of the ORD properties of collagen in the solid state will provide the basis for direct comparison of the chain conformation of collagen in the two different states.

3.2 Experimental

A. Materials

Collagen solution was prepared from rat tail tendon as described in Chapter II of the extraction process. Gelatin solution was prepared by heating the collagen solution at 50° C. for one hour and allowed to cool at room temperature for several hours before its use. Collagen and gelatin films were prepared from the solutions by evaporation. Films used for the ORD measurement in the visible to near UV regions were prepared in the manner described in the section of solution casting in Chapter II. Films for the measurements in the Cotton effect region (250 m μ to 200 m μ) were prepared by casting directly on the quartz plate.

B. Instrument Description

A Cary 60 Spectropolarimeter (manufactured by Cary Instruments, Monrovia, Calif.) was used. Basic features of this instrument are as follows: the light source is a 450-500 Watt Xenon lamp. The monochromator is double prism. The angle of rotation is found by using the Faraday cell which is made of a silica cylinder, surrounded by a coil through which an alternating current is passed. The polarizer and analyser prisms are made of ammonium dihydrogen phosphate and are immersed in cyclohexane. Details of the instrument are described in a publication of Cary

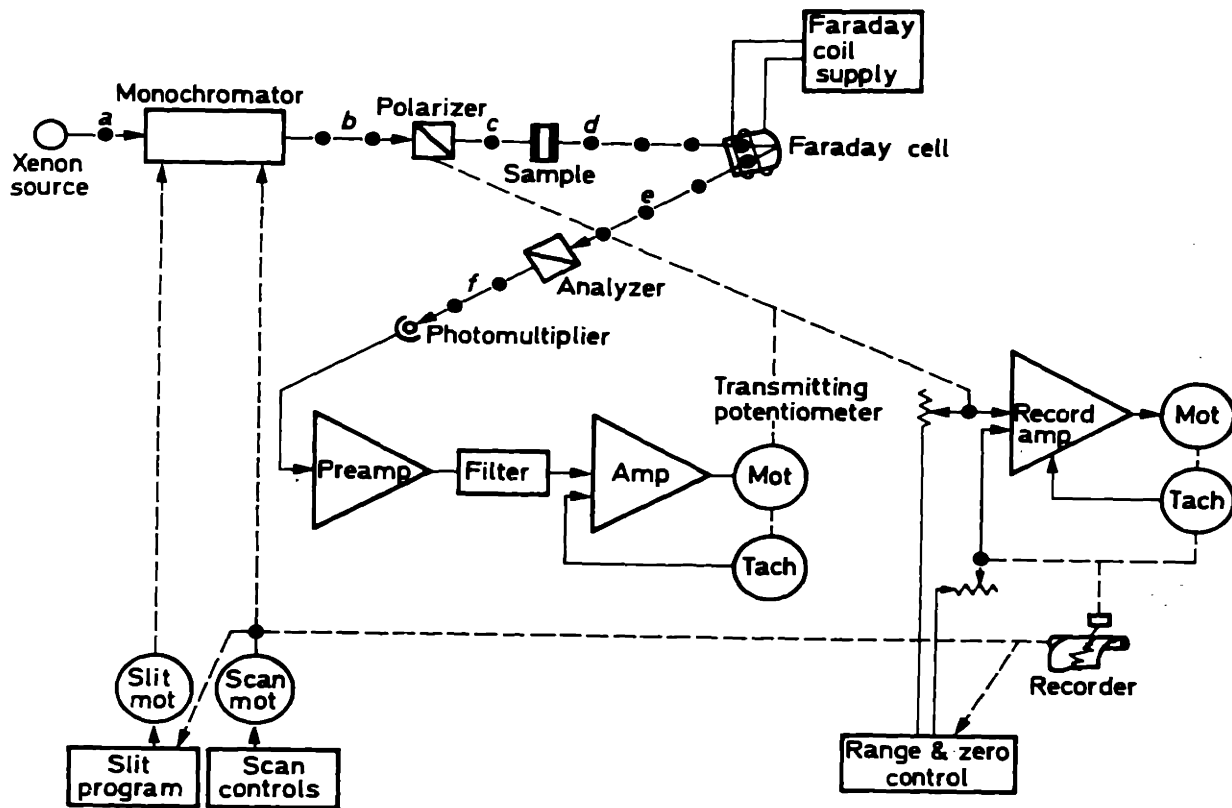
et al. (48). A schematic representation of the instrument is shown in Figure IV-6. The Cary 60 was also equipped with a CD dichrograph (Model 6002), an attachment for CD measurements. The principal part in the CD dichrograph is an electrobirefringent crystal, known as a Pockell cell, which resolves the plane polarized ray into two circularly polarized parts. The principles of the CD measurements are outlined in the book of Velluz, Legrand and Grosjean (54).

C. ORD Measurements from the Visible to Near UV Region
(600 m μ - 250 m μ)

Two factors are dominating in the precision of the measurement of ORD aside from the quality of the machine. They are the absorbance of the sample and the magnitude of the OR of the sample. An ideal sample is one which has high OR with negligible absorbance. Collagen and gelatin solutions are good samples in this respect.

Measurements of the solution were done using a solution cell which is made of spectrograde fused quartz and has an optical pathlength of 1 cm. The concentration of the solution was approximately 0.08%-wt. For each measurement, a baseline was obtained with blank specimen (solvent only). The baseline for 0.05 M acetic acid solution was the same as the baseline for air. The rotation angle was recorded in a continuous manner with changing wavelengths from 600 m μ to 250 m μ .

As in the dilute solution specimen, no difficulties



a=Undispersed, non-polarized beam
b=Monochromatic non-polarized beam
c=Monochromatic polarized beam

d=Beam "c" rotated by sample
e=Beam "d" cyclically displaced by Faraday cell
f=Component transmitted by analyzer

Figure IV-6 Schematic diagram of Cary 60 spectropolarimeter (10)

arose from absorption in the measurements of the collagen and gelatin films. The thickness of the film used for the measurement of ORD in this wavelength region varied from 5 to 10 μ for collagen and 10 to 100 μ for cold- and hot-cast gelatin. Thicker films were not appropriate because the maximum rotation angle the Cary 60 can measure is limited to two degrees, one degree each for positive and negative rotation.

A round brass tube (the inner and outer diameters are 2.0 cm and 2.5 cm, 2.5 cm in length) with degree scales engraved every 3°, 0° to 360°, on the outside wall, was used for a specimen holder on which round specimens of the film (2.5 cm in dia.) were mounted with Scotch Tape. The mounted specimen was placed in front of the polarized light beam such that the plane of the film was perpendicular to the direction of the propagation of the light which passed through the central area of the specimen. This was done by placing the brass sample holder on the V-shaped solution cell holder; the solution cell holder has three adjustable legs and has been prealigned so that when a solution cell or the brass film holder is placed, the beam is normal to the plane of the cell of the film.

Measurements were carried out in three steps. First, the baseline was obtained without a specimen. Second, the OR was measured at a fixed wavelength (normally at 365 m μ) with the specimen rotated around the axis of light propagation. This step was necessary to examine the uniform-

ity of the film and to detect any birefringence the film might have (see Figures II-10, II-11 in Chapter II). If the variation of OR values measured at different positions of the specimen was within 10 % of its average value, the specimen was considered as an acceptable one and a position for the ORD measurement was selected which gave the exact average value of OR. Third, ORD was run with a fixed specimen position from 600 m to 250 m and recorded in the same chart paper on top of the baseline.

D. ORD Measurements in the Far UV Region (250 m μ - 200 m μ)

ORD measurement in the far UV region is more difficult experimentally than in the visible region. Collagen and gelatin, as most other proteins, have absorption bands in this wavelength range which give rise to the Cotton effect. Accordingly, the magnitude of OR increases enormously (i.e. the maximum value of OR in the Cotton region is about 40 times higher than the OR at 365 m μ) as the wavelength approaches an absorption band. This requires a reduction of sample size by the same order of magnitude. At the same time, absorption of the light beam by the specimen increases rapidly as the wavelength approaches 200 m μ and as a result the absolute noise level of the instrument rises to the extent that reliable measurement becomes practically impossible.

For a collagen solution, the appropriate concentration

range was approximately 0.01 %-wt. and that of a gelatin solution was about three or four times higher than collagen. The solution samples were prepared easily by dilution. Film specimens were prepared by casting directly on the quartz surface from the dilute solution. Measurements were done in the same manner as described above.

E. CD Measurements

The procedure for the measurement of CD is exactly the same as that of ORD. The same specimens used for ORD measurements in the Cotton effect region were used also for CD measurements. CD was recorded in terms of the ellipticity θ , expressed in degrees (equation (7)). The molecular ellipticity, $[\theta]$ was calculated according to equation (9). The CD measurements were made in the far UV region (below 260 $m\mu$) because collagen does not have any CD effect in the higher wavelength region. Again, due to the increasing absorption of light by the specimen, as the wavelength approaches 200 $m\mu$, CD measurements were not possible below ca. 200 $m\mu$, especially with gelatin films, which have a lower CD and therefore, thicker films were needed.

F. Other Measurements

In order to calculate the specific rotation $[\alpha]$, (equation (3)), the concentration of the solution, or the density of the film and the optical path length of the specimen used

for each measurement, must be determined.

The concentration of the solution was determined by a gravimetric method as already described in Chapter II. The optical path of the solution samples was 1 cm, which is the fixed dimension of the solution cell used for the entire solution measurements. The thickness of the film was measured by a mechanical method using an Ames dial guage (B.C. Ames Co., Waltham, Mass.) which has a sensitivity of 1.25 μ .

The density of the films was obtained by independent measurements of weight, thickness and area of the film. In order to reduce the relative errors involved in each measurement, thick films (about 100 μ thick) were used. When thin films were used, the apparent density appeared to be much higher than that of thick films (see Figure IV-7). This was interpreted as follows: the water absorbed on the surface of the film will give an error in the measured weight of collagen without affecting the thickness of the film, and thereby yields a higher apparent density due to the false, excessive weight. This effect will be more significant when the film is thin. Therefore, density data were taken only from measurements with thick films where absorbed water contributes a negligible error to the total weight of the film. Average water content of the films were about 15%-wt.

No appreciable difference was found between the densities of collagen and gelatin films obtained by this method,

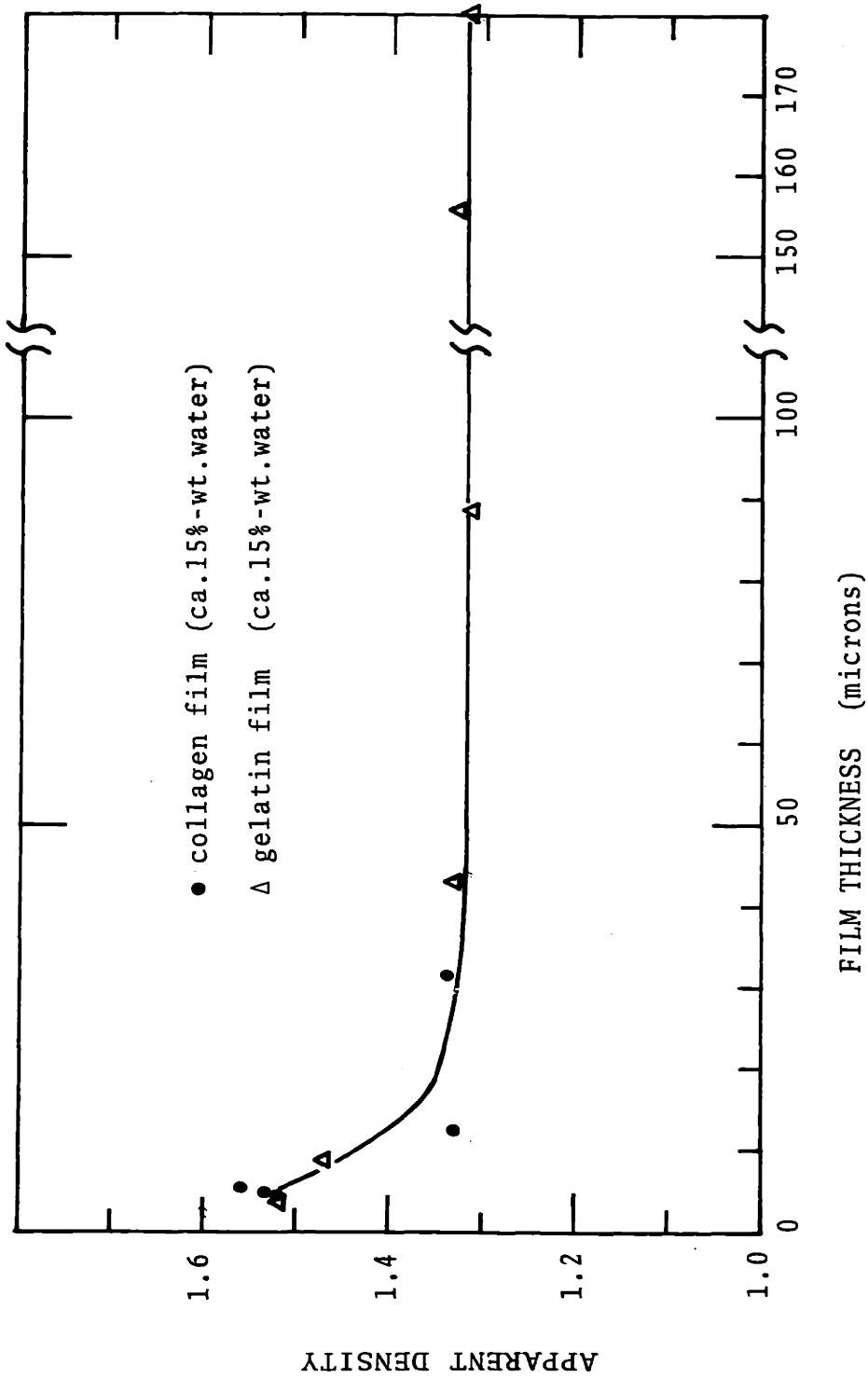


Figure IV-7 Apparent density of collagen and gelatin films as a function of thickness

and the value of 1.32 was used as a standard density for ORD calculation. The thickness of the films used for ORD measurements in the Cotton effect region was too small (order of 1 μ) to be measureable by mechanical means and therefore the ORD data was normalized by superposing the data in the 240 $m\mu$ - 300 $m\mu$ regions on the already established ORD curves in the visible—near UV regions which were obtained from thick films. (Note: IR interference fringes can be used to measure the film thickness, however, the film used in this work was too thin (less than 1 μ) to be measured by this technique, which is useful for thickness larger than a few microns.)

3.3 Results

The optical rotatory dispersion of collagen and gelatin in solution is shown in Figure IV-8 for wavelengths of 600 $m\mu$ to 250 $m\mu$. The optical rotation is expressed as the specific rotation $[\alpha]$ which has a dimension of degrees-cm³/dm-gr. The ORD of collagen and gelatin in solution in the far UV region is shown in Figure IV-9.

Figure IV-10 shows the ORD of collagen, cold-cast, and hot-cast gelatin films in the visible—near UV region. The ORD of collagen film in the far UV region is presented in Figure IV-11. Because of the excessive noise level arising from absorption of the light beam by the collagen film, measurement of ORD of the collagen film was not possible below 220 $m\mu$.

The CD of collagen and gelatin solutions is shown in Figure IV-12, and the CD of collagen and cold-cast gelatin films is shown in Figure IV-13.

3.4 Discussion

A. Dilute Solution Studies

The ORD of native and denatured rat tail collagen shown in Figure IV-8 confirms earlier findings (42-47). Gelatin, like many other random coil proteins (6,10,42), shows an ORD of simple dispersion (Figure IV-14), which can be expressed by a one term Drude equation. While the helical polypeptides and proteins exhibit complex dispersion (6,42), the ORD of collagen is also that of simple dispersion as illustrated in Figure IV-15. The dispersion constants λ_c of collagen and gelatin were found to be $205 \pm 10 \text{ m}\mu$ and $209 \pm 10 \text{ m}\mu$ respectively. The difference between the two values is within experimental error and λ_c does not change significantly upon denaturation, which agrees well with earlier findings reported by Cohen (43) and Harrington (42). The rotatory constants A of collagen and gelatin (obtained from Figures IV-14 and IV-15) were -1.19×10^8 and -0.41×10^8 respectively (Table IV-1). The high levorotation of collagen (i.e. $[\alpha]_{365} = -1300$) was, therefore, reduced by denaturation to about one third of its value in gelatin (i.e. $[\alpha]_{365} = -450$), indicating that about two thirds of the optical rotation of collagen comes from its conformational contribution.

As shown in Figure IV-9, collagen has a large negative Cotton effect with a minimum peak at around 207-208 $m\mu$, and an inflection point (estimated from Figure IV-9) at about 195 $m\mu$. Gelatin shows a similar Cotton effect with a minimum at around 208-209 $m\mu$ and an inflection point (estimated) at around 200 $m\mu$. Both collagen and gelatin appear to have a simple Cotton effect, but the magnitude in gelatin is much lower than in collagen. This indicates that the Cotton effect of collagen depends heavily on conformation. The Cotton effect of rat tail collagen presented here agrees well with those published for calf skin collagen (49), guinea pig skin collagen (53) and ichthyocol collagen (59). Blout et al. (49) studied the Cotton effect of both polyproline II and calf skin collagen and concluded that the similarity in Cotton effects of the two indicates that the structure of collagen is very closely related to the left-handed poly-L-proline II helix, which favors the earlier findings from X-ray diffraction studies (58). The absence of a 225 $m\mu$ Cotton effect, which is a characteristic of α -helical conformations (13,56,57) was also recognized as evidence for the absence of an α -helix in the collagen conformation (49).

Even though the Cotton effects of both collagen and gelatin appeared to be simple, with one dominant absorption band, and are also qualitatively the same in that the minimum peaks are at around 207-209 $m\mu$, the CD spectra of collagen and gelatin shown in Figure IV-12 are slightly dif-

ferent from each other. The CD spectrum of collagen has two distinctive peaks, a strong negative peak at 198 $m\mu$ and a weak positive peak at 222 $m\mu$. On the other hand, that of gelatin shows only a negative peak at about 200 $m\mu$ and no apparent positive peak is found. The apparent simple Cotton effect of collagen is, therefore, a double Cotton effect, where a weak positive Cotton effect of 222 $m\mu$ is overshadowed by a strong negative Cotton effect of 198 $m\mu$. The Cotton effect of gelatin, however, seems to be a simple one. Recently, Timasheff et al. (14) reported the CD spectrum of calf skin collagen, which is essentially identical (a strong negative band at 198 $m\mu$ and a weak positive band at 223 $m\mu$) with the CD of rat tail collagen presented here. The CD spectrum of ichthyocol collagen, reported by Madison and Schellman (59), also showed a strong negative peak at 198 $m\mu$ and a weak positive peak at 220 $m\mu$, which is in good agreement with our data on rat tail collagen. The presence of the two prominent peaks in the ORD and CD spectra of collagen can, therefore, be recognized as distinctive features of collagen in contrast to the ORD and CD of gelatin, showing only one apparent peak. The optical activity of collagen in the wavelength regions far from these bands is due to contributions from these two bands.

The CD spectrum of denatured collagen has not been reported previously. However, the CD spectra of many other random coil polypeptides have been reported (14,36). It

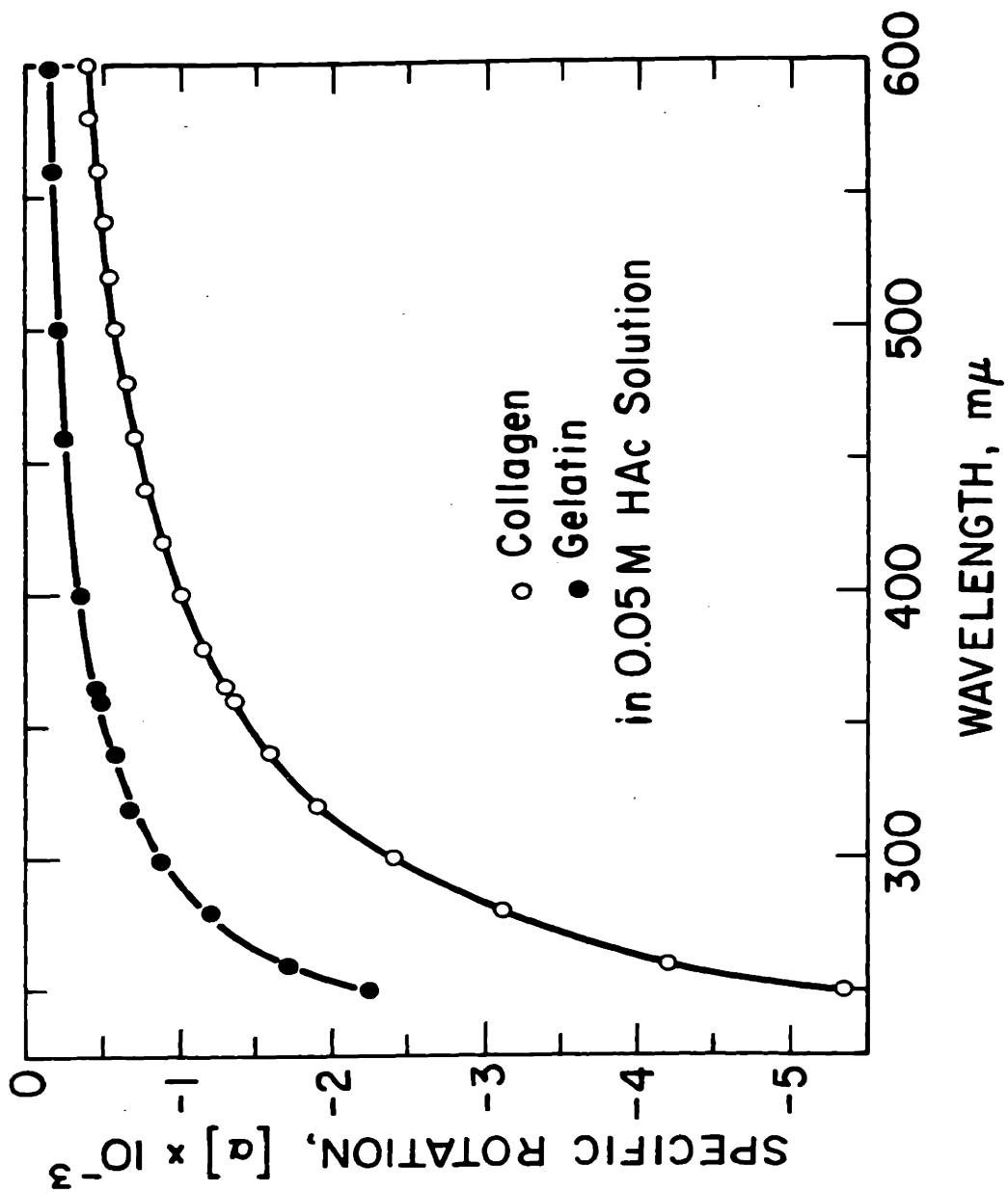


Figure IV-8

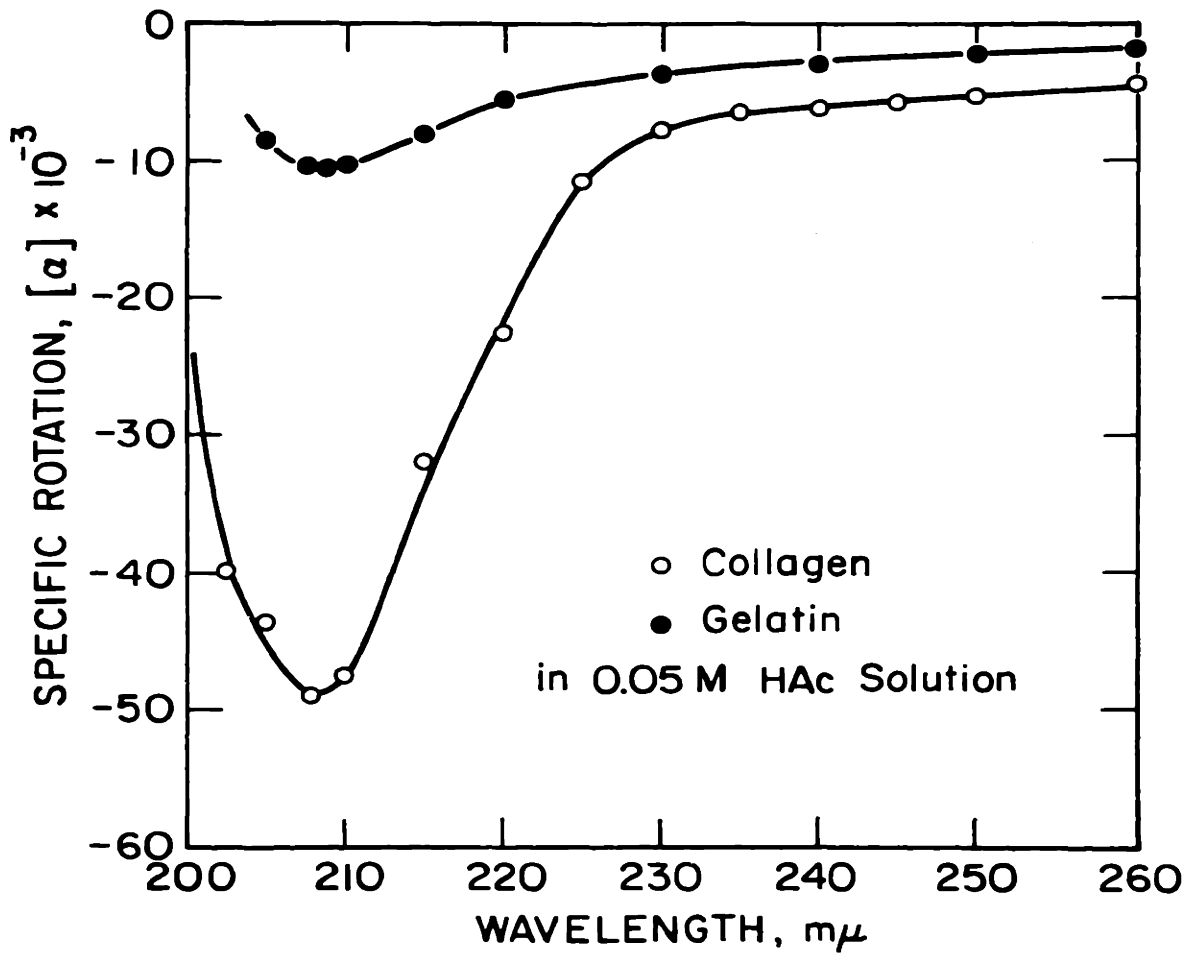


Figure IV-9 ORD of collagen and gelatin in dilute solution(0.05M HAc) in far UV region

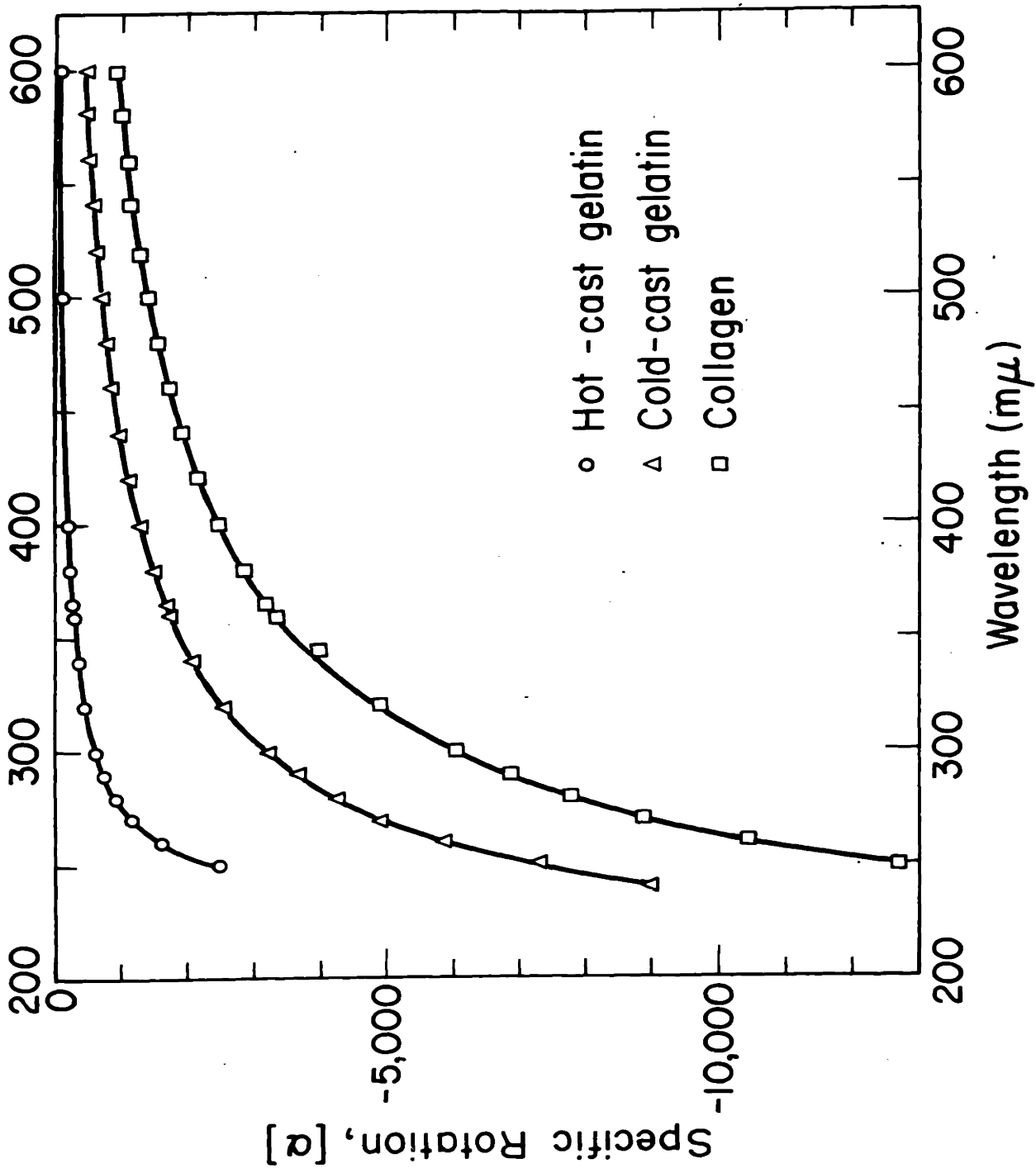


Figure 117

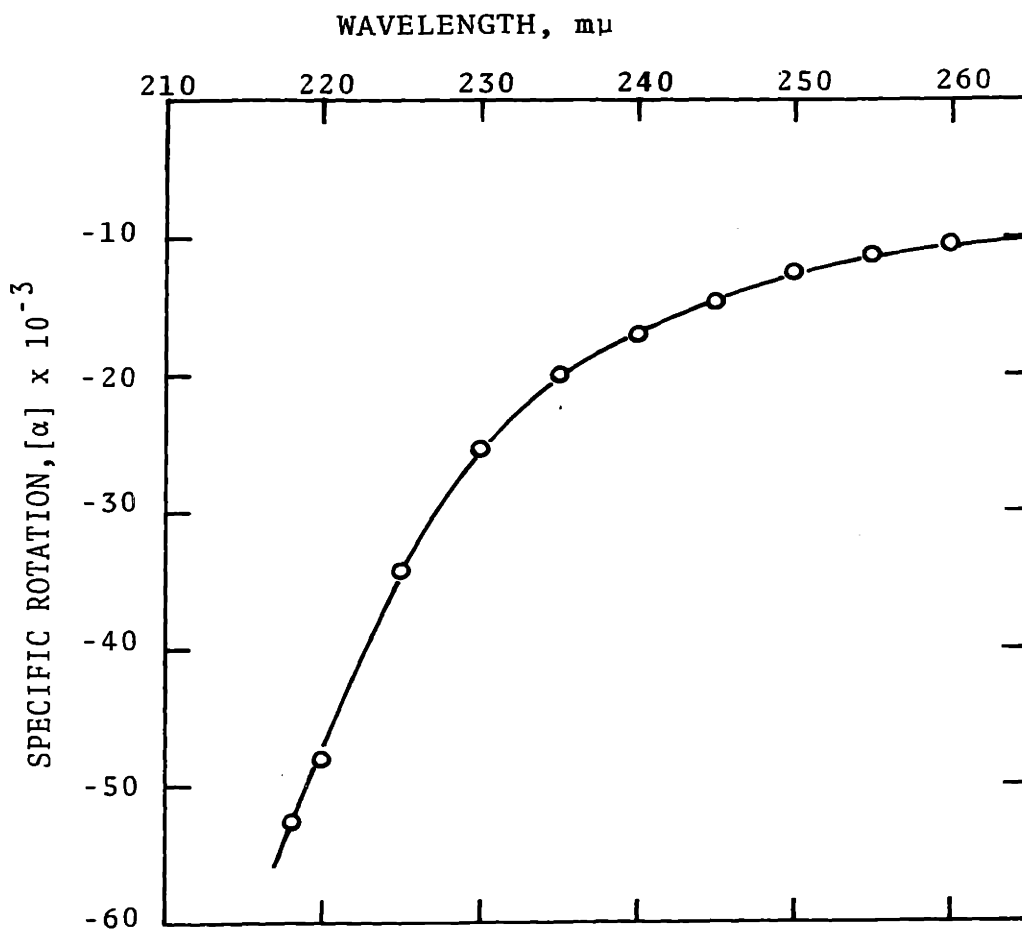


Figure IV-11 ORD of collagen film in far UV region

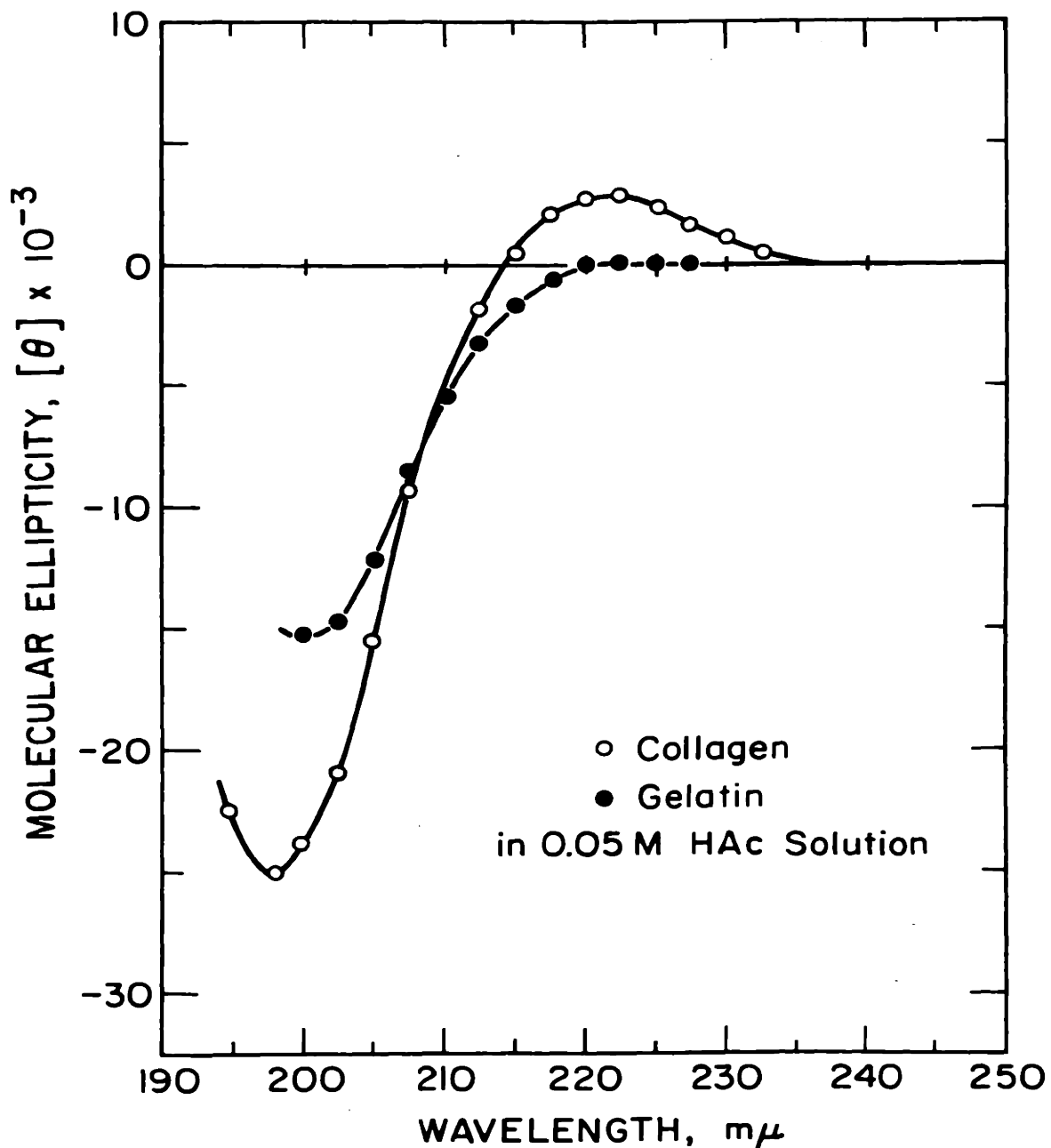


Figure IV-12 CD spectra of collagen and gelatin in dilute solution (0.05M HAc)

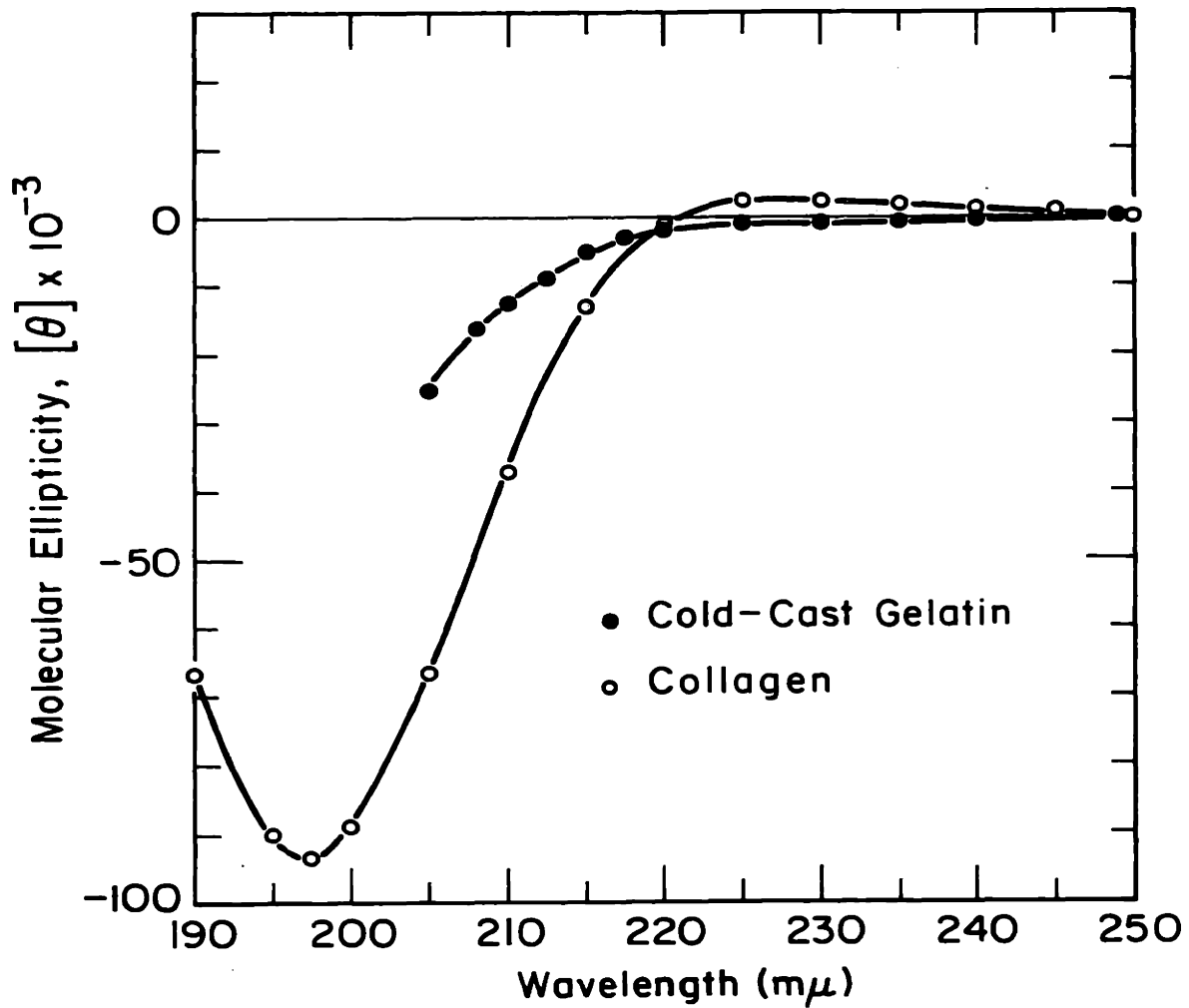


Figure IV-13 CD spectra of collagen and cold-cast gelatin films

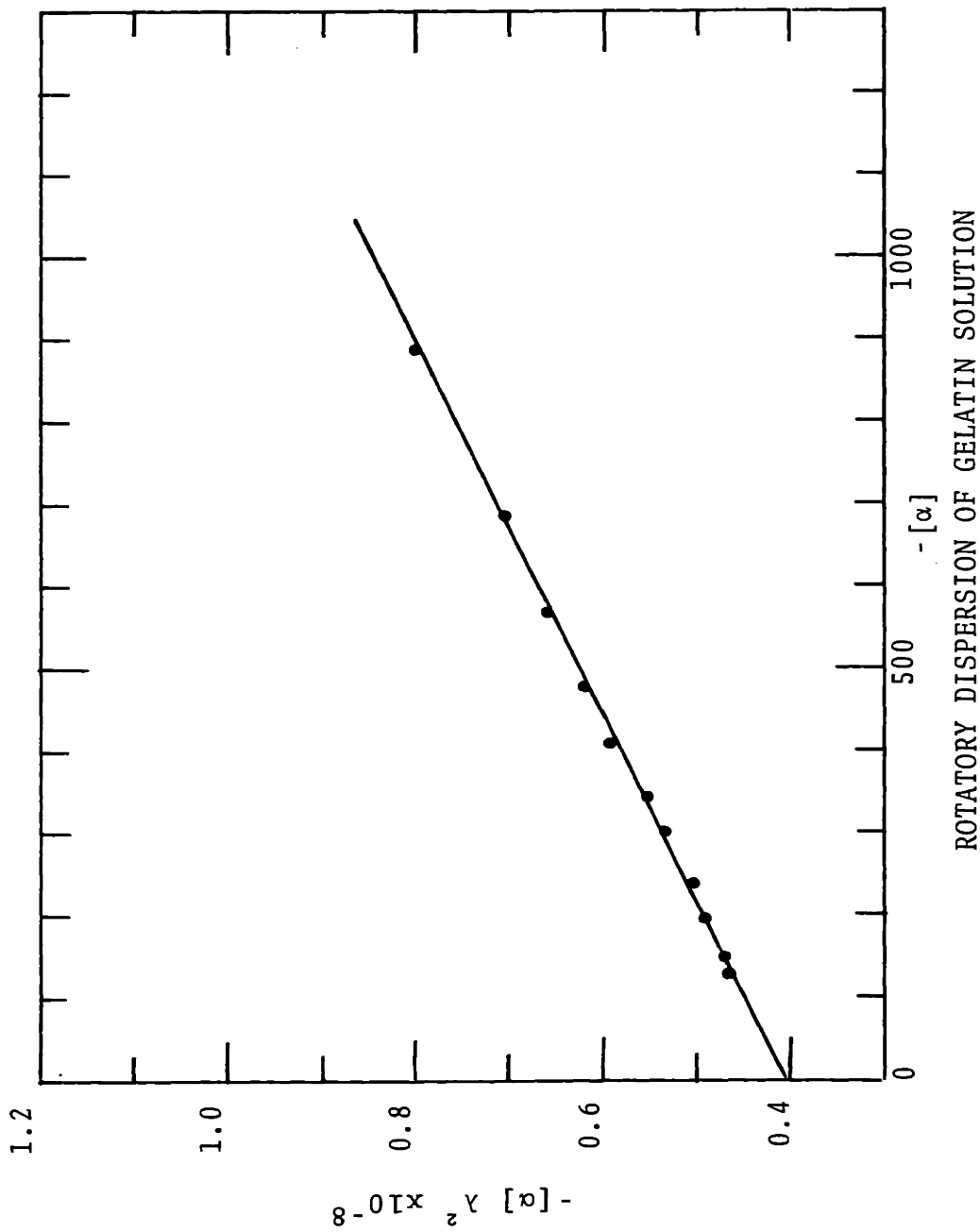
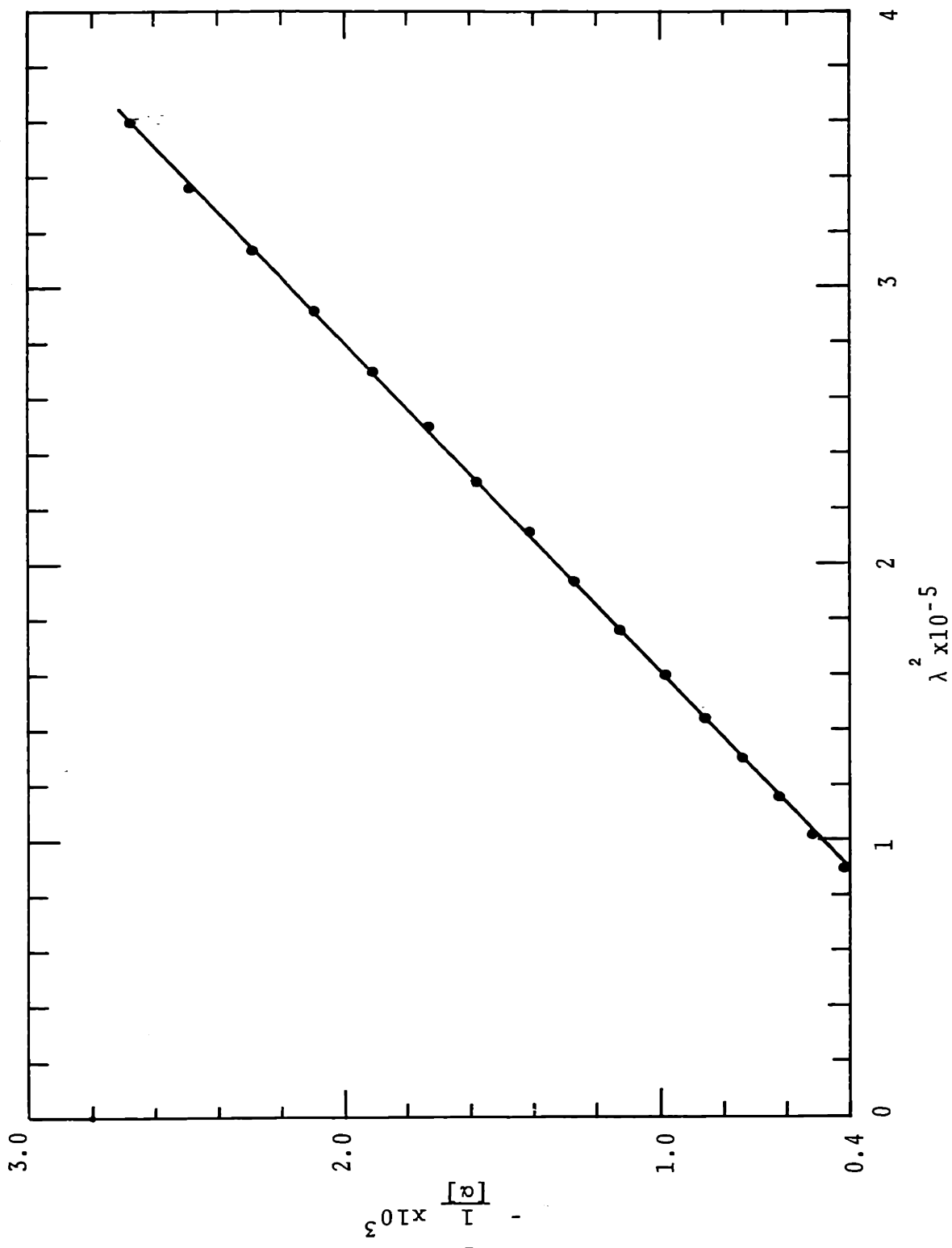


Figure IV-14



ROTATORY DISPERSION OF RTT COLLAGEN SOLUTION

Figure IV-15

has been found that the CD spectra of such polypeptides as poly-L-glutamic acid in water and poly-L-lysine in water (random coil conformations) (14,36) show three absorption bands: a strong negative band at 196-202 $m\mu$, a weak positive band at 217 $m\mu$, and another weak positive band at 235-238 $m\mu$. Considering these findings, it might be possible that gelatin also has three bands and that two of the bands are too weak to be detected, due to the presence of the strong negative band and as a result only a negative band appears as shown in Figure IV-12. Whether or not this is true, it must be concluded that the CD spectra of collagen shows two distinctive absorption bands, whereas that of gelatin shows only one absorption band. The difference is directly attributable to the difference in chain conformations.

B. Studies of Films

The ORD of collagen and of cold-cast and hot-cast gelatin films, in the visible to near UV wavelength regions, are shown in Figure IV-10. As in the dilute solution, the ORD of all three different films exhibit a simple dispersion which can be expressed by a one term Drude equation. This is shown in Figures IV-16, IV-17 and IV-18 where straight lines were obtained in the plot of $1/[\alpha]$ against λ^2 . Values of the dispersion constant λ_c were obtained from the intercepts of the lines (intercept = $-\lambda_c^2/A$), and the rotatory constant A was obtained from the slopes of the

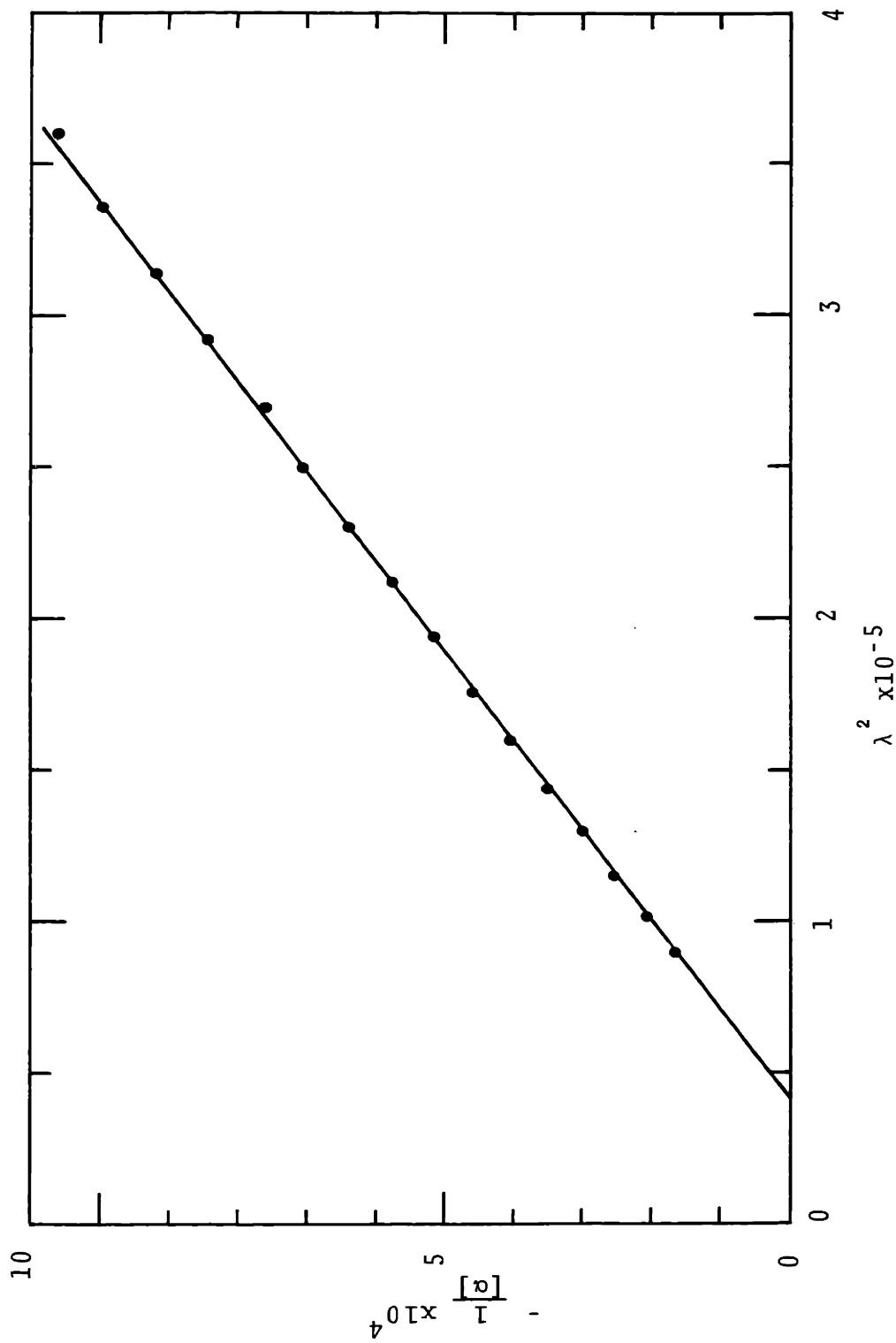


Figure IV-16 Drude plot of the ORD of collagen film (600m μ -300m μ)

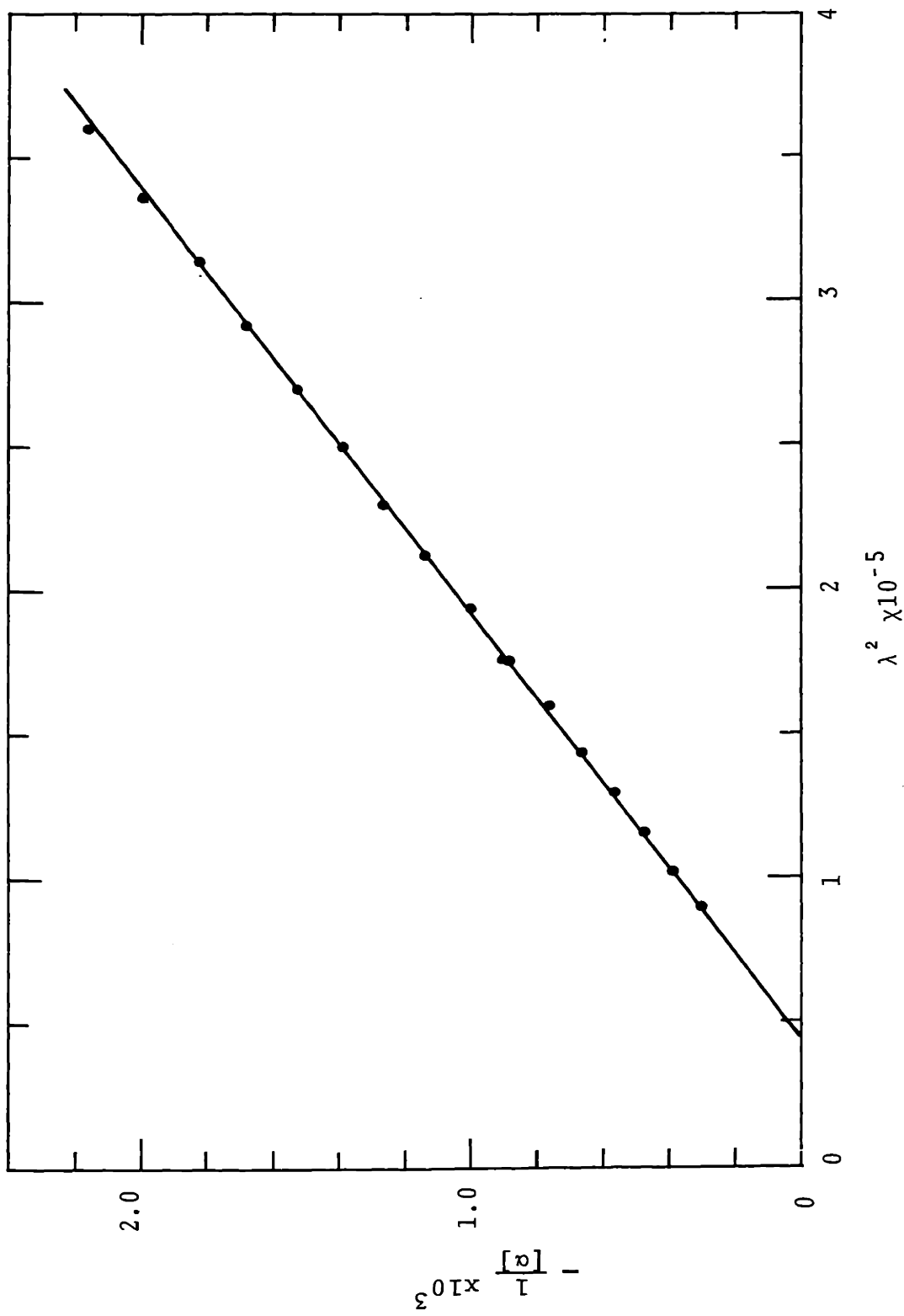


Figure IV-17 Rotatory dispersion of cold-cast gelatin film

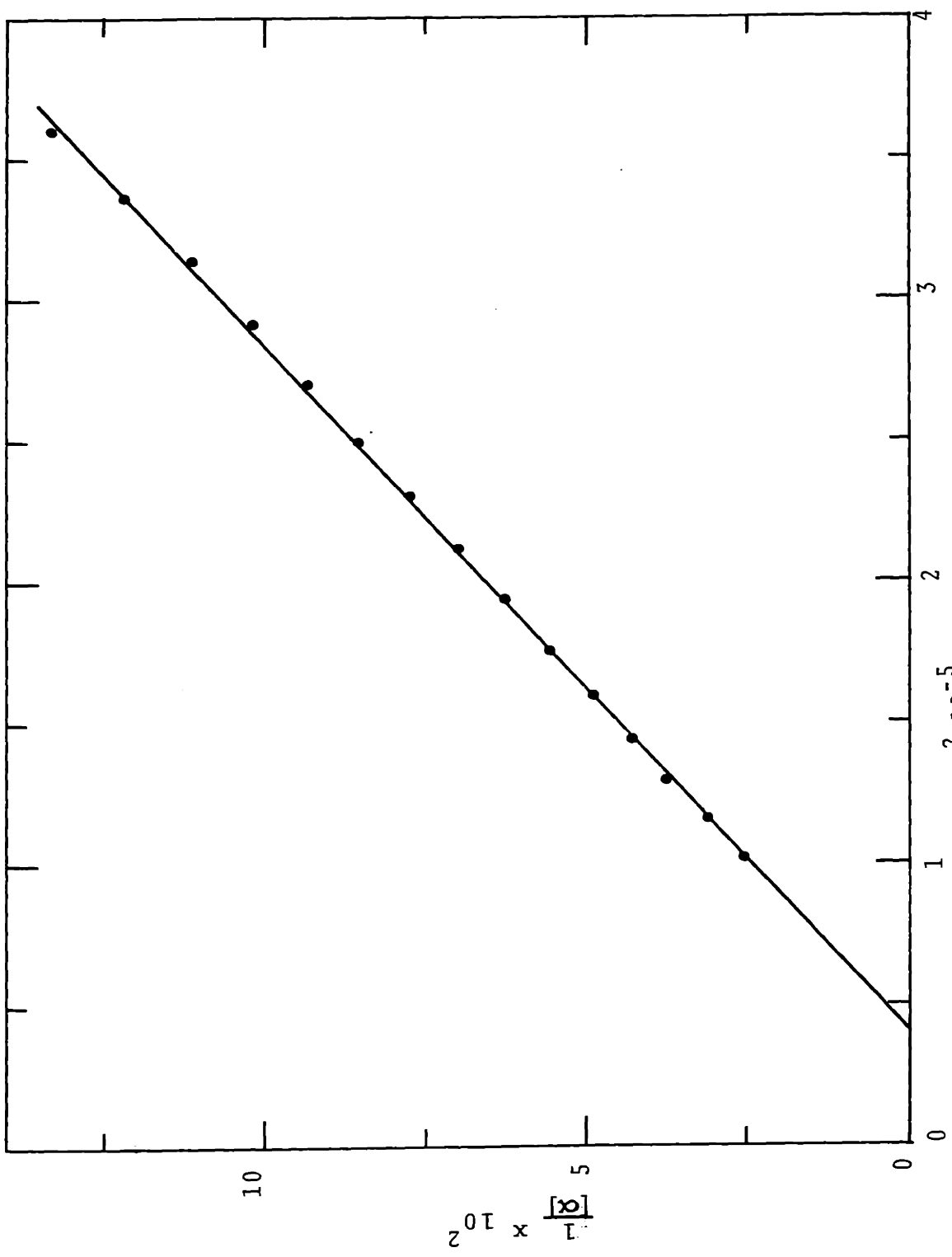


Figure IV-18 ORD of hot-cast gelatin film (600m μ - 300m μ)

straight lines (slope = $-1/A$). These are summarized in Table IV-1, together with solution data.

The values of λ_c are $204 \pm 10 \text{ m}\mu$, $209 \pm 10 \text{ m}\mu$, and $200 \pm 10 \text{ m}\mu$ for collagen, cold-cast and hot-cast gelatin films respectively. The three values are not considered to be significantly different from each other because they are well within the limit of the error range. The values of the rotatory constant A show large differences among the three films. At $365 \text{ m}\mu$, for example, the specific rotation of the collagen film is -3200 ± 200 , those of the cold-cast and the hot-cast films are -1700 ± 150 and -260 ± 30 as shown in Table IV-1.

The specific rotation of cold-cast and hot-cast gelatin films was reported earlier (43,93,94). Robinson and Bott (93) found that gelatin film prepared by evaporation of solution at room temperature (cold-cast) showed much higher values of the specific rotation ($[\alpha]_D = -1000$) than film cast at above 35° C . (hot-cast gelatin), which had almost the same value ($[\alpha]_D = -128$) as the hot gelatin solution. Cohen (43) also observed that the films formed by evaporation in the cold showed very high specific rotation ($[\alpha]_D = -600$) whereas the films produced at higher temperature (presumably at above 35° C .) gave too low rotation to be measured. Elliott (94) also observed that cold-cast gelatin films had significantly higher specific rotation than hot-cast gelatin films.

All these results are consistent in that cold-cast

TABLE IV-1 ORD DATA OF COLLAGEN AND GELATIN IN VARIOUS STATES

	$A \times 10^{-8}{}^a$	$\lambda_c (m\mu) {}^a$	$[\alpha]_{365}$
Collagen solution ^b	1.19	205 ± 10	-1300 ± 50
Gelatin solution ^b (cold)	0.40	209 ± 10	-450 ± 30
Gelatin solution ^c (hot)	----	-----	-300 ± 30
Collagen film ^d	2.97	204 ± 10	-3200 ± 200
Cold-cast gelatin film ^e	1.47	210 ± 10	-1700 ± 150
Hot-cast gelatin film ^e	0.24	200 ± 10	-260 ± 30

Note:

a: A , λ_c are the rotatory constant and dispersion constant in Drude equation $[\alpha] = A/\lambda - \lambda_c^2$

b: Ca. 0.08%-wt. in 0.05 M acetic acid at 23° C.

c: Measured at 65° C.

d: Cast at 23° C.

e: Cast at 65° C.

gelatin films (prepared at 23° C.) showed specific rotation values several times higher than the hot-cast gelatin films (prepared above 35° C.). This is directly attributable to the difference in secondary and tertiary structure of the chain conformation in the two films. The presence of the helical structure of collagen in cold-cast gelatin films, which was partially formed during the casting process, was already demonstrated by X-ray diffraction patterns in Chapter III. While the specific rotation of the hot-cast gelatin films is almost the same as that of the gelatin solution (43,93), that of cold-cast gelatin films is much higher than cold gelatin solution (43,93). At 365 m μ , for example, the specific rotation of hot gelatin solution (65° C.) is ca. -300, vs. -260 of hot-cast gelatin films (65° C.); whereas the cold-cast gelatin film shows ca. -1700, vs. -450 of gelatin solution at room temperature. More significant differences were observed between collagen film (ca. -3200) and collagen solution (ca. -1300).

No explanation has previously been give for such an apparent discrepancy, the understanding of which seems to be of great importance in the use of ORD data as a probe to the conformation of molecular chains in these films. Some of the details in ORD and CD data of collagen films and solutions will, therefore, now be discussed in a comparative manner in an attempt to answer this question.

C. Comparison of Data Obtained in Solution and Solid State

In the visible to near UV regions, the ORD of collagen in both dilute solution and film are of simple dispersion as shown in Figures IV-14 and IV-16. The dispersion constant λ_c has essentially the same value of about 205 m. in both ORD data. Qualitatively, therefore, the ORD of collagen film appears to be the same as the ORD of collagen solution. However, the magnitude of the OR in the film is much higher than the OR in the solution (i.e. $[\alpha]_{365}^{\text{film}} = -3200$, $[\alpha]_{365}^{\text{solution}} = -1300$). The ORD of collagen film in comparison with solution is shown in Figures IV-19 and IV-20. The OR of collagen film is consistently higher than that of collagen solution in entire wavelength from visible (Figure IV-19) to far UV region (Figure IV-20).

The circular dichroism spectra of collagen film and collagen solution are shown in Figure IV-21. As discussed in previous section, the CD of collagen in solution has two extrema which are characteristic features of the collagen triple helix. The CD spectrum of film has also two extrema, a strong negative band at about 198 m μ and a weak positive peak near 225 m μ . This is exactly the same feature as the CD of collagen in solution except a slight shift in frequency of the positive peak from 222 m μ to 225 m μ . This strongly supports the presence of native collagen molecules in the film. The magnitude of the molecular el-

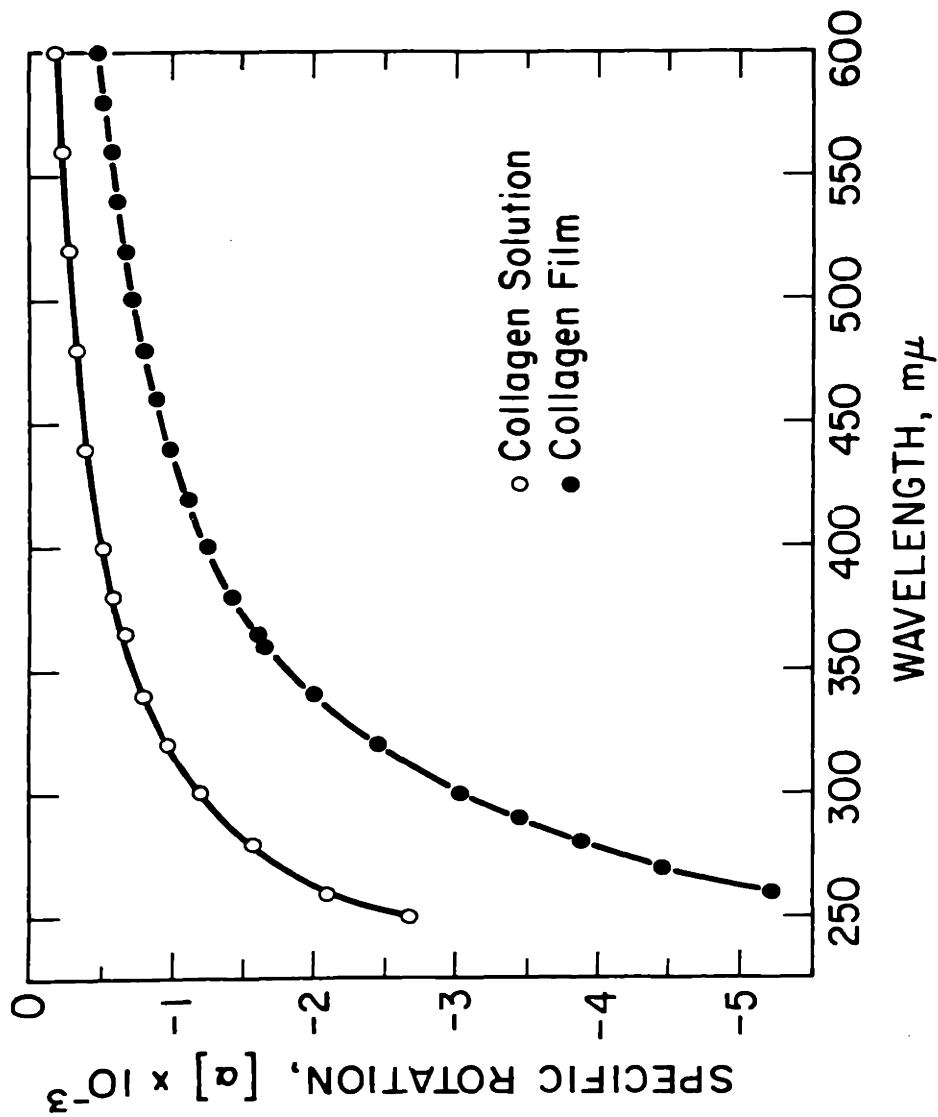


Figure IV-19 Comparison of ORD of collagen solution (in 0.05M HAC) and collagen film (Visible to near UV region)

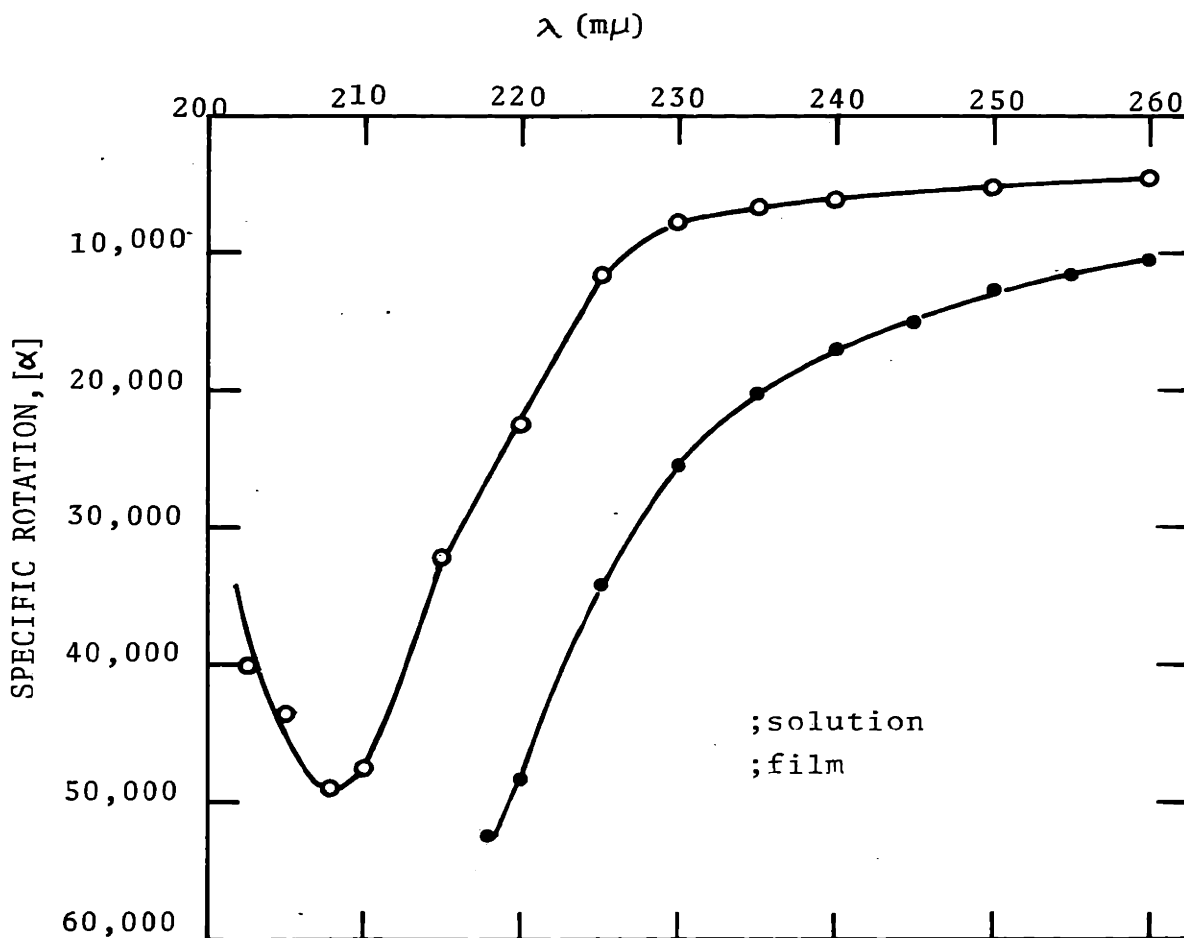


Figure IV-20 Comparison of the ORD of collagen solution (in 0.05M HAC) and collagen film (far UV region)

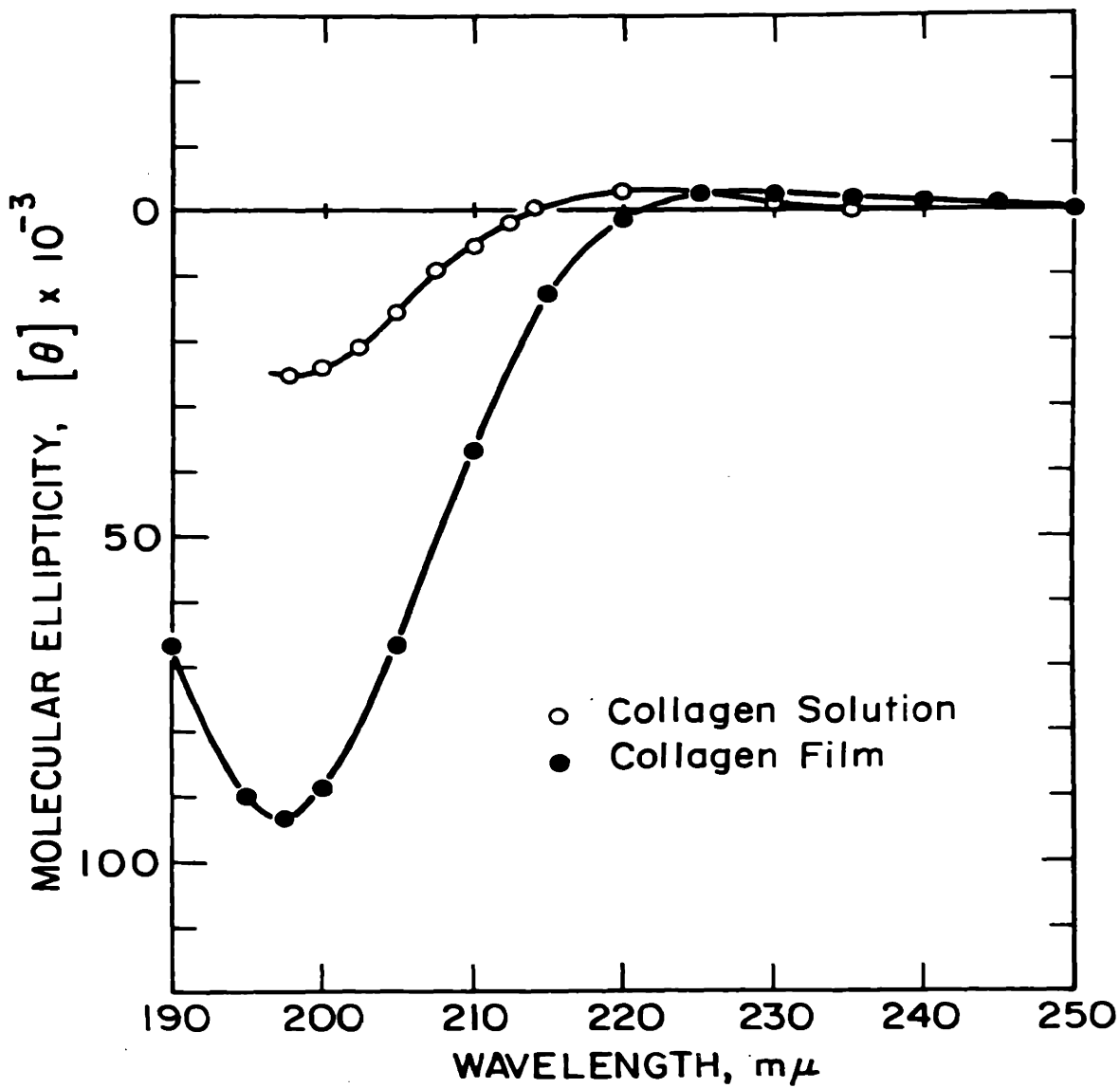


Figure IV-21 Comparison of CD spectra of collagen solution (in 0.05M HAC) and collagen film

lipticity is, however, much higher in film ($[\theta]_{198}^{\text{film}} = -93,000$) than in solution ($[\theta]_{198}^{\text{solution}} = -25,000$), which is qualitatively consistent with the ORD data.

These apparent discrepancies in the magnitude of the values of ORD and CD of collagen in dilute solution and the solid film immediately raise a question as to whether the chain conformations in solution and in the solid state are the same, even though the characteristic features of ORD and CD spectra appear to be the same.

Recently, comparative studies of ORD and CD have been reported (60-62, 66-68) on the conformations of several polypeptides in dilute solution and the solid film. The positive Cotton effect of poly-O-acetyl-hydroxyl-L-proline I film was reported to be shifted to lower wavelengths by ca. 40-60 $m\mu$ as compared with the ORD curves in solution (60). While the CD spectra of poly-L-proline I and II have been reported to be the same in both film and solution (61), the Cotton effect of poly-L-proline I in solution was suggested to be negative (49) and that of poly-L-proline I in the form of film was reported to be positive by the same authors (68) which clearly contradicts each other. The optical rotation of polyalanine in solution was found to be positive (67) but that of film was reported to be negative by the same authors (66). The reported CD spectra of poly-L-lysine (unordered form) obtained with film and solution showed differences in both magnitude and the position of peaks (62). The unordered

poly-L-proline, however, has been suggested to have the same CD spectra in solution and the solid film (61). No clear explanations are available at present for the account of such discrepancies. Implications have, however, been made of different conformations in dilute solution and the solid state (62). The difference in magnitudes of ORD and CD of collagen between in solution and the solid state could conceivably be due to the change in conformation of collagen chains.

On the other hand, the aspect of anisotropy in the optical activity of the macromolecules has been studied both theoretically (65,70-72) and experimentally (63-65). By applying the electric field to the solution of poly-L-benzyl-L-glutamate (PBLG) in 1,2-dichloroethane, Tinoco (63) measured the optical rotation of the oriented PBLG molecules in the solution. He showed that the specific rotation of PBLG in solution was positive along the helical axis (i.e. $[\alpha]_{33}^{365} = +670$) and was negative perpendicular to the helical axis (i.e. $[\alpha]_{11}^{365} = -400$). Similar study was reported by Hoffman and Ullman (73) on PBLG. The dependence of optical activity on the orientation of the molecules attained by applying the static electric field was also discussed by Troxell and Scheraga (74) on poly-n-butyl isocyanate. These studies well demonstrated that the optical activity of the anisotropic macromolecules is different along the different molecular axes and the measured rotation values depend on the direction and the degree

of orientation of molecules with respect to the propagation direction of the light.

Direct comparison of the specific rotation of collagen in solution and in film can, therefore, be further complicated by the difference in orientation of collagen molecules if the optical activity of collagen molecule is, indeed, different along the different molecular axes. Any attempt to interpret the difference in ORD and CD in terms of structural change of the molecule must be made with the complete understanding of the aspect of anisotropy of the molecule and the orientation of the molecules in the sample. For this, analysis of optical activity tensor of collagen molecule and the dependence of the OR on the direction of the light propagation as well as the orientation of the collagen molecule in solution and film are discussed in the next sections.

3.5 Tensorial Character of Optical Activity

A. Gyration Tensor g_{ij}

In crystal optics, it is general practice to describe the anisotropy of crystals by following a set of so-called material equations which relates excitation vector \tilde{D} and the field strength \tilde{E} (electric vector) by a linear vector function (75,76).

$$\begin{aligned} D_1 &= \epsilon_{11}E_1 + \epsilon_{12}E_2 + \epsilon_{13}E_3 \\ D_2 &= \epsilon_{21}E_1 + \epsilon_{22}E_2 + \epsilon_{23}E_3 \\ D_3 &= \epsilon_{31}E_1 + \epsilon_{32}E_2 + \epsilon_{33}E_3 \end{aligned} \tag{20}$$

where subscripts 1,2,3 are the three mutually perpendicular coordinates. (In the isotropic case, a simple proportionality $D = \epsilon E$ holds). The nine quantities $\epsilon_{11}, \epsilon_{22}, \dots$ are constants of the medium and constitute the "dielectric tensor" of rank two. In shorter form, equation (20) can be written

$$D_i = \epsilon_{ij} E_j \quad i, j = 1, 2, 3 \quad (21)$$

The dielectric tensor is known to be "symmetric" so that

$$\epsilon_{ij} = \epsilon_{ji}$$

The material equation (20) is originally developed for a medium which is homogeneous, non-conducting and magnetically isotropic but electrically anisotropic (76). For optically active medium, which is not only electrically anisotropic but also magnetically anisotropic, the real symmetric tensor ϵ_{jk} is replaced by the complex tensor;

$$\epsilon_{jk} + ig_{jk} \quad (23)$$

The additional terms g_{jk} is called "gyration tensor" which represents the amount of optical activity. This gyration tensor is supposed (76) to be small and does not contribute to the electric energy W_e ; $W_e = 1/2(\tilde{D} \cdot \tilde{E})$. Because of this requirement, gyration tensor forms an "antisymmetric tensor" of rank two (76). Sommerfeld (76) showed that only a crystal without symmetry can possess gyration tensor.

The gyration G , which gives the amount of optical activity, varies with direction and can be written in gen-

eral form (72),

$$G = g_{11}l_1^2 + g_{22}l_2^2 + g_{33}l_3^2 + 2g_{12}l_1l_2 + 2g_{23}l_2l_3 + 2g_{31}l_3l_1 \quad (24)$$

or

$$G = g_{ij}l_i l_j \quad i, j, = 1, 2, 3 \quad (25)$$

where i, j are the indices for coordinates and l_1, l_2, l_3 are direction cosines between wave normal (or the direction of light propagation) and the crystal axes.

The relationship between the optical rotatory power R and the gyration G is given by Nye (72) for uniaxial crystals,

$$R = \frac{\pi G}{\lambda_0 \bar{n}} \quad (26)$$

where λ_0 is the wavelength of the light, \bar{n} is the average refractive index of the crystal along the optic axis for ordinary and extraordinary waves (or left and right handed polarized light).

B. Gyration Tensor Components in a Uniaxial Crystal and Collagen Molecule

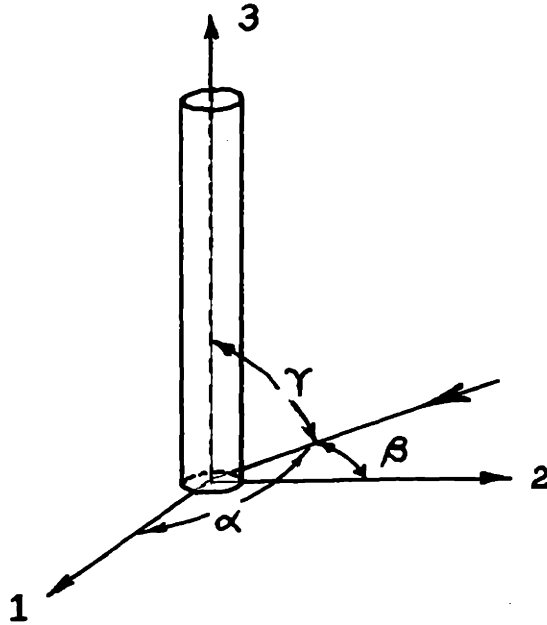
Depending on the crystal symmetry, the gyration tensor g_{ij} has some zero components and the number of independent components are reduced. Extensive table was given by Nye (72) for the forms of gyration tensor g_{ij} for all different classes of the crystal symmetry.

In this section, however, the form of gyration tensor for the uniaxial crystal with a cylindrical symmetry and,

specifically, for collagen molecule is discussed in detail.

Before applying the symmetry operation to the gyration tensor, it is necessary to note the following: first, conventionally, the rotatory power is called "positive" if the sense of the rotation is the same as the handedness of the coordinate axes. If the symmetry operation changes the handedness of the reference axes, rotatory power will change sign too and such physical quantities are called "pseudo-scalar". Secondly, if the tensor changes its sign when the reference axes changes its handedness, it is called "axial tensor". The gyration tensor g_{ij} in equation (25) is the "axial second rank tensor".

Now, it is assumed that the tropocollagen molecule is a uniaxial crystal with an optic axis along the axis of helix and has a three-fold rotational symmetry. (It should be noted that this assumption is reasonable, considering the fact that the tropocollagen molecule is composed of three polypeptide chains of left-handed helices which intertwined each other to form right-handed super-helix.) Under the assumption made above, and molecular axes assigned as below, we want to find out the form of gyration tensor for collagen molecule.



For the general case, where the incident light propagates along the direction which has direction cosines of $l_1 = \cos \alpha$, $l_2 = \cos \beta$ and $l_3 = \cos \gamma$ with respect to the axes 1, 2 and 3 of collagen (See Figure above), the gyration G can be expressed according to the equation (24) which is

$$G = g_{11}l_1^2 + g_{22}l_2^2 + g_{33}l_3^2 + 2g_{12}l_1l_2 + 2g_{23}l_2l_3 + 2g_{31}l_3l_1 \quad (24)$$

where

$$l_1 = \cos \alpha$$

$$l_2 = \cos \beta$$

$$l_3 = \cos \gamma$$

If crystal is rotated around axis 3 by an angle of θ (see Figure 22), direction cosines will be changed accordingly so that new directional cosines are $l_1' = \cos \alpha'$, $l_2' = \cos \beta'$ and $l_3' = \cos \gamma'$ and the gyration G' will be

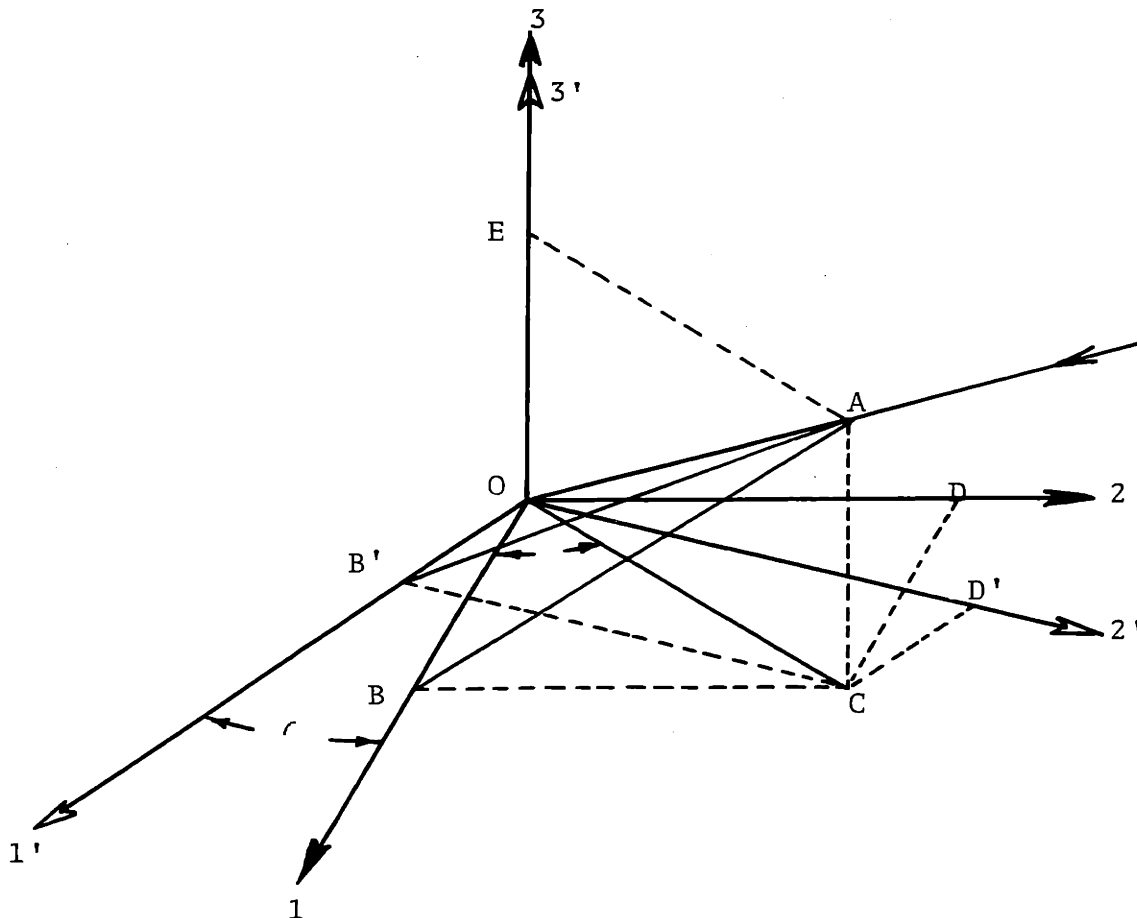


Figure IV-22

1,2,3-----original axes of collagen molecule
 1',2',3'--new axes of collagen molecule after
 rotating around axis 3 by angle of
 (to be continued in the following page)

$$l_1 = \cos\alpha = \cos(\text{AOB})$$

$$l_1' = \cos\alpha' = \cos(\text{AOB}')$$

$$l_2 = \cos\beta = \cos(\text{AOD})$$

$$l_2' = \cos\beta' = \cos(\text{AOD}')$$

$$l_3 = \cos\gamma = \cos(\text{AOE})$$

$$l_3' = \cos\gamma' = \cos(\text{AOE})$$

If OA is taken as a unit length, from triangle OBC
 $OB = \cos\alpha$, $OC = \sin\gamma$ and, therefore

$$\cos\varphi = OB/OC = \cos\alpha/\sin\gamma \quad \text{----- (1)}$$

The relationship is held in triangle OB'C so that

$$\cos(\varphi + \theta) = OB'/OC = \cos\alpha'/\sin\gamma \quad \text{---- (2)}$$

From (1) and (2),

$$\begin{aligned} \cos\alpha' &= \cos(\varphi + \theta) \sin\gamma = \sin\gamma [\cos\varphi \cos\theta - \sin\varphi \sin\theta] \\ &= \sin\gamma [\cos\alpha \cos\theta / \sin\gamma - \sin\varphi \sin\theta] \\ &= \cos\alpha \cos\theta - \sin\gamma \sin\varphi \sin\theta \quad \text{----- (3)} \end{aligned}$$

$$\text{Now } \sin\varphi = BC/OC = OD/OC = \cos\beta/\sin\gamma \quad \text{----- (4)}$$

By introducing (4) into (3),

$$\cos\alpha' = \cos\alpha \cos\theta - \cos\beta \sin\theta$$

In the same manner,

$$\cos\beta' = \cos\alpha \sin\theta + \cos\beta \cos\theta \text{ and}$$

$$\cos\gamma' = \cos\gamma$$

$$l_1 = \cos\alpha = \cos(\text{AOB})$$

$$l_1' = \cos\alpha' = \cos(\text{AOB}')$$

$$l_2 = \cos\beta = \cos(\text{AOD})$$

$$l_2' = \cos\beta' = \cos(\text{AOD}')$$

$$l_3 = \cos\gamma = \cos(\text{AOE})$$

$$l_3' = \cos\gamma' = \cos(\text{AOE})$$

If OA is taken as a unit length, from triangle OBC
 $OB = \cos\alpha$, $OC = \sin\gamma$ and, therefore

$$\cos\varphi = OB/OC = \cos\alpha/\sin\gamma \quad \text{----- (1)}$$

The relationship is held in triangle OB'C so that

$$\cos(\varphi + \theta) = OB'/OC = \cos\alpha'/\sin\gamma \quad \text{---- (2)}$$

From (1) and (2),

$$\begin{aligned} \cos\alpha' &= \cos(\varphi + \theta) \sin\gamma = \sin\gamma [\cos\varphi \cos\theta - \sin\varphi \sin\theta] \\ &= \sin\gamma [\cos\alpha \cos\theta / \sin\gamma - \sin\varphi \sin\theta] \\ &= \cos\alpha \cos\theta - \sin\gamma \sin\varphi \sin\theta \quad \text{----- (3)} \end{aligned}$$

$$\text{Now } \sin\varphi = BC/OC = OD/OC = \cos\beta/\sin\gamma \quad \text{----- (4)}$$

By introducing (4) into (3),

$$\cos\alpha' = \cos\alpha \cos\theta - \cos\beta \sin\theta$$

In the same manner,

$$\cos\beta' = \cos\alpha \sin\theta + \cos\beta \cos\theta \text{ and}$$

$$\cos\gamma' = \cos\gamma$$

$$G' = g_{11}l_1'^2 + g_{22}l_2'^2 + g_{33}l_3'^2 + 2g_{12}l_1'l_2' + 2g_{23}l_2'l_3' + 2g_{31}l_3'l_1' \quad (27)$$

The general relationship between original (l_1, l_2, l_3) and new direction cosines (l_1', l_2', l_3') can be represented by an adjoining matrix, (derivation of this is shown in the text in Figure IV-22).

	l_1	l_2	l_3	
l_1'	$\cos \theta$	$-\sin \theta$	0	
l_2'	$\sin \theta$	$\cos \theta$	0	
l_3'	0	0	1	(28)

so that

$$\begin{aligned} l_1' &= l_1 \cos \theta - l_2 \sin \theta = \cos \alpha \cos \theta - \cos \beta \sin \theta \\ l_2' &= l_1 \sin \theta + l_2 \cos \theta = \cos \alpha \sin \theta + \cos \beta \cos \theta \\ l_3' &= l_3 = \cos \gamma \end{aligned} \quad (29)$$

Since the rotation of molecule around the axes 3 does not change the hand of the reference axes 1,2 and 3, neither the gyration G nor its component tensor g_{ij} changes its sign. If rotation angle θ is 120° (this operation will bring the collagen molecule in identical position due to the 3-fold symmetry), new direction cosines become

$$\begin{aligned} l_1' &= -1/2 \cdot l_1 - \sqrt{3}/2 \cdot l_2 \\ l_2' &= \sqrt{3}/2 \cdot l_1 - 1/2 \cdot l_2 \\ l_3' &= l_3 \end{aligned} \quad (30)$$

By substituting the eqs. (30) into eq. (27) and rearranging the right hand side, we get

$$\begin{aligned}
 G' = & (1/4 \cdot g_{11} + 3/4 \cdot g_{22} - \sqrt{3}/4 \cdot g_{12}) \ell_1^2 + (3/4 \cdot g_{11} + \\
 & + 1/4 \cdot g_{22} + \sqrt{3}/4 \cdot g_{12}) \ell_2^2 + g_{33} \ell_3^2 + 2(\sqrt{3}/2 \cdot g_{11} - \\
 & - \sqrt{3}/2 \cdot g_{22} - 1/2 \cdot g_{12}) \ell_1 \ell_2 + 2(-1/2 \cdot g_{23} - \sqrt{3}/2 \cdot g_{13}) \\
 & \ell_2 \ell_3 + 2(\sqrt{3}/2 \cdot g_{23} - 1/2 \cdot g_{13}) \ell_1 \ell_3
 \end{aligned} \quad (31)$$

In the same way, if $\theta = 240^\circ$ (which will bring the collagen molecule in the identical position), we have

$$\begin{aligned}
 G'' = & (1/4 g_{11} + 3/4 g_{22} + \sqrt{3}/4 g_{12}) \ell_1^2 + (3/4 g_{11} + \\
 & + 1/4 g_{22} - \sqrt{3}/4 g_{12}) \ell_2^2 + g_{33} \ell_3^2 + 2(-\sqrt{3}/2 g_{11} + \\
 & + \sqrt{3}/2 g_{22} - 1/2 g_{12}) \ell_1 \ell_2 + 2(-\sqrt{3}/2 g_{23} - \\
 & - 1/2 g_{13}) \ell_1 \ell_3 + 2(-1/2 g_{23} + \sqrt{3}/2 g_{13}) \ell_1 \ell_3
 \end{aligned} \quad (32)$$

Since the rotation around axis -3 by 120° and 240° should not affect the gyration G,

$$G = G' = G'' \quad (33)$$

By identifying each term in eqs (25), (31) and (32), we get

$$g_{12} = g_{13} = g_{23} = 0 \quad (34)$$

$$g_{11} = g_{22} \quad (35)$$

Therefore, from six components of gyration tensor only diagonal components g_{11} , g_{22} , g_{33} are non-zero and $g_{11} = g_{22}$ and tensor reduced to

$$G = \begin{bmatrix} g_{11} & 0 & 0 \\ 0 & g_{22} & 0 \\ 0 & 0 & g_{33} \end{bmatrix}, \quad g_{11} = g_{22} \quad (39)$$

The optical activity of the tropocollagen molecules can, therefore, be described completely by three components α_{11} , α_{22} and α_{33} which are associated with gyration tensor

components g_{11} , g_{22} and g_{33} . The general expression is from eq. (25), (26) and (39), (α is equivalent to rotatory power R in eq. (26), the exact relation of which to the gyration G is shown in eq. (16)),

$$\alpha = \alpha_{11}\ell_1^2 + \alpha_{22}\ell_2^2 + \alpha_{33}\ell_3^2 \quad (40)$$

or, since $\ell_1^2 + \ell_2^2 + \ell_3^2 = 1$,

$$\alpha = \alpha_{11}(1-\ell_3^2) + \alpha_{33}\ell_3^2 \quad (40)'$$

where

α_{11} , α_{22} are the optical rotation along the direction perpendicular to the axis of the collagen helix,

α_{33} is the optical rotation along the axis of collagen helix,

ℓ_1 , ℓ_2 , ℓ_3 are the direction cosines of the incident light with respect to the molecular axes 1, 2, 3 of collagen molecule.

C. Interpretation of ORD of Collagen in Solution and in Film

In dilute solution, collagen molecules are randomly oriented in space and, therefore, the measured rotation will be the average of the three components α_{11} , α_{22} and α_{33} . For random orientation in 3-dimension, the average of the direction cosines will be equal in all directions so that $\overline{\ell_1^2} = \overline{\ell_2^2} = \overline{\ell_3^2} = 1/3$. The specific rotation of collagen in solution is, therefore,

$$[\alpha]_{\text{solution}} = [\alpha]_{\text{solution}} = [\alpha_{11}]\ell_1^2 + [\alpha_{22}]\ell_2^2 + [\alpha_{33}]\ell_3^2 = 1/3([\alpha_{11}] + [\alpha_{22}] + [\alpha_{33}])$$

$$= 1/3(2[\alpha_{11}] + [\alpha_{33}]) \quad (41)$$

In film, as discussed already in Chapter III of X-ray diffraction studies, collagen molecules are mostly lying in the plane of the film and randomly oriented within the plane. When such film is subjected to the measurement of the optical rotation with the beam perpendicular to the plane of the film, the angle between the axis of collagen helix and the direction of the beam is 90 degrees and the direction cosine ℓ_3 becomes zero. On the other hand, the axes 1 and 2 of the collagen molecules are equivalent to each other and randomly oriented with respect to the direction of the incident beam so that $\ell_1^2 = \ell_2^2 = 1/2$. The specific rotation of a collagen film assumed to possess perfectly planar orientation, therefore, will be

$$\begin{aligned} [\alpha]_{\text{film}} &= [\alpha_{11}]\ell_1^2 + [\alpha_{22}]\ell_2^2 \\ &= 1/2([\alpha_{11}] + [\alpha_{22}]) = [\alpha_{11}]_{\text{solid}} = [\alpha_{22}]_{\text{solid}} \end{aligned} \quad (42)$$

From equations (41) and (42), it is apparent that the specific rotation of collagen obtained with dilute solution will be different from that obtained with solid film, as long as $[\alpha_{11}]$ is not equal to $[\alpha_{33}]$.

It is interesting to see how the measured optical rotation will change when the film is tilted such that the angle between the normal of the film plane and the light

propagation direction is θ . The general relationship between the optical rotation and the angle of tilt θ can be derived as follows:

Let's consider the situation shown in Figure IV-23. x, y, z are the three orthogonal laboratory coordinates, where light propagates along the y direction and film is tilted by an angle of θ around the x axis. (When $\theta = 0$, this is the case discussed above where equation (42) is applied.) If OA represents the helical axis of collagen molecule lying in the plane of the film, at an angle ϕ from the x -axis, by tilting the plane by θ degrees, OA will be tilted to OA' . Now the direction cosine λ_3 , between the direction of the light propagation OY and OA' , becomes a function of the angles θ and ϕ , namely,

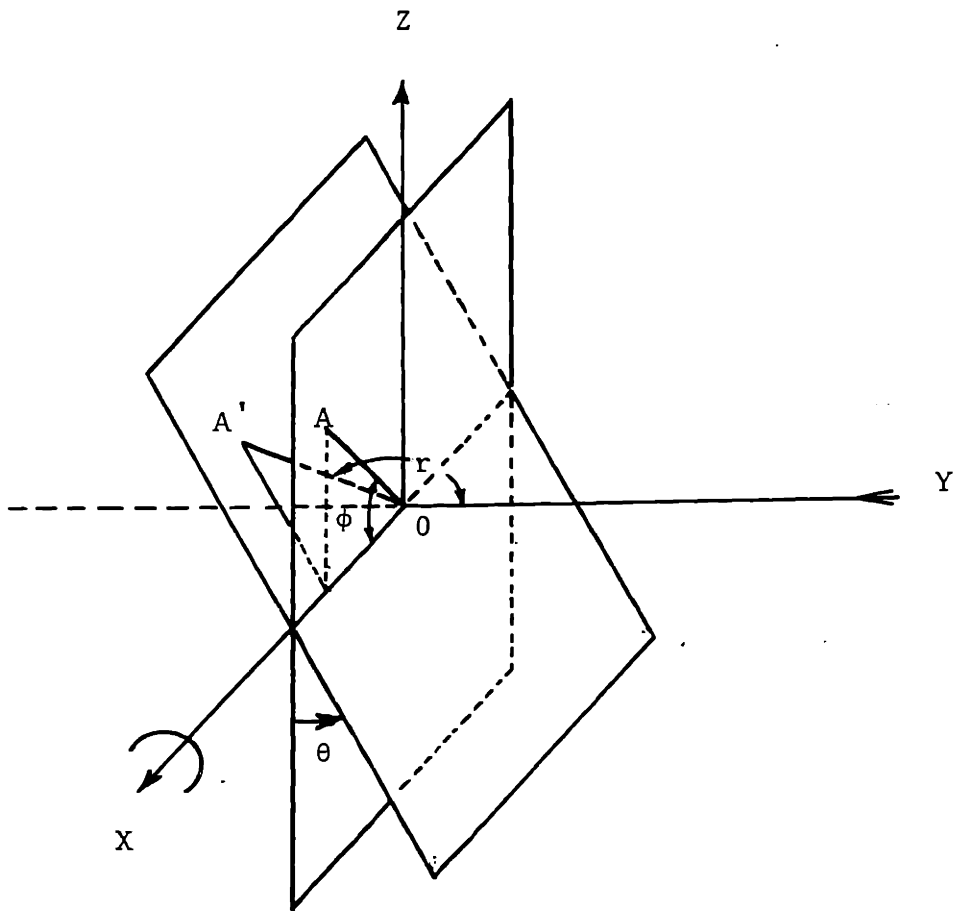
$$\lambda_3 = \cos \gamma = \sin \phi \sin \theta \quad (43)$$

at a fixed angle of θ , the average of the square of the direction cosine, λ_3^2 for all possible values of the angle will be

$$\overline{\lambda_3^2} = (\sin^2 \theta) \frac{\int_0^{2\pi} \sin^2 \phi \, d\phi}{\int_0^{2\pi} d\phi} = 1/2 \sin^2 \theta \quad (44)$$

At any given position of the molecule specified by angle θ and ϕ , the axis 3 of the molecule is fixed, but the axes 1 and 2 are perfectly random within the plane normal to the axis 3. Therefore, $\lambda_1^2 = \lambda_2^2$ and, since

$$\lambda_1^2 + \lambda_2^2 + \lambda_3^2 = 1$$



X,Y,Z-----laboratory coordinates
 Light propagates along the Y axis and film is tilted
 by angle θ around the x axis
 OA,OA'-----represents the helical axis of the collagen
 molecule

Figure IV-23 Geometry of tilted collagen film

$$\ell_1^2 = \ell_2^2 = 1/2(1 - \ell_3^2) = 1/2 \left(\frac{1 - \sin^2 \theta}{2} \right) \quad (45)$$

the specific rotation at tilted angle θ becomes

$$\begin{aligned} [\alpha_\theta] &= [\alpha_{11}]\ell_1^2 + [\alpha_{22}]\ell_2^2 + [\alpha_{33}]\ell_3^2 \\ &= [\alpha_{11}] (\ell_1^2 + \ell_2^2) + [\alpha_{33}] \ell_3^2 \\ &= [\alpha_{11}] \frac{1 - \sin^2 \theta}{2} + [\alpha_{33}] \frac{\sin^2 \theta}{2} \\ &= [\alpha_{11}] + \frac{\sin^2 \theta}{2} ([\alpha_{33}] - [\alpha_{11}]) \end{aligned} \quad (46)$$

It is possible to use eq. (46) to measure the $[\alpha_{33}]$ indirectly. Application of eq. (46) requires, however, the absence of birefringence in the specimen, a correction for change in sample thickness with tilt angle and a correction applied to the apparent tilt angle to account for the effect of refraction of the medium.

In order to have a meaningful comparison between the specific rotation values of collagen solution and films one should compare the average values $[\bar{\alpha}]_{\text{solution}}$ with $[\bar{\alpha}]_{\text{solid}}$, or its component $[\alpha_{11}]_{\text{solution}}$ with $[\alpha_{11}]_{\text{solid}}$; $[\alpha_{33}]_{\text{solution}}$ with $[\alpha_{33}]_{\text{solid}}$. Since $[\alpha]_{\text{solution}} = [\bar{\alpha}]_{\text{solution}}$, it is desirable to obtain the value of $[\bar{\alpha}]_{\text{solid}}$. Experimental difficulties in preparing such specimen of solid collagen in random orientation discouraged the direct measurements of $[\bar{\alpha}]_{\text{solid}}$. Instead, an attempt was made to measure $[\alpha_{33}]_{\text{solid}}$ using oriented fibers and thereby estimate the $[\bar{\alpha}]_{\text{solid}}$ by making use of the $[\alpha]_{\text{film}} = [\alpha_{11}]_{\text{solid}}$ value and the equation (40). The next section

is devoted to a description of such an attempt.

3.6 Optical Rotation of Collagen Fiber, $-\alpha_{33}$ solid

A. Experimental

Sample Preparation: Rat tail tendon fibers were pre-extracted in 0.5 M NaH_2PO_4 solution and dried in the air under the tension to keep the fibers in uncrimped straight configuration during the drying. Dried fibers were then mounted in a finely drilled hole in stainless steel plate. The plate was 0.132 mm in thickness and the diameter of the hole was 0.73 mm. The mounting was done as follows: the dry tendon fibers were tapered in one end with a razor blade and then thin end of the fibers were placed in the hole. The fibers were then pulled through the hole until they filled and plugged tightly the entire hole. After fibers were firmly held in the hole, both ends of the fibers were carefully trimmed with a very sharp razor blade. At this step, extreme care was taken not to pull out the fibers from the hole while trimming and also to produce as smooth a surface as possible. Then both sides of the hole were covered with thin cover glasses of ca. 0.2 mm thick. The specimen thus prepared, contained collagen fibers aligned parallel along the direction normal to the plane of the steel plate. The optical micrograph of the specimen is shown in Figure IV-24, which shows the cross sectional view of the fibers (magnification ca. 125) in

the hole with light underneath the plate.

Measurement of Optical Rotation, $[\alpha_{33}]$: Optical rotation was measured using Cary 60 Spectropolarimeter. The specimen was mounted on the special sample holder, supplied with Cary 60 for the use of cubic solution cell, so that the specimen plate was perpendicular and, therefore, fiber axes were parallel to the direction of the light propagation (Figure IV-25). The use of stainless steel plate reduced the area of the cross-section of the beam to ca. 1/10 of its normal size. Any effect that the reduced beam size might have on the measurement was examined by running the baseline of the machine and measuring the optical rotation values for known specimen (i.e. collagen solution) with and without using the plate. When the sample holder was used, the response time necessary for the compensator of the Cary 60 to reach its equilibrium position was slightly extended; however, no appreciable difference was observed in measured value of the optical rotation.

The ORD was run from 600 μ to lower wavelengths and when rotation angle exceeded the limits of the instrument, (1°), samples of the opposite rotation, placed in series, were used to bring down the rotation angle within the measurable limit. (As shown in next section, $[\alpha_{33}]_{\text{solid}}$ was positive and, therefore, collagen solution of high concentration (ca. 1.5%-wt.) was used to reduce the rotation angle to a measurable level).



Figure IV-24 Optical micrograph of the cross-sectional view of the tendon specimen used for the optical rotation measurements (magnification, ca. x125)



Figure IV-14 Optical micrograph of the cross-sectional view of the tendon specimen used for the optical rotation measurements (magnification, $\times 200$)

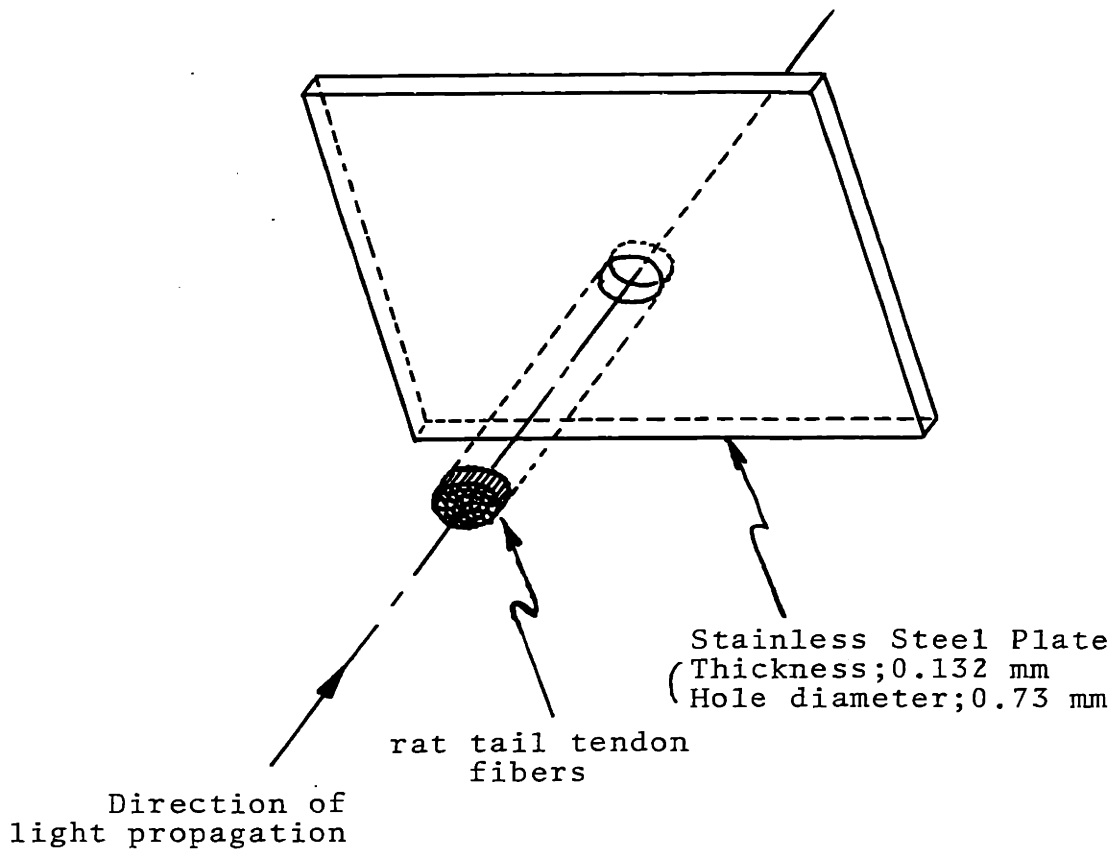


Figure IV-25 Specimen holder for the tendon fibers in the measurements of the optical rotation

Measurement of Thickness and Density: In order to convert the measured rotation angle to the specific rotation, it is necessary to know exact thickness and packing density of the tendon specimen used. (i.e. $[\alpha] = 10 \cdot \alpha / \ell \cdot c$ where α is the measured angle of rotation, ℓ is thickness of the specimen in cm, c is the density of the specimen in gr/cm^3 , so $\ell \cdot c$ is surface density, g/cm^2 .) When examined under the microscope, the overall surface of the cross-sections of the fibers was fairly smooth and in the same plane as the surface of the metal plate. The thickness of the specimen (average length of the fibers in the hole), therefore, was taken to be the same as the thickness of the metal plate which was 0.132 mm. The packing density (% cross sectional area occupied by fibers) of each specimen used was determined by visual examination under the microscope. For a completely filled specimen (i.e. no apparent vacant area is seen in the entire cross sectional area of the hole), the hexagonal packing was assumed for the packing of fibers inside the hole and a factor of 0.91 was applied to the density 1.32 to obtain the bulk density of the fiber specimen. (The density 1.32 measured with dry collagen films (ca. 15%-wt. water) was also assumed to be the density of dry collagen fibrils (ca. 15%-wt. water)). The value for $\ell \cdot c$ in the above equation was, therefore, obtained by multiplying the density 1.32 by a factor 0.91 and by the thickness 0.132 mm.

B. Results and Discussion

The ORD of dry rat tail tendon fibers (ca. 15%-wt. moisture), measured along the fiber axis (therefore, along the axis of collagen helix) is shown in Figure IV-26. Each point in the Figure IV-26 represents one measured value. The filled circles are all from the same specimen, showing the variation in repeated measurements and open circles are from different specimens indicating the specimen-to-specimen variations. Such scattered values are considered to be due to the variation in packing densities of collagen fibers in different specimens and the possible misalignment of the specimen position with respect to the light propagation direction, which will introduce birefringence effect in the measured values. Line was drawn through the average values of the scattered points.

Contrary to the negative rotation values of collagen solution and film, $[\alpha]_{\text{tendon}}$ was positive in the entire wavelength range measured. At 365 m μ , for example, $[\alpha]_{\text{tendon}}$ is $+1500 \pm 200$, whereas $[\bar{\alpha}]_{\text{solution}}$ is -1300 ± 50 and $[\alpha]_{\text{film}}$ is -3200 ± 200 . The dispersion of the quantities $[\alpha]_{\text{film}} = [\alpha_{11}]_{\text{solid}}$ and $[\alpha]_{\text{tendon}} = [\alpha_{33}]_{\text{solid}}$ of collagen in dry solid state is shown in Figure IV-27.

The $[\alpha_{33}]$ of the elastoidine fiber was reported by McGavin (64), who measured the optical rotation along the fiber axis using polarized microscope. At wavelength of sodium D line, reported values were +958 and +887 for the

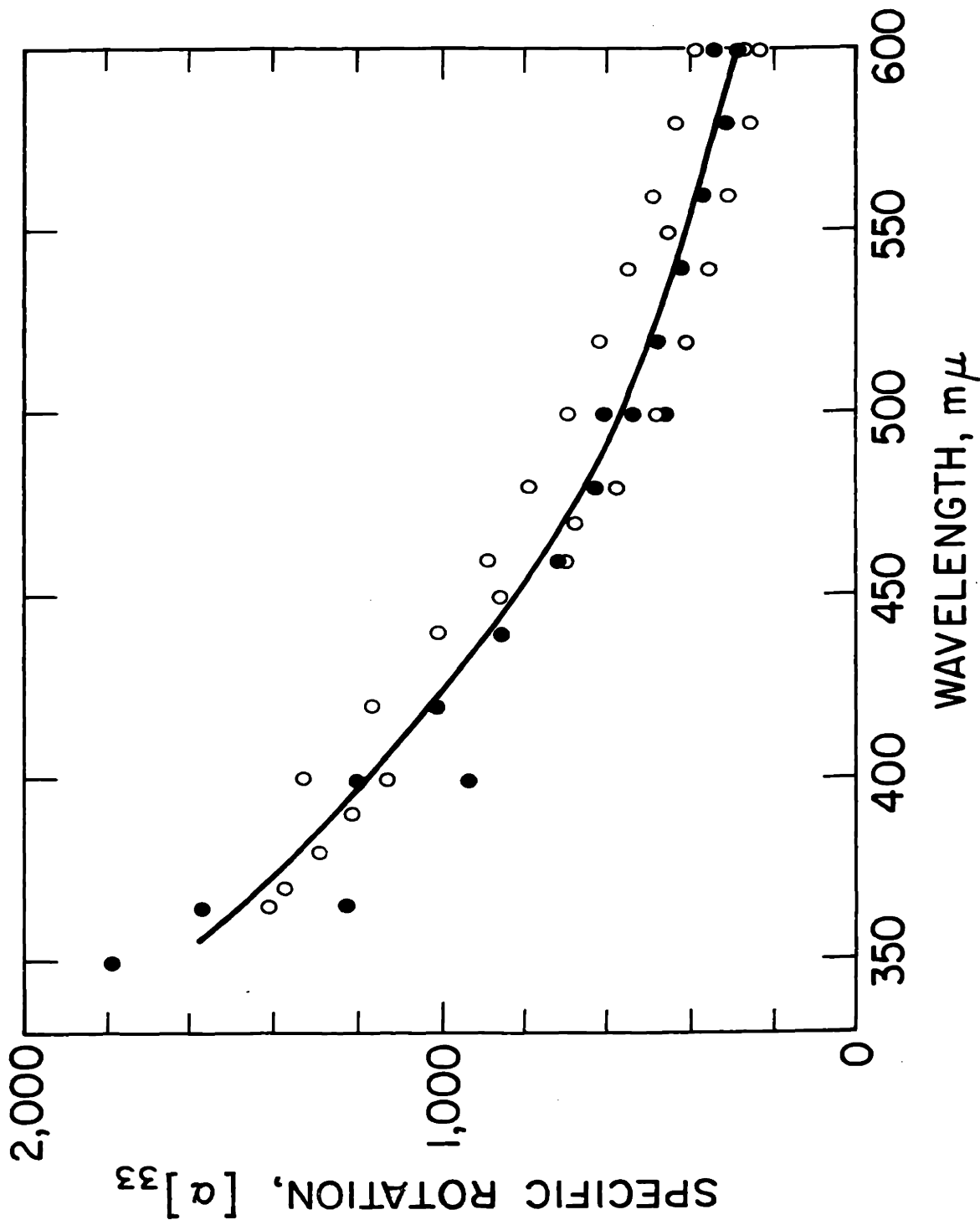


Figure IV-26 ORD of dry collagen fiber (ca.15%-wt. water) measured along the axis $[\alpha]_{33}$

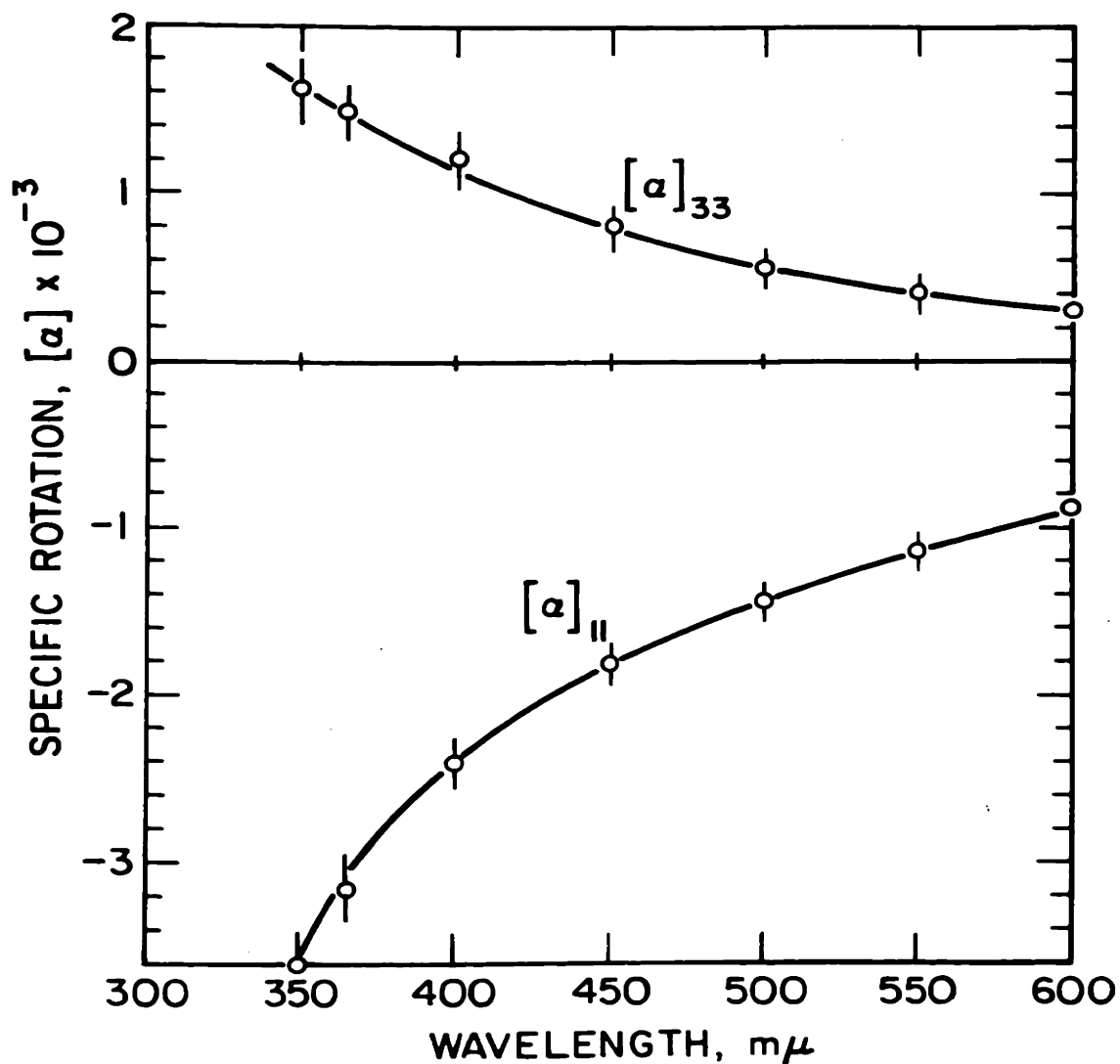


Figure IV-27 Comparison of the ORD of collagen measured along the helical axis of molecule ($[\alpha]_{33}$) and in perpendicular to the helical axis ($[\alpha]_{\perp}$)

wet and acid-swollen elastoidine fibers, however, $[\alpha_{33}]$ of the collagen fiber was mentioned to be negative (64). It seems unlikely, however, that $[\alpha_{33}]$ of collagen fiber is quite different from that of elastoidin fiber, because the chemical composition (55) and the X-ray diffraction patterns (77,81,82) of the two fibers are known to be very similar and, therefore, collagen and elastoidin have been considered as of the same triple helical structures. (82). The $[\alpha_{33}]$ of collagen measured in this work was, indeed, positive as elastoidin fiber, but the magnitude of the rotation was much lower for the relatively dry collagen used in that work than for the wet elastoidin fiber used by McGavin. (for a discussion of the effect of moisture content on optical activity, see below).

The significance of the resolution of optical activity in its tensorial components should be such that the anisotropy of the optical activity should provide more information on the structure of the molecules than the average optical rotation. The $[\alpha_{33}]$, for example, should be able to indicate the helix sense better than the $[\bar{\alpha}]$ can. At the present time, however, a complete theory does not exist which allows us to assign the helix sense unequivocally.

For example, Moffitt (83) has suggested that $[\alpha_{33}]$ is much larger than $[\alpha_{11}]$ in algebraic values for right-handed α -helix, whereas, Tinoco et al. (50) showed that $[\alpha_{33}]$ is negative and $[\alpha_{11}]$ is positive for right-handed α -helix, which contradicts each other. Although the right-handed assumption

tion of Moffitt et al. (83) and Fitts and Kirkwood (97) receives support from experimental data (i.e. b_0 in the Moffitt-Yang equation has negative value if right-hand α -helix, which is consistent with observed b_0 values in PBLG), theoretical calculation by Tinoco and Woody (84) using the polarizability theory showed that if PBLG is left-handed helix $[\alpha_{33}]$ will be positive which is consistent with the experimental observation (63).

The $[\alpha_{33}]$ value and its positive sign of collagen cannot, therefore, provide any clearer answer to the question of helix sense of collagen (in fact, there is no independent evidence to support the presently assumed left-handed minor helices and right-hand superhelix which is based mostly on the stereochemical considerations (82). Nonetheless, there is no doubt that the components $[\alpha_{11}]$, $[\alpha_{33}]$ will give more sensitive measure of conformational changes than the average $[\bar{\alpha}]$, and can provide more well-defined basis for the estimation of helical content of film together with the information on orientation.

C. Indirect Measurement of $[\alpha_{33}]$

Recently, an attempt was made to estimate the $[\alpha_{33}]_{\text{solid}}$ by measuring the specific rotation of the collagen film at various tilt angles, a technique which has been described in the previous section of the tensor analysis. The details of the experiment can be found in the report (95) by Mr. Chor Huang, my colleague, to the depart-

ment of Mechanical Engineering, M.I.T.

In brief, the optical rotation angle of a uniform, non-birefringent collagen film, cast on the surface of fused quartz plate, was measured at various angles of tilt (θ). According to eq. (46), derived in the previous section, one would expect that the specific rotation at a tilt angle θ , $[\alpha]_{\theta}$ will be

$$[\alpha]_{\theta} = [\alpha_{11}] + \frac{\sin^2 \theta}{2} ([\alpha_{33}] - [\alpha_{11}]) \quad (46)$$

However, correction is necessary of the optical path length of the specimen and the direction cosines of the beam with respect to the molecular axes 1, 2, 3 of collagen for the refractive index of the medium (95). In other words, apparent tilt angle β is different from the actual tilt angle θ due to the refractive index n , with the relationship $\sin \beta = n \cdot \sin \theta$. After introducing the above correction and assuming the $[\alpha]_{\theta=0} = [\alpha_{11}]$, the following equation was obtained (95):

$$\frac{\alpha_{\beta}}{\alpha_0} \cos \theta = 1 + \frac{\sin^2 \beta}{2n^2} \cdot \frac{[\alpha_{33}] - [\alpha_{11}]}{[\alpha_{11}]} \quad (47)$$

where α_{β} is the rotation angle of the specimen at tilt angle β ,

α_0 is the rotation angle of the specimen at $\beta = 0$, therefore, corresponds to $[\alpha_{11}]$ in actual rotation in degree,

n is the refractive index of collagen film (n is assumed to be 1.525 ± 0.025 for 85%-wt. collagen, 15%-wt. water (96),

β is the actual tilt angle between the beam direction and the normal of the film plane ,

θ is tilt angle corrected for refractive index of the sample .

The experimental data were presented in Figure IV-29 where plot was made for $(\alpha_{\beta}/\alpha_0 \cdot \cos \theta)$ vs $(\sin^2 \beta)$.

As shown in Figure IV-28, linear dependence of $(\alpha_{\beta}/\alpha_0 \cdot \cos \theta)$ on $(\sin^2 \beta)$ was well demonstrated by a straight line. This result is consistent with the analysis of the tensorial nature of the optical activity of collagen. The α_{33} can be estimated from the slope of the plot and the estimated value was $+1900 \pm 300$. This result is not far from the value of $+1500 \pm 200$ obtained by the direct measurements.

3.7 Comparison of the Optical Rotation of Collagen in Dilute Solution and in Solid State

For the purpose of the comparison of optical rotation, the specific rotation values at a fixed wavelength, namely $365 \text{ m}\mu$, are examined here.

In dilute solution state, the specific rotation of the collagen is the average value of the three components of $[\alpha_{11}]$ $[\alpha_{22}]$ and $[\alpha_{33}]$.

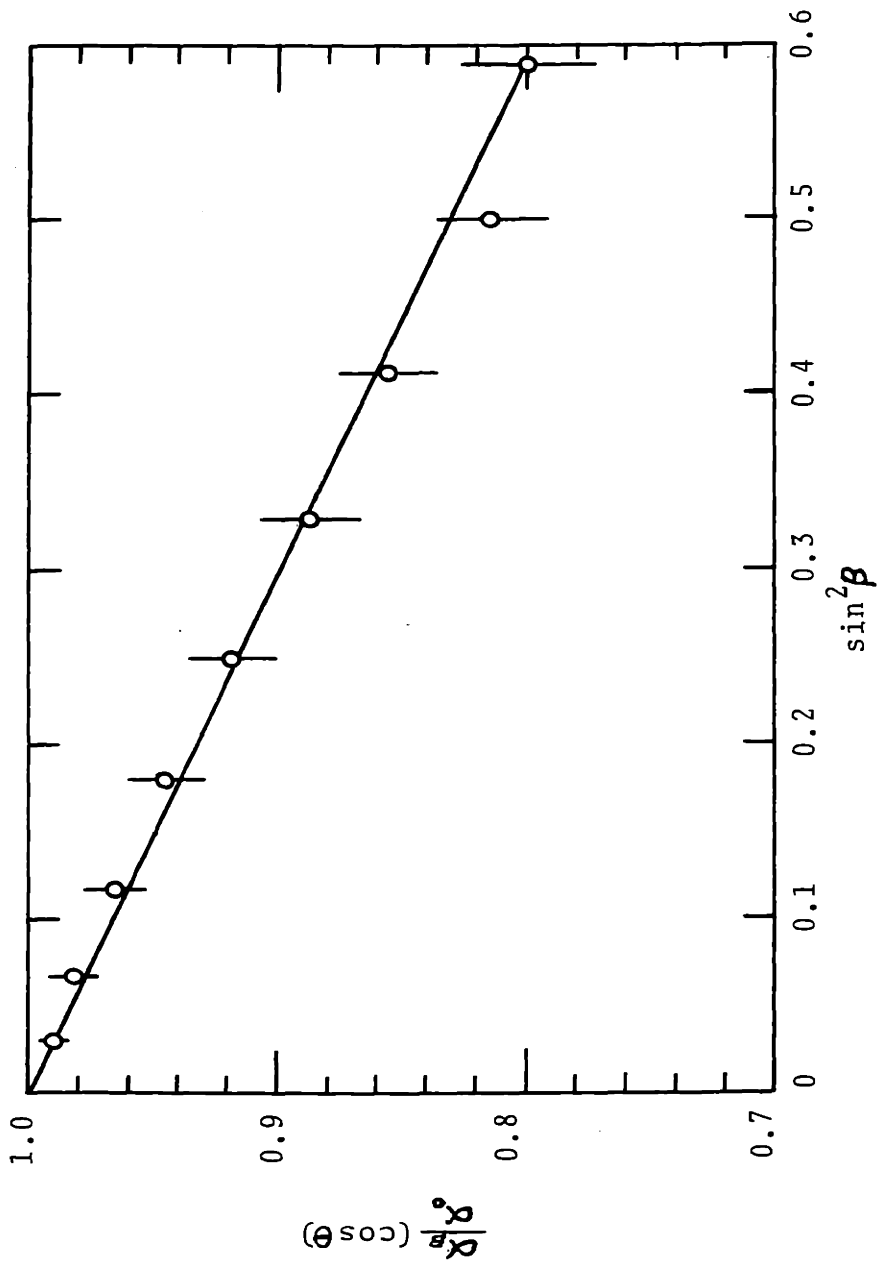


Figure IV-28 Specific rotation of the collagen films at various tilted positions (Tilt angle β)

$$[\alpha]_{\text{solution}} = [\bar{\alpha}]_{\text{solution}} = 1/3 (2[\alpha_{11}]_{\text{solution}} + [\alpha_{33}]_{\text{solution}} = -1300 \pm 50 \quad (47)$$

In solid state (ca. 15%-wt. moisture),

$$[\alpha]_{\text{film}} = -3200 \pm 200 \quad (48)$$

$$[\alpha]_{\text{tendon}} = +1500 \pm 200$$

As discussed in previous section, $[\alpha]_{\text{film}}$ and $[\alpha]_{\text{tendon}}$ can be interpreted as $[\alpha_{11}]_{\text{solid}}$ and $[\alpha_{33}]_{\text{solid}}$ respectively. In actuality, however, the orientation of the collagen molecules in the film is not perfectly planar. So is the orientation in the tendon fiber. As already discussed in Chapter III, such disorientation was estimated from the X-ray patterns and found to be 12° for the average out-of-plane orientation in the films and 9° for the misorientation of collagen molecules along the axis of tendon fiber. When corrections are made,

$$\text{for film: } \bar{\alpha}_3^2 = \overline{\cos^2 \gamma} = \overline{\cos^2(90-12)} = 0.043$$

$$\bar{\alpha}_1^2 = \bar{\alpha}_2^2 = 1/2 (1 - \bar{\alpha}_3^2) = 1/2 (0.957),$$

γ being the average angle between the helical axis of collagen molecules and the direction of the light propagation.

$$[\alpha]_{\text{film}} = [\alpha_{11}] \bar{\alpha}_1^2 + [\alpha_{22}] \bar{\alpha}_2^2 + [\alpha_{33}] \bar{\alpha}_3^2 = \quad (49)$$

$$= 0.957 [\alpha_{11}] + 0.043 [\alpha_{33}]$$

$$\text{for tendon: } \bar{\alpha}_3^2 = \overline{\cos^2 \gamma} = \overline{\cos^2 9} = 0.976$$

$$\bar{\alpha}_1^2 = \bar{\alpha}_2^2 = 1/2 (1 - \bar{\alpha}_3^2) = 1/2 (0.024)$$

$$[\alpha]_{\text{tendon}} = 0.024 [\alpha_{11}] + 0.976 [\alpha_{33}] \quad (50)$$

By solving the two eqs. (49) and (50) above, we get

$$\begin{aligned} [\alpha_{11}]_{\text{solid}} &= -3400 \pm 200 \\ [\alpha_{33}]_{\text{solid}} &= +1600 \pm 200 \end{aligned} \quad (51)$$

(It should be reminded here again that the values of the specific rotation of film and tendon in eq. (48) is the actual measured values with collagen films and tendon fibers. The values in eq. (51) are the components of the specific rotation of collagen molecules.)

It has been shown in eq. (6) that, for the purpose of comparing optical activity of different proteins or the same protein in different solvents, correction is necessary to eliminate the variation in rotation values due to the different refractive index of the medium. Since there is a significant difference in refractive index between a dilute solution specimen and a solid specimen, the Lorentz correction factor $3/(n^2 + 2)$ has been applied to the values in eqs. (48) and (51). For dilute solution of collagen (ca. 0.08%-wt.) in 0.05 M acetic acid, the refractive index is assumed to be 1.33, the same value as water, because of the very low concentration) and the refractive index of solid collagen (ca. 15%-wt. water) is taken to be 1.525. (The value is obtained from the linear interpolation between 1.33 for 100%-wt. water and 1.55 [6] for 100%-wt. collagen). The specific rotation values, reduced in this manner, are as

follows, which are denoted by the subscript r:

$$\text{for solution: } [\bar{\alpha}]_r = -1035 \pm 40 \quad (52)$$

$$\text{for solid: } [\alpha_{11}]_r = -2360 \pm 140$$

$$[\alpha_{33}]_r = +1110 \pm 140$$

and, therefore,

$$[\bar{\alpha}]_r = -1200 \pm 240 \quad (53)$$

(For $[\alpha_{33}] = 1900 \pm 300$, obtained from the indirect measurements, $[\alpha_{33}]_r$ is 1310 ± 190 and, accordingly,

$$[\bar{\alpha}]_r = -1140 \pm 275 \quad (54)$$

When the solid state values of -1200 ± 240 , -1140 ± 275 are compared with the solution value of -1035 ± 40 , two values are seen to be essentially the same within exper-

imental error range. The significance of this finding is that the large apparent difference between the optical activity of collagen in dilute solution and of collagen film is, in fact, largely due to the difference in orientation of the molecules in the two specimens and that the "structure" of collagen molecules in the solid state is substantially the same in dilute solution state. (The "structure" used here by this author refers to the basic features of secondary and tertiary structure of three-stranded coiled-coil, established as the standard structure of tropocollagen molecule by X-ray diffraction studies (82). The minor distortion of chain conformation, which might be occurred due to factors such as the distortion of the side chains, having arisen from the close packing, is not considered as the different structure where secondary and tertiary structure of the chains assume different conformations, as often found in the conformational transitions between α , β and random-coiled structures in polypeptides).

A small difference could exist between the values of $[\bar{\alpha}]_r^{\text{solution}}$ and $[\bar{\alpha}]_r^{\text{solid}}$ which this work has not resolved due to the large error range involved in the measurement. Even if there were, this would not be necessarily attributable to the difference in the tertiary structure of collagen in two states because the following effects could result in such small difference without altering the main chain conformation. For example, small difference in op-

tical activity can be observed due to the effect of environment on optical rotation (66) which is similar in nature to the effect of solvent observed in dilute solution studies (79,80). Or closely packed molecules in the solid state increase the side-group interactions which may affect the electronic π - π^* transition of the peptide bonds in backbone chains, thereby affecting the optical activity of the molecules observed. It may also be possible that the steric constraints imposed on polypeptide chains in the solid state, (which is absent in dilute solution), may distort the side chains yielding a slight distortion of the backbone chains.

All these contentions are, however, not considered by the author as the change in the secondary and tertiary structure of collagen triple helix. It must be emphasized that the comparison of the average optical rotation of collagen in dilute solution and the solid state provides the unique basis for the direct comparison of the structure of collagen in the two states. (It is unique in that ORD can be used for the study of the structure in both dilute solution and the solid states whereas the other classical physicochemical techniques are applicable only to one of either in dilute solution or in the solid state.) The result of such comparison strongly suggests that some of the confusion and the discrepancies, arising from the comparisons of ORD and CD of polypeptides between in solution and the solid states (which has been described in section

3.4-C) may be resolved by the analysis of the tensorial components of the optical activity of the polypeptides.

3.8 Assay of Helical Contents in Collagen/Gelatin System in Solid State

Several different techniques can be used to distinguish the helical structure of native collagen from the denatured random coil gelatin in solid state. Among these are the X-ray diffraction and infrared spectroscopy, details of which have already been discussed in Chapter III. Other methods are differential thermal analysis (88) and viscoelastic measurements (89). In DTA method, it has been demonstrated that collagen helix gives rise to a melting peak at $215 \pm 10^{\circ}$ C., whereas gelatin, in absence of such peak, shows a glass transition temperature at $196 \pm 3^{\circ}$ C. (88). A clear distinction was also shown (89) by the viscoelastic measurements of collagen and gelatin films, diluted with glycerol; the stress relaxation modulus of collagen-glycerol film is about ten times lower than that of gelatin-glycerol film and while the collagen-glycerol films show permanent plastic deformation, gelatin-glycerol films are rubbers.

Even though these methods can differentiate clearly the native, helical structure of collagen from the completely denatured, random-coiled gelatin, the characterization of intermediates, or the partially helical molecules are often very difficult, especially when the quantitative as-

say of helix content is attempted, primarily due to the lack of sensitivity. In this section, use of the ORD measurements for the estimation of helix content is discussed for the collagen/gelatin system in solid state. The ORD technique has been widely used for the estimation of helical content of many biopolymers and proteins in dilute solution.

Several methods have been proposed including the so-called "b₀ method" (90, 91), the "[α]_D method" (92) and the 'λ_c method" (92). Recently two measures based on the Cotton effect (40), shown in Figure IV-5 are added. Details on each method can be found elsewhere (90,91,92, 40,6,22) and so will not be discussed here. It must, however, be noted that all these methods are based on the linear model (i.e. linear interpolation between 100% helix and 100% random coil).

Several facts established already in earlier sections on the specific rotation of collagen and gelatin are of importance to the estimation of helical content which are summarized as follows:

(i) ORD of collagen, cold-cast and hot-cast gelatin films are all of the simple dispersion, which can be described as one term Drude equation (section 4(b))

$$[\alpha]_{\lambda} = A/(\lambda^2 - \lambda_c^2)$$

(ii) The only difference in ORD of collagen, cold-cast and hot-cast gelatin is the values of the rotatory

constant A (Table IV-1 in section 3), which gives the value of $[\alpha]_{\text{film}}^{365}$ -3200, -1700 and -260 respectively. The dispersion constant λ_c is essentially the same for three different films with a value of $205 \pm 10 \text{ m}\mu$. (section 4(b)).

(iii) Collagen film represents the native collagen molecules in the solid state, as seen by the characteristic CD spectrum (Figure IV-13) and by the comparison of $[\bar{\alpha}]_r^{\text{sol'n}}$ and $[\bar{\alpha}]_r^{\text{solid}}$ (section 7)

(iv) Hot-cast gelatin film is totally an amorphous random coil form of collagen as proven by the X-ray diffraction pattern (Chapter III) and the comparison of $[\bar{\alpha}]_{\text{sol'n}}^{\text{gelatin}}$ (ca. -300 at 365 $\text{m}\mu$) and the $[\bar{\alpha}]_{\text{solid}}^{\text{gelatin}}$ (ca. -260 at 365 $\text{m}\mu$) (section 4(b)).

From facts (i) and (ii), it is obvious that neither the " b_0 method" nor the " λ_c method" are applicable to collagen/gelatin system. (The " b_0 method" is for macromolecules of ORD of complex dispersion, where Moffitt-Yang equation is applicable (i.e. PGLG) and the " λ_c method" was proposed for proteins where λ_c in the Drude equation is changed upon denaturation).

The specific rotation is the only variable associated with conformational changes from collagen triple helix to random coil and, therefore, $[\alpha]$ can be used as a parameter to define the various states of conformation between native helical to denatured random coil conformations.

From facts (iii) and (iv), the specific rotation values of collagen and hot-cast films can be assigned as

the values for $[\alpha]_{\text{film}}$ of 100% native helix and 100% random coil, respectively. Therefore, at 365 $m\mu$, for example,

$$[\alpha]_{\text{film}}^{\text{collagen}} = -3200 \pm 200 \text{ represents 100\% native}$$

$$[\alpha]_{\text{film}}^{\text{hot-gelatin}} = -260 \pm 30 \text{ represents 100\% random coil}$$

(It should be noted that 100% helical, referred to native collagen, does not necessarily mean that tropocollagen is totally of helical conformation in entire length of the molecule. The controversy on the question of the absolute level of the helicity in collagen structure has been well discussed by Carver and Blout (53). Instead, the 100%-helical refers to the level of helicity of the native collagen per se).

Now, one can estimate the helical contents of films of any semi-crystalline (or partially helical) form of collagen by measuring the specific rotation value of the film and using the following linear relationship:

$$\% \text{ Helix} = \frac{[\alpha]_{\text{film}}^{\text{unknown}} - [\alpha]_{\text{film}}^{\text{hot-gelatin}}}{[\alpha]_{\text{film}}^{\text{collagen}} - [\alpha]_{\text{film}}^{\text{hot-gelatin}}} \times 100 \quad (55)$$

By using this equation (55), the helical contents of the cold-cast gelatin film is estimated to be as follows:

$$[\alpha]_{\text{film}}^{\text{cold-gelatin}} = -1700 \pm 150 \text{ at } 365 \text{ } m\mu$$

TABLE VI-2 COMPARISON OF THE ORD AND IR METHODS IN EVALUATING THE HELICAL CONTENTS OF COLD-CAST GELATIN FILMS

	ORD ($[\alpha]_{365}^{\text{films}}$)	IR (A_{1235}/A_{1450})
Collagen	-3200 ± 200	1.35 ± 0.10
Cold-cast	-1700 ± 150	1.10 ± 0.05
Hot-cast	-260 ± 30	0.89 ± 0.03
	$\frac{(1700 \pm 150) - (260 \pm 30)}{(3200 \pm 200) - (260 \pm 30)}$	$\frac{(1.10 \pm 0.05) - (0.89 \pm 0.03)}{(1.35 \pm 0.10) - (0.89 \pm 0.03)}$
	$= \frac{1440 \pm 153}{2940 \pm 202}$	$= \frac{0.21 \pm 0.059}{0.46 \pm 0.105}$
	$= 0.49 \pm 0.06$	$= 0.45 \pm 0.16$
% Helix	$49\% \pm 6\%$	$45\% \pm 16\%$

Note:

1. Error in original data of each film is the standard deviation
2. For $z = x + y$ $\Delta z = (\Delta x^2 + \Delta y^2)^{1/2}$
3. For $z = x/y$ $(\Delta z/z)^2 = (\Delta x/x)^2 + (\Delta y/y)^2$
4. Error in the final results is the absolute error.

$$\% \text{ Helix} = \frac{(-1700) - (-260)}{(-3200) - (-260)} \times 100 = 49\% \pm 6\%$$

The result is in good agreement with the result 45% obtained from the IR data (Chapter III). The error in ORD method ($\pm 6\%$) is, however, much less than the IR method ($\pm 16\%$) indicating that ORD method is much more sensitive than IR method. Detailed analysis of the errors are shown in Table IV-2 for comparison.

3.9 Optical Activity of Collagen at Different Hydration Levels

The purpose of this experiment was to monitor the structure of tropocollagen molecules during casting operation and also to understand how the specific rotation of collagen changes from its dilute solution value (ca. -1300 at 365 $m\mu$) to the solid film value (ca. -3200 at 365 $m\mu$) as the level of hydration changes during casting. For this, the measurements of the optical rotation of dilute solution of collagen were followed as the solution was being evaporated and subsequently dehydrated to solid film.

A. Experimental

At a fixed reference wavelength of 365 $m\mu$, the specific rotation of collagen solution was measured using the standard solution cell in the same manner as described earlier in this chapter. Depending on the level of the concentration of collagen, three different solution cells

of optical path length of 1.0 cm, 0.1 cm and 0.01 cm were used for the range of concentrations from 0.08% to 0.4%-wt. collagen, from 0.4% to 1.0%-wt. and from 1.0% to about 5%-wt. respectively. At higher concentration than 5%-wt. collagen, solution became very viscous and the solution cell could not be used any further. An aliquot of a very viscous solution (ca. 7%-wt. collagen) was, therefore, transferred onto the surface of quartz cell where further dehydration was carried out. The optical rotation was measured quickly while the concentrated collagen solution was in the liquid state. At around 7% to 10%-wt. collagen, the flow of the solution was barely noticeable during the measurement of rotation as seen by changes in the measured angles. Measurements were, however, made quickly at different positions of the cell by rotating the cell by 180° around the direction of the light propagation. At about 20%-wt. collagen, solution acquired gel-like state and the flow of the concentrated collagen was negligible. Due to the relatively rapid change in concentration at above 20%-wt. collagen, measurements were carried out more or less in continuous manner and the weight of the whole specimen (quartz cell and the collagen gel) was measured before and after the each rotation measurements. The concentration of the collagen for each measurement was determined by the average weight of the sample measured before and after that measurement based on the final dehydrated collagen weight. (Dehydrated at 105° C., vacuum for 72 hours.) At

higher concentration levels of ca. 40%-wt. - 60%-wt. collagen, significant error was introduced in determining the concentration of the sample due to the non-uniform dehydration in the direction from the center of the cell, where the actual measurement was made, to the outside circumference of the sample. The error was, however, not considered as vital in this experiment. The approximate error in concentration was estimated to be not more than $\pm 5\%$ in the concentration range of 40% - 60%.-wt.

B. Results and Discussion

The specific rotation of collagen measured at 365 m μ at various hydration levels was plotted against the concentration of water and is shown in Figure IV-29. As results show, from the dilute solution state to about 30%-wt. collagen, the specific rotation remained unchanged at a value of -1300. It therefore can be concluded immediately that in this concentration range there is no evidence of collagen molecules undergoing any structural changes or of interaction between them leading, for example, to formation of aggregates (i.e. liquid crystal formation), which may affect the optical rotation. It should be noted that, as already described in the section of solution casting in Chapter II, onset of gel-like state occurred at around 20%-wt. collagen level, as seen by the visual observation as well as shown by the associated drastic changes in the ratio of dehydration (see Figure II-5). Such a change in the

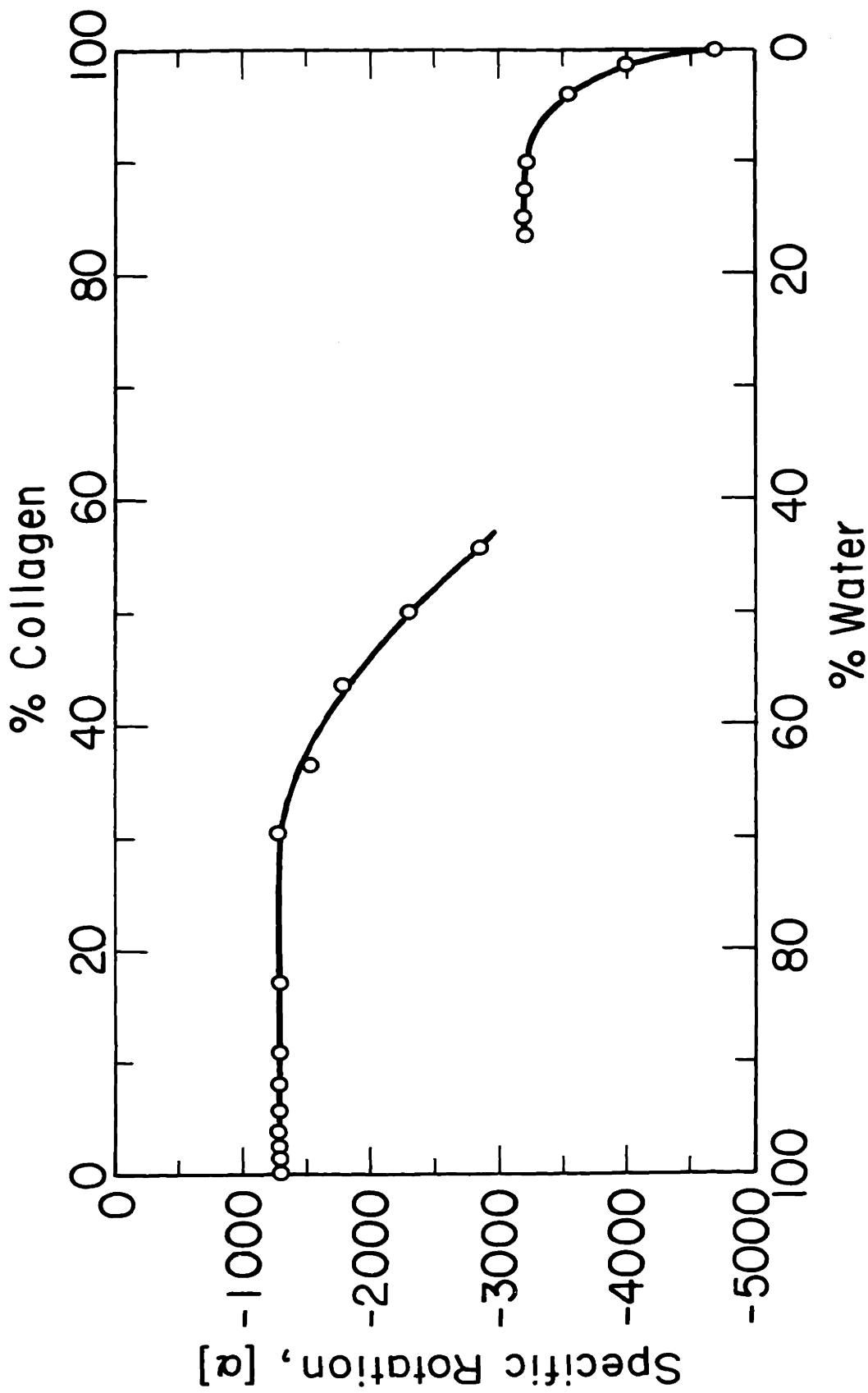


Figure IV-29 Specific rotation of collagen at various hydration levels from in dilute solution to anhydrous states

viscoelastic character of the collagen solution apparently has no effect on the structure of tropocollagen molecules. From about 30%-wt. collagen, however, the specific rotation gradually increased in its magnitude from -1300 to about -2800 as concentration increased to ca. 56%-wt. collagen. Considering the fact (discussed earlier in section 3.7) that the higher magnitude of the specific rotation value of the collagen film (ca. -3200) is largely due to the planar orientation of the collagen molecules in the film against the random orientation in dilute solution, and that the average specific rotation of collagen is almost the same in both states, it seems to be clear that the increase in the optical rotation observed in the higher concentration range must be due to the gradual attainment of the orientation by collagen molecules in the plane of the film as the gel-like collagen becomes dry film. (Discussion on the data above 85%-wt. collagen to anhydrous state, shown in Figure IV-29 will be presented in next chapter).

3-10 Summary and Conclusions

A. A brief review has been made on the phenomenon of optical activity and its use on the study of secondary and tertiary structure of biopolymers and polypeptides. General aspects of the Drude and the Moffitt-Yang equations and Cotton effects have been discussed.

B. To explore the optical rotation measurement in the use

of the characterization of collagen and gelatin in the solid state, optical rotatory dispersion (ORD) and circular dichroism (CD) measurements were made on collagen of various conformational states in the solid state as well as in dilute solution. The following results were obtained:

(i) In dilute solution, both collagen and gelatin (denatured collagen) show ORD behavior (250 $m\mu$ - 600 $m\mu$) known as simple dispersion which can be expressed by a one-term Drude equation with dispersion constant λ_c of $205 \pm 10 m\mu$. A large difference in optical rotation was observed (i.e. at 365 $m\mu$ $[\alpha]_{\text{collagen}}^{\text{sol'n}} = -1300 \pm 50$, $[\alpha]_{\text{gelatin}}^{\text{sol'n}} = -450 \pm 30$) which confirms the earlier findings (42; 43). In the Cotton effect region (250 - 200 $m\mu$), both collagen and gelatin showed simple negative Cotton effect with minimum at around 207 - 209 $m\mu$, which also agrees well with the reported results (49,53,54). Despite the apparent simple Cotton effect shown in the ORD of both collagen and gelatin, CD spectrum of collagen showed two distinctive peaks, a strong negative one at ca. 198 $m\mu$ and a weak positive one at ca. 222 $m\mu$, while that of gelatin showed only a negative peak at about 200 $m\mu$.

(ii) In the solid state, the ORD spectra (in the range 250 - 600 $m\mu$) of collagen (crystalline), cold-cast (semi-crystalline) and hot-cast (amorphous) gelatin films were also of simple dispersion as in dilute solution (i).

The differences in the degree of structural order at secondary and tertiary levels among the above three films (Chapter III) were sensitively reflected in the magnitude of the optical rotation. At 365 m μ , for example, the specific rotation values were -3200 ± 200 , -1700 ± 150 and -260 ± 30 for collagen, cold-cast and hot-cast gelatin films respectively. The ORD and CD spectra in the solid state showed essentially the same basic features (i.e. the position and the sign of the extrema) as in dilute solution. The large differences were, however, observed between the magnitude of the optical rotation of collagen film ($[\alpha]_{365} = -3200$) and solution ($[\alpha]_{365} = -1300$), and between that of cold-cast gelatin film ($[\alpha]_{365} = -1700$) and gelatin solution ($[\alpha]_{365} = -450$ at 23° C.), while those of hot-cast gelatin film ($[\alpha]_{365} = -260$) and hot gelatin solution ($[\alpha]_{365} = -300$ at 65° C.) were almost identical.

C. The apparent difference shown above raised a question as to whether the triple helical structure of the collagen molecule assumes different conformations in solution and the solid state. In an attempt to answer the question, analysis has been made of the optical activity tensor of the collagen molecule assuming the collagen molecule is a uniaxial crystal with a 3-fold symmetry. As a result of the analysis, following equation was derived;

$$\alpha = \alpha_{11} l_1^2 + \alpha_{22} l_2^2 + \alpha_{33} l_3^2$$

and

$$\alpha_{11} = \alpha_{22}$$

where $\alpha_{11} = \alpha_{22}$, α_{33} are the optical activity measured with the light beam perpendicular and parallel to the helix axis of collagen molecule, l_1 , l_2 , l_3 are the direction cosines. The components α_{11} and α_{33} of the collagen molecule in the solid state (ca. 15%-wt. water) has been determined by measuring the optical rotation of the collagen film and the tendon fibers. The specific rotation $[\alpha_{11}]$ and $[\alpha_{33}]$, thus, obtained are, at 365 m μ ,

$$[\alpha_{11}]_{\text{solid}} = - 3400 \pm 200$$

$$[\alpha_{33}]_{\text{solid}} = + 1600 \pm 200$$

D. Proper comparison was made between the optical activity of collagen in solution and in the solid state by taking the average of the three components, reduced by the Lorentz correction factor.

$$\text{At } 365 \text{ m}\mu, [\alpha]_{\text{r}}^{\text{solution}} = \frac{2 [\alpha_{11}]_{\text{r}}^{\text{sol'n}} + [\alpha_{33}]_{\text{r}}^{\text{sol'n}}}{3} = -1035 \pm 40$$

$$[\alpha]_{\text{r}}^{\text{solid}} = \frac{2 [\alpha_{11}]_{\text{r}}^{\text{solid}} + [\alpha_{33}]_{\text{r}}^{\text{solid}}}{3} = -1200 \pm 240$$

From this, it is concluded that the triple helical structure of collagen is essentially the same in both dilute solution and the solid state and that the large apparent difference between the optical activity of collagen in

dilute solution and in solid film is largely due to the difference in the degree of orientation of the molecules.

E. With the establishment of the nativity of the collagen molecules in the solid film (D), assay of the helical contents of semi-crystalline collagen films (cold-cast gelatin) was made using the following equation;

$$\% \text{ Helix} = \frac{[\alpha]_{\text{cold-gelatin}} - [\alpha]_{\text{hot-gelatin}}}{[\alpha]_{\text{collagen}} - [\alpha]_{\text{hot-gelatin}}}$$

The result gives the relative helicity of the specimen with respect to the native collagen helix.

Helical contents of the cold-cast gelatin films were found to be 49% ± 6% which is in good agreement with the result 45% ± 16%, obtained from the IR method. As proven by the smaller error in the result, ORD method was much more sensitive than the IR method in assaying the helical contents of collagen-gelatin specimen.

REFERENCES FOR CHAPTER IV

1. Djerassi, C. (1960) Optical Rotatory Dispersion, McGraw-Hill, N.Y.
2. Pauling, L. and Corey, R.B (1951), Proc. Natl. Acad. Sci., U.S. 37, 235
3. Watson, J. and Crick, F.H.C. (1953), Nature, 171, 737
4. Poly- α -amino Acids, Protein models for conformational studies, Ed. by G.D. Fasman, M. Dekker Inc. N.Y. (1947)
5. Jirgenson, B. (1961), Tetrahedron, 13, 166
6. Urnes, P. and Doty, P. (1961), Adv. Prot. Chem. 16, 401
7. Schellman, J.A. and Schellman, C.G. (1961), J. Poly. Sci. 49, 129
8. Drude, P. (1900), Lehrbuch der Optik, 2nd Ed. S. Hirzel Verlag Leipzig.
9. Moffitt, W. and Yang, J.T. (1956), Proc. Natl. Acad. Sci. U.S. 42, 598
10. Jirgenson, B. (1969) Optical Rotatory Dispersion of Proteins and Other Macromolecules, Springer-Verlag, N.Y.
11. Simmons, N.S. and Blout, E.R. (1960), Biophys. J. 1, 55
12. Simmons, N.S., Cohen, C., Szent-Gyorgyi, A.G., Wetlaufer, D.B. and Blout, E.R. (1961), J. Am. Chem. Soc. 83, 4766
13. Blout, E.R., Schmier, I. and Simmons, N.S. (1962), J. Am. Chem. Soc., 84, 3193
14. Timasheff, S.N., Townend, R., Susi, H., Stevens, L., Gorbunoff, M.J. and Kumosinski, T.F. (1967), in Conformation of Biopolymers Vol. 1. p 173, Ed. by Ramachandran, G.N. Academic Press
15. Lowry, T.M. (1935), Optical Rotatory Power, Longsman, Green, London
16. Kuhn, W. (1958), Ann. Rev. Phys. Chem. 9, 417
17. Rosenfeld, L. (1928), Z. Physik, 52, 161
18. Kirkwood, J.G. (1937), J. Chem. Phys. 5, 479

19. Condon, E.U., Altar, W. and Eyring, H. (1937), J. Chem. Phys. 5, 753
20. Moffitt, W. (1956), J. Chem. Phys. 25, 467
21. Moscowitz, A. (1960), Rev. Mod. Phys. 32, 440
22. Yang, J.T. (1967), In Poly- α -Amino Acids, Ed. by Fasman, G.D., Dekker, N.Y. P239
23. Beychok, S. (1967), In Poly- α -Amino Acids, Ed by Fasman, G.D., Dekker, N.Y. P 293
24. Eyring, H., Liu, H.C. and Caldwell, D. (1968), Chem. Reviews, 68, 525
25. Kauzmann, W.J., Walter, J.E. and Eyring, H. (1940), Chem. Review, 26, 339
26. Mitchell, S. (1933) "The Cotton Effect" G. Bell & Sons, Ltd. London
27. Moscowitz, A. (1960), In ORD, by Djerassi, C. Chapter 12. McGraw-Hill, N.Y.
28. Beychok, S. (1966), Science, 154, 1288
29. Heller, W. (1958), J. Phys. Chem. 62, 1569
30. Yang, J.T. and Doty, P. (1957), J. Am. Chem. Soc. 79, 761
31. Doty, P. and Yang, J.T. (1956) J. Am. Chem. Soc. 78, 493
32. Blout, E.R. (1960), In ORD, Ed. Djerassi, C. McGraw-Hill N.Y. Chapt. 17
33. Kauzmann, W. (1957), Quantum Chemistry, Acad. Press N.Y. p 616
34. Bradbury, E.M., Downie, A.R., Elliott, A. and Hanby, W.E. (1960), Proc. Roy. Soc. A259, 110
35. Karlson, R.H., Norland, K.S., Fasman, G.D. and Blout, E.R. (1960), J. Am. Chem. Soc. 82, 2268
36. Yang, J.T. (1967), In Conformation of Biopolymers, Vol. 1. Ed. by Ramachandran, G.N. Acad. Press p 157
37. Kauzmann, W. (1957), Ann. Rev. Phys. Chem. 8, 413

38. Kuhn, W. and Freudenberg, K. (1932), In Hand- und Jahrbuch der Chemischen Physik, Vol. VIII, part c. Akademische Verlag. Leipzig
39. Moffitt, W. and Moscowitz, A. (1959), J. Chem. Phys. 30, 648
40. Greenfield, N. and Fasman, G.D. (1969), Biochem. 8, 4108
41. Urry, D.W. and Eyring, H. (1966), In Perspectives in Biology and Medicine, p 450-475
42. Harrington, W.F. and von Hippel, P.H. (1961), Adv. Protein Chem. 16, 1
43. Cohen, C. (1955), J. Biophys. Biochem. Cytol. 1, 203
44. Harrington, W.F. (1958), Nature, 181, 997
45. Burge, R.E. and Hynes, R.D. (1959), Nature, 184, 1562
46. Lewis, M.S. and Piez, K.A. (1961), Federation Proc. 20, 380
47. Doty, P. and Nishihara, T. (1958), In Recent Adv. in Gelatin and Glue Res., G. Stainsby Ed. p.92 Pergamon Press, London
48. Cary, H., Hawes, R.C., Hooper, P.B., Duffield, J.J. and George, K.P. (1964), Appl. Optics, 3, 329
49. Blout, E.R., Carver, J.P. and Gross, J. (1963), J. Am. Chem. Soc., 85, 644
50. Caldwell, D.J. and Eyring, H. (1971), The Theory of Optical Activity, Wiley- Interscience
51. Gratzer, W.B., Rhodes, W. and Fasman, G.D. (1963), Biopolymers, 1, 319
52. von Hippel, P.H. (1967), In Treatise on Collagen, Vol. 1, G.N. Ramachandran Ed. Chapt. 6, Academic Press, London and New York
53. Carver, J.P. and Blout, E.R. (1967) In Treatise on Collagen, Vol. 1, G.N. Ramachandran Ed. Chapt. 9 Acad. Press, London and New York
54. Velluz, L., Legrand, M. and Grosjean, M. (1965), Optical Circular Dichroism, Acad. Press, London and New York

55. Damodaran, M. et al. (1956), Biochem. J. 62, 621
56. Sarkar, P.K. and Doty, P. (1966), Proc. Natl. Acad. Sci. U.S. 55, 981
57. Greenfield, N., Davidson, B. and Fasman, G.D. (1967), Biochem., 6, 1630
58. Cowan, P.M. and McGavin, S. (1955), Nature, London 176, 501
59. Madison, V. and Schellman, J. (1970), Biopolymers, 9, 65
60. Fasman, G.D. (1966), Biopolymers, 4, 509
61. Tiffany, M.L. and Krimm, S. (1968) Biopolymers, 6, 1767
62. Fasman, G.D., Hoving, H. and Timasheff, S.N. (1970), Biochem. 9, 3316
63. Tinoco, Jr., I. (1959), J. Am. Chem. Soc. 81, 1540
64. McGavin, S. (1964), J. Mol. Biol. 9, 601
65. Troxell, T.C. and Scheraga, H. A. (1971), Macromolecules 4, 519
66. Elliott, A., Hanby, W.E. and Malcolm B.R. (1958), Disc. Faraday Soc. 25, 167
67. Downie, Elliott, A, Hanby, W.E. and Malcolm, B. R. (1957), Proc. Royal Soc. A242, 325
68. Blout, E.R. and Spector, E. (1963), Biopolymers, 1, 565
69. Kauzmann, W. (1971), Private Communication
70. Tinoco, Jr., I. (1957), J. Amer. Che. Soc. 79, 4248
71. Gō, N. (1965), J. Chem. Phys. 43, 1275, (1967) J. Phys. Soc. of Japan, 23, 83 and 1094
72. Nye, J.F. (1957) Physical Properties of Crystals Oxford Press
73. Hoffman, S.J. and Ullman, R. (1970), J. Poly. Sci. No. 31, 205
74. Troxell, T.C. and Scheraga, H.A. (1971), Macro-molecules, 4, 527

75. Born, M. (1933), Optik, Springer Verlag, Berlin
76. Sommerfeld, A. (1954), Optics, Academic Press, N.Y.
77. Bear, R.S. (1952), Adv. Protein Chem. 7, 69
78. Urry, D.W. and Ji, T.H. (1968), Arch. Biochem. Biophys. 128, 802
79. Adler, A.J. et al. (1968), J. Amer. Chem. Soc. 90, 4763
80. Urry, D.W. (1968), Ann. Rev. Phys. Chem. 19, 477
81. McGavin, S. (1962) J. Mol. Biol. 5, 275
82. Ramachandran, G.N. (1967), In Treatise on Collagen Vol. 1, Chapt. 3. Acad. Press, London and New York
83. Moffitt, W., Fitts, D.D. and Kirkwood, J.G. (1957), Proc. Nat'l. Acad. Sci. U.S. 43, 723
84. Tinoco, Jr., I. and Woody, R.W. (1960), J. Chem. Phys. 32, 461
85. Boedtker, H. and Doty, P. (1956), J. Amer. Chem. Soc. 78, 4267
86. Piez, K. (1967), In Treatise on Collagen Vol. 1, Chapt. 5, Ed. by Ramachandran, G.N. Acad. Press, London and New York
87. Hodge, A.J. (1967), In Treatise on Collagen Vol. 1, Chapt. 4, Ed. by Ramachandran, G.N. Acad. Press, London and New York
88. Yannas, I.V. (1972), J. Macromol. Sci. c7, 49
89. Yannas, I.V. and Huang, C. (1972), Macromolecules, 5 99
90. Cohen, C. and Szent-Györgi, A. (1957), J. Amer. Chem. Soc. 79, 248
91. Carver, J.P., Shacter, E. and Blout, E.R. (1966), J. Amer. Chem. Soc. 88, 2562
92. Yang, J.T. (1957), J. Amer. Chem. Soc. 79, 761
93. Robinson, C. and Bott, M.J. (1951), Nature, 168, 325
94. Elliott, A. (1958), In Recent Adv. in Gelatin and Glue Research, Ed. by Stainsby, G. Pergammon Press

95. Huang, Chor (1972), Report to the Dept of Mech. Eng., M.I.T.
96. Benedek, G.B. (1972), Private Communication
97. Fitts, D.D., and Kirkwood, J.G. (1957), Proc. Natl. Acad. Sci. U.S. 43, 1046

CHAPTER V
EFFECT OF DEHYDRATION ON THE STRUCTURE
AND PROPERTIES OF COLLAGEN

V-1 Introduction

One of the major differences between the environment of collagen in the native state and in the bulk state lies in its degree of hydration. In the native state, collagen exists in highly hydrated form (i.e. native tendon contains ca. 65%-wt. water), whereas in dry bulk state, it contains approximately 10-15%-wt. water. Due to the large amount of polar amino acid residues, about 15-20%-wt. (18-25g/100g collagen) of water is believed to be bound directly to the primary chains of the collagen molecule (10,11). The role of such bound and free water in the biological functions and the stability of the structure of biological macromolecules is often very difficult to assess.

The question naturally arises as to whether or not the structure of collagen triple helix is affected by different levels of hydration. Several independent studies (9-13) put forward the hypothesis that water plays an important role in the stabilization of triple helix. In particular, von Hippel and Harrington (11,14) proposed that water is essential in the formation and the maintenance of collagen triple helix. The characterization of collagen structure in the non-fibrous bulk state, therefore, necessitates further investigation of the structure of anhydrous collagen. In this chapter, the effect of dehydration on

the structure of collagen at different levels (primary, secondary, tertiary and quaternary) were studied using the techniques described in earlier chapters.

In addition to the structural aspect of the effect of dehydration on collagen triple helix, another feature of it was found to be the insolubilization of the soluble collagen (23). It has been found by Yannas and Tobolsky (24) that gelatin becomes covalently cross-linked when it is dehydrated below 0.3%-wt. moisture content. These authors suggested that interchain amide bonds are formed via a condensation reaction between carboxylic and amino groups. Even though the dehydration per se was not recognized as the process causing cross-linking, similar behavior was reported earlier (25-27) that soluble gelatin becomes insoluble when it is treated under various conditions of high temperature, indicating some kind of cross-links has developed (26,27). Since collagen and gelatin are identical in their primary structure (i.e. some constituent amino acids), the nature of the dehydrative cross-linking in collagen may well be the same as that in gelatin. With collagen in vivo, however, intermolecular cross-linking is suggested (28,29) to be formed through the aldol condensation reaction between lysine-derived aldehydes. It is not known yet whether the intermolecular cross-linking produced biosynthetically in vivo is related at all to the dehydrative cross-linking produced in collagen in vitro.

Besides the intrinsic interest in assessing the role of traces of water in collagen molecule, since the change in the solubility of collagen film poses a practical importance in its use (i.e. as membrane), investigation has been made to study the solubility of the anhydrous collagen and to elucidate the mechanism of dehydrative cross-linking.

V-2. Amino Acid Analysis of Anhydrous Collagen

The purpose of this experiment was to investigate the effect of dehydration and the experimental conditions employed for the dehydration on the primary structure of collagen, namely the constituent amino acids of the polypeptide chains of collagen molecule. Comparisons were made between the amino acid compositions of the native and the dehydrated rat tail tendon collagen.

2.1 Experimental

Tendon fibers extracted from fresh rat tails were pre-extracted in 0.5M $\text{NaH}_2\text{B}_4\text{O}_7$ solution for a few hours to remove the non-collagenous portions, washed with distilled water and then dried in the open air. Portions were dehydrated at 105°C under vacuum (ca. 3×10^{-4} mmHg) for five days. Approximately 30 mg each of the native and the dehydrated collagen were weighed into 250 ml ampules and 6M HCl was added at a ratio of 5 ml/1 mg collagen. Ampules were then sealed under the vacuum by a torch burner. Acid hydrolysis was carried out at 120°C, for

22 hours. Upon completing the hydrolysis, HCl was removed by a rotating vacuum evaporator and dried hydrolysate was washed three times with distilled water before finally redissolved in "Trisol" buffer solution. Approximately 10 ml of Trisol buffer was used to dissolve the hydrolysate obtained from 30 mg of collagen. Aliquots of the final hydrolysate in Trisol buffer solution were taken to the analyser.

Analysis was carried out using Beckman Automatic Amino Acid Analyser (Model 121, Beckman Instruments, Fullerton, Calif.). Three separate specimens were analyzed from each hydrolysate of the untreated and the dehydrated collagen and for each specimen, one reference solution was also analyzed. The reference solution was made up of about 25 different amino acids, each with exact amount of 25 μ moles/ml. The output data from the Analyser was the integrated area of the absorption peaks of each amino acid. The amount of each amino acid in the sample was, therefore, obtained in μ moles/ml from the ratio of the data of sample to the reference standard solution for each amino acid, multiplied by 25 μ moles/ml. For complete analysis of one specimen, approximately 9 hours were needed.

2.2 Results and Discussion

The final data of the amino acid composition of the native untreated and the dehydrated (105°C vacuum for 3 days) collagen are presented in Table V-1, where each

number represents the number
total of 1000 amino acids.
and hydroxylysine in the st
data were not obtained for
numbers in the parentheses
et al. (1). As already dis
result of native collagen i
those published data shown
difference was found in the
the untreated and the dehyd
by Cassel (2) and by Bowe a
heating on the degradation
of amino acids due to the t
extensive with methionine,
serine, threonine and valine
showed quantitative results
in amino acid residue was re
collagen at 140°-150°C for
amino acids were lost at 170
ten days at 140°-150°C were
in one day at 170°C. They a
at 105°C did not cause any a
acid in the air for ten days

The result obtained in
confirm these observations.
under vacuum for three days,
amino acid composition of co
susceptible amino acids such

Table V-1. Amino Acid Composition at Native and Dehydrated Rat Tail Tendon Collagen

	<u>Native</u>	<u>Dehydrated</u> *
Alanine	102.0	100.5
Glycine	336.0	338.0
Valine	22.7	22.6
Leucine	27.4	26.3
Iso-Leucine	11.5	10.9
Proline	121.0	122.0
Phenylalanine	13.5	12.7
Tyrosine	4.7	4.4
Serine	33.9	37.2
Threonine	18.0	19.2
Methionine	5.3	4.8
Arginine	(50.0)	(50.0)
Histidine	3.9	4.0
Lysine	31.2	30.3
Aspartic Acid	46.3	46.4
Glutamic Acid	71.3	71.0
Hydroxyproline	95.2	91.5
Hydroxylysine	(6.6)	(6.6)

* Dehydration was carried out at 105° C, under vacuum (3x10⁻⁴ mmHg) for 3 days.

NOTE: Data represents the number of amino acid residue per total of 1000 residues.

arginine, lysine, serine.
that the primary structure
the dehydration carried out
vacuum.

V-3 Effect of Dehydration Diffraction Pattern of

In this experiment, wi
patterns of rat tail tendon
different hydration levels
to anhydrous state. Change
associated with dehydration
were made to interpret the
to the secondary, tertiary
the collagen in tendon.

3.1 Experimental

The preparation of the
procedures for the X-ray ex
were already described in Ch
two specimens were prepared
and the other for the deter
water content of the specime
was gradually reduced to var
under different conditions c
The X-ray diffraction patter
single specimen after each c
moisture was determined with
vacuum drying method. The c

dehydration steps and the water content attained thereby, are listed in chronological order in Table V-2.

For the wet specimen pattern (#1), fibers were kept wet by a few drops of distilled water supplied at constant intervals of ca. 10 minutes during the exposure time of about 50 minutes. The patterns #2 and #3 were obtained in the open air because water content is close to the equilibrium water content of ca. 15% at ambient conditions. For X-ray patterns (#4-#8) of the dehydrated fibers, the following experimental steps were taken to keep the fibers at relatively constant moisture levels during the X-ray exposure. The fiber specimen mounted on the sample holder was placed in a weighing bottle and was dehydrated in the vacuum oven. After each dehydration step the specimen was kept in the weighing bottle while it was being taken to the X-ray instrument.

The entire section of the diffraction unit of the X-ray instrument was enclosed, air tight, by transparent mylar films (ca. 0.05 mm thick) and inside of the enclosure (where the specimen and the X-ray source were) was continuously flushed with dry air. The dry air was supplied from a compressed air cylinder through the series of drying tubes containing NaOH, CaCl_2 silica gel and finally the anhydrous P_2O_5 . This provided the nearly perfect anhydrous environment for the specimen fibers while it was exposed to the X-ray. Each time, the weighing bottle containing the specimen holder with the fiber specimen mounted on it was placed inside of the mylar chamber and

Table V-2. Dehydration History of the Tendon Fiber

<u>x-ray pattern number</u>	<u>T(°C)</u>	<u>P(mmHg)</u>	<u>Time(hr.)</u>	<u>Water Content (%-wt.)</u>
1		completely wet		65
2	23	760	24	20
3	23	760	48	16.5
4	23	3×10^{-4}	2	9.2
5	23	3×10^{-4}	72	3.9
6	45	3×10^{-4}	24	2.2
7	65	3×10^{-4}	48	0.95
8	105	3×10^{-4}	120	< 0.1
9	23	immersed in water	48	65

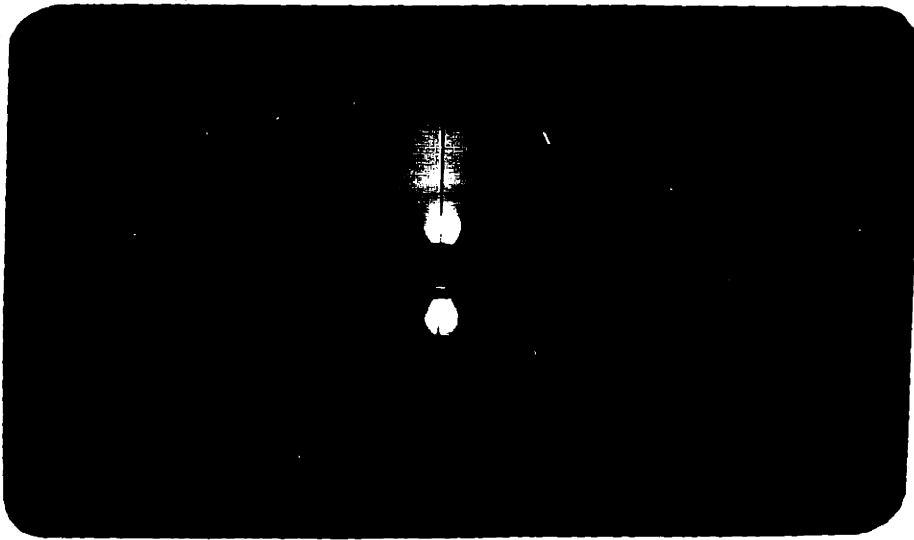
Note: Each step represents the additional treatment to the previous steps in the order

then the chamber was air tightened, flushed with dry air for at least ten minutes before the specimen was taken out of the bottle and placed in front of the X-ray beam. The steps were taken in reverse order after the exposure and the specimen was subjected to further treatment.

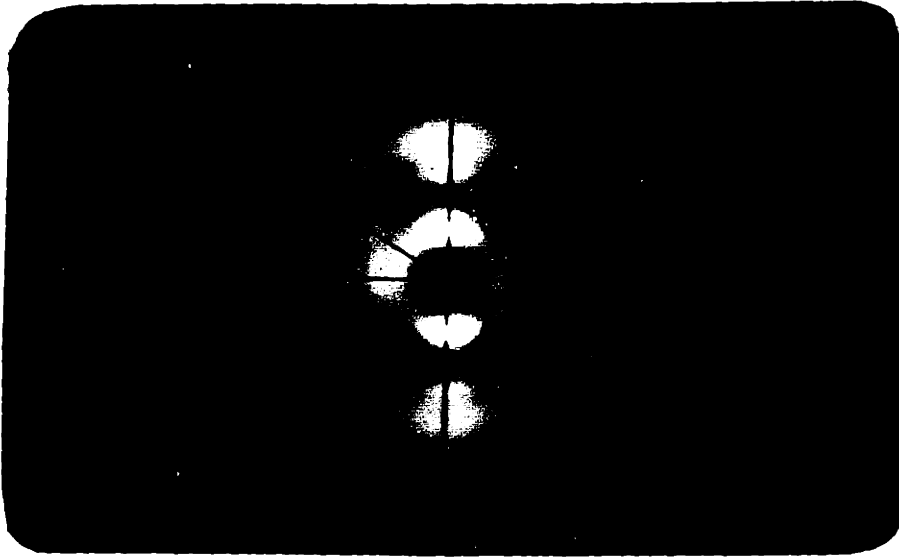
The moisture regain during the exposure time of ca. 50 minutes was negligible at dehydration levels of 1 ~ 2%-wt. (#6 and #7) and was less than 0.1%-wt. with anhydrous fibers (#8). After X-ray pattern was obtained with the anhydrous fiber, it was rehydrated by immersing in distilled water for two days at 23°C to obtain the pattern of rehydrated fibers (#9).

3.2 Results

The wide-angle X-ray fiber diagrams of native wet tendon (#1) and dry tendon (#3) are shown in Fig. V-1. Patterns of partially dehydrated (#5) and anhydrous specimen (#8) are shown in Fig. V-2. Figure V-3 shows the pattern of the rehydrated tendon (#9) in comparison with the original native wet tendon (#1). The layer line spacings were computed from each pattern and shown in Figs. V-4 and V-5. Figure V-4 shows the 10th, 7th and 3rd layer line spacings plotted against the moisture content. Figure V-5 shows the changes in the equatorial spacings of d_{100} , d_{200} reflections at different hydration levels. The helical parameter, unit twist, obtained from the ratio of d_{10}/d_3 is also plotted against water content in Fig. V-6(a).

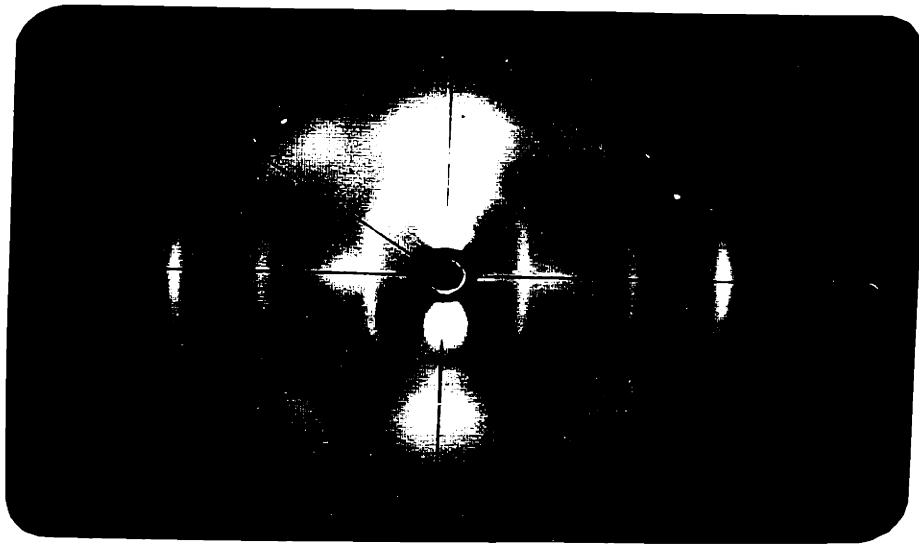


NATIVE WET TENDON
(ca. 65%-wt. water)
PATTERN #1

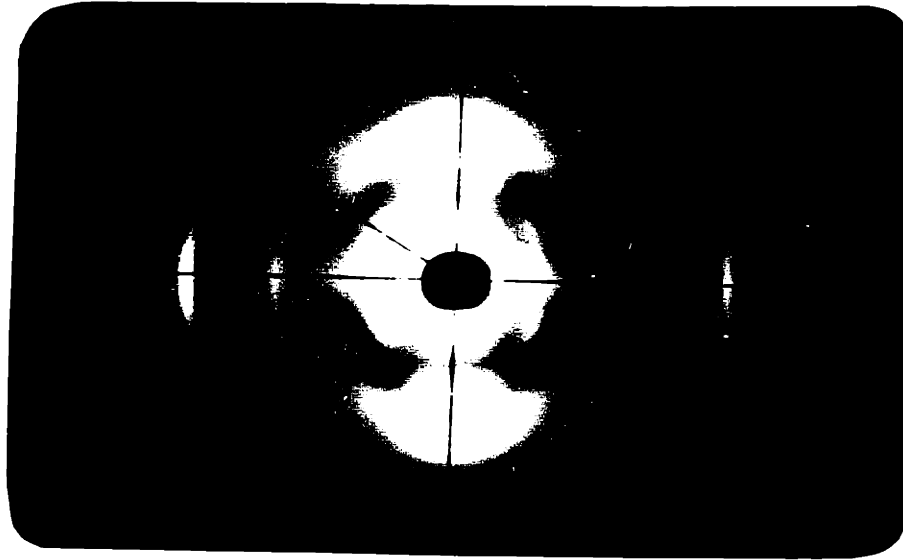


DRY TENDON
(16.5%-wt. water)
PATTERN #3

Figure V-1 Wide-Angle X-Ray Diffraction Pattern of
Collagen Fibers

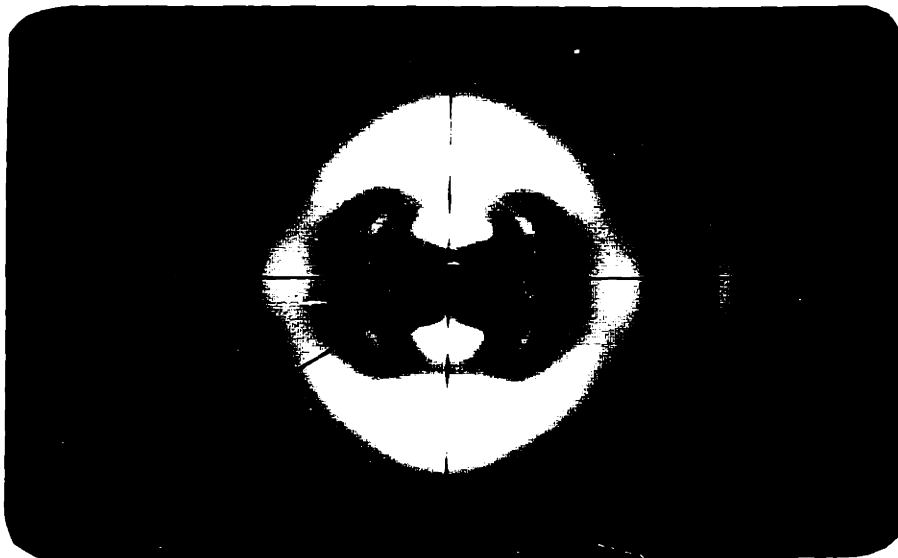


SAMPLE WITH HEADS
(Co. 057, Al. water)
PATTERN #1

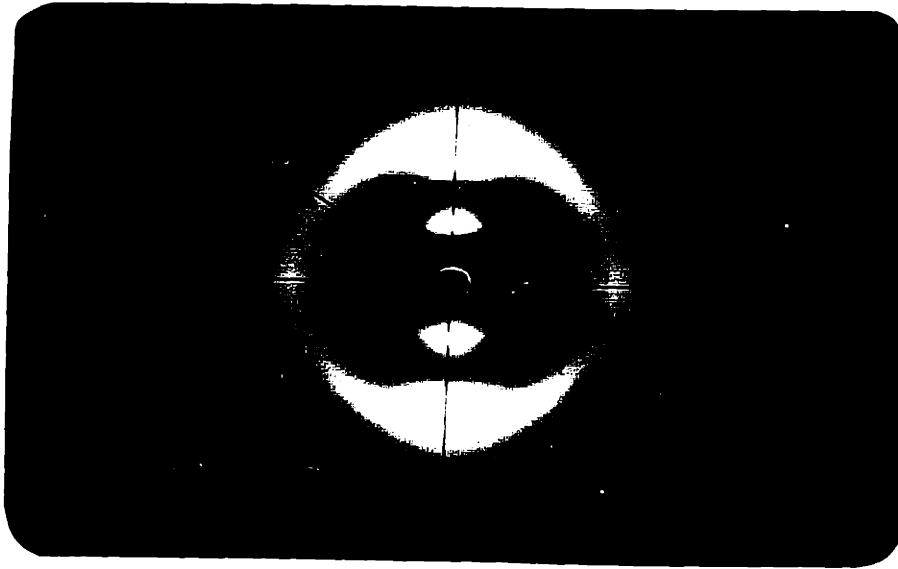


DRY HEADS
(Co. 057, Al. water)
PATTERN #3

Figure A-1 With and Without Head Pattern of
Cotton Fibers

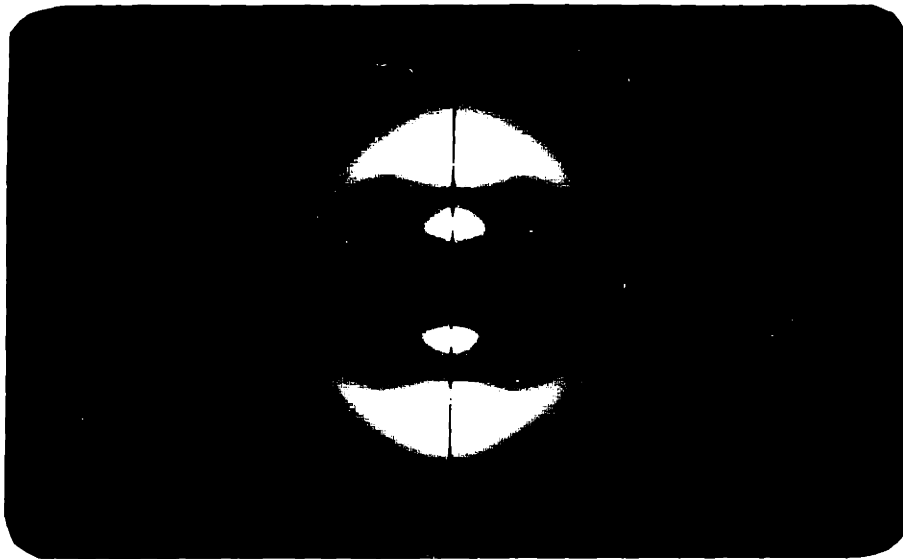


PARTIALLY DEHYDRATED CELLULOSE
 (5.9% wt. water)
 PATTERN #3

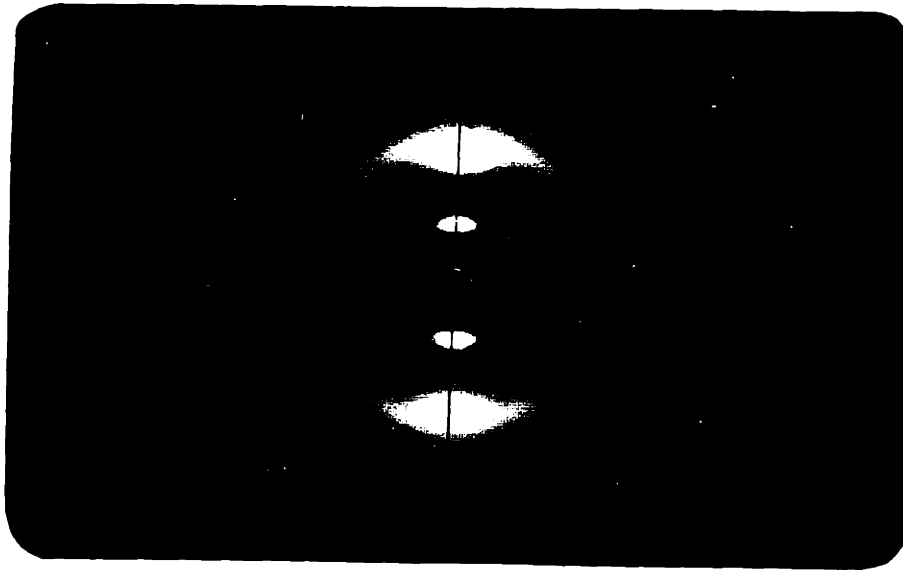


ANHYDROUS CELLULOSE
 (0.1% wt. water)
 PATTERN #8

Figure V.2. Wide Angle X-Ray Diffraction Pattern of Cellulose

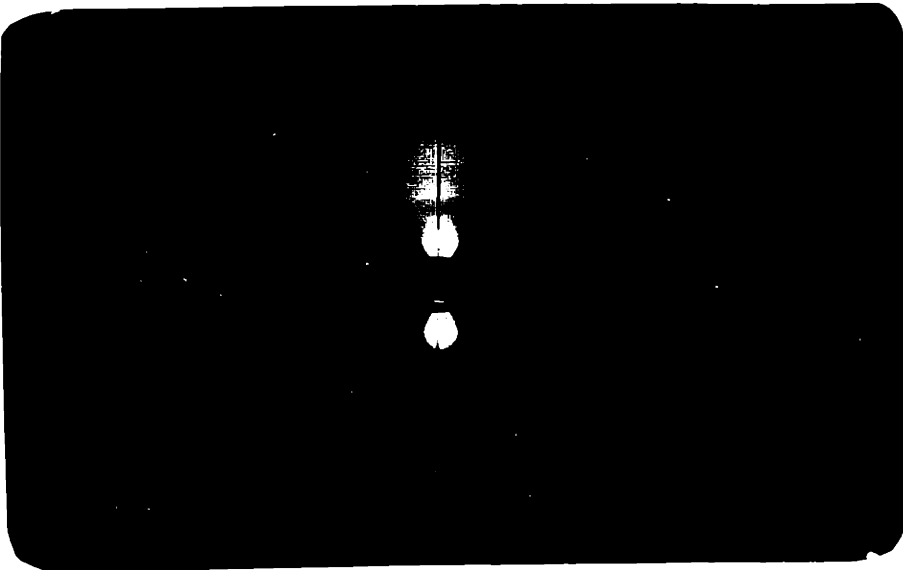


PARTIALLY DEHYDRATED TENDON
(3.9%-wt. water)
PATTERN #5

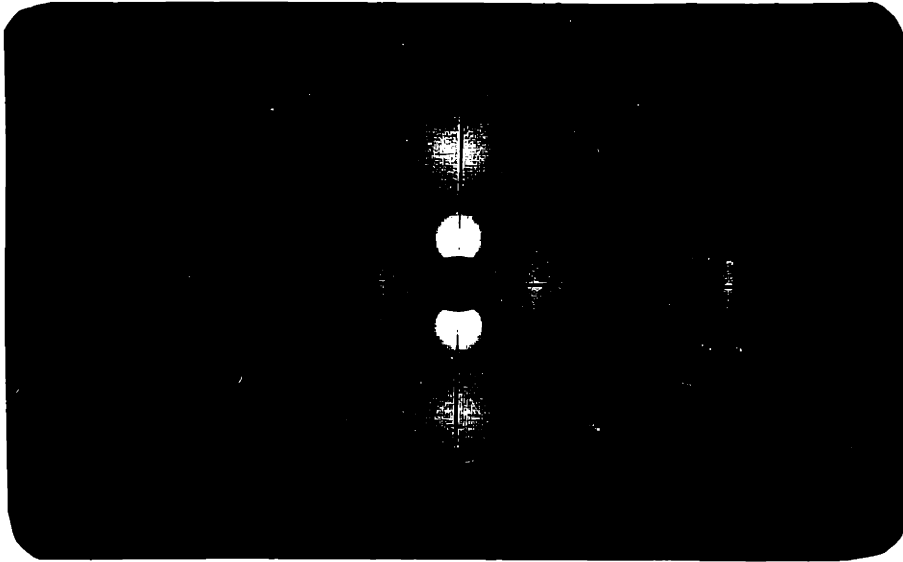


ANHYDROUS TENDON
($< 0.1\%$ -wt. water)
PATTERN #8

Figure V-2 Wide-Angle X-Ray Diffraction Pattern of Collagen

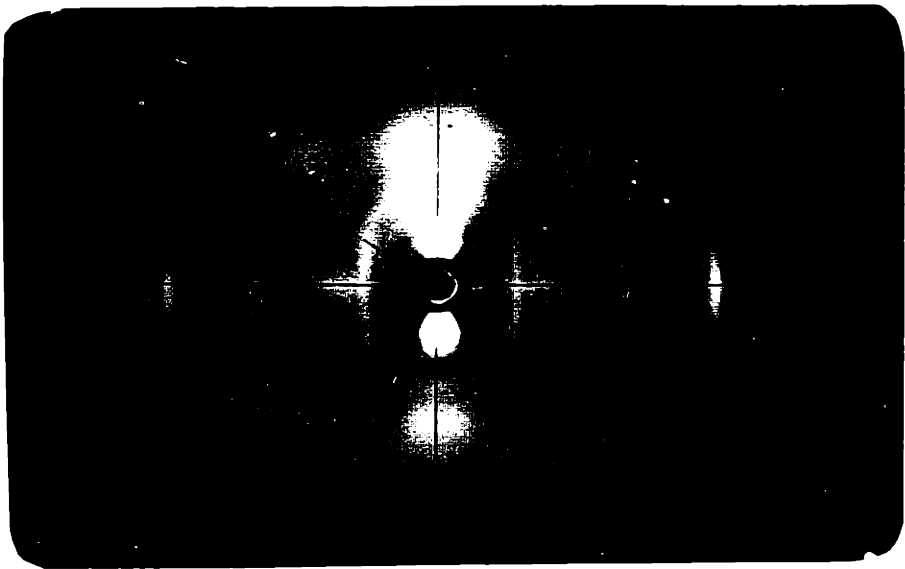


NATIVE WET TENDON
(ca. 65%-wt. water)
PATTERN #1

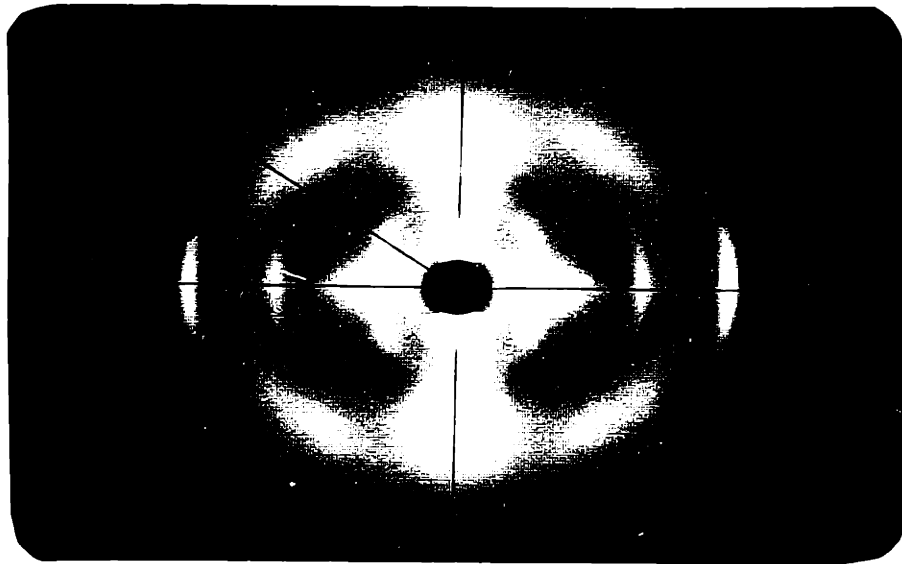


REHYDRATED TENDON
(ca. 65%-wt. water)
PATTERN #9

Figure V-3 Comparison of the Wide-Angle X-Ray Pattern of Wet and Rehydrated Collagen Tendon



SAMPLE WITH 65%
WATER
PATTERN #1



REHYDRATED SAMPLE
65% WATER
PATTERN #2

Figure 3. Comparison of the X-ray diffraction patterns of the sample and rehydrated collapsed template.

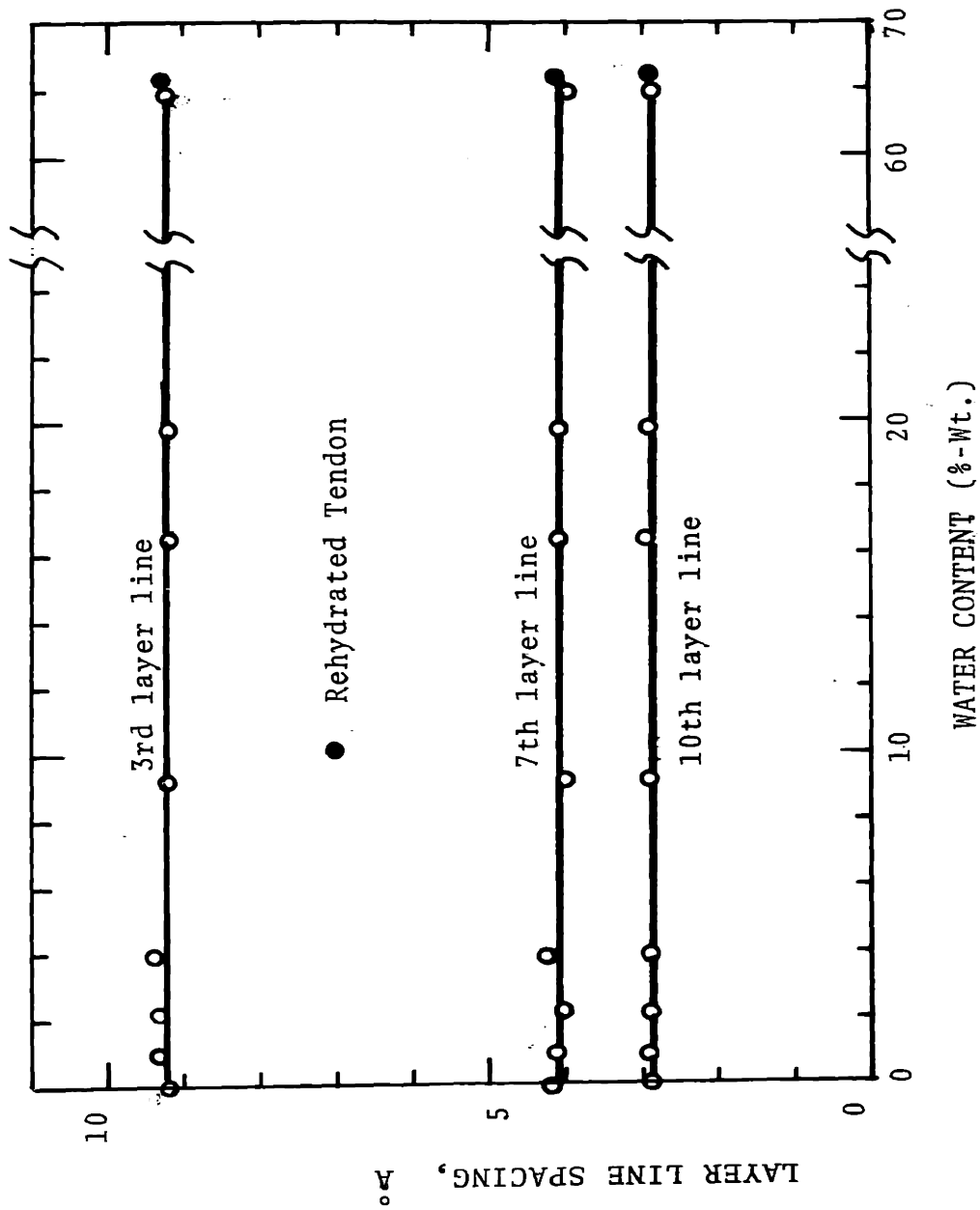


Figure V-4 Layer Line Spacings of the X-Ray Fiber Pattern of Collagen at Different Levels of Dehydration

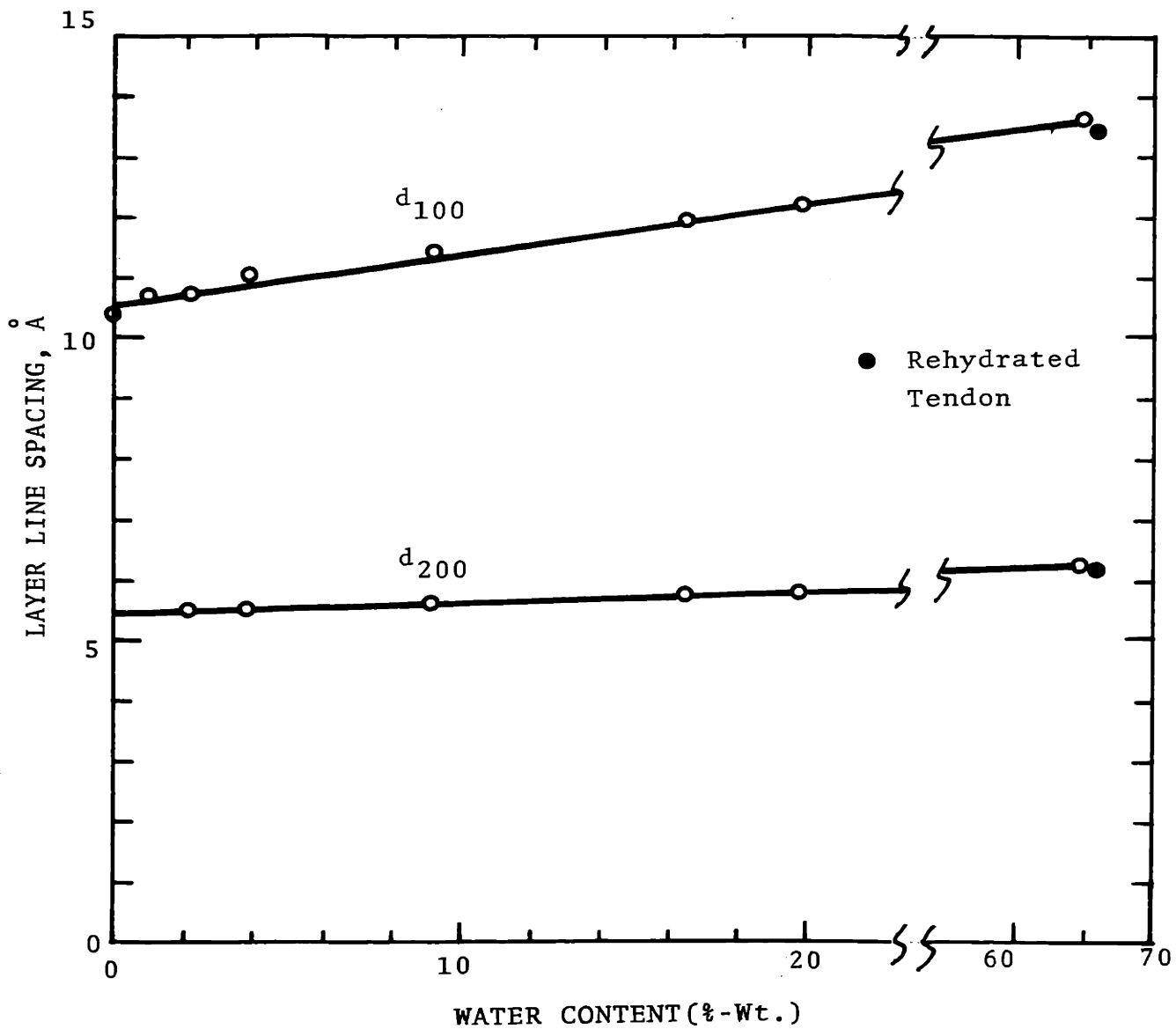


Figure V-5 Changes in Equatorial Spacings in the Wide-Angle X-Ray Fiber Pattern

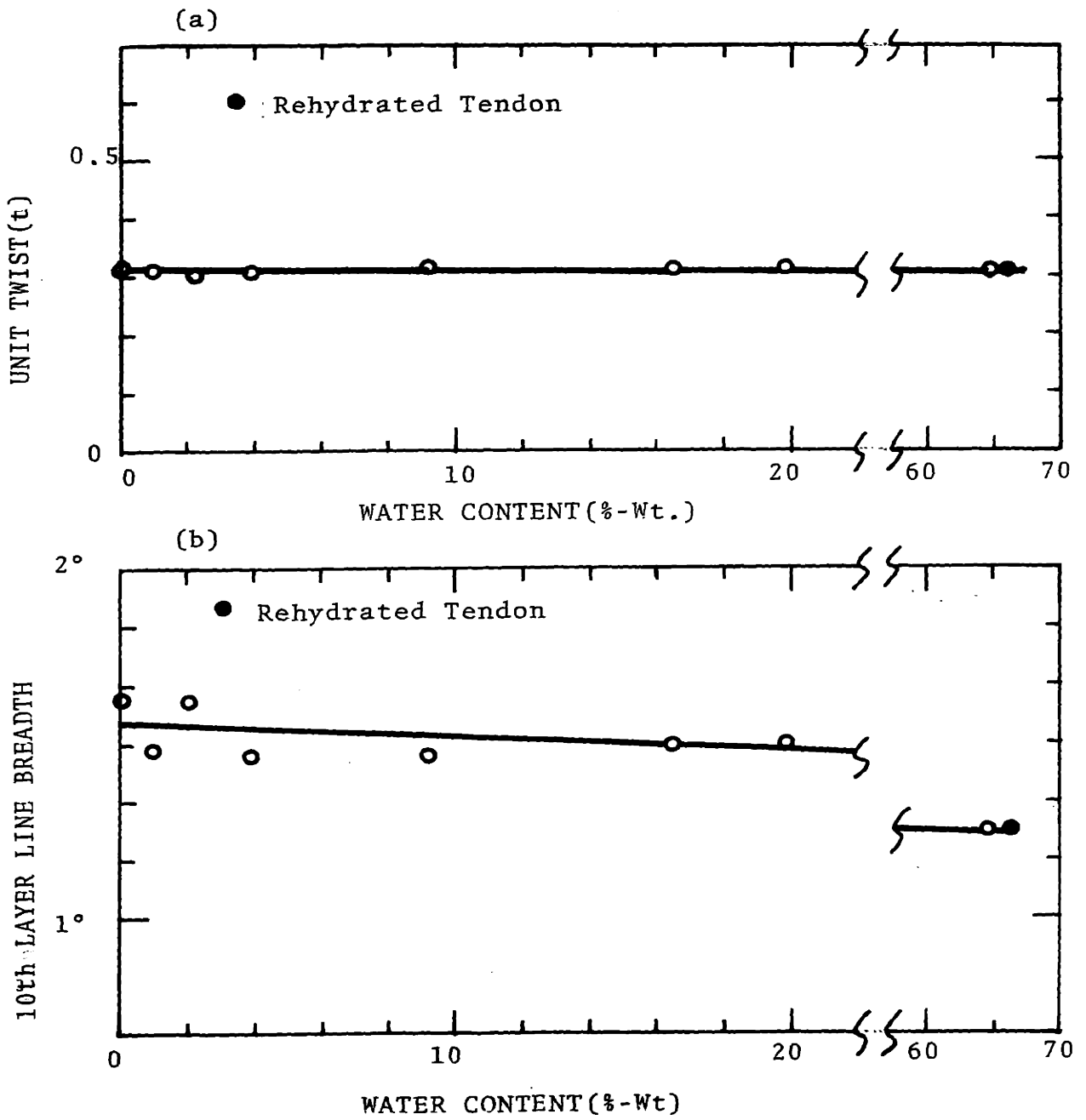


Figure V-6 Unit Twist and 10th Layer Line Breadth at Different Levels of Dehydration

3.3 Discussion

As shown in Figs. V-1, V-2 and V-3, the patterns become, in general, more diffuse as the fibers were dehydrated. The loss of the sharpness in the reflections is well demonstrated by the increase in arc length and the line breadth of the meridional (10th) and equatorial (d_{100}) reflections. The changes in line breadth of the meridional reflection are shown in Fig. V-6(b), where $1^{\circ}15'$ in wet fiber pattern has changed to ca. $1^{\circ}34'$ in the anhydrous fiber pattern. The sharp spot-like reflection of equatorial peak in wet fiber pattern also has changed distinctively to the arc reflection as the fibers were dehydrated.

Despite the increased differences, the layer line spacing of the 10th, 7th and 3rd layer lines remained unchanged at 2.9 Å, 4.1 Å and 9.25 Å, respectively, throughout the entire dehydration levels. Remarkable changes were, however, observed in the spacings of the d_{100} , d_{200} equatorial reflections which are illustrated in Fig. V-5. In the wet fiber pattern, d_{100} is ca. 13.6 Å which was reduced to ca. 10.5 Å in anhydrous fiber pattern.

The characteristics of the dry fiber pattern have been previously reported by others (4-9). The most unequivocal distinction between wet and dry fiber patterns was drawn from the equatorial reflection (d_{100}), the origin of which lies in the lateral packing of the tropo-collagen molecules in the fibrils. Besides the hydration sensitive spacings, recognized by many others (5,6,7), the

increased diffuseness of the spot-like reflection into arc-shaped reflection, with dehydration, was interpreted as the evidence of the disorientation of the tropocollagen molecules in the fibrils. This was substantially supported also by the low angle diffraction studies by Rougvie and Bear (5) who showed that the fanning angle of the low angle diffraction pattern increased from 0° to ca. 20° upon dehydration. The nature of the disorientation was explained by the model of wavy or crinkled structure of tropocollagen (a structure where lateral distance between tropocollagen molecules varies along the length of the molecule in dry state in contrast to the relatively constant spacing in wet state where water molecules filled the space between the molecules) in the dry fibers by Bear (7). This seems to be reasonable model due to the following grounds: (i) Bear (7) and Rougvie and Bear (5) showed that the macro period of 700 \AA observed in low angle diffraction pattern of the wet fiber decreased to 640 \AA in dry fiber pattern, which is associated with macroscopic shrinkage.

(ii) The result shown in Fig. V-4 indicates, however, that the spacings of 10th, 7th and 3rd layer lines did not change by dehydration and therefore the helical parameters (unit height and unit twist) are unchanged. The apparent discrepancy in (i) and (ii) leads to the support to the crinkled model for the dry collagen. In dry state, therefore, collagen has defects (or imperfections) in the quaternary structural level. In wet collagen,

water molecules fill the space between the tropocollagen molecules, thereby increase the inter-tropocollagen spacings and also promote the arrangement of molecules yielding the highly ordered quaternary structure (4).

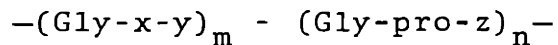
The question now is how such lattice defects occur at quaternary level and how such defects would be related to the tertiary structure of collagen helix. Contribution of water to the intramolecular stabilization of triple helix has been proposed by independent studies in dilute solution (11,14) and the X-ray diffraction studies on tendon (9). In particular, von Hippel and Harrington (11, 14) have suggested that water plays an important role in the formation as well as in the stabilization of the collagen triple helix in dilute solution. An array of water bridges through the oxygens of the carbonyl groups of the collagen chains has been proposed by these authors (11,14). Fessler and Hodge (13) observed an increase in density when collagen was denatured to gelatin by heating in CsCl solution and considered this fact to be consistent with the hypothesis proposed by previous authors. Esipova et al. (9) also suggested that water bridges between the carbonyl groups are responsible for the stabilization of the triple helix based on the wide-angle X-ray diffraction studies on tendon fibers.

At the present time, the proposed sites for water molecules to form systematic water bridges are not clearly known. Esipova et al. (9) have proposed that water forms intrachain bridge between carbonyl groups of one amino

acid to the next within the same primary chains. von Hippel and Harrington (11) suggested that array of water bridges through the oxygens of carbonyl groups may form around the individual primary chains. Burge et al. (12) have found two possible positions of systematic interchain water bridges between carbonyl oxygens within the tropocollagen molecule, although they also pointed out that neither is entirely satisfactory. Even though the exact sites are not known, there is no doubt that both carbonyl oxygen and polar groups are primary sites for water.

At this point, we should therefore examine the distribution of such polar groups along the collagen triple helix.

Both by chemical method (15,16) and transmission electron microscopy (7,17), alternate regions of "polar" and "apolar" blocks of tripeptides have been suggested to be present along the collagen triple helix. Excellent review on the concept of block copolymer of "polar" and "apolar" for collagen molecule in solid state has been given by Yannas (22), who represented the typical sequence in collagen by the following approximation:



where x, y represent mostly (though not exclusively) the polar amino acids and z being one of Hypro, Ala, Gly, Glu, Arg, Asp, Phe, The, or Ser; m, n are known to be about 4-7 (22). Even though no sharp distinctions could

be made between polar and apolar regions (22), it is generally true that polar region contains few imino acids and a large portion of polar amino acids, whereas apolar region contains a large portion of imino acids, proline and hydroxyproline (18). Due to the rotational barrier provided by the pyrrolidine rings of proline and hydroxyproline it is expected that the apolar regions may be more stable than the polar regions. An interesting aspect of this is that apolar regions in the tropocollagen are responsible for the triple helical nature of collagen structure (20) and polar regions are less ordered and may even be different from the triple helical structure (18,19). X-ray studies of model peptides showed that many of the tripeptides found in the apolar region are capable of forming collagen-like helices (20), whereas those found in the polar regions are not (19). The evidence of the order-disorder nature of apolar-polar regions has been suggested by Schwartz et al. (21). They showed by electron microscopy of the stretched reconstituted fibrils on a mylar substrate that less ordered polar regions are more extensible (~50% extension) than the more ordered, rigid apolar region (~9%). It appears, therefore, appropriate to consider the tropocollagen molecule as being a block copolymer of highly ordered, rigid apolar regions alternated by less ordered, more flexible polar regions.

Based on the above copolymer model, following interpretation is made on the X-ray patterns of the

tendon fibers: At highly swollen state (ca. 65%-wt.), the wide-angle X-ray diffraction pattern (#1) showed relatively sharp spot of equatorial and meridional reflections and also small-angle X-ray pattern showed zero fanning angle (5), indicating that the quaternary lattice structure is highly ordered. It has been shown independently by von Hippel and Harrington (11) and by Bradbury et al. (10) that about 15-20%-wt. of water (18-25 g water/100 g collagen) can be bound directly to collagen. Therefore, at this hydration level, about 45%-wt. water is free water which presumably fills the inter-tropocollagen space through the multilayer sorption, thereby increasing the spacings and also bringing the collagen chains straight.

When swollen tendon is dried to ca. 15-20%-wt. moisture level, much of the losses in sharpness of the reflections occur in wide-angle pattern (#3 in Fig. V-1). The 10th layer line breadth increases from ca. $1^{\circ}15'$ to ca. $1^{\circ}30'$ (Fig. V-6(b)) and equatorial reflection (d_{100}) changes from spot-like to arc-shape reflections. The spacing d_{100} decreases from ca. 13.6 \AA to ca. 12 \AA (Fig. V-5). The low-angle pattern by Rougvie and Bear (5) showed the increase in fanning angle from zero to ca. 20° , and decrease in macro period from ca. 700 \AA to ca. 640 \AA . All these changes are consistent with the view that the tropocollagen molecules become wavy or crinkled (4,7). Since water lost is mostly free water (ca. 65%-wt.) the effect on the tertiary structure of collagen is con-

sidered to be minor. (It should be reminded that, in fact, collagen molecule in the dry solid film (ca. 15%-wt.) is proven to be essentially of the same structure as in dilute solution (Chapter IV)). Therefore, the loss of free water brings about merely the lattice defects in the quarternary level and the disorientation of the collagen helix and has no appreciable effect on the structure of collagen at tertiary level.

Further dehydration of relatively dry collagen (pattern #3 in Fig. V-1) to anhydrous state (pattern #8 in Fig. V-2) causes the changes in diffraction pattern in the same manner as the previous dehydration of wet to dry state. The loss of sharpness in reflections of the wide angle pattern is more intense (i.e., 10th layer line breadth changed from $1^{\circ}30'$ to $1^{\circ}34'$) and the characteristic macro period in small-angle patterns was also reported to reduce from 640 Å in dry fibers to ca. 600 Å in anhydrous fibers (5). Even though the layer line reflections are more diffuse, the 10th, 7th and 3rd layer line spacings remain unchanged even at anhydrous state. It appears, therefore, the collagen molecules become more disoriented. Since water removed in this step is mostly bound water, it is possible that such increase in crinkleness of the collagen helix may be associated with some effect on the tertiary structure of collagen, such as local distortion of polypeptide chains. The perturbation of the tertiary structure of collagen chain is more likely to

occur in polar regions where structure is less ordered and more polar sites are presented for bound water than in apolar regions where structure is more ordered, rigid and less polar sites are presented. The unchanged helical parameters (unit height and unit twist) are therefore considered to be largely due to the apolar regions where structural integrity seems to be largely intact. Such non-uniform effect will cause internal shrinkage stresses at the tertiary level resulting in further lattice defects at quaternary level (inter-tropocollagen lattice).

The effect of such severe dehydration (water less than 0.1%-wt.) on the X-ray pattern was almost completely recovered by rehydrating the anhydrous fiber in water for two days as shown in Fig. V-3, as well as in Figs. V-4, V-5 and V-6. This clearly shows that the effect of dehydration on collagen fiber is almost completely reversible, indicating that the changes in structure of polar regions of the collagen helix is minor and reversible. The significance of this finding is that collagen helix survives excessive dehydration and the presence of water is not necessary for the maintenance of the collagen triple helix.

V-4 Effect of Dehydration on the Optical Rotation of Collagen.

In this study, optical rotation of the collagen films was studied at different hydration levels from ca. 15%-wt. water to anhydrous state.

4.1 Experimental

The optical rotation of the collagen films (non-birefringent, uniform thickness of ca. 10 μ) were measured at different hydration levels using Cary 60 Spectropolarimeter. Films were placed in a Beckman VLT-2 heating unit (an accessory for infrared spectrophotometer) with NaCl windows and dehydrated to various levels of moisture under different conditions of temperature and vacuum. In order to prevent any shrinkage stresses building up during dehydration, films were allowed free to contract. The conditions employed for the dehydration are summarized in Table V-3.

Table V-3. Dehydration history of the collagen films

<u>Temp</u> ($^{\circ}$ C)	<u>Press.</u> (mmHg)	<u>Time</u> (h)	<u>Moisture</u> (%-wt.)
23 $^{\circ}$ C	760	0 (Control)	14.5-15.0
35 $^{\circ}$ C	10 $^{-4}$	6	4.0
35 $^{\circ}$ C	10 $^{-4}$	28	2.7
70 $^{\circ}$ C	10 $^{-4}$	21	1.6
70 $^{\circ}$ C	10 $^{-4}$	20	1.5
105 $^{\circ}$ C	10 $^{-4}$	65	0

Note: each dehydration step is the additional treatment to the previous treatment in the descending order. After each step of dehydration, the Beckman VLT-2 unit with the specimen inside was kept under vacuum and placed in the sample chamber of Cary 60 Spectropolarimeter and the optical rotation was measured with the light beam perpendicular to the plane of the film at a fixed

reference wavelength of 365 m μ .

Following the measurement of anhydrous collagen film, the film was rehydrated by exposing to open air for three days. This was done by the removal of the NaCl windows from the VLT-2 unit and therefore, without taking out the specimen from the VLT-2 unit. Moisture determination was made on control specimen which was dehydrated independently.

4.2 Result and Discussion

The values of the specific rotation $[\alpha]_{365}$ of the collagen film measured at different hydration levels were shown in Fig. V-7 where $[\alpha]_{365}$ was plotted against moisture content. The original value, -3200, of the dry film (ca. 14-15%-wt. water) remained more or less constant in the water content range of 15%-wt. to ca. 8%-wt. Then the magnitude of the rotation gradually increased monotonically from -3200 to ca. -4500 as the level of dehydration decreased to anhydrous state. After exposure to open air for three days at 23°C, the anhydrous film regained its original equilibrium moisture of ca. 15%-wt. and the specific rotation returned to its original value of -3200. (Filled circle in Fig. V-7.)

The significance of the changes in optical rotation caused by dehydration could be attributable to the changes in the secondary and tertiary structure of collagen triple helix. It was not clear, by X-ray diffraction study alone in the previous section, to what extent the

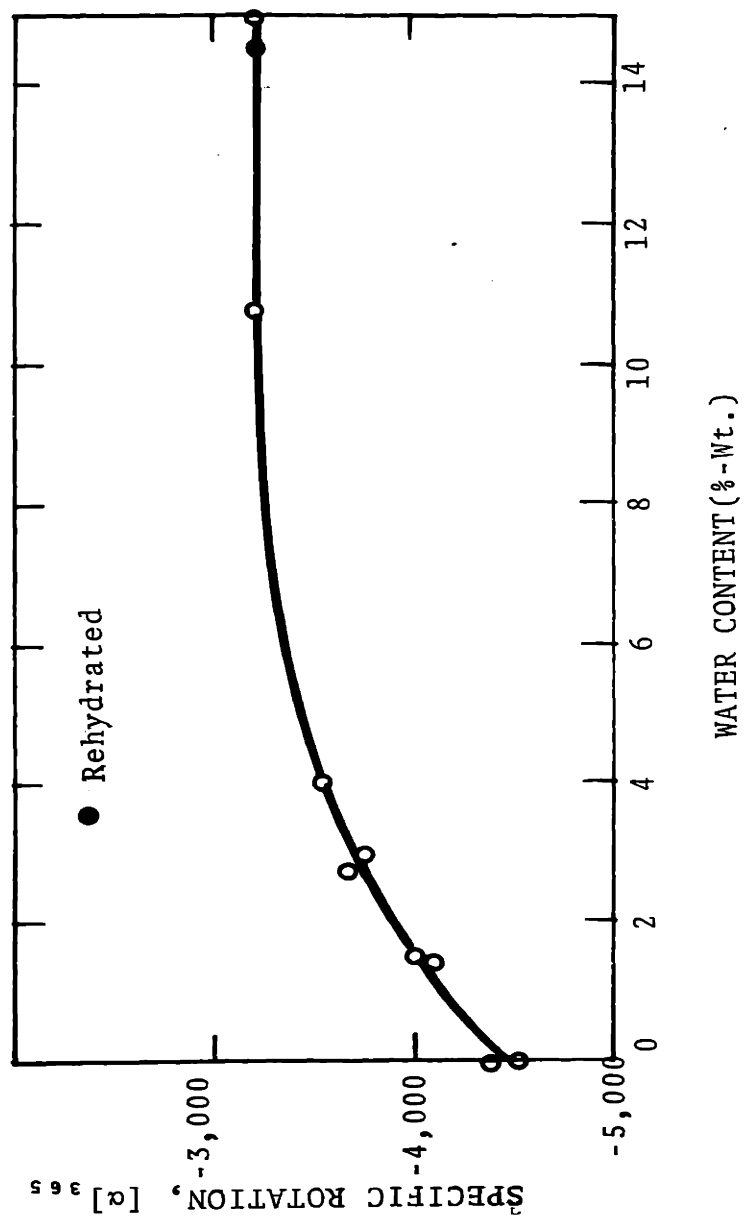


Figure V-7 Specific Rotation of the Collagen Film at Various Levels of Dehydration

tertiary structure of collagen helix is affected by dehydration. It seems that the local distortion of the individual chains in collagen helix brought about by dehydration which would occur mostly in polar regions is associated with the increased specific rotation observed at anhydrous state. Unfortunately, it is not possible to predict the exact nature and type of the deformation of the chains from the value of observed specific rotation. An interesting point is, however, that the level of optical rotation never decreased in its magnitude below the original level of -3200 and therefore the distortion of the chain caused by dehydration does not appear to be that of the randomization of the triple helical chains, which would decrease the level of optical activity as demonstrated by cold-cast ($[\alpha]_{365} = -1700$) and hot-cast ($[\alpha]_{365} = -260$) gelatin. The complete reversibility of the effect of dehydration on the structure of collagen is again clearly demonstrated by the completely recovered specific rotation value of the rehydrated collagen film, which is consistent with the X-ray diffraction study. The collagen helix, therefore, survives the severe dehydration (anhydrous state).

V-5 Effect of Dehydration on the Infrared Spectrum of Collagen

Infrared absorption spectra of dry (ca. 15%-wt. water) and anhydrous (<0.1%-wt. water) collagen films were obtained and the comparisons were made to examine

the effect of dehydration on the spectra and its relation to the structure of collagen.

5.1 Experimental

Infrared absorption spectrum of dry collagen film (ca. 3 μ thick) was obtained for the wavelengths from 2.5 μ to 50 μ using a Perkin-Elmer Infrared Spectrophotometer 621, as previously described in Chapter III. Following the measurements, the same film was placed in a Beckman VLT-2 heating unit with NaCl windows and was dehydrated at 105°C under vacuum (3×10^{-4} mmHg) for three days. After the completion of the dehydration, the temperature was reduced to room temperature (23°C) and the absorption spectrum was recorded. During the entire experiment, the Beckman VLT-2 unit was connected to a vacuum line so that the anhydrous specimen was kept free of moisture. In addition to the full spectra, repeated measurements were made at the following five absorption bands in particular, i.e. 3330 cm^{-1} , 1650 cm^{-1} , 1550 cm^{-1} , 1450 cm^{-1} , and 1235 cm^{-1} .

5.2 Results and Discussion

The comparisons were made specifically on the five major absorption bands between the two spectra of dry and anhydrous collagen and summarized below.

The 3330 cm^{-1} Band: No appreciable change was observed in band frequency. The intensity, however, was reduced slightly in the spectrum of anhydrous specimen.

The Amide I Band (1640 cm^{-1} -1660 cm^{-1}): The intensities of the sub-bands did not change and, therefore, the band contour and the apparent frequency remained unchanged at 1655 cm^{-1} .

The Amide II Band (1535 cm^{-1} -1550 cm^{-1}): The apparent frequency has shifted from 1550 cm^{-1} to 1530 cm^{-1} in anhydrous specimen as a result of the changes in relative intensities of sub-bands.

The 1450 cm^{-1} Band: Neither the frequency nor the intensity of the band has changed.

The Amide III Band (1235 cm^{-1}): No appreciable change was found in intensity of the band. Slight shift of the band frequency was observed, however, from 1235 cm^{-1} to 1230 cm^{-1} in the spectra of anhydrous collagen film. The changes in the IR absorption bands of collagen, brought about by dehydration, are largely different from the changes observed in the spectra of denatured collagen, described in Chapter III. First of all, the frequency of the NH stretching vibrational band did not change upon dehydration from the characteristic value, 3330 cm^{-1} of the collagen helix to the value 3300 cm^{-1} of random-coiled molecules. Secondly, the intensity of the Amide III band (1235 cm^{-1}) was not reduced by dehydration, whereas a large reduction of the intensity was observed in denatured collagen (Chapter III). Since the intensity of the 1450 cm^{-1} band remained unchanged, the ratio of the

absorbance of the two bands, 1235 cm^{-1} and 1450 cm^{-1} , (A_{1235}/A_{1450}) did not change from its characteristic value of 1.35 for the collagen helix (Chapter III). The above two facts strongly suggest that the chain conformation of the collagen molecule is largely undisturbed from its triple helical structure by dehydration.

While the Amide I band was not changed at all, slight shifts were found in the Amide II and III bands which is consistent with the earlier work by Bradbury et al. (10). The exact nature of the frequency shifts in these bands is not clearly understood due to the lack of knowledge in details of these bands. It seems, however, probable that such changes may be associated with the minor chain distortion of the individual chains of collagen helix which would occur in mostly polar regions during dehydration as discussed in previous sections. The slightly reduced intensity in 3330 cm^{-1} band is attributable to the loss of bound water as discussed by Bradbury et al. (10).

V-6 Conclusion on the Effect of Dehydration on the Structure of Collagen.

6.1 The loss of free water during the dehydration from highly swollen state (ca. 65%-wt. water) to dry state (ca. 15%-wt. water) causes the defects in the structural order primarily at the quarternary level (the level of order produced by packing of tropocollagen molecules), by developing the wavy or crinkled structure (4,7).

This is evidenced by the wide- and small-angle X-ray diffraction pattern of fibers, which showed the increasing disorientation without changing the dimension of the triple helical structure. The extent to which the tertiary structure (triple helix) of collagen is affected is considered to be minimal based on the ORD measurement (Chapter IV) and the fact that most of the water lost is unbound free water.

6.2 When dehydrated further to anhydrous state (0.1%-wt. water), the loss of bound water causes minor distortion of the secondary and tertiary structure of collagen primarily in the polar regions. The apolar regions remain unaffected, being responsible for the constant layer line spacings, thus, constant helical parameters, observed in wide-angle X-ray pattern. The non-uniform effect in polar and apolar regions of tropocollagen molecule, probably, causes the internal stresses contributing the further development of lattice defects in the quaternary level.

6.3 The minor distortion of the tertiary structure in polar regions of the tropocollagen molecule is considered to be responsible for the increased magnitude of the optical activity ($[\alpha_{11}]_{365} = -3200$ for dry film and $[\alpha_{11}]_{365} = -4500$ for anhydrous film) and the slight shift in the frequencies of the Amide II and III bands in the infrared absorption spectrum of anhydrous collagen.

6.4 The basic feature of the triple helical structure of

collagen is largely unaffected even at completely anhydrous state. This is evidenced by the ORD measurement (the specific rotation values never decreased in magnitude below the value of dry film $[\alpha]_{365} = -3200$), in magnitude by the infrared measurements (A_{1235}/A_{1450} remains unchanged at a value of ca. 1.35 even at anhydrous state) and, in part, by the X-ray data (the layer line spacings did not change even at anhydrous state).

6.5 The effect of dehydration on the structure of collagen is almost completely reversible as seen by the X-ray diffraction pattern and the optical activity measurements. Therefore, collagen triple helix survives the severe dehydrative state and the presence of water is not considered necessary to retain the helical structure of collagen.

6.6 The complete dehydration did not cause any loss of amino acids in collagen indicating that the primary structure of the collagen is intact during the dehydrative process.

V-7. Dehydrative Cross-Linking in Collagen and Gelatin.

7.1 Solubility of the Dehydrated Collagen Film

In this experiment, quantitative analyses of the solubility of the collagen films were made which has been dehydrated to various levels of moisture content, ranging from ca. 95%-wt. water to the anhydrous state, under different conditions.

a. Experimental

The collagen films were cast under blowing air at 23°C from a dilute solution of rat tail collagen in 0.05 M acetic acid solution. The film specimens (average wt. ca. 0.15 g) were then dehydrated to the various levels of water content under different conditions, which have been summarized in Table V-4. The water content of the specimens, used for the solubility test, was determined by the vacuum drying method (see Chapter II) on control specimens which had been dehydrated under identical conditions. On the average, eight specimens were used for each dehydration level, four for the solubility test and four for the determination of water content. The solubility test was done as follows: the specimen film was solubilized in 0.05 M acetic acid solution (100 ml/0.1 g collagen) at 23°C for two days with occasional stirring. Then, gel fraction was separated from sol using a coarse glass frit. Both sol and gel were then dried in air and dehydrated at 105°C under vacuum to determine the weight. To ensure the accuracy of the experiment, the total weight of the sol and gel fractions were compared with the original weight of the film specimen, and data were taken only when the difference between the latter and former was not more than 5% of the original weight. The percent weight of the sol fraction was used as the percent solubility. Several highly cross-linked specimens were subjected to the solubility test in

different solvents (10M LiBr solution, 5M guanidine hydrochloride solution) for various lengths of time over a period of a month at 23°C, as well as in 0.05 M acetic acid solution at higher temperatures up to 100°C for half an hour.

b. Results and discussion

The result of the experiment is summarized in Table V-4 where the %-weight of the sol and the gel are tabulated at various levels of water content. The solubility in %-wt. of the sol fraction is also plotted against water content in Fig. V-8.

The result shows that the collagen film remains completely soluble in acetic acid solution down to a water content of about 3%-wt. The onset of insolubilization occurs very sharply at water content between 2.5%-wt. and 1%-wt. and below 1%-wt. Soluble collagen becomes almost completely insoluble. It appears that in collagen, insolubilization sets in at slightly higher level of moisture content (below ca. 1%-wt.) than in gelatin (below ca. 0.2%-wt. [24]). This was confirmed by independent experiments with gelatin, the result of which is shown in Table V-5. It shows that gelatin remains soluble at water content as low as about 0.3%-wt.

Soluble collagen which has been dehydrated below water content of 1%-wt. does not dissolve even when immersed in 5 M guanidine chloride solution or in 10 M LiBr solution over several weeks at 23°C. It also

TABLE V-4 Solubility of the Dehydrated
Collagen Films

Sample #	Treatment	Water (%-wt.)	Sol (%-wt.)	Sel (%-wt.)
1	Wet film removed before casting is over	94.6	100	0
2	Wet film removed before casting is over	87.3	100	0
3	Dry film	15.0	100	0
4	Dehydrate at 23°C vacuum, 4 hr	4.7	100	0
5	Dehydrate at 23°C vacuum, 25 hr	2.8	100	0
6	Dehydrate at 65°C vacuum, 4 hr	2.5	97 ± 3	3 ± 3
7	Dehydrate at 65°C vacuum, 25 hr	1.7	91 ± 3	9 ± 3
8	Dehydrate at 65°C vacuum, 170 hr	1.5 ± 0.1	87 ± 2	13 ± 2
9	Dehydrated, vacuum at 23°C, 75 hr at 85°C, 16 hr	0.6 ± 0.1	2 ± 1	98 ± 1
10	Dehydrated, vacuum at 23°C, 75 hr at 85°C, 24 hr at 105°C, 45 hr	0.3 ± 0.1	1 ± 1	99 ± 1
11	Dehydrated vacuum at 65°C, 170 hr at 105°C, 100 hr	~0.0	0	100
12	Dehydrated, vacuum at 23°C, 75 hr. at 85°C, 24 hr at 105°C, 100 hr	~0.0	0	100

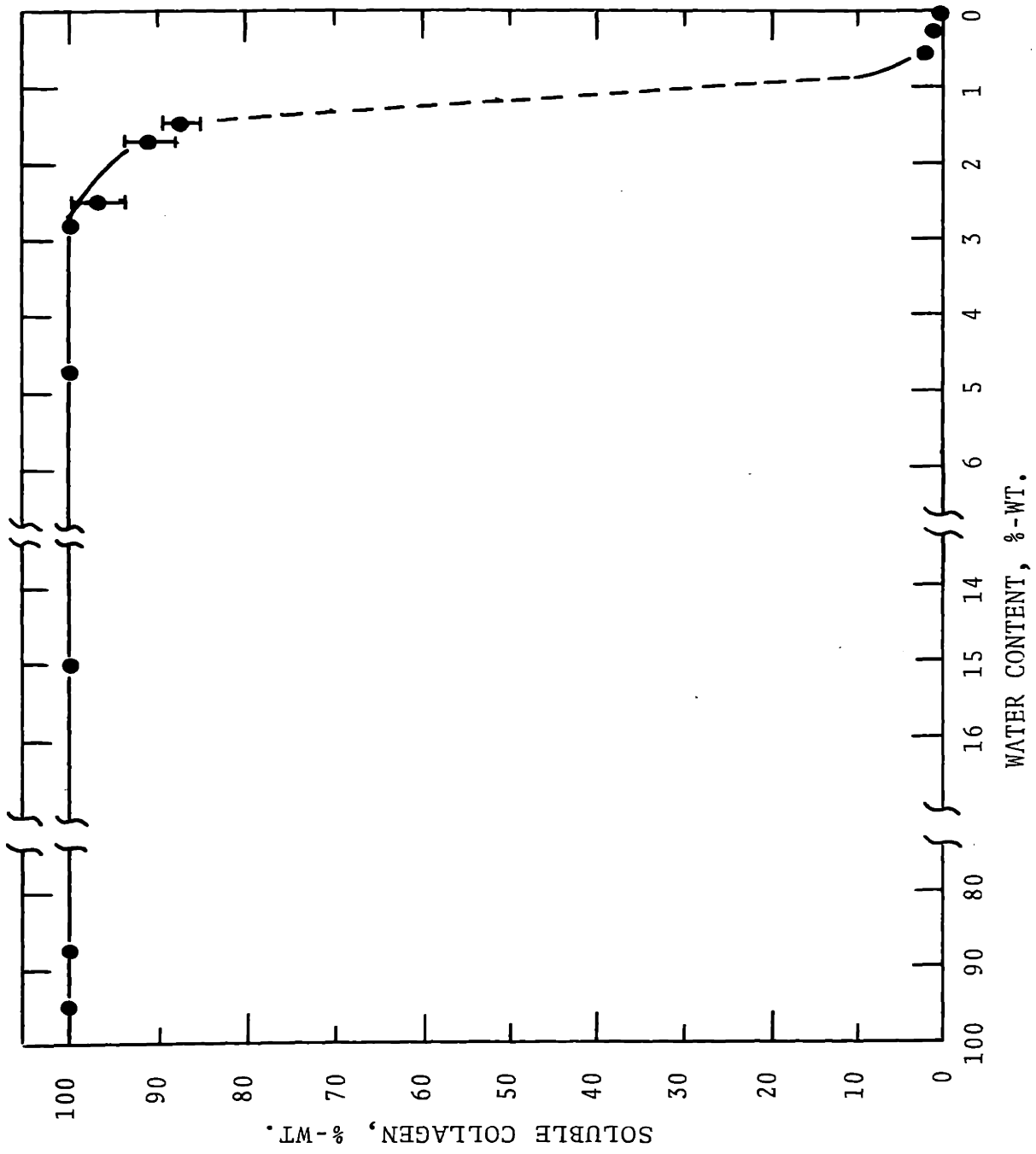


Figure V-8 Solubility of Dehydrated Collagen

Table V-5 Solubility of Dehydrated Gelatin Film

<u>Sample#</u>	<u>Water(%-wt.)</u>	<u>Solubility(in water, at 40°C)</u>
1	48.0	completely soluble
2	32.6	completely soluble
3	18.2	completely soluble
4	12.0	completely soluble
5	10.4	completely soluble
6	1.9	completely soluble
7	0.6	completely soluble
8	0.5	completely soluble
9	0.3	completely soluble
10	< 0.3	insoluble

does not dissolve in 0.05 M acetic acid solution even at 100°C for half an hour. It appears rather clear, therefore, that the irreversible loss of the solubility in dehydrated soluble collagen is due to the formation of intermolecular cross-links which are primary (covalent) bonds.

7.2 Study on the Mechanism of Dehydrative Cross-linking

It has been proposed by Yannas and Tobolsky (24) that the dehydrative cross-linking in gelatin occurs through the simple condensation reaction between carboxylic groups of one chain and amino groups of the other chain. The credibility of this proposal was well demonstrated recently by Soignet et al. (30) who successfully use the vacuum drying method to cross-link cotton cellulose containing both carboxylic and amine groups. Possibility has, however, not been clarified whether the cross-linking, developed in gelatin and collagen by dehydration, is conceivably formed via free radicals, which have been observed to be present in many biological materials (31). The concentration of the free radicals present in food materials was also reported to be increased significantly by a lyophilization process (32). To test the hypothesis that the dehydrative cross-linking of gelatin and collagen occurs by means of a free radical mechanism, the following experiment was carried out.

a. Experimental

Effect of free radical scavenger: Samples of

gelatin (Ossein gelatin, $\bar{M}_w \approx 300,000$) films were prepared by admixing different amounts of free radical scavengers in a solution of gelatin in distilled water and then subsequently casting this solution at room temperature. Hydroquinone and thiourea were used as the scavengers which were reported (33) to be effective inhibitors in irradiation cross-linking of collagen. Concentration of scavenger was varied from 0.1-4.0 g/100 g gelatin. Films were then dehydrated at 105°C under vacuum (3×10^{-1} mmHg) for three days and subjected to the solubility test. Three different solvents were used: water at 40°C, 5 M guanidine hydrochloride and 10 M LiBr solution at 23°C.

b. Results and Discussion

Table V-6 shows the summarized results of the effect of free radical scavengers on the dehydrative cross-linking in gelatin. The presence of either hydroquinone or thiourea of various amounts (up to 4.0%-wt.) in the gelatin film did not inhibit the formation of the cross-links in the films when dehydrated below 0.1%-wt. moisture level and no appreciable effect was noticed even after the prolonged solubility tests over several weeks. The result provides evidence that free radical is not responsible for the dehydrative cross-links in gelatin. In fact, the electron paramagnetic resonance (EPR) measurements by Chien (34) on collagen films which were either untreated (therefore soluble) or dehydrated, showed no appreciable EPR signals which can be directly

TABLE V-6 Effect of Free Radical Scavengers on the Solubility of Dehydrated Gelatin

a. Gelatin/Hydroquinone Films

Solvent	Concentration of Hydroquinone (g/100g gelatin)				
	0.1	0.5	1.0	2.0	4.0
1 Water (40°C)					
2 5 M guanidine -HCl (23°C)					All insoluble
3 10 M LiBr (23°C)					

b. Gelatin/Thiourea Films

Solvent	Concentration of Thiourea (g/100g gelatin)				
	0.1	0.5	1.0	2.0	4.0
1 Water (40°C)					
2 5 M guanidine -HCl (23°C)					All insoluble
3 10 M LiBr (23°C)					

NOTE: Solubility tests were carried over 2 days with solvent 1; 7 days with solvent 2 and 3 at indicated temperatures. All the films were dehydrated at 105°C under vacuum for 3 days.

associated to an intrinsic paramagnetic species in collagen, indicating that the amount of free radicals, if any are present, is minimal in collagen. The above findings, therefore, favor the earlier proposal (34) that the dehydrative cross-linking is via a condensation reaction mechanism.

7.3 Solubility of the Dehydrated Lathyrivic Collagen.

In collagen in vivo, evidence has been accumulated (28,29,36,37) that cross-links are developed via an aldol condensation reaction between lysine-derived aldehydes (α -amino adipic- δ -semialdehyde) and ϵ -amino groups in the form of Schiff's base (38) or between two residues of α -amino adipic- δ -semialdehyde (28,36). The role of aldehyde groups in the formation of cross-links in the native state was strongly supported by lathyrivic collagen (28), a collagen extracted from the animal which does not have structural integrity of the tissue. The lathyrivic collagen is known to be deficient of aldehydes (39) and thereby unable to be cross-linked biosynthetically (39,40). In an attempt to find out whether the cross-links produced biosynthetically via aldolcondensation in the native state are related to the dehydrative cross-links in vitro, or specifically whether aldehyde plays any role in the formation of cross-linking by dehydration, several experiments were conducted as described below.

a. Experimental

NaBH₄ reduced collagen: the reduction of collagen

by sodium borohydride was reported elsewhere (37,41) to reduce aldehyde to alcohol. The method by Blumenfeld and Gallop (37) was used in this work. Collagen solution, containing about 0.1%-wt. collagen in 0.05 M acetic acid solution (pH \approx 3.6) was adjusted its pH to 8.0 by adding 0.5 M NaH_2PO_4 solution at 23°C. Then, about 7 mg of solid NaBH_4 powder (Merck Co.) was added to approximately 50 ml of the collagen solution at 3°C. Addition of NaBH_4 yielded bubbles vigorously, a qualitative indication that the quality of NaBH_4 was satisfactory. The reaction mixture was kept at 3°C in a refrigerator for 4 hours before the pH was lowered to 4.0 by dropwise addition of 1 M HCl to destroy excess NaBH_4 . The solution was, then, dialysed against water for one day at 23°C and cast into films. The films of reduced collagen were subsequently dehydrated at 105°C, under vacuum, for 3 days and the solubility of thus dehydrated films was tested in the same way as described in previous section.

Solubility of the Dehydrated Films in Cysteamine Solution:

Collagen films which have been dehydrated and thus cross-linked were extracted with 0.2 M cysteamine solution as follows.

The solution of 0.2 M cysteamine was prepared by dissolving 6.82 g of cysteamine-HCl (Mercaptoethylamine, M.W. = 113.6) in 300 ml of 0.45 M NaCl solution. The pH of the solution was adjusted to 7.0 by addition of 1 M NaOH solution. Extraction was carried out by immersing

the collagen film in the 0.2 M cysteamine solution and kept over a week in a refrigerator at 3°C. After extraction, gel was separated from the solution, dialysed against distilled water for one day and then dehydrated to determine the weight. Soluble fraction was determined by the difference of the weight of collagen before and after the extraction.

Solubility of the Dehydrated Lathyrivic Collagen: Films were cast from the dilute solutions of normal acid soluble collagen and lathyrivic collagen (extracted from the skin of young rats treated with lathyrogen). The lathyrivic collagen was kindly donated by Dr. Nimni at the University of Southern California, Department of Medicine and Biochemistry. The properties of the lathyrivic collagen was reported by Nimni and coworkers previously (41,42). Both lathyrivic and normal collagen films were dehydrated at 23°C under vacuum ($\sim 10^{-6}$ mmHg) for 40 days, as well as at 105°C, under vacuum (3×10^{-4} mmHg) for 3 days. The solubility of the dehydrated films way then tested in the way described earlier in this section.

b. Results and Discussion

The solubility of the collagen films treated under various conditions was summarized in Table V-7. First, the result shows that the NaBH_4 reduced collagen becomes insoluble after dehydrated at 105°C under vacuum for three days, indicating that the reduction of collagen with NaBH_4 does not affect the dehydrative cross-linking.

TABLE V-7 Solubility of Normal and Lathyritic Collagen with Various Treatments

<u>Specimen</u>	<u>Treatment</u>	<u>Water (%-wt.)</u>	<u>Solubility</u>
Acid soluble rat tail collagen	1. Reduced with NaBH ₄	~0%	Completely insoluble ^d
	2. Dehydrated at 105°C, vacuum ^a 3 days		
Acid soluble rat tail collagen	1. Dehydrated 105°C, vacuum ^a 3 days	~0%	No soluble fraction was found after 7 days extraction at 3°C
	2. Extracted with 0.2 M cycteamine at 23°C		
Acid soluble rat skin collagen	1. Dehydrated at 23°C, vacuum ^b 40 days	~1% ^c	Partially insoluble ^d
	2. Dehydrated at 105°C, vacuum ^a 3 days	~0%	Completely insoluble ^d
Rat skin lathyritic collagen	1. Dehydrated at 23°C, vacuum ^b 40 days	~1% ^c	Partially insoluble ^d
	2. Dehydrated at 105°C, vacuum ^a 3 days	~0%	Completely insoluble ^d

NOTE: a: vacuum by rotatory pump $\sim 3 \times 10^{-4}$ mm Hg
b: vacuum by diffusion pump $\sim 10^{-6}$ mm Hg
c: estimated
d: Tested in 0.05 M acetic acid at 23°C for a week

Second, both normal and lathyrctic rat skin collagen becomes insoluble when dehydrated to anhydrous state. Third, the dehydrated, therefore cross-linked, collagen is not solubilized even to a small extent in 0.2 M cysteamine solution, which is known to solubilize the insoluble (cross-linked in vivo) collagen (41).

The reduction of collagen with NaBH_4 has been known (37) to reduce the aldehyde to alcohol and thereby served as the method of providing aldehyde-deficient collagen (41). Like lathyrctic collagen, collagen reduced by NaBH_4 is known to be unable to form stable intermolecular cross-links in vitro (41) due to the lack of aldehyde. The fact that the NaBH_4 -reduced collagen becomes also cross-linked by dehydration suggests that the dehydrative cross-linking in collagen is formed in the absence of aldehydes and, therefore, not via an aldol condensation reaction.

Stronger evidence is provided by the lathyrctic collagen. It has been well established that the lathyrctic collagen is identical in chemical and physicochemical properties with normal collagen (43) except the former contains far less amount of aldehyde groups (ca. 1/2) than the latter. The cause of lathyrism was identified at the β -amino propionitrile (BAPN) which inhibits the conversion of lysine to aldehyde, thereby inhibiting the intermolecular cross-linking (44). The lathyrctic collagen, which is not capable of forming intermolecular cross-links biosynthetically in vivo, however, becomes cross-linked

when dehydrated to anhydrous. Indication of this result in cross-linking is not related to the number of cross-links in vivo.

Nimni and coworkers (46) showed that reagents such as penicillamine, cysteamine, and cysteine, could solubilize insoluble collagen. In particular, the collagen extracted from rat skin by cysteamine but not by penicillamine or cysteine solubilized collagen (47) but was found to have a lower amino acid content. Based on this finding, it was suggested that cysteamine may break the bonds of similar nature as S-S bonds in the form of intermolecular cross-links synthesized synthetically (28), and as a result the solubilized collagen contains more amino acids. The above suggestion is correct if the mechanism of intermolecular cross-linking is the same. In fact (Table V-7) that cysteamine solubilized collagen of the insoluble collagen, and this is therefore indicative of that the mechanism is different from aldol condensation reactions.

7.4 Summary and Conclusions Linking in Collagen and

It has been shown that various chemical scavengers did not inhibit the

linking in collagen and gelatin and that the EPR measurements of the untreated and dehydrated collagen did not show appreciable signals attributable to free radicals (34). One of the most probable routes to produce the free radical would be the thermal degradation.

As already discussed, dehydration at 105°C under vacuum for 5 days did not cause any loss of amino acid, indicating that thermal degradation is negligible. It appears, therefore, rather clear that the dehydrative cross-linking in gelatin and collagen is not through the free radical mechanism and therefore via a condensation reaction which favors the hypothesis by Yannas and Tobolsky (24).

In vivo, cross-linking of collagen is known to be formed by the aldol condensation reaction between aldehyde groups or between aldehyde and ϵ -amine groups (28,29,36,37,38). Furthermore, the presence of aldehyde in collagen is identified (37,40,44,41) as the indispensable factor in the formation of cross-links biosynthetically. It has been shown in this work that the presence and the absence of the aldehydes in collagen have no effect in the development of cross-links in vitro by dehydration. Furthermore, such dehydrative cross-linking is not cleaved by cysteamine which is known (45, 46) to cleave the intermolecular cross-links developed biosynthetically in vivo. These results clearly show the evidence that the dehydrative cross-linking in

collagen and gelatin is not related to the mechanism of the biosynthesis of cross-links in vivo.

Rough estimation shows that there are approximately 360 carboxylic groups ($-\text{COOH}$), 240 primary amine groups ($-\text{NH}_2$), 160 secondary amine groups ($=\text{NH}$), and 470 hydroxyl groups ($-\text{OH}$) in one tropocollagen molecule. It appears that the condensation reaction is possible not only between carboxylic groups and amino groups to form amide links, but also between carboxylic groups and hydroxyl groups to form ester links. This work was not able to resolve the exact chemical nature of dehydrative cross-linking. However, none of the evidence is inconsistent with the mechanism of a condensation reaction as suggested by Yannas and Tobolsky (24) for the cross-linking in dehydrated gelatin.

Because of the high temperature (105°C) at which collagen and gelatin is subjected for dehydration, the question arises as to what effect the temperature itself has on the dehydrative cross-linking and, more specifically, whether cross-linking is the consequence of dehydration alone. The results in Table V-7 show that dehydration causes partial insolubilization in rat skin collagen even at 23°C . It appears, therefore, that dehydration per se is the cause of the formation of cross-links. (Under identical conditions, however, lathyritic collagen was soluble. Due to the limited amount of the lathyritic collagen, it was not confirmed by repeated experiment.) Additional work may be

necessary to draw a clear distinction between cross-linking caused by dehydration alone (i.e. dehydration at temperatures below, say, 37°C) and that caused by a pyrolytic reaction occurring at temperatures considerably in excess of about 50-60°C.

REFERENCES FOR CHAPTER V

1. Piez, K.A., Eigner, E.A. and Lewis, M.M. (1963),
Biochemistry, 2, 58
2. Cassel, J.M. (1966) J. Amer. Leather Chem. Assoc., 53, 215
3. Bowe, J.H. and Taylor, J.E. (1971) J. Amer. Leather Chem.
Assoc. 66, 96
4. Ramachandran, G.N. (1967) IN Treatise on Collagen
Vol.1 Chap.3, Academic Press
5. Rougvie, M.A. and Bear, R.S. (1953) J. Amer. Leather Chem.
Assoc., 48, 735
6. Zaides, A.L. (1954), Kolloid Z., 16, 267
7. Bear, R.S. (1953) Adv. Prot. Chem., 7, 69
8. Cowan, P.M., North, A.C.T. and Randall, J.T. (1955)
Symp. Soc. Exp. Biol., 9, 115
9. Esipova, N.G., Andreeva, N.S. and Gatovskaia, T.V. (1958)
Biofizika, 3, 529
10. Bradbury, E.M., Burge, R.E., Randall, J.T. and Wilkinson,
G.R. (1958) Disc. Faraday Soc., 25, 173
11. von Hippel, P.H. and Harrington, W. (1960) Brookhaven
Symp. Quan. Biol., 13, 213
12. Burge, G.E., Cowan, P.M. and McGavin, S. (1957) In Recent
Advances in Gelatin and Glue Research Ed. by
G., Pergammon, London
13. Fessler, J.H., and Hodge A.L. (1962) J. Mol. Biol., 5, 446
14. Harrington, W.F. and von Hippel, P.H. (1961) Archs. Biochem.
Biophys., 92, 100
15. Grassman, W., Hannig, K., Endres, H. and Riedel, A. (1956)
Z. Physiol. Chem., 306, 123
16. Grasman, W., Hannig, K. and Schleyer, M. (1960) Z. Physiol. Chem.
322, 71
17. Bear, R.S., Boldnan, O, E.A. and Salo, T.P. (1951) J. Am.
Leather Chem. Assoc. 46, 107

-
18. Hopfinger, A. J. and Wal
9, 433
 19. Anderson, J. M., Rippon,
Biochem. Biophys. Res. C
 20. Traub, W. and Yonath, A.
 21. Schwartz, A., Geil, P. H.
Biophys. Acta., 194, 130
 22. Yannas, I. V. (1972) J. Ma
 23. Sung, N. H. (1970) Repor
 24. Yannas, I. V. and Tobols
 25. Bougoin, D. and Joly, M.
 26. Ouchi, E. and Noda, H. (1
 27. Bello, J. and Riese-Bel
Photograph, 29, 361
 28. Piez, K. A. (1968) Ann. R
 29. Bornstein, P., Kang, A. H
Nat'l, Acad. Sci., 55,
 30. Soignet, D. M., Benerito
Text. Res. J., 39, 485
 31. Commoner, B., Townsend,
Nature, 174, 689
 32. Munday, K. A., Edward, M.
Food Agric., 13, 455
 33. Bailey, A. J. and Rhodes
22, 606
 34. Chien, J. C. W. (1970) Pr
 36. Kang, A. H., Faris, B. and
Biophys. Res. Comm., 39
 37. Blumenfeld, O. O. and Ga
Acad. Sci., U. S., 56, 126
 38. Bailey, A. J. and Peach,
Res. Comm., 33, 812

39. Levene, C. I. (1962) J. Exp'tl. Med., 116, 119
40. Martin, G. R., Piez, K. A. and Lewis, M. S. (1963) Biochim. Biophys. Acta, 69, 472
41. Deshmukh, K. and Nimni, M. E. (1969) J. Biol. Chem., 244, 1787
42. Nimni, M. E., Deshmukh, K., Gerth, N. and Bavetta, L. A. (1969) Biochem. Pharma., 18, 707
43. Tanzer, M. L. (1965) In "International Review of Connective Tissue Research" Vol. 3 Ed. by Hall, D. A. Acad. Press, N. Y.
44. Piez, K. A., Martin, G. R., Kang, A. H. and Bornstein P. (1966) Biochem., 5, 3813
45. Nimni, M. E. (1966) Biochem. Biophys. Res. Comm., 25, 434
46. Nimni, M. E., Deshmukh, K. and Bavetta, L. A. (1967) Arch. Biochem. Biophys., 144, 292
47. Deshmukh, K. and Nimni, M. (1968) Biochim. Biophys. Acta, 154, 258

BIOGRAPHICAL NOTE

Mr. Nak-Ho Sung was born on September 30, 1940 in Seoul, Korea. He was raised and educated mostly in Seoul, except for those years of Korean War when fled in country side. After graduating from Seoul High School in 1960, he entered the Seoul National University, where he earned his B.S. degree in chemical engineering in 1964. He worked for two years from 1964 to 1966 in Hanil Nylon Industry Co., Korea as an engineer.

In 1966, Mr. Sung was accepted as a graduate teaching assistant at the University of Chicago. He obtained the M.S. degree in physical chemistry from the University of Chicago in 1967, before he came to M.I.T. From 1967 to 1972, he has been a graduate research assistant in the Fibers and Polymers Division in Mechanical Engineering.

Since 1967, he has been a member of American Chemical Society and in 1969 he became a member of Sigma Xi. He took the office of M.I.T. Korean Alumni Assos. in 1970-1971, and has been a fund raiser for Seoul High School Scholarship Fund. in the past two years.

Publications

- * I.V.Yannas, N-H. Sung, A.C.Lunn: The transition from linear to non-linear viscoelastic behavior, Part II: Stress relaxation of polycarbonate, (1971) J. Macromol. Sci., B5(3), 487
- * I.V.Yannas, N-H. Sung: Optical Rotatory Dispersion of Collagen in the Solid State: A sensitive assay of helical content, (1972) Polymer preprints, 13, 123
- * I.V.Yannas, A.C.Lunn, and N-H. Sung: Mechanical Softening: a precursor to cold drawing (1969) Polymer preprints, 10, 1113